Exploring integrin and growth factor receptor crosstalk mechanisms

Thesis submitted in accordance with the requirements of the University of Liverpool for the degree of Doctor in Philosophy by Joanna Ruth Thomas.

July 2018

Abstract

Joanna R. Thomas; Exploring integrin and growth factor receptor crosstalk mechanisms.

The pro-invasive integrin αvβ6 is upregulated in a range of carcinomas, from normally very low levels, and is associated with poor prognosis. Therapeutic targeting of αvβ6 with inhibitory antibodies has produced promising results in breast cancer models *in vivo*. Preclinical evidence has suggested that αvβ6 and EGFR expression correlate in disease, and that a co-operative relationship between αvβ6 and EGFR may exist *in vivo*. This study aimed to determine if αvβ6 and EGFR are functionally integrated, and to investigate wider mechanisms of integrin and growth factor receptor crosstalk.

Immunofluorescent imaging, under steady-state conditions, demonstrated co-localisation between αvβ6 and EGFR in MDA-MB-468 cells in protrusive structures and endosomes. In addition, imaging and integrin-associated complex (IAC) enrichment approaches revealed that EGFR was recruited to sites of αvβ6 engagement on the αvβ6-selective ligand, latency-associated peptide (LAP). Importantly, reciprocal EGF or LAP stimulation increased EGFR and αvβ6 co-localisation with early endosomes, indicative of co-internalisation. Together, these data suggest a co-regulatory relationship between αvβ6 integrin and EGFR that impacts receptor trafficking mechanisms. Stimulation with LAP caused the phosphorylation of ERK, indicating αvβ6 positively regulates MAPK pathway signalling, and that signalling crosstalk may also exist between αvβ6 and EGFR.

Bioinformatic interrogation of αvβ6-IACs revealed αvβ6-medated adhesions are conducive sites of EGFR signalling. The identification of proteins associated with endocytosis and receptor trafficking highlighted liprin α1 as an important potential mediator of αvβ6 and EGFR crosstalk. The over-representation of Hippo pathway regulators at αvβ6-IACs led to on-going work that has identified αvβ6 as a regulator of YAP nuclear localisation and suggests that αvβ6-EGFR crosstalk is a determinant of this function.

Proteomic analysis of EGF regulated IAC components led to the identification of the adaptor protein Eps8 as a novel mediator of integrin and EGFR crosstalk. Eps8 functions to constrain endocytosis of α5β1 and EGFR and is required for adhesion organisation. These functions have direct consequences for adhesion and cytoskeletal dynamics.

On-going analysis of candidates identified from αvβ6-IAC proteomics will elucidate how αvβ6 and EGFR signalling networks and trafficking are integrated. In the future we aim to determine how these mechanisms contribute to αvβ6-dependent breast cancer cell invasion, and how αvβ6-EGFR receptor crosstalk understanding may contribute to the success of αvβ6-targeted therapeutics.

Dedication

To my parents Sue and Paul for their love and support,

my grandmother Ruth for her wisdom and inspiration,

and my cousin Charlie whose memory I honour at all my milestones.

Acknowledgements

Thank you to my supervisors Mark Morgan and Ian Prior for their unfaltering support and guidance throughout my PhD. You have helped mould me into the scientist I am today and for that I am truly grateful.

Thank you to all members of the Morgan lab past and present; especially Daniel Newman, Heather Swift, Katarzyna Wolanska, Horacio Maldonado and Stephanie Mo.

Our work on αVβ6 is based on a strong collaboration with John Marshall's lab at Barts Cancer Institute, London. John's postdoc Kate Moore and former PhD student Caroline Sproat have contributed significantly. Kate Moore has performed all the αVβ6 invasion and *in vivo* xenograft studies, and Caroline Sproat has performed important proteomic experiments. John, Kate and Caroline have been fundamental collaborators, and are duly referenced throughout this thesis. Louise Jones from Barts Cancer Institute is also an important collaborator and has provided clinical and pathological data on αVβ6.

The Eps8 project also represents a substantial collaborative effort. The project was started by Nikki Paul during her PhD in the Martin Humphries and Charles Streuli labs at the University of Manchester. Mark Morgan has performed immunofluorescence experiments, internalisation assays and assisted with calculations for the membrane dynamics experiments. Katarzyna Wolanska performed the live-cell imaging, and Rac1 activity experiments. Horacio Maldonado has also contributed to the project analysing Rab5 activity.

Dean Hammond has been a greatly aided the Morgan lab in our bioinformatic analyses. Dean has taught me a lot about bioinformatics and been a great source of information and guidance. Tobias Zech and his lab members have provided useful advice and interesting discussions relating to actin and trafficking. A particular mention goes to Tobias's former postdoc Ewan MacDonald who greatly advanced my understanding of EGFR trafficking. Claire Wells (King's College London) enlightened us to the importance of palmitoylation in the regulation of adhesion biology, and her unpublished data has informed our hypotheses significantly and is duly referenced. Additional thanks go to Sylvie Urbe and her former postdoc Yvonne Tang for their expertise on EGFR and provision of antibodies.

Thank you to the Wellcome Trust for generously supporting my PhD and academic development.

Contents

List of Figures

List of Tables

Abbreviations

a.u.	Arbitrary units
Abi1	Abl interactor 1
ABTS	2,2’-Azino-bis(3-ethylbenzothiazoline-6-sulfonic acid) diammonium salt
ACN	Acetonitrile
AEBSF	4-(2-Aminoethyl)benzenesulfonyl fluoride hydrochloride
AFM	Atomic force microscopy
Ambic	Ammonium bicarbonate
AMSH	Associated molecule with the SH3 domain of STAM
ANOVA	Analysis of variance
Arf6	ADP-ribosylation factor 6
ARVC	Arrhythmogenic right ventricular cardiomyopathy
ATP	Adenosine triphosphate
Bad	Bcl-2-associated death promoter
BFP	Biomembrane force probe
BSA	Bovine serum albumin
Cbl	Casitas B-lineage lymphoma proto-oncogene
Cdc42	Cell division cycle 42
COLL	Collagen
CST	Cell Signalling Technologies
DAG	Diacylglycerol
DCIS	Ductal carcinoma in situ
DMEM	Dulbecco’s Modified Eagle’s Medium
DMSO	Dimethyl sulfoxide
DNA	Deoxyribonucleic acid
DTBP	Dimethyl 3,3'-dithiobispropionimidate
DTT	Dithiothreitol
DUB	Deubiquitinating enzyme / Deubiquitinase
ECM	Extracellular matrix
EDTA	Ethylenediaminetetraacetic acid
EEA1	Early endosome antigen 1
EGF	Epidermal growth factor
EGFR	Epidermal growth factor receptor
EGTA	Ethylene glycol-bis(2-aminoethylether)-N,N,N’,N’-tetraacetic acid

ELISA	Enzyme Linked Immunosorbent Assay
EMT	Epithelial-to-mesenchymal transition
Eps8	Epidermal growth factor receptor kinase substrate 8
Eps8l2	Epidermal growth factor receptor kinase substrate 8-like protein 2
ER	Oestrogen receptor
ERK	Extracellular signal-regulated kinase
ESCRT	Endosomal Sorting Complex Required for Transport
Ets-1	Eukaryotic translation initiation factor
FA	Formic acid
F-actin	Filamentous actin
FAK	Focal adhesion kinase
FAT	Focal-adhesion targeting
FCS	Foetal calf serum
FERM	Four-point-one, ezrin, radixin, moesin
FN	Fibronectin
FRAP	Fluorescence recovery after photobleaching
GAGs	Glycosaminoglycans
GAP	GTPase-activating proteins
GEF	Guanine nucleotide exchange factors
GFP	Green fluorescent protein
GFR	Growth factor receptor
Grb2	Growth factor receptor-bound protein 2
GTPase	Guanosine triphosphatase
HAX1	HCLS-1-associated protein X1
HER	Human EGFR
HGF	Hepatocyte growth factor
HRS	Hepatocyte growth factor-regulated tyrosine kinase substrate
IA	Iodoacetamide
IAC	Integrin-associated complex
ICAP-1	Integrin cytoplasmic domain-associated protein-1
ILK	Integrin-linked kinase
IP3	Inositol 1,4,5-triphosphate
JC-virus	John Cunningham polyoma virus
KD	Knock-down

KEGG	Kyoto encyclopedia of genes and genomes term
KSEA	Kinase Substrate Enrichment Analysis
LAMP2	Lysosome-associated membrane protein 2
LANCL2	LanC-like protein 2
LAP	Latency associated peptide (Transforming Growth Factor-β1)
LATS1/2	Serine/threonine-protein kinase LATS1/2
LC-MS	Liquid chromatography-mass spectrometry
LIM	Lin-11, Isl1, and Mec-3
mAb	Monoclonal antibody
MAPK	Mitogen-activated protein kinase
MDGI	Mammary-derived growth inhibitor
MesNa	Sodium 2-mercaptoethanesulfonate
Met	Hepatocyte growth factor receptor
MIDAS	Metal ion-dependent adhesion site
MMPs	Matrix metalloproteinases
MS	Mass spectrometry
MST1/2	Mammalian STE20-like protein kinase 1/2
MT1-MMP	Membrane-type 1 matrix metalloproteinase
mTOR	Mammalian target of rapamycin
MVBs	Multivesicular bodies
Nrp1	Neuropillin-1
NSAF	Normalized spectral abundance factor
NSCLC	Non-small-cell lung carcinoma
OSCC	Oral squamous cell carcinoma
p…	Phosphorylated
pAb	Polyclonal antibody
PanIN	Pancreatic intraepithelial neoplasia
PBS	Phosphate buffered saline
PBST	Phosphate buffered saline with tween-20
PDAC	Pancreatic ductal adenocarcinoma
PDGFR	Platelet-derived growth factor receptor
PDK1	Phosphoinositide-dependent protein kinase 1
PET	Positron emission tomography
PG	Progesterone receptor

PI3K	Phosphoinositide 3-kinase
PINA	Protein Interaction Network Analysis
PIP2	Phosphatidylinositol (4,5)-bisphosphate
PIP3	Phosphatidylinositol (3,4,5)-trisphosphate
PKC	Protein kinase C
PKD	Protein kinase D
PMA	Phorbol 12-myristate 13-acetate
PML	Progressive multifocal leukoencephalopathy
PP1	Protein phosphatase 1
PP2A	Protein phosphatase 2 A
PPI	Protein-protein interaction
PSI	Plexin-semaphorin-integrin
PTB	Phosphotyrosine-binding domain
PTEN	Phosphatase and tensin homolog
Rac1	Rac family small GTPase 1
RACK1	Receptor of activated protein C kinase 1
RalGDS	Ral guanine nucleotide dissociation stimulator
RCC2	Regulator of chromosome condensation–2
RCP	Rab-coupling protein
RIAM	Rap1 GTP–interacting adaptor molecule
RIPA	Radio Immunoprecipitation Assay buffer
RNA	Ribonucleic acid
ROCK	Rho-associated kinase
RTK	Receptor tyrosine kinase
SDS	Sodium dodecyl sulfate
SDS-PAGE	Sodium dodecyl sulfate polyacrylamide gel electrophoresis
SH2	Src homology 2
SHANK	SH3 and multiple ankyrin repeat domains
SHARPIN	SHANK associated RH domain interactor
siRNA	Small interfering RNA
Sos	Son-of-sevenless
STAM	Signal-transducing adaptor molecule
TAZ	Transcriptional coactivator with PDZ-binding motif
TBST	Tris buffered saline with tween-20

TCL	Total cell lysate
TCPTP	T-cell protein tyrosine phosphatase
TFM	Traction-force microscopy
TGFα	Tumour transforming growth factor alpha
TGFβ	Transforming growth factor beta
TNBC	Triple-negative breast cancer
uPA	Urokinase plasminogen activator
uPAR	Urokinase plasminogen activator receptor
VASP	Vasodilator-stimulated phosphoprotein
VCAM-1	Vascular cell adhesion molecule-1
VEGF	Vascular endothelial growth factor
YAP	Yes-associated protein

1. Introduction

This thesis project studies mechanisms of crosstalk between integrins and growth factor receptors (GFRs). Receptor crosstalk can impact the function of both receptor families and must be fully understood to aid the development of targeted therapies, as unanticipated crosstalk mechanisms can hinder therapeutic efficacy. To put this into context, the canonical functions of the receptor families, modes by which they are regulated, and current targeted therapeutics are outlined. Known mechanisms of crosstalk between integrins and growth factor receptors are discussed. Particular focus has been given to the pro-invasive integrin αVβ6 and the ErbB family GFR EGFR in the context of triple-negative breast cancer (TNBC), as these receptors and their crosstalk represents novel and clinically relevant targets for the TNBC sub-type of breast cancer which currently has no targeted therapies (Andreopoulou et al., 2017).

1.1 Extracellular Matrix

Integrins are the main extracellular matrix (ECM) engaging surface receptors and function to integrate signals between cells and their microenvironment (Hynes, 2014). The ECM is the non-cellular component of tissues and organs that, in addition to physical support, can also regulate the behaviour of cells within, through biochemical and biophysical cues. The properties of the ECM can vary greatly between tissues (e.g. calcified bone vs the cornea) dependent on function, and in different physiological states (e.g. fibrotic or cancerous) (Frantz et al., 2010). The ECM is secreted and locally assembled primarily by fibroblasts. The three major classes of macromolecules that comprise the ECM are glycosaminoglycan (GAG)-associated proteoglycans, fibrous proteins and glycoproteins (Frantz et al., 2010).

GAGs and proteoglycans are strongly hydrophilic and adopt highly extended conformations. Consequently they form hydrogels that occupy a large volume relative to their mass, and are able to withstand compressive forces (Schaefer and Schaefer, 2010). Collagens are the major family of fibrous proteins, that constitute the main structural integrity of the ECM. Collagens can assemble into collagen fibrils, which often aggregate forming fibres that resist tensile force (Rozario and DeSimone, 2010). Inelastic collagen fibrils can be associated with elastin-rich elastic fibres to limit the extent of stretching, preventing tearing of elastic tissues (Frantz et al., 2010). Glycoproteins such as fibronectin (FN) and laminins typically contain multiple domains with binding sites for ECM macromolecules and cell surface receptors (Frantz et al.,

2010). These proteins are therefore able to contribute to the organisation of the ECM, cellular signalling and mechanochemical stimuli.

The ECM is dynamic, constantly being synthesised, remodelled and degraded. Some self-assembly of ECM fibrils can occur *in vitro*, however cell driven organisation of fibrils is the predominant mechanism (Humphrey et al., 2014; Hynes, 2014). The ability of cells to apply force to ECM macromolecules via ECM binding receptors linked to the actin cytoskeleton is crucial to this process (Wolanska and Morgan, 2015). Force application to ECM proteins, such as FN, can cause conformational changes revealing cryptic binding sites (Smith et al., 2007; Vogel, 2006). Fibres within the ECM may also be cross-linked by enzymes such as Lysyl oxidase (LOX) and transglutaminase 2, resulting in matrix stiffening (Griffin et al., 2002; Levental et al., 2009). Proteolytic degradation of ECM is primarily mediated by matrix metalloproteinases (MMPs) and serine proteases (Frantz et al., 2010).

The ECM binds a range of growth factors, essentially acting as a reservoir, with a role in establishing stable gradients. Growth factors can function as soluble ligands released as a consequence of ECM degradation, or as bound ligands with proteoglycan involvement as a co-factor (Hynes, 2009). Many ECM proteins also contain domains that can act as ligands for growth factor receptors (GFRs), allowing the establishment of concentration gradients. Consequently, GFRs and ECM receptors in the cell plasma membrane can be bound simultaneously, to spatially localise and constrain initiation of multiple signalling mechanisms (Hynes, 2009).

1.2 Integrin Family

Cellular binding to the ECM is mediated primarily by the integrin family of receptors. Additional ECM binding receptors include the syndecan family of membrane spanning proteoglycans that can bind a wide range of ligands, and the discoidin domain receptor family of receptor tyrosine kinases (RTKs) that bind collagens (Couchman et al., 2001; Valiathan et al., 2012). All metazoan express at least one β and two α integrin subunits (Whittaker and Hynes, 2002). Evolutionary expansion of the family has produced the complete mammalian set of integrins comprised of 8 β- and 18 α-subunits that are known to assemble into 24 distinct heterodimers (Figure 1.1) (Hynes, 2002). The family is further diversified by alternative spicing variants and post-translational modifications that may affect ligand binding (van der Flier and Sonnenberg, 2001). Integrin α- and β-subunits associate non-covalently, and both span the plasma membrane with small intracellular C-terminal

cytoplasmic domains, and large extracellular N-terminal extracellular domains (Alberts et al., 2015).

Integrin heterodimers have specific non-redundant functions, as evidenced by their distinct knock-out mouse phenotypes, ranging from a block in pre-implantation development (β1 knock-out) (Fassler and Meyer, 1995), to different developmental defects and post-natal phenotypes (Hynes, 2002). Ligand specificity is mediated by both the α- and β-subunits, contributing to an array of binding capabilities and affinities. Integrin binding to ECM macromolecules is normally mediated by a short motif, such as the *Arg-Gly-Asp* (RGD) motif (Hynes, 2002), that interacts with a divalent-cation-binding site within the integrin (Humphries et al., 2003b). Integrin heterodimers can be subcategorised by their structure and ligand binding profiles (Figure 1.1). The two most evolutionarily ancient sub-categories are the RGD-binding and laminin-binding integrins. The insertion of an A-domain in the α-subunit created a collagen binding subgroup. α4β1 and α9β1 recognise an acidic *Leu-Asp-Val* (LDV) motif that is related to the RGD motif (Hynes, 2002). Vertebrates also express leukocyte specific integrins (αL, αM, αX, and αD that dimerise with β2, and αEβ7) that mediate cell-cell adhesion through immunoglobulin family cell surface receptors, such as ICAM (intercellular adhesion molecule) (Hynes, 2002).

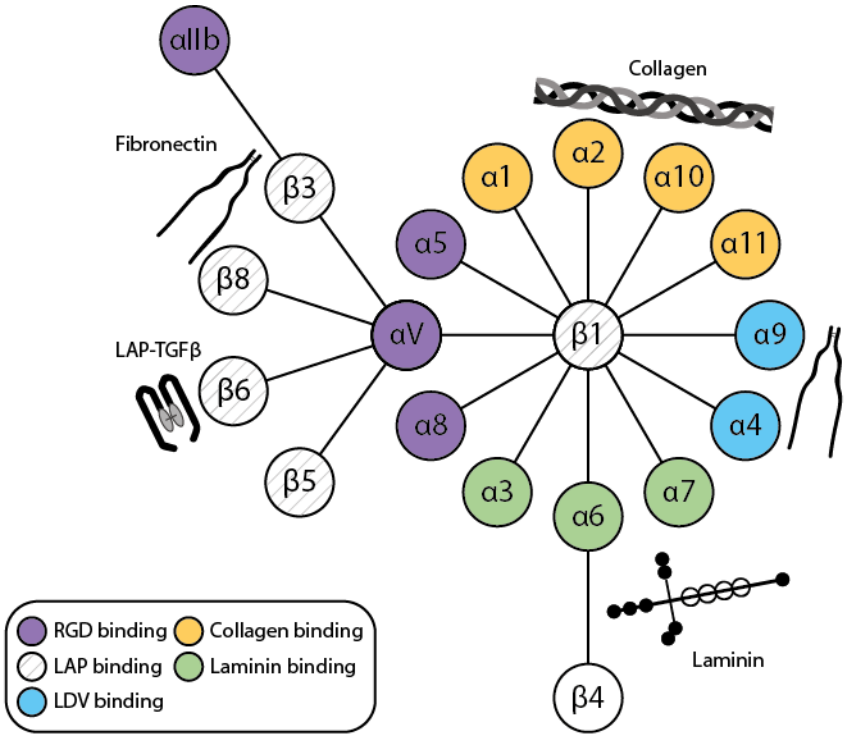

Figure 1.1 The integrin receptor family. Heterodimers formed by integrin α- and β-subunits, omitting the leukocyte-specific β2, β7, αL, αM, αX, and αD (Hynes, 2002). Subfamilies based on ligand specificities are depicted (colouring of α-subunits). All five αV heterodimers, α5β1, α8β1, and αIIbβ3 recognise the RGD tripeptide sequence (purple) in ligands such as fibronectin and vitronectin. α4β1 and α9β1 recognise an acidic LDV motif (blue) that is functionally related to the RGD motif. α1, α2, α10 and α11 that pair with β1 contain an inserted A domain, forming a subfamily that can bind collagens and laminins (yellow). α3, α6 and α7 paired with β1, and α6β4 selectively bind laminins (green), however do not contain an A domain in the α-subunits. β-subunits with grey hatching can bind latency associated peptide (LAP) when paired with αV. The ligands fibronectin, LAP-TGFβ, collagen and laminin are depicted proximal to the integrins that they are engaged by (Humphries et al., 2006).

1.2.1 Integrin Structure

Integrins have large extracellular domains (>1,600 amino acids) and typically short cytoplasmic domains (20 – 50 amino acids) (Hynes, 2002) (Figure 1.2). The β4 subunit is a notable exception to this, as its cytoplasmic domain is larger (~1,000 amino acids), allowing it to connect to intermediate filaments instead of actin, as is the case for all other integrin β-subunits (Hynes, 2002). The first crystal structure of an integrin dimer was reported for the extracellular region of αVβ3 in (Xiong et al., 2001), followed by the structure in complex with an RGD ligand (Xiong et al., 2002).

The extracellular domain contains a head, followed by the leg domain of each subunit, single pass transmembrane helices, ending a cytoplasmic domain (Figure 1.2). The major ligand binding site is formed by contact between the α-subunit β propeller, the β subunit A-domain, and the α-subunit A-domain if present (Humphries et al., 2003b). The A-domain contains a

metal ion-dependent adhesion site (MIDAS) site that binds cations and is responsible for the cation dependency of integrin ligand binding (Humphries et al., 2003a).

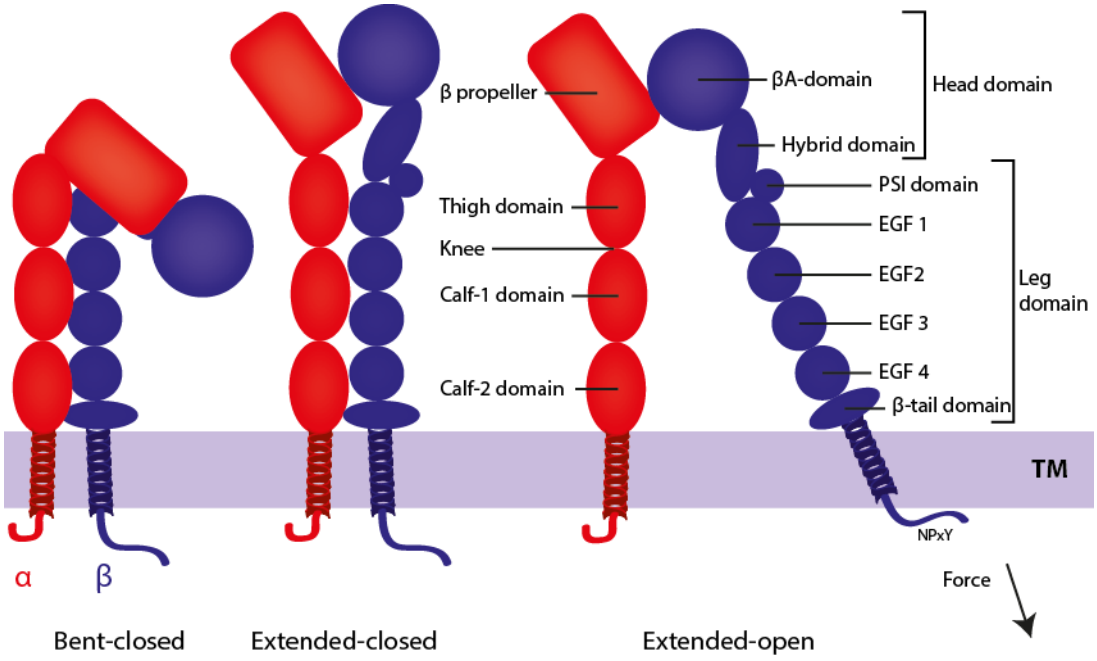

Figure 1.2 Integrin structure and conformation. Integrin heterodimers are formed from an α (red) and a β subunit (blue). The α-subunit has a β propeller domain comprised of seven blades, followed by three β-sandwich domains termed thigh, calf-1 and calf-2 domains (Campbell and Humphries, 2011). If present, the αA domain is inserted between β propeller blades. The β-subunit head domain contains a βA-domain and hybrid domain, followed by a leg with a plexin-semaphorin-integrin (PSI) domain, followed by 4 EGF repeats and a β-tail domain. The head region is the primary site for ligand binding. The membrane-proximal regions of the cytoplasmic domains of both subunits contains an α helix. The C-terminal residues of the α-subunit cytoplasmic domain loop back to contact the membrane-proximal region. The terminal residues of the β-subunit cytoplasmic domain are disorganised and contain a NPxY motif responsible for interacting with talin (Travis et al., 2003). Integrins can broadly form three different structures, a bent-closed with low ligand affinity, extended-closed primed structure with low ligand affinity, and an extended-open conformation with separated leg and cytoplasmic domains, which is active and has a high affinity for ligands (Askari et al., 2009).

The α-subunit cytoplasmic domain has three β-sandwiches, termed thigh, calf-1 and calf-2 domains. A flexible region between the thigh and calf-1 is termed the knee, which can adopt a 135° bend (Humphries et al., 2003a). The β-subunit has a 'hybrid' domain in the head region, that can move to promote a conformational changes that create high affinity binding sites in the integrin head and cytoplasmic regions (Liddington, 2014). The β-subunit leg domain contains a plexin-semaphorin-integrin (PSI) domain, four epidermal growth factor (EGF)-like repeats and a β-tail domain with a cystatin-like fold (Humphries et al., 2003a).

The first 10 amino acids of the α- and 20 amino acids of the β-subunit cytoplasmic regions form α-helices. The remaining C-terminal residues of the α-subunit loop back to contact the

membrane-proximal region of its cytoplasmic domain. The final residues of the β-subunit cytoplasmic domain are disordered and contain a NPxY motif that mediates binding to talin via its four-point-one, ezrin, radixin, moesin (FERM) domain. The degree of conservation between β cytoplasmic domains is higher than between α-subunits, leading to the theory that the β-subunit is the principal binding site for cytoplasmic interactors, and the α-subunit may have a more regulatory role (Humphries et al., 2003a).

1.3 Regulation of Integrins

Integrin activity is tightly regulated for the spatial and temporal control of adhesion formation and detachment, which is essential to processes such as cell migration and vascular extravasation of leukocytes. Integrin structural conformation can be separated into three states; an inactive bent low ligand affinity conformation with inhibitory contact between the cytoplasmic domains, a primed extended low affinity conformation, and an active high affinity conformation with separated legs and cytoplasmic domains (Figure 1.2) (Liddington, 2014). Integrins exist in an equilibrium between these three states, that can be influenced to favour either direction (Pouwels et al., 2012). Cytoplasmic domain truncated mutants result in a constitutively high affinity state integrin, highlighting the important regulatory role of the cytoplasmic domains (Mehta et al., 1998). The inactive bent state of integrins is maintained by non-covalent interactions between α- and β-subunits in the transmembrane and cytoplasmic domains (Shattil et al., 2010). A salt bridge is formed between the membrane-proximal cytoplasmic domains of α- and β-subunits, which if disrupted results in integrin activation (Hughes et al., 1996). A conserved GFFKR motif within the α-subunit cytoplasmic domain is required for the formation of the salt bridge, and therefore for maintaining the inactive integrin conformation (O'Toole et al., 1991).

1.3.1 Positive Regulation

The extracellular microenvironment critically influences integrin activity. Integrin binding is affected by the extracellular concentration of Ca^{2+} and Mg^{2+}, due to the MIDAS divalent cation binding domains in integrins. Divalent cations can affect the affinity and specificity of integrin ligand binding (Humphries et al., 2003a). Binding to extracellular multi-valent ligands triggers the clustering of integrins, which increases their ligand avidity (Shattil et al., 2010). ECM rigidity is important for the response to intracellular force applied to integrins by actomyosin-dependent contractility, which increases binding strength (Friedland et al., 2009; Kong et al., 2009).

Talin binding to the integrin β cytoplasmic domain is a crucial step in integrin activation. The head domain of talin binds via its FERM domain to the NPxY motif of the β cytoplasmic domain, whilst the talin rod domain has multiple actin-binding sites. Talin exists in an autoinhibited conformation, which must be released to allow integrin binding (Moser et al., 2009). Talin binding to the β-cytoplasmic domain disrupts the salt bridge connecting the cytoplasmic α- and β-subunits, resulting in a change in position of the β transmembrane helix, consequently activating the integrin by separating the cytoplasmic domains (Figure 1.2) (Banno and Ginsberg, 2008). The small guanosine triphosphatase (GTPase) Rap1 and its adaptor Rap1 GTP–interacting adaptor molecule (RIAM) are drive recruitment of talin to integrin β-subunit cytoplasmic domains (Lee et al., 2009). Kindlin is able to bind the integrin β-subunit cytoplasmic domain at sites distinct from talin, and functions to co-activate integrins potentially in a subunit specific manner (Ye et al., 2014).

1.3.2 Negative Regulation

Interference of talin or kindlin binding to the β cytoplasmic domain is a major inhibitory mechanism. Proteins containing a phosphotyrosine-binding (PTB) domain, such as tensins 1 – 4, bind to the NPxY motif and compete with talin (Pouwels et al., 2012). Phosphorylation of the NPxY motif is required for PTB domain binding (Forman-Kay and Pawson, 1999), and inhibits talin binding (Anthis et al., 2009). Integrin cytoplasmic domain-associated protein-1 (ICAP-1) also competes with talin binding, however does not require tyrosine phosphorylation of the NPxY motif for its interaction (Bouvard et al., 2003). Filamins also inhibit talin binding, by engaging with a filamin binding site that overlaps with the talin binding site on the β cytoplasmic domain (Kiema et al., 2006).

Integrin α-subunit cytoplasmic domain binding negative regulators of integrin activity can bind to a conserved membrane-proximal region, or to poorly conserved membrane distal regions with potential to regulate integrin activity in a heterodimer specific manner (Pouwels et al., 2012). SHARPIN (SHANK associated RH domain interactor) binds the conserved WKxGFFKR motif in the α-subunit and has been shown to inhibit β1 activity by inhibiting talin and kindlin binding to the β-subunit (Rantala et al., 2011). Mammary-derived growth inhibitor (MDGI) binds several α-subunits and inhibits integrin activity in breast cancer cells, most likely by reducing the association between active β1 and kindlin (Nevo et al., 2010). The existence of negative regulators of integrin activity that exhibit specificity for specific α-subunits is less clear (Pouwels et al., 2012).

In addition to direct integrin binding, integrin activity can be regulation by sequestration of integrin regulators. For example, the actin cytoskeletal regulators SHANK 1 (SH3 and multiple ankyrin repeat domains) and SHANK 3 indirectly inhibit integrins by sequestering integrin activators (Atherton and Ballestrem, 2017). SHANK interacts with active GTP-bound Rap1, and sequesters it limiting its bioavailability for activating integrins at the plasma membrane (Lilja et al., 2017).

1.3.3 Integrin Trafficking

The control of integrin bioavailability at the plasma membrane is key to regulating their function. Integrins are internalised in a constitutive and often ligand-independent manner via clathrin-dependent or clathrin-independent endocytosis (Bridgewater et al., 2012). Recruitment of endocytic regulators to integrins can influence and drive internalisation (Bridgewater et al., 2012). Cargo usually associates with clathrin-coated structures via an adaptor protein. HCLS-1-associated protein X1 (HAX1) is involved in clathrin-mediated endocytosis, and directly binds the cytoplasmic domain of β6 integrin. The interaction between HAX1 and β6 is essential for the clathrin-mediated endocytosis ofαVβ6 (Ramsay et al., 2007). The binding of protein kinase C α (PKCα) to β1 via the NPxY motif promotes caveolin dependent internalisation of β1 (Ng et al., 1999; Parsons et al., 2002). Active and inactive integrins can be trafficked differentially (Arjonen et al., 2012). One example of this is that efficient internalisation of active α5β1 requires the transmembrane glycoprotein neuropillin-1 (Nrp1), whereas inactive α5β1 internalisation is unaffected by Nrp1 silencing (Valdembri et al., 2009). Recruitment factors can also bind the α-subunit mediating heterodimer specific trafficking, for example p120RasGAP (RASA1) is able to bind α cytoplasmic domains, compete with Rab21 binding, facilitating integrin recycling (Mai et al., 2011).

Integrins rapidly traffic to early endosomes, where cargos are sorted either for degradation or recycling back to the plasma membrane (Figure 1.3) (Caswell and Norman, 2006; Sorkin and von Zastrow, 2009). Degradation of integrins is influenced by their level of ubiquitination (Caswell et al., 2009), however integrins can be retrieved from lysosomal degradation pathways by sorting nexin SNX17, and subsequently recycled (Steinberg et al., 2012). Proteins that predominantly localise to specific trafficking compartments can be used to identify different endosomal sub-types such as EEA1 (early endosomal antigen 1) which is present on early endosomes, HRS (hepatocyte growth factor-regulated tyrosine kinase substrate) which is a component of ESCRT that localises predominantly to the MVB, and LAMP2 (lysosome-associated membrane protein 2) which is present on lysosomes (Figure

1.3) (Braulke and Bonifacino, 2009; Goh and Sorkin, 2013). These markers will be utilised to investigate receptor trafficking in this thesis.

The majority of integrins are sorted for recycling (Bretscher, 1989; Bretscher, 1992), either through a fast 'short-loop' or slow 'long-loop' pathway (Figure 1.3) (Bridgewater et al., 2012). The short-loop pathway recycles cargo from early endosomes, and is controlled by Rab4 and Rab35 (Grant and Donaldson, 2009). The long-loop pathway recycles cargo that have transited from early endosomes to the perinuclear recycling compartment and is Rab11 and/or Arf6 (Figure 1.3) (ADP-ribosylation factor 6) dependent (Grant and Donaldson, 2009; Stenmark, 2009). The rate of integrin recycling can be affected by switching between the pathways. Stimulation with platelet derived growth factor (PDGF) switches αVβ3 from the long-loop Rab11 dependent recycling pathway, to the short-loop Rab4 dependent pathway (Roberts et al., 2001).

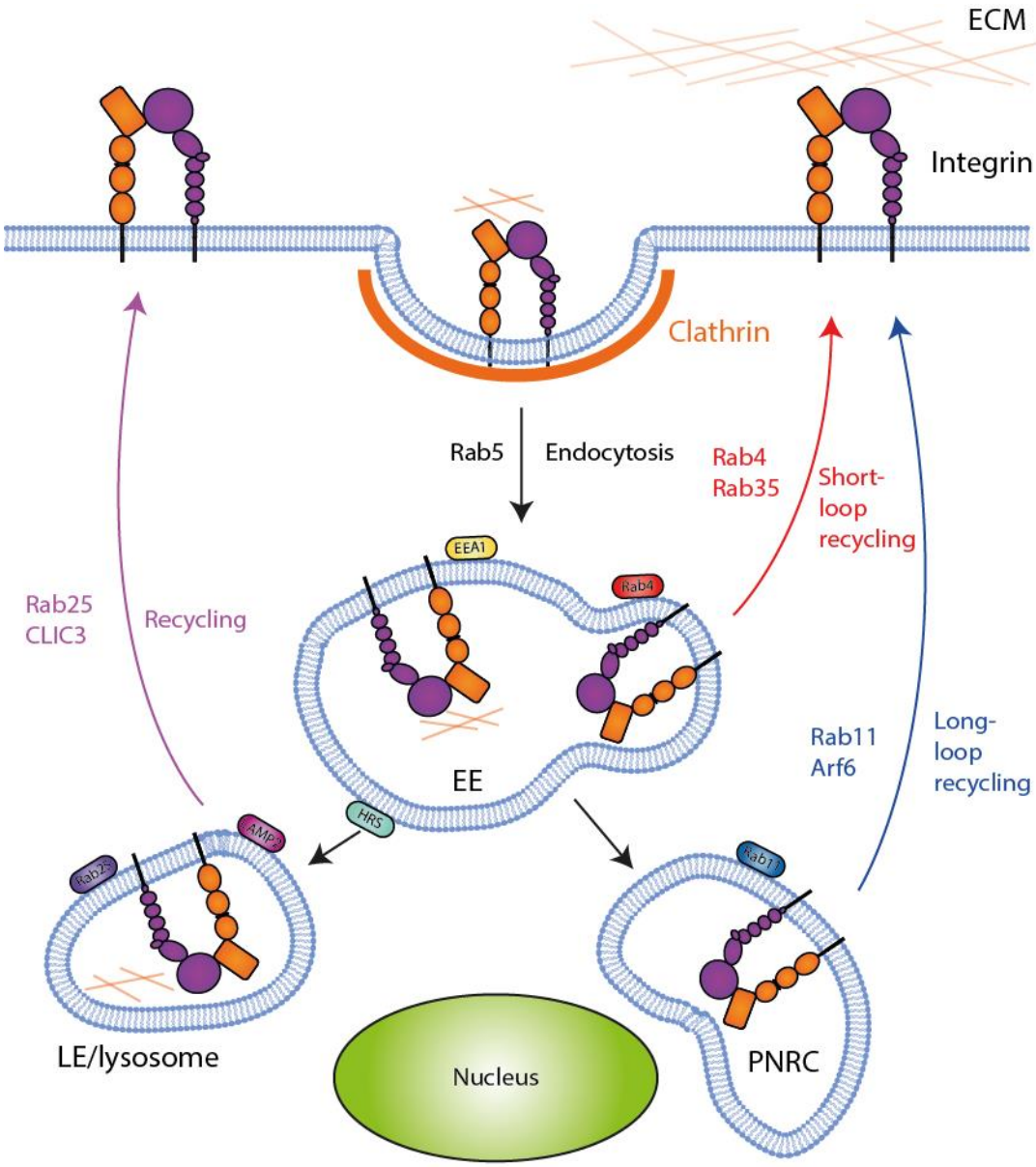

Figure 1.3 Integrin trafficking. Integrins can be endocytosed via clathrin-dependent (shown) and clathrin-independent routes, and traffic to the early endosome (EE). Integrins are predominantly recycled rather than degraded (De Franceschi et al., 2015). Integrin recycling is broadly associated with a fast short-loop pathway from the EE which is dependent on Rab4 and Rab35, or a slower long-loop pathway from the perinuclear recycling compartment (PNRC) which is dependent on Rab11 and Arf6 (Bridgewater et al., 2012). Integrins trafficked to the late endosome (LE) or lysosome can also be recycled, and the ECM ligand is degraded. This process has been shown to be mediated by CLIC3 for α5β1 (Dozynkiewicz et al., 2012).

1.4 Integrin Function

1.4.1 Bidirectional Signalling

Integrins are so named for their ability to 'integrate' signals from the extracellular and intracellular environments. Central to this is their ability to transduce signals from the ECM to the cell, termed 'outside-in signalling', and the converse transmission of signals from the cell to the ECM termed 'inside-out signalling'. 'Outside-in' signalling relies on ligand binding by the integrin extracellular head domain, to induce conformational changes that propagate down the structure and induce reorganisation of the cytoplasmic domains (Figure 1.2). The reverse is true for 'inside-out' signalling whereby cytosolic proteins alter the cytoplasmic regions to induce conformational changes in the extracellular domain of the integrin that affect ligand binding capabilities (Liddington, 2014). Outside-in signalling results in the dynamic recruitment of cytosolic proteins to integrin adhesions, that relay diverse intracellular signals mediating core processes such as cell survival, proliferation, spreading and migration (Harburger and Calderwood, 2009). Integrins lack intrinsic enzymatic activity and therefore initiate signalling through the dynamic recruitment of signalling moieties (Caswell et al., 2009). Inside-out signalling is able to modulate adhesion strength, transmit force required for cell migration and influence ECM assembly and remodelling (Shattil et al., 2010).

1.4.2 Mechanotransduction

A key feature of integrin adhesions is their ability to sense mechanical force externally from the ECM, or internally from actomyosin contractility and respond with biochemical signals. The cytoplasmic domains of integrins do not contain actin-binding sites, therefore they are linked via proteins such as talin and vinculin to the actin cytoskeleton and its associated actomyosin contractility (Sun et al., 2016). Integrin mechanotransduction is essential for the mechanical homeostasis of the ECM to maintain tissue structural integrity (Humphrey et al., 2014). The ability of cells to generate traction forces is also essential for membrane protrusions and cell migration.

Polymerisation of actin filaments perpendicular to the plasma membrane can cause distention and protrusion formation. In a situation where the actin cytoskeleton is not coupled to integrin adhesions, the polymerising end of the actin filament cannot distend the plasma membrane, and instead results in actin retrograde flow, where the actin filament is pushed backwards towards the cell body with the addition of new monomers (Sun et al., 2016). When filamentous actin (F-actin) is linked to integrin adhesions, actin polymerisation

and actomyosin contractility can be converted into traction forces, which push the plasma membrane forward and apply force to the ECM (Sun et al., 2016).

Integrin-mediated adhesion to the ECM is required for the generation of traction force, and the bond strength between integrins and ligands is regulated by force (Kong et al., 2009). The interaction is an example of a force-stabilised 'catch bond', where the application of force allosterically activates protein-protein interactions resulting in increased bond lifetime (Sun et al., 2016). Repeated cycles of force application and release was shown to strengthen the bond between α5β1 and FN, using atomic force microscopy (AFM) and a biomembrane force probe (BFP) (Kong et al., 2013).

Proteins recruited to integrin-mediated adhesions can be regulated by mechanical force. Talin is a mechanosensitive protein, which undergoes force-dependent conformational changes (Jansen et al., 2017). Cytoplasmic talin is present in an inactive autoinhibited conformation, that can be relieved by Kank2 or RIAM binding (Sun et al., 2016). Actomyosin contractility is able to stretch talin that is simultaneously bound to integrins and actin (Sun et al., 2016). The talin rod domain contains 13 subunits (R1-13) which can be unfolded through application of force, with differential kinetics (Yao et al., 2016). The R3 domain is the most mechanically weak and is therefore considered to be the first mechanosensor. Unfolding of talin disrupts binding sites for proteins that bind its folded form and exposes new cryptic binding sites for proteins such as vinculin. The number of exposed vinculin binding sites increases with talin stretch, consequently increasing vinculin binding (Yao et al., 2016). Vinculin binds talin and F-actin, strengthening the linkage and further recruiting F-actin, thus re-enforcing coupling of the integrin-mediated adhesion to the cytoskeleton (Sun et al., 2016). Talin and vinculin are able to mediate the recruitment of other proteins at integrin adhesions depending on their activation states and structures (Jansen et al., 2017).

Proteins involved in integrin adhesion signalling and actin regulation can be differentially recruited and activated in a force-dependent manner, demonstrated collectively through a meta-analysis of adhesion enriched mass spectrometry (MS) datasets sensitive to the myosin II inhibitor blebbistatin (Horton et al., 2016a). Focal adhesion kinase (FAK) and paxillin can both be phosphorylated in response to mechanical stimuli (Jansen et al., 2017). FAK-null fibroblasts have impaired migration and lose the ability to migrate preferentially towards stiffer substrates in a mechanosensitive process termed 'durotaxis' (Wang et al., 2001). Paxillin phosphorylation status is also important in durotaxis, and may be involved in vinculin

recruitment (Plotnikov et al., 2012). Mechano-regulated proteins recruited to integrin-mediated adhesions are required for mediating downstream responses to mechanical force.

Sensation of force at adhesions can result in transcriptional changes. Stem cell differentiation is influenced by ECM rigidity, demonstrated by mesenchymal stem cells cultured on soft substrates differentiating towards neurogenic lineages, intermediate substrates producing myogenic linages, and stiff substrates inducing osteoid phenotypes (Engler et al., 2006). YAP (Yes-associated protein) and TAZ (transcriptional coactivator with PDZ-binding motif) were identified as key force sensitive transcription factors, that translocate to the nucleus in response to ECM stiffness (Dupont et al., 2011). Mechanical force application at integrin-mediated adhesions is therefore important in regulating the function and composition of adhesions and can mediate long-term transcriptional changes that impact on cellular function and differentiation.

1.5 Adhesion Dynamics

Integrin-mediated adhesions are traditionally thought to exist in three major forms (nascent, focal and fibrillar adhesions) that develop sequentially and can co-exist simultaneously in the same cell. Nascent adhesions are initial contacts formed in lamellipodial protrusions. They consist of a small number of integrins, and are independent of myosin contractility (Wolfenson et al., 2013). Integrins are activated and cluster in nascent adhesions. Integrin clustering can be positively regulated by multi-valent ECM ligands, intracellular adhesion components, and the glycocalyx (Iwamoto and Calderwood, 2015; Paszek et al., 2014). Nascent adhesions can progress to form adhesion complexes, through actomyosin contractility strengthening the adhesions and recruiting cytosolic proteins to adhesion sites (Wolfenson et al., 2013).

Nascent adhesions can either disassemble or mature to form focal adhesions in a force-dependent process. The transition involves reinforcement with increased mechanical force and the formation of anchored actomyosin-containing stress fibres (Byron et al., 2010). Focal adhesions have a longer lifetime than nascent (~20 minutes compared to ~1 minute), and are key in supporting forward protrusions (Wolfenson et al., 2013). Controlled assembly and disassembly of focal adhesions is required for coordinated cell migration. Focal adhesions are disassembled predominantly at the rear of the migrating cell, primarily by microtubule-mediated destabilisation (Kaverina et al., 1999; Wolfenson et al., 2013).

Focal adhesions can mature into fibrillar adhesions, that are more elongated and located centrally in the cell (Wolanska and Morgan, 2015). Fibrillar adhesions are the main sites of fibronectin deposition and fibrillogenesis (Byron et al., 2010). The formation of fibrillar adhesions is actomyosin force-dependent, however the maintenance of fibrillar adhesions is less sensitive to force than focal adhesions (Wolfenson et al., 2013).

The coordination of adhesion formation and turnover is tightly regulated and intrinsically related to mechanical force. The Rho GTPases are central to the regulation of actin polymerisation and generation of intracellular contractility and force (Byron et al., 2010). Rac1 (Rac family small GTPase 1) and Cdc42 (cell division cycle 42) promote the formation of focal complexes, whereas RhoA is implicated in maturation into focal adhesions. RhoA promotes myosin activity through myosin light chain phosphorylation via Rho-associated Kinase (ROCK) and induces the formation of bundled actin stress fibres (Byron et al., 2010; Wolfenson et al., 2013). RhoA is also involved in generating fibrillar adhesions, by promoting the translocation of ligated α5β1 integrin (Pankov et al., 2000). The regulation of integrin-mediated adhesion formation and maturation is required for the control of adhesion-related functions such as coordinated cell migration and ECM production and remodelling.

1.5.1 The Adhesome

Integrin adhesions recruit large associated cytosolic multiprotein complexes, termed the integrin 'adhesome'. Advances in adhesion isolation techniques and proteomics have enabled the unbiased identification of thousands of associated proteins, compared with previous literature-curated databases estimating over 200 (Winograd-Katz et al., 2014). 3D super-resolution microscopy demonstrates the adhesome is a stratified and highly organised structure (Kanchanawong et al., 2010). The adhesome can be categorised into three functionally distinct layers: a membrane-proximal integrin signalling layer containing integrin cytoplasmic domains, FAK and paxillin; an intermediate force transduction layer of predominantly talin and vinculin; and a distal actin regulatory layer composed of zyxin, VASP (vasodilator-stimulated phosphoprotein) and α-actinin. Talin spans all three layers in a highly polarised orientation, with its head domain bound to integrin cytoplasmic domains, and the tail spanning to actin and overlapping with actin regulatory layer components (Kanchanawong et al., 2010).

The integrated proteomic analysis of seven adhesome proteomic datasets generated a 2,412 protein meta-adhesome (Horton et al., 2015a). The datasets were generated by different laboratories with varying methods and a range of cells, using the ligand fibronectin. A core

'consensus' adhesome of 60 proteins identified in at least five of the datasets was produced, which broadly clustered into four theoretical protein-protein interaction axes comprising α-actinin, zyxin and VASP; talin and vinculin; FAK and paxillin; and integrin-linked kinase (ILK) and kindlin. 29 of the 60 consensus proteins were not present in the literature-curated adhesome, and had varying degrees of known protein interactions with canonical adhesome components (Horton et al., 2015a).

Temporal changes in adhesome composition were examined during adhesion assembly and disassembly, which supported the theory of a hierarchical distribution of components (Horton et al., 2015a). Integrins remained most stable compared to other proteins at the adhesion site throughout disassembly, and integrin-actin links were also disrupted late in the disassembly process. Adaptor proteins were lost earlier and faster in disassembly, indicating they may be primary targets for the initiation of this process. Components displayed different kinetics in adhesion assembly and disassembly, indicating that these processes are differentially regulated and not reciprocal (Horton et al., 2015a). Myosin II dependent adhesomes were highly enriched in LIM (Lin-11, Isl1, and Mec-3) domain containing proteins (Horton et al., 2016a; Horton et al., 2015a), demonstrating their force dependency as LIM domains are biosensors of mechanical tension (Schiller et al., 2011).

Integrin adhesions are highly dynamic and exhibit constant turnover, enabling rapid and sensitive responses to external cues (Wolfenson et al., 2013). In addition to varying adhesion composition, protein interactions can be modulated in response to adhesion turnover. Differing interaction combinations can greatly influence the composition of the adhesome, particularly if centred on a core component. Conformational changes can produce open active or closed inactive protein forms, that if force regulated can have roles in mechanosensation (Zaidel-Bar and Geiger, 2010). Adhesion components can also be highly phosphorylated, which may create docking sites for interacting proteins or illicit a conformational change (Zaidel-Bar and Geiger, 2010). Rho GTPases at adhesions are activated by guanine nucleotide exchange factors (GEFs) and inactivated by GTPase-activating proteins (GAPs), and primarily alter adhesion composition indirectly through actin cytoskeleton regulation (Zaidel-Bar and Geiger, 2010).

Whilst proteomic approaches have greatly advanced the understanding of the complexity of integrin adhesions, many questions remain. The composition of adhesions on different ligands, engaging different integrin heterodimers, and in different cell types remains to be elucidated (Horton et al., 2015a). Analysis of adhesions on cells in more complex

microenvironments such as cell-derived ECM matrices and pliable 3D substrates will also be key to informing knowledge of adhesome components that may be functional *in vivo*.

1.6 Integrins in Cancer

Integrin-mediated regulation of biological processes such as proliferation, gene expression, cell survival and cell motility are exploited by tumour cells to promote cancer progression and invasion (Hamidi et al., 2016). Expression of integrins αVβ3, α5β1, αVβ5, α6β4, αVβ1 and αVβ6 correlate with tumour progression of various types (Desgrosellier and Cheresh, 2010). Integrins αVβ3, α5β1 and αVβ6 are usually expressed at very low or undetectable levels in normal epithelia, but are greatly upregulated in some cancers, and their expression correlates with a poor prognosis (Desgrosellier and Cheresh, 2010). Integrins have therefore been recognised as clinically relevant targets for cancer therapeutics.

Normal non-circulating cells typically exhibit anchorage-dependent survival as a mechanism to prevent inappropriate proliferation. In such instances, loss of cell adhesion triggers anoikis (detachment induced apoptosis). Ligand-engaged integrin-mediated signalling promotes cell survival primarily by promoting the phosphoinositide 3-kinase (PI3K)-Akt pathway activity (Hager et al., 2013). Integrins can also control the expression of key cell cycle proteins, such as cyclin D1 (Fournier et al., 2008). Integrins have been shown to continue signalling within endosomes, conferring a resistance to anoikis (Alanko et al., 2015). Cancer cells typically exhibit anchorage-independent growth, whereby suppression of anoikis enables tumours to survive in circulation and therefore metastasise to distant sites.

The tumour stromal microenvironment is recognised as a key mediator of tumour progression, and can actively promote malignant conversion (Micke and Ostman, 2004). The tumour stroma consists of fibroblasts, inflammatory cells, blood vessels, and ECM (Dvorak, 2015). Increased matrix stiffness within tumours is linked to a more invasive tumour phenotype. Increased ECM rigidity due to collagen cross-linking enhances integrin signalling and induces a more invasive tumour phenotype (Levental et al., 2009). Increased collagen deposition in desmoplasia (the growth of fibrous or connective tissue) is able to promote tumour cell survival and proliferation through integrin signalling (Desgrosellier and Cheresh, 2010). Integrins also have a well-established role in promoting tumour angiogenesis. Integrin αVβ3 and α5β1 expression on endothelial cells promotes tumour vascularisation, by allowing endothelial cells to engage initial matrix proteins such as vitronectin and fibrinogen, that are deposited at tumour sites (Desgrosellier and Cheresh, 2010).

Metastasis is responsible for up to 90% of cancer-related mortality (Chaffer and Weinberg, 2011). For metastasis to occur, tumour cells must be able to invade local tissue, intravasate, survive in the circulation, extravasate, then colonise and proliferate at a metastatic site. Cell motility and protrusions are intrinsically related to invasion as this process is dependent on cell migration. Local invasion can be collective, where cells maintain cell-cell contacts that are cadherin and integrin-mediated (Hager et al., 2013); however single cell detachment is often considered to be required for distant metastases. Epithelial-to-mesenchymal transition (EMT) is key in this process, as it involves the downregulation of cell-cell adhesions and induces scattering. The loss of epithelial morphology results in an invasive phenotype that is more likely to induce metastasis (Hager et al., 2013). Invasion into the microenvironment can require the degradation of the ECM if it is a physical barrier. This process is primarily mediated by MMPs that are secreted or surface bound in the case of membrane-type 1 MMP (MT1-MMP) (Page-McCaw et al., 2007). Integrins can affect the localisation and activity of MMPs, promoting invasion (Gonzalo et al., 2010; Morgan et al., 2004).

Integrins are important for the colonisation of and proliferation in a new metastatic site. The combination of integrins expressed by a tumour cell dictate tumour cell binding abilities, potentially to very different ECM compositions at metastatic sites compared to the primary tumour (Seguin et al., 2015). Integrins may also be involved in priming pre-metastatic niche formation. Exosomes secreted by the primary tumour can be sequestered by cells at metastatic destinations. Distinct integrin expression patterns within exosomes were identified directing metastases for tissue/organ specific colonisation, such as α6β4 and α6β1 directing metastases to the lung, and αVβ5 to the liver (Hoshino et al., 2015).

Integrins therefore have roles in many of the hallmarks of cancer, including adhesion-independent growth, invasion, angiogenesis and metastasis. Integrin-targeted therapeutics could therefore be used to target multiple aspects of cancer biology.

1.6.1 Integrin Targeted Therapies

Integrins have been identified as potential therapeutic targets since the discovery that they may promote pathogenic processes, such as cancer. Integrins are amenable to pharmacological inhibitors, as their binding sites and some regulatory sites are extracellular and therefore accessible. Integrin inhibitory antibodies are mostly either competitive inhibitors obstructing the ligand binding site, or allosteric inhibitors that can, for example, prevent activating conformational changes (Byron et al., 2009).

Nineteen of the 24 integrin heterodimers have been targets for therapeutic drugs, either alone or as multi-chain families (e.g. αVβx), with 480 integrin targeting drugs identified (July 2017 survey cut-off) (Raab-Westphal et al., 2017). Seven drugs targeting integrins have reached clinical market: abciximab (anti-β3), tirofiban (anti-αIIbβ3), eptifibatide (anti-αIIbβ3), natalizumab (anti-α4), vedolizumab (anti-α4β7) and lifitegrast (anti-αLβ2), with efalizumab (anti-αLβ2) having been withdrawn (Millard et al., 2011; Raab-Westphal et al., 2017). Integrins are also in development for use in diagnostic imaging, and as a mechanism for drug delivery (Raab-Westphal et al., 2017).

The four β1 collagen binding integrins have been targeted, with the focus on α1β1 for rheumatoid arthritis (SAN-300 Valent, Quebec, QC, Canada) and α2β1 as an anti-thrombotic and potentially a cancer therapeutic; with phase two clinical trials active for both (Raab-Westphal et al., 2017). Fibronectin binding integrins β1 (α4, α5, α8) and αV (β1, β3 and β6) have been prominent targets for drug design, as they are extensively linked to cancer, fibrosis, inflammation and autoimmune diseases (Raab-Westphal et al., 2017). α4β1 binds VCAM-1 (vascular cell adhesion molecule 1) and is involved in homing activated T-cells to sites of inflammation. The pan-α4 inhibitor natalizumab (Tysabri®) is used clinically for the treatment of multiple sclerosis and Crohn's disease (Raab-Westphal et al., 2017).

αV integrins are interesting as cancer therapeutics, as they are involved in angiogenesis, tumour growth, immunomodulation and metastases. Two pan αV inhibitors abituzumab (Merck KGaA (Darmstadt, Germany) and intetumumab (Centocor (Malvern, PA, USA) have been evaluated in late-stage clinical trials, for colorectal cancer and melanoma respectively (Raab-Westphal et al., 2017). No drugs specifically targeting laminin-binding integrins have reached clinical trials (Raab-Westphal et al., 2017).

Targeting of leukocyte specific integrins that mediate cell-cell adhesion have produced three therapeutics that have made it to market. The β2 inhibitor Lifitegrast (Xiidra®) is a licenced local inflammation suppressant for the treatment of dry-eye disease. The αLβ2 inhibitor efalizumab (Raptiva®) was launched in 2003 for the treatment of psoriasis, but was associated with 3 cases of progressive multifocal leukoencephalopathy (PML), and subsequently withdrawn in 2009 after treatment of 45,000 patients (Raab-Westphal et al., 2017). Vedolizumab (Entyvivo®) was launched in 2014 after clinical trials in Crohn's disease and ulcerative colitis. Vedolizumab inhibits the interaction between α4β7 and Mad-CAM-1 (mucosal vascular addressin cell adhesion molecule 1), blocking homing of activated T-cells to Peyer's patches in the gut (Wagner et al., 1996).

The majority of successful integrin therapeutics are anti-thrombotics, targeting αIIbβ3 expressed on platelets. αIIbβ3 has a low affinity for fibrinogen on resting platelets, but is converted to a high-affinity form upon platelet activation, and induces platelet aggregation during blood clotting (Coller and Shattil, 2008). The pan β3 inhibitor abciximab (Reopro®) was the first integrin inhibitor to reach therapeutic market, in 1995 (Goodman and Picard, 2012). The success of abciximab in clinic prompted the development of tirofiban (Aggrastat®) and eptifibatide (Integrilin®) which were both launched in 1998 for the treatment of acute coronary syndrome (Raab-Westphal et al., 2017).

The development of integrin targeting drugs has not been very successful, with only 7 of the 480 that entered clinical trials reaching market, compared to the 10% average for drugs that have entered phase one clinical trials (Raab-Westphal et al., 2017). Animal models have been particularly misleading for integrins, hindered by inherent difficulties with models such as xenografts that cannot accurately represent the clinical scenario; although these can be improved using patient-derived explant models (Yada et al., 2018).

Success has also been restricted by a lack of knowledge regarding the complexities of integrin biology. This issue is exemplified by the αVβ3- and αVβ5-specific inhibitor Cilengitide (Merck KGaA) which was identified as a promising anti-angiogenic and anti-tumour therapeutic in phase one and two preclinical studies. Cilengitide failed phase three clinical trials for the treatment of glioblastoma, showing no clinical benefit (Stupp et al., 2014). Crosstalk between αVβ3 and vascular endothelial growth factor (VEGF) is a potential contributor to the failure of cilengitide. Mice deficient in αVβ3 have enhanced tumour growth and angiogenesis, likely due to a compensatory upregulation of VEGF receptor, which promotes angiogenesis in response to VEGF (Reynolds et al., 2002). Nanomolar concentrations of cilengitide were shown to promote VEGF receptor-mediated angiogenesis, and increased recycling of αVβ3 and VEGF receptor to the plasma membrane (Reynolds et al., 2009). The failure of cilengitide is a direct example of integrin and GFR mediated crosstalk resulting in an unanticipated biological outcome that resulted in failure of the drug to meet clinical trial outcomes. This highlights the importance of understanding and considering integrin and GFR crosstalk in the development of integrin-targeted therapeutics.

Despite disappointing outcomes in clinical trials, patient stratification can determine clinical contexts where integrin-targeting therapies may yet become effective therapies. Natalizumab was withdrawn a year after launch after three patients developed PML. This was found to be an on-target side-effect due to T-cell immunosuppression leading to the

induction of John Cunningham polyoma virus (JC-virus). Screening patients for JC-virus antibodies allowed the renewed use of natalizumab (Raab-Westphal et al., 2017). The pan-αV inhibitor abituzumab was evaluated compared to standard of care in a phase two clinical trial for metastatic colorectal cancer (Elez et al., 2015). Whilst the progression-free survival endpoint was not met, overall survival was longer in patients with high integrin αVβ6 expression. These patients represent a subgroup for cohort-stratification that abtituzumab could benefit (Elez et al., 2015). Patient-stratification is likely to be important in identifying sub-groups of patients where integrin-targeted therapeutics may be clinically successful. The potential target αVβ6 will be discussed further in section 1.7.5.

1.7 Integrin αVβ6

Integrin αVβ6 was identified in epithelial cells as an RGD-binding integrin (Busk et al., 1992). with an expression pattern exclusive to epithelia (Breuss et al., 1995). The β6 subunit can only associate with αV, whereas αV can additionally associate with β1, β3, β5 and β8 (Figure 1.1) (Hynes, 2002). Under homeostatic conditions αVβ6 is expressed at very low, or undetectable, levels in most tissues, except secretory glands in the endometrium and the luminal surface in colon epithelia (Breuss et al., 1995). αVβ6 is upregulated, however, during epithelial remodelling in circumstances such as embryogenesis, wound healing and tumourigenesis (Breuss et al., 1995; Haapasalmi et al., 1996). αVβ6 is upregulated in a range of cancers including breast, oral squamous, pancreatic, colon, cervical and non-small cell lung carcinomas; and this upregulation is usually associated with poor prognosis and survival (Bates et al., 2005; Elayadi et al., 2007; Hazelbag et al., 2007; Moore et al., 2014; Thomas et al., 2001b).

Little is known about the control of αVβ6 expression levels. High cell density is known to enhance αVβ6 expression levels in colon cancer cells mediated via protein kinase C (PKC) activity (Niu et al., 2001). TGFβ and tumour necrosis factor alpha (TNFα) have both been shown to upregulate αVβ6 expression (Scott et al., 2004; Zambruno et al., 1995), potentially synergistically through upregulating the transcription factor Ets-1 (eukaryotic translation initiation factor) (Bates et al., 2005). These mechanisms may be important in stimulating the upregulation of αVβ6 expression that is observed in cancer.

Trafficking is an important mechanism of regulation of αVβ6 and has been shown to influence αVβ6 biological function. Integrin αVβ6 is internalised via clathrin-dependent endocytosis (Berryman et al., 2005; Ramsay et al., 2007). HS1-associated protein X-1 (HAX-1) was identified in a yeast-two hybrid screen for novel interactors of the β6 cytoplasmic domain

and is required for αVβ6 dependent migration and invasion (Ramsay et al., 2007). HAX-1 and clathrin heavy chain are both required for αVβ6 internalisation, and HAX-1 is hypothesised to regulate clathrin-mediated endocytosis of αVβ6, which is required for coordinated receptor turnover crucial to cellular migration and invasion (Ramsay et al., 2007). Activation of PKC with phorbol 12-myristate 13-acetate (PMA) increases αVβ6 internalisation and recycling rates, which theoretically could also enhance αVβ6 receptor redistribution and promote motility, although this has not been assessed (Wang et al., 2011a).

Knock-out mouse phenotypes provided initial information regarding the physiological functions of αVβ6. The αVβ6-null mouse phenotype has inflammation of the skin and airways (Huang et al., 1996), and is protected from pulmonary fibrosis (Munger et al., 1999). Similarities between the phenotypes of αVβ6- and TGFβ-null mice led to the observation that αVβ6 can function through promoting TGFβ activity (Munger et al., 1999). Constitutive over-expression of αVβ6 in epithelium also resulted in a mouse phenotype with increased TGFβ activity and spontaneous chronic fibrotic lesions, supporting these conclusions (Hakkinen et al., 2004). Regulation of TGFβ activity is therefore considered to be the primary physiological function of αVβ6.

1.7.1 TGFβ Signalling

TGFβ is a pleotropic cytokine that exists in three isoforms, TGFβ1, TGFβ2 and TGFβ3, which are widely expressed and conserved, with different functions demonstrated by unique knock-out mouse phenotypes (Khan and Marshall, 2016). TGFβ is important during development for body patterning, ECM production, cell proliferation, differentiation and apoptosis. In the adult, TGFβ primarily functions during tissue repair and is involved in immune regulation (Massague, 2008). TGFβ binding to its receptor stimulates serine/threonine kinase domain activity of the receptor, which then phosphorylates Smad2/Smad3. Phosphorylated Smad2/3 dissociates from the receptor, and associates with the co-smad Smad4, to form a complex that translocates to the nucleus to associate with other transcriptional regulators, and control the transcription of target genes (Alberts et al., 2015). TGFβ signalling is dynamically regulated at multiple levels. Partner proteins in the nucleus which vary depending on cell type and state, can affect which genes are influenced by TGFβ (Alberts et al., 2015).

Different routes of TGFβ receptor trafficking can either further activate or inactivate the signalling pathway. Smad shuttling in and out of the nucleus also allows for differential responses depending on TGFβ concentration and signal duration. Inhibitory Smads -6 and -7 can inhibit signalling through competitive binding. TGFβ signalling can also stimulate

mitogen-activated protein kinase (MAPK) and PI3K signalling pathways in addition to its canonical Smad cascade (Alberts et al., 2015). Dysregulated TGFβ signalling can lead to chronic fibrosis, which is an inappropriate response to organ injury resulting in excessive ECM deposition, ultimately leading to organ failure (Margadant and Sonnenberg, 2010).

1.7.2 TGFβ Activation

Control of TGFβ activity is a key regulatory mechanism, as TGFβ is always produced in an inactive form. TGFβ genes encode a 25 kDa latency associated peptide (LAP) and a 12.5 kDa TGFβ moiety, forming a propeptide complex. LAP and TGFβ are cleaved in the Golgi, but remain non-covalently associated upon secretion in a conformation that renders TGFβ inactive (Worthington et al., 2011). The LAP- TGFβ small latent complex (SLC) can associate with the latent TGFβ binding protein (LTBP) to form the large latent complex (LLC), which can be anchored to the ECM through LTBP binding fibronectin (Worthington et al., 2011). TGFβ can be activated by pH, reactive oxygen species, proteases and the glycoprotein thrombospondin-1 (Annes et al., 2003). More recently however, integrins have been identified as key activators of TGFβ.

LAP associated with TGFβ contains an RGD motif theoretically bound by all RGD-binding integrins, and demonstrably can be bound by αVβ3, αVβ5, αVβ6 and αVβ8 (Humphries et al., 2006; Worthington et al., 2011). A point mutation in the TGFβ1 LAP RGD motif to RGE produces a mouse phenotype seemingly identical to TGFβ1 knockout, strongly suggesting integrin-mediated activation of TGFβ1 is key for its function, as defects occur despite the availability of non-integrin-mediated activation mechanisms (Yang et al., 2007). The integrin αV knockout mouse develops abnormalities in vasculogenesis and cleft palate, in common with TGFβ1 and -3 knockout mice (Bader et al., 1998; Dickson et al., 1995; Kaartinen et al., 1995). The presence of the RGD motif within LAP and the overlap between TGFβ-null and integrin-null mouse phenotypes provided initial evidence of a link between integrins and the regulation of TGFβ activity.

Integrins αVβ3 and αVβ5 are unlikely to have crucial roles in TGFβ activation, as neither of their knockout mouse phenotypes exhibit pathology associated with TGFβ deficiency (Worthington et al., 2011). αVβ8 and αVβ6 are considered the most important integrins for mediating TGFβ activation (Aluwihare et al., 2009). αVβ8 is required for TGFβ activation controlling neurovascular development and stability (Mu et al., 2008). αVβ6 is important for the localised activation of TGFβ in epithelium, and has a role in immune cell control at

epithelial barriers. (Worthington et al., 2011). This indicates integrin heterodimer specificity in controlling different functions related to TGFβ activity.

Integrin αVβ6 activates TGFβ by binding LAP and applying tension-mediated force to produce a conformational change, releasing TGFβ from its inactive complex (Worthington et al., 2011). Protease inhibitors do not prevent αVβ6-mediated activation of TGFβ, indicating the process is not cleavage mediated (Munger et al., 1999). Traction force microscopy of pancreatic cancer cell lines on LAP-coated substrates demonstrated increased Rho activity promoted force application on LAP, which correlated with TGFβ activity levels (Tod et al., 2017). Integrin αVβ8 activation of TGFβ is mediated by proteolytic cleavage of LAP by MT1-MMP (Mu et al., 2002). This indicates αVβ6 has specialised mechanism for the activation of TGFβ, that is not common to αVβ8.

TGFβ has differential effects in cancer and can function as a tumour suppressor or promoter. TGFβ inhibits cell proliferation mainly by blocking cell cycle progression in the G1 growth phase, therefore suppressing tumour growth (Massague, 2008). TGFβ promotes EMT in part by activating the transcription of Snail and Slug, which are key mediators of the EMT process (Naber et al., 2013). TGFβ-mediated EMT has been linked to increased tumour cell invasion and metastases, and modulation of the tumour stroma promoting a myofibroblast rich environment involved in promoting an invasive and fibrotic tumour phenotype (Khan and Marshall, 2016; Naber et al., 2013). TGFβ tumour suppressor functions are thought to predominate in the early stages of tumour progression, and then become pro-oncogenic in later stages, as the cancer becomes less responsive to external control over its proliferation (Thomas et al., 2006).

1.7.3 αVβ6 in cancer

Wound healing and carcinogenesis have many biological processes in common, to the extent that tumours have been described as wounds that cannot heal (Dvorak, 2015). Commonality exists between the advancing edge of a wound, and the invasive edge of a carcinoma, both requiring tissue remodelling. Tumours are thought to hijack these physiological mechanisms to aid their progression. An important differential between the two processes for αVβ6 is a permanent ‘on’ state in tumours, rather than the temporal regulation observed in wound healing (Thomas et al., 2006). αVβ6 is elevated in one third of carcinomas and correlates with poor survival (Raab-Westphal et al., 2017). Higher levels of αVβ6 are commonly observed at the invasive edge of the tumour, indicating a relationship with tumour invasiveness (Niu and Li, 2017).

Integrin αVβ6 has been extensively studied in colon cancer, with early observations showing αVβ6 enhances cell proliferation (Agrez et al., 1994). αVβ6 is upregulated in 34 – 37% of colon cancer patient samples, and in 70% of patients with liver metastases (Yang et al., 2008). Colorectal cancer patients with high αVβ6 levels have statistically significantly reduced median survival times (Bates et al., 2005). αVβ6 expression is increased during adenoma-to-carcinoma progression, indicating a role in this process and implying potential for αVβ6-targeted therapeutics in inhibiting this process (Brunton et al., 2001).

High levels of αVβ6 have been observed in 15 – 16% of invasive ductal breast carcinomas and is associated with a poor prognosis (Moore et al., 2014). αVβ6 has been identified as a marker of ductal carcinoma in situ (DCIS) progression, as it is associated with progression to invasive cancer (Allen et al., 2014a). αVβ6 promotes tumour cell invasion *in vitro* and growth *in vivo*, through modulation of the microenvironment (Allen et al., 2014b). αVβ6 is statistically significantly associated with the incidence of distant metastases (Moore et al., 2014) and lymph node positive tumours (Desai et al., 2016).

Integrin αVβ6 is expressed in the majority of oral squamous cell carcinomas (OSCC) (Jones et al., 1997a), and is associated with malignant transformation (Thomas et al., 2006). αVβ6 promotes migration and invasion of squamous carcinoma cells *in vitro* (Thomas et al., 2001b) and tumour growth *in vivo* (Ramos et al., 2002). αVβ6 is expressed at moderate to high levels in 45% of pancreatic ductal carcinomas (PDAC) and correlates with a more advanced state and lymph node metastases (Li et al., 2016). αVβ6 promotes PDAC cell proliferation and invasion, and tumour growth *in vivo* (Li et al., 2016). The role of αVβ6 in pancreatic cancer is complicated however by the TGFβ paradox, as TGFβ activation can also suppress tumour progression if TGFβ is functioning as a tumour suppressor (Hezel et al., 2012). Integrin αVβ6 expression is therefore associated with a poor prognosis in a range of cancers, where it has been shown to mediate cancer-related processes such as cellular invasion, malignant transformation and metastases.

1.7.4 αVβ6 is a Pro-Invasive Integrin

Integrin αVβ6 enhances cell invasion in a range of models, and therefore is widely considered to be a pro-invasive integrin. αVβ6 upregulates the expression of proteinases such as MMPs and urokinase plasminogen activator (uPa), which mediate degradation of the ECM that can be a physical barrier to cell invasion. αVβ6 positive ovarian cancer cells express elevated levels of pro-MMP-9 and uPa, which results in increased plasminogen-dependent ECM degradation (Ahmed et al., 2002b). αVβ6 expression in oral keratinocytes increases MMP-2

and MMP-9 expression and enhances cellular migration and invasion in an MMP-9 dependent manner (Thomas et al., 2001a; Thomas et al., 2001c). αVβ6 is also implicated in the regulation of MMP-3, which is associated with increased invasion (Ramos et al., 2002). A region of the β6 cytoplasmic domain was demonstrated to mediate the pro-invasive effects mediated by MMP-2 and MMP-9 (Morgan et al., 2004).

Local activation of TGFβ by αVβ6 can also increase cell invasion, due to TGFβ-mediated EMT which promotes single cell motility and invasion (Li et al., 2014). Interestingly, predominantly local and reversible rather than constitutive activation of TGFβ appears to mediate the switch from collective to single cell motility in breast cancer (Giampieri et al., 2009). αVβ6 activation of TGFβ also has a role in regulating the tumour microenvironment, modulating the stroma to enhance tumour invasive capacity (Khan and Marshall, 2016). Key known mechanisms by which αVβ6 facilitates cellular invasion are therefore regulating the expression and activity levels of proteases and TGFβ.

Rac1 activity is associated with increased invasion of αVβ6 positive oral squamous and pancreatic cancer cells (Nystrom et al., 2006; Tod et al., 2017). A switch between Rac1 activity and RhoA activity regulated by Eps8 (epidermal growth factor receptor kinase substrate 8) differentially regulates the pro-migratory and TGFβ-activating functions of αVβ6 in PDAC cell lines (Tod et al., 2017). Eps8 activates Rac1 when in complex with Abi1 and the Rac1 GEF Sos1 (Di Fiore and Scita, 2002). Down-regulation of Eps8, Sos1 or Rac1 inhibited αVβ6-mediated cell motility, and promoted αVβ6-mediated TGFβ activation which corresponded with increased RhoA activity (Tod et al., 2017). Rac1 is reported to antagonise RhoA activity directly (Sander et al., 1999), and mathematical modelling has predicted inhibition of Eps8-mediated Rac1 activation promotes RhoA activation (Hetmanski et al., 2016). This demonstrates the pro-migratory and TGFβ-activating functions of αVβ6 are distinct, and are regulated by Eps8.

1.7.5 αVβ6 Targeting for Imaging and Therapy

αVβ6 meets requirements for an imaging and therapeutic target, as it is expressed on the cell surface, at low levels normally, but at higher levels in tumours compared to the surrounding areas (Thomas et al., 2006). αVβ6 has been targeted in two clinical trials for the treatment of idiopathic pulmonary fibrosis. The antibody BG00011 (STX-100) from Biogen-Idec completed phase 2 trials in March 2017 (NCT01371305) for idiopathic pulmonary fibrosis and nephropathy, however no results have been released to date (Raab-Westphal et al., 2017). The αVβ6 positron emission tomography (PET) imaging agent GSK3008348 (GSK (Brentford,

UK)) is in phase 1 clinical trials (NCT03069989) for the therapy of idiopathic pulmonary fibrosis (Raab-Westphal et al., 2017).

Additional inhibitors of αVβ6 are also in development. The selective αVβ6 inhibitor 6.3G9 inhibited tumour growth and TGFβ activation in Detroit 562 pharyngeal carcinoma cell xenografts *in vivo* (Van Aarsen et al., 2008; Weinreb et al., 2004). The humanised monoclonal antibody 264RAD, developed by Astra Zeneca, has also produced promising results in *in vivo* xenograft models. 264RAD is a potent inhibitor of αVβ6 with some additional inhibitory activity against αVβ8 (Eberlein et al., 2013). 264RAD treatment reduced the rate of tumour growth in a dose-dependent manner in Detroit 562 xenografts, and caused a regression of tumour size at the highest dose of 20 mg/kg (Eberlein et al., 2013). 264RAD treatment slowed tumour growth and statistically significantly reduced the number of lung metastases of 4T1 breast tumour xenografts, which metastasise to the lung (Eberlein et al., 2013). 264RAD also successfully inhibited tumour growth in HER2 positive breast cancer xenografts as a monotherapy, and effectively prevented tumour growth when in combination with the HER2 inhibitor trastuzumab even in trastuzumab resistant MCF-7/HER2-18 xenografts (Moore et al., 2014). 264RAD continued to be effective in a long term (six week) treatment (Moore et al., 2014).

A20FMDV2 peptide derived from foot and mouth virus is in development for PET imaging of αVβ6 positive tumours using a radiolabelled form (Slack et al., 2016). Specific binding to αVβ6 can also be utilised for drug delivery if the peptide or antibody is internalised (Man et al., 2018). An antibody-drug conjugate (15H3, Seattle Genetics (Bothell, USA)) is in early development for this purpose (Raab-Westphal et al., 2017).

Targeting αVβ6 as a therapeutic is complicated by its role in TGFβ activation (Hezel et al., 2012). The αVβ6 inhibitor 3G9 was assessed in KRas driven pancreatic ductal adenocarcinoma (PDAC) mouse model. αVβ6 and TGFβ inhibition promoted the progression of premalignant pancreatic intraepithelial neoplasia (PanIN) lesions into PDAC and a decrease in 'survival', defined as the point at which signs of illness facilitated euthanasia (Hezel et al., 2012). αVβ6 inhibition was repeated in a Smad4-null version of the mouse model, and had no effect on 'survival', suggesting the tumour promoting effects of αVβ6 were due to its activation of TGFβ (Hezel et al., 2012). This highlights the importance of TGFβ tumour sensitivity in the response to αVβ6 therapeutics and suggests Smad4 status could be important patient stratification criteria for future clinical trials.

The targeting of αVβ6 represents an exciting clinical therapeutic for the treatment of a range of different cancers, however the development of αVβ6 therapeutics is likely to require careful consideration of patient stratification criteria to identify sub-sets of patients where the therapy is most likely to be clinically effective or could be contraindicated. Utilisation of αVβ6 as a clinical imaging target also represents an interesting avenue for αVβ6 in cancer treatment.

1.8 The ErbB Growth Factor Receptor Family

The ErbB growth factor receptor family (originally named for homology to the erythroblastoma viral gene product, v-erbB), are RTKs that are activated upon ligand binding, and stimulate intracellular signalling pathways to promote cell growth, survival, proliferation and differentiation into different cell subtypes (Alberts et al., 2015). There are four members of family; EGFR (ErbB1; HER1, human EGFR 1), ErbB2 (HER2; Neu), ErbB3 (HER3) and ErbB4 (HER4). The ligands for the ErbB receptors are the 11 ligands of the EGF-family, which can be grouped into three according to receptor affinity. Specific EGFR binding ligands are EGF, tumour transforming growth factor α (TGFα), amphiregulin and epigen; ligands with dual specificity for EGFR and ErbB4 are betacellulin, heparin-binding EGF and epiregulin, and the final group neuregulins (NRGs) (also termed heregulins) bind both ErbB3 and ErbB4 (NRG-1 and NRG-2) or ErbB4 only (NRG-3 and NRG-4) (Hynes and MacDonald, 2009).

The ErbB family receptors have an extracellular domain with a ligand-binding cleft and dimerisation loop, a helical transmembrane domain, and a cytoplasmic region with a tyrosine kinase domain and ATP (adenosine triphosphate) binding site, and a c-terminal tail with phosphorylatable tyrosines (Yarden and Pines, 2012). ErbB receptors exist in either a unliganded autoinhibited 'closed' formation, where the loop that mediates receptor dimerisation is occluded, or an 'open' form that results from the structural rearrangement of the extracellular domains upon ligand binding (Cho et al., 2003). ErbB receptors function as homodimers or heterodimers, for which ErbB2 is a preferential binding partner (Hynes and MacDonald, 2009). Each dimer exhibits distinct functional properties such as ligand binding affinities, receptor trafficking routes, and effector activation (Citri and Yarden, 2006).

ErbB2 is a notable exception to the ErbB family, as it has no identified high affinity ligands, and exists in a fixed conformation resembling a ligand-activated state, and consequently ErbB2 is readily able to function as a co-receptor for ErbB binding partners that may become available (Cho et al., 2003). ErbB3 is also atypical as it has low kinase activity (~1,000 fold less than EGFR) (Shi et al., 2010). Despite their respective lack of ligands and kinase activity, the

ErbB2 ErbB3 heterodimer is one of the most potent for promoting cell growth and differentiation (Citri et al., 2003).

1.8.1 EGFR Activation

EGFR can function as a homodimer, or as a heterodimer with ErbB2, ErbB3 or ErbB4 (Citri and Yarden, 2006). EGFR homodimers and heterodimers with ErbB2 form with similar affinities, however heterodimers formed with ErbB3 or ErbB4 are much weaker (Graus-Porta et al., 1997; Hendriks et al., 2003). The *ErbB1* knockout mouse is lethal mid-gestation or at postnatal day 20, dependent on genetic background (Miettinen et al., 1995; Sibilia and Wagner, 1995; Threadgill et al., 1995). The phenotypes of multi-organ failure revealed the importance of EGFR in epithelial cell proliferation, migration and differentiation (Citri and Yarden, 2006). EGFR ligand knockout mouse phenotypes were milder and did not phenocopy *ErbB1* knockout, indicating redundancy between ligands despite distinct functions (Luetteke et al., 1999; Mann et al., 1993; Sweeney et al., 2001).

EGFR is activated upon ligand binding, resulting in activation of its kinase domain and consequent autophosphorylation. Ligand binding does not act as a physical bridge between the two monomers, as the ligand binding clefts are distal to the dimerisation loop, resulting in a 'back-to-back' conformation (Figure 1.4) (Garrett et al., 2002; Ogiso et al., 2002). In the classical model of EGFR activation, ligand binding to EGFR monomers at the plasma membrane results in a conformational change in the extracellular domain, releasing the dimerisation loop motif from an inactive tethered state (Alberts et al., 2015; Ferguson et al., 2003). EGFR then forms a dimer with another ligand bound monomer, where the interaction is primarily mediated by the dimerisation loop with stabilisation facilitated by other regions such as the transmembrane domain (Mendrola et al., 2002).

Receptor dimerisation orients the intracellular domains, forming an asymmetric structure where one kinase domain is termed the 'activator', and the other the 'receiver' (Figure 1.4). Activation of the kinase domains depends on an intermolecular interaction, as opposed to trans-autophosphorylation exhibited by other RTKs (Alberts et al., 2015). The C-lobe of the 'activator' kinases interfaces with the N-lobe of the 'receiver' kinase and stabilises it in an active conformation (Zhang et al., 2006). The active 'receiver' then phosphorylates multiple tyrosine residues on the C-terminal tails of both receptors (Alberts et al., 2015).

More recent evidence has suggested EGFR dimers can be present in a preformed state, prior to ligand-engagement (Tao and Maruyama, 2008). Ligand-induced activation is still required for receptor activation however and can additionally result in further aggregation of dimers

into oligomers forming competent signalling platforms (Bessman et al., 2014; Needham et al., 2016). Discrepancies in the literature are likely the result of a wide range of experimental techniques with varying cellular contexts, confounded by a potential context dependent equilibrium. The essential role of EGFR is reflected in the multi-modal regulation of its activity, indicating the importance of fine control over its function.

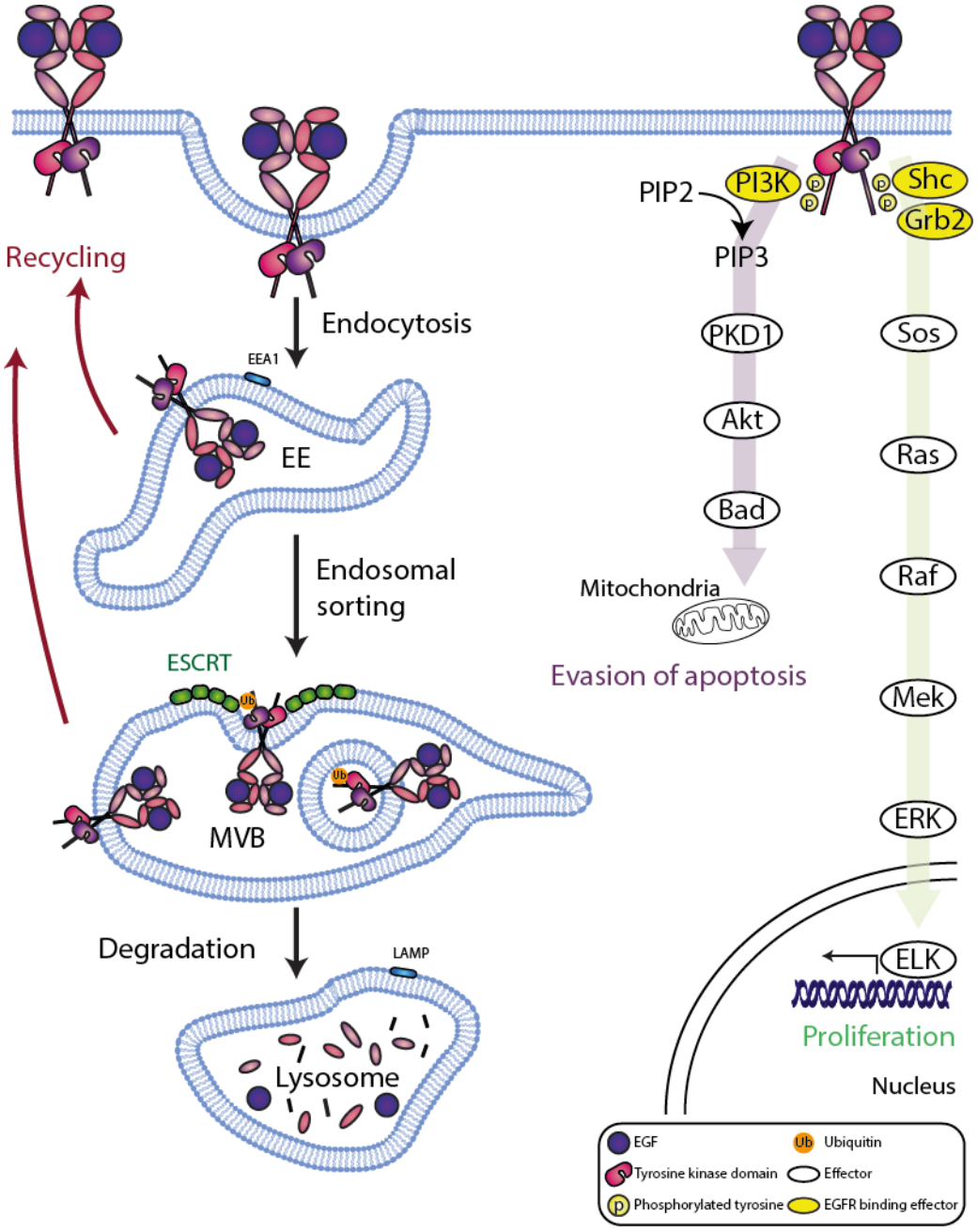

Figure 1.4 EGFR signalling and trafficking. Active ligand bound EGFR is a back-to-back homodimer, interacting primarily through the trans- and juxta-membrane domains. EGFR activation induces an asymmetrical orientation of the tyrosine kinase domains (visualisation aided by monomers as different colours), which triggers autophosphorylation (Lemmon, 2009). Signalling effectors are recruited to phosphorylated tyrosines, and mediate downstream signalling (PI3K-Akt and MAPK pathways shown in purple and green, respectively) (Yarden and Shilo, 2007). EGFR activation stimulates receptor internalisation via clathrin-dependent and independent routes (Sorkin and Goh, 2009). Ubiquitin moieties on EGFR are detected by the ESCRT complex which sorts EGFR for lysosomal degradation (Raiborg and Stenmark, 2009).

1.8.2 EGFR Signalling

Phosphorylated tyrosine residues primarily on the C-terminal tail of EGFR are docking sites for proteins that contain Src homology 2 (SH2) or PTB domains, that recognise peptide motifs containing phosphorylated tyrosines (Guo et al., 2003). Proteins can either be recruited directly to phosphorylated tyrosines on EGFR, or indirectly via phosphorylated docked proteins or adaptors. Many of the proteins recruited are signalling effectors, that become activated by docking either through phosphorylation or an induced conformational change (Alberts et al., 2015).

EGFR activates the Ras-MAPK signalling pathway which stimulates cell proliferation (Figure 1.4). The adaptor protein Grb2 (growth factor receptor-bound protein 2) binds EGFR directly at Y1068 (Rojas et al., 1996), or via the adaptor Shc which docks to EGFR at Y1148 and Y1173 (Zwick et al., 1999). Grb2 recruits the Ras-GEF Sos (son-of-sevenless), which activates Ras. Active Ras results in the sequential recruitment and phosphorylation of the kinases Raf (MAPKKK), Mek (MAPKK), and finally Erk (MAPK). Erk then translocates to the nucleus and phosphorylates transcription regulators that promote proliferation and cell cycle progression (Yarden and Shilo, 2007). The Ras-MAPK pathway is tightly regulated, and usually only transiently activated. Tyrosine specific phosphatases reverse phosphorylation at multiple levels in the cascade. Ras activation is terminated by Ras-GAPs that inactivate Ras. MAPK activates a negative feedback loop by increasing transcription and inhibiting degradation of MAPK phosphatases, that inactivate MAPKs (Alberts et al., 2015; Caunt and Keyse, 2013). There are multiple parallel MAPK pathways with different MAPKs involved, that can be differentially regulated and constrained by scaffold proteins that spatially restrict their signalling (Alberts et al., 2015).

The PI3K-Akt pathway is also stimulated by EGFR and promotes cell survival by inhibiting apoptosis (Figure 1.4). The membrane bound enzyme PI3K is activated by EGFR, and phosphorylates PIP2 (phosphatidylinositol (4,5)-bisphosphate), producing PIP3 (phosphatidylinositol (3,4,5)-trisphosphate) (Alberts et al., 2015). PIP3 recruits PDK1 (phosphoinositide-dependent protein kinase 1), which phosphorylates Akt. Akt phosphorylates multiple proteins, including pro-apoptotic Bcl-2-associated death promoter (Bad). Phosphorylation of Bad creates a binding site for 14-3-3, which then sequesters Bad preventing its action thereby evading apoptosis (Avraham and Yarden, 2011). The PI3K-Akt pathway is also able to promote cell growth, through the indirect activation of mTOR (mammalian target of rapamycin). The phosphoinositide phosphatase PTEN (phosphatase

and tensin homolog) inhibits the conversion of PIP2 to PIP3 and therefore all Akt downstream signalling.

Phospholipase C γ (PLCγ) becomes activated after docking to EGFR. PLCγ converts PIP2 into inositol 1,4,5-triphosphate (IP3) and diacylglycerol (DAG) (Alberts et al., 2015). IP3 raises intracellular calcium levels, and DAG activates PKC (Oda et al., 2005). Both of these signalling pathways have downstream effects on cell motility (Yarden and Shilo, 2007). EGFR signalling can therefore function to promote cellular proliferation, survival and motility.

1.8.3 EGFR Trafficking

Un-ligated EGFR is constitutively endocytosed slowly, and rapidly recycled to maintain predominant membrane localisation (Sorkin and Goh, 2008). The rate of EGFR endocytosis is increased following ligand stimulation, and EGFR is efficiently targeted for lysosomal degradation (Figure 1.4) (Sorkin and Goh, 2008; Wiley et al., 1991). This ligand-mediated downregulation of EGFR levels is an important negative feedback mechanism for attenuating signalling. The majority of EGFR signalling occurs at the plasma membrane (Brankatschk et al., 2012; Sousa et al., 2012), however it can continue from endosomal vesicles and is required for some specific signalling pathways and optimal activation of subsets of transducers at intracellular sites (Vieira et al., 1996). EGFR internalisation can therefore have both negative and positive effects on signalling.

EGFR is internalised predominantly via clathrin-mediated endocytosis, however when this pathway is saturated due to high ligand or receptor concentrations, slower clathrin-independent routes are additionally employed (Sigismund et al., 2005). Grb2 binding to pY1068 and pY1086 on EGFR promotes its internalisation and is involved in its recruitment to clathrin-coated pits (Fortian and Sorkin, 2014; Jiang et al., 2003). The E3 ubiquitin ligase Cbl (Casitas B-lineage lymphoma proto-oncogene) recruited to EGFR via pY1045 or indirectly through GRB2 is also involved in EGFR internalisation (Waterman et al., 2002) is, however this is independent of EGFR ubiquitination (Huang et al., 2007; Huang et al., 2006).

After internalisation EGFR containing clathrin coated vesicles fuse with early endosomes. EGFR is then either rapidly recycled to the plasma membrane, or remains in the endosomes as they fuse with each other and mature into multivesicular bodies (MVBs) and late endosomes (Sorkin and von Zastrow, 2009). EGFR can be recycled through tubular extensions of the MVB, or via a Rab11 pathway from late endosomes (Tomas et al., 2014). Ligands dissociate from EGFR with different pH sensitivities, for example TGFα dissociates at endosomal pH, whereas EGF remains bound until lysosomal acidification (French et al.,

1995). Ligand release leads to receptor dephosphorylation and deubiquitination, and consequent receptor recycling influencing EGFR trafficking fates. Ligand release is not a pre-requisite for recycling however, demonstrated by the recycling of EGF bound EGFR (Sorkin et al., 1991).

Ubiquitinated EGFR interacts with ubiquitin binding domains of ESCRT-0 (Endosomal Sorting Complex Required for Transport) (primarily comprised of HRS (hepatocyte growth factor-regulated tyrosine kinase substrate) and STAM (signal-transducing adaptor molecule)), which triggers its incorporation into internal vesicles within the MVB (Eden et al., 2012). The MVB then fuses with lysosomes, resulting in the degradation of EGF and EGFR. c-Cbl is recruited to active EGFR promoting its ubiquitination and subsequent degradation (Waterman et al., 2002); therefore linking ubiquitination to EGFR activation status and mediating termination of active signalling (Lemmon and Schlessinger, 2010).

EGFR degradation is also influenced by deubiquitinating enzymes (DUBs) that remove ubiquitin from proteins (Clague et al., 2012). An example of this is the DUB AMSH (associated molecule with the SH3 domain of STAM) that deubiquitinates EGFR, opposing its ubiquitin-dependent sorting for lysosomal degradation (McCullough et al., 2004). Proteasomal degradation is also implicated for EGFR (Longva et al., 2002), however this is potentially an indirect mechanism influencing protein levels of the ESCRT complex (Sorkin and von Zastrow, 2009). Trafficking of EGFR is therefore an important mechanism for regulating its surface bioavailability and total protein levels, which has direct consequences for its function.

1.8.4 EGFR in Cancer

EGFR signalling can be dysregulated in cancer, contributing to uncontrolled cell growth and evasion of apoptosis. Overexpression of EGFR due to gene amplification is reported in a wide range of cancers including lung and breast, where it can correlate as an indicator of recurrence or shorter survival (Yarden and Pines, 2012). EGFR can also be mutated primarily in the extracellular and kinase domains, resulting in enhanced signalling. Signalling effectors and mediators are also frequently mutated in cancer, for example pro-oncogenic active Ras mutations, and PTEN deficiencies (Alberts et al., 2015).

The most common EGFR mutant is the truncated EGFR vIII (deletion of residues 6-273) that lacks a proportion of the extracellular ligand binding domain (Pedersen et al., 2001). This mutant is constitutively phosphorylated independent of ligands, and is pro-tumourigenic (Pedersen et al., 2001). EGFR vIII hypophosphorylation at the c-Cbl docking site Y1048 reduces receptor ubiquitination, allowing degradation evasion (Grandal et al., 2007; Han et

al., 2006). The most frequent mutation in the kinase domain is an L858R point mutation (Sigismund et al., 2017). L858R EGFR has impaired c-Cbl-mediated ubiquitination, slower internalisation rates and enhanced heterodimerisation with ErbB2 (Shtiegman et al., 2007).

EGFR targeted therapies are in clinical use for a range of cancers, primarily non-small-cell lung carcinoma (NSCLC), head and neck squamous cell carcinoma and colorectal cancer (Yarden and Pines, 2012). EGFR therapeutics can be divided into antibodies and small molecule kinase inhibitors. Cetuximab (Erbitux®, Bristol-Myers Squibb) and panitumumab (Vectibix®, Genentech) are the most commonly used antibodies (Sigismund et al., 2017). Cetuximab was licensed in 2004 for the treatment of wild type KRAS colorectal cancer and head and neck cancer (Roskoski, 2014). Panitumumab was licensed in 2006 as a second line treatment for metastatic colorectal cancer (Roskoski, 2014).

First generation small molecule tyrosine kinase inhibitors gefitinib (Iressa®, AstraZeneca) and erlotinib (Tarceva®, OSI/Genentech) were approved in 2003 and 2004, respectively (Cohen et al., 2005; Cohen et al., 2003). Gefitinib is a second line treatment for NSCLC, and erlotinib is licensed for NSCLC and as a combination therapy for pancreatic cancer (Roskoski, 2014). EGFR therapies are often hindered by the development of resistance. The most common mechanism of EGFR kinase inhibitors is a T790M point mutation in the EGFR kinase domain (Mazza and Cappuzzo, 2017). The third generation EGFR kinase inhibitor Osimertinib (Tagrisso®, Astra Zeneca) was licensed in 2017 for the treatment of metastatic NSCLC with the T790M mutation (AURA3 clinical trial NCT012151981) (Mazza and Cappuzzo, 2017). Resistance-causing mutations are also implicated in downstream effectors of EGFR in KRAS, BRAF, PI3K and PTEN (Yarden and Pines, 2012). Combination therapies with non-overlapping targets are a potential means of more effectively targeting EGFR and delaying resistance (Sigismund et al., 2017).

In conclusion, EGFR is frequently mutated or overexpressed in cancer, which results in a poor prognosis due to the dysregulation of EGFR functions such as mitogenic signalling, protection from apoptosis and promotion of cell motility. EGFR has been successfully targeted by antibodies and small molecule inhibitors in a range of cancers and has been particularly successful in NSCLC, head and neck squamous cell carcinoma and colorectal cancer. EGFR therefore represents a clinical relevant and therapeutically amenable target that is relevant to a wide range of cancers.

1.9 Integrin and Growth Factor Receptor Crosstalk

Crosstalk between cell-ECM adhesions and GFRs has long been evident in the phenomenon of cell survival anchorage dependence. Detachment from solid substrates initiates anoikis (detachment-induced apoptosis) in adherent cell types, due to impaired growth factor and cytokine signalling (Alberts et al., 2015). Attachment-independent survival is a hallmark of metastatic cancer, and is required for distant spread via circulation (Liotta and Kohn, 2004). GFRs signal inefficiently without integrin-mediated adhesions, and signalling is cell-type and matrix specific (Ivaska and Heino, 2011). Crosstalk between integrins and GFRs affects the activity, expression level, signalling and trafficking of both.

1.9.1 Regulation of Receptor Activity

Integrins and GFRs often co-localise at the cell surface, however few examples of direct binding exist (Ivaska and Heino, 2011). Aggregation of integrins causes GFR co-clustering, creating a permissive environment by bringing GFR monomers into proximity with each other and common downstream signalling effectors (Figure 1.5) (Yamada and Even-Ram, 2002). GFRs may also influence integrin clustering, for example knockdown of EGFR results in increased membrane diffusion and decreased clustering of *Drosophila* orthologs of integrin β1 (Arora et al., 2012). Lipid raft plasma membrane microdomains have been implicated as specialised regions that gather integrins and GFRs into signalling platforms (Decker et al., 2004). Other transmembrane receptors such as tetraspanins and syndecans may act as physical bridges between integrins and GFRs (Charrin et al., 2014; Morgan et al., 2007; Streuli and Akhtar, 2009). Some ECM components can be engaged both by integrins and by GFRs, for example tenascin-C can be bound by both EGFR and αVβ3, and therefore function as linkers (Jones et al., 1997b; Swindle et al., 2001). Integrins can also regulate the activity of GFRs by mechanisms that are more direct that creating a permissive environment.

Integrins are reported to activate GFRs in a ligand-independent manner. Cell adhesion to FN or collagen, has been shown to stimulate EGFR phosphorylation under serum free conditions (Moro et al., 1998). This effect was recapitulated by binding antibodies against integrin αV and β1 indicating an integrin-dependent mechanism. Activation of the adaptor p130cas and kinase Src was also required, indicating the mechanism may not be solely receptor mediated (Moro et al., 2002). Interestingly ligand-independent activation of EGFR produces a different pattern of receptor tyrosine phosphorylation, omitting Y1148 which is phosphorylated with EGF (Moro et al., 2002). Phosphorylated Y1148 is a docking site for Shc which is important for Ras-MAPK signalling (Zwick et al., 1999). Integrin-mediated activation may therefore have

unique signalling consequences compared to canonical ligand stimulation. Integrin-mediated ligand-independent activation of GFRs has been demonstrated for multiple other integrin subtypes and GFRs including hepatocyte growth factor receptor (Met) and platelet-derived growth factor receptor (PDGFR) (Ivaska and Heino, 2011; Veevers-Lowe et al., 2011). Adhesion stimulated activation of GFRs does not appear to be a universal phenomenon and may be ligand and cell type specific. Adherence to laminin-332 is demonstrated to have no effect on EGFR phosphorylation status, however it enhances EGFR phosphorylation following EGF stimulation, compared to cells in suspension or adhered to poly-L-lysine (Alexi et al., 2011). The amount of receptor at the cell surface also appears to be an important determinant (Moro et al., 2002).

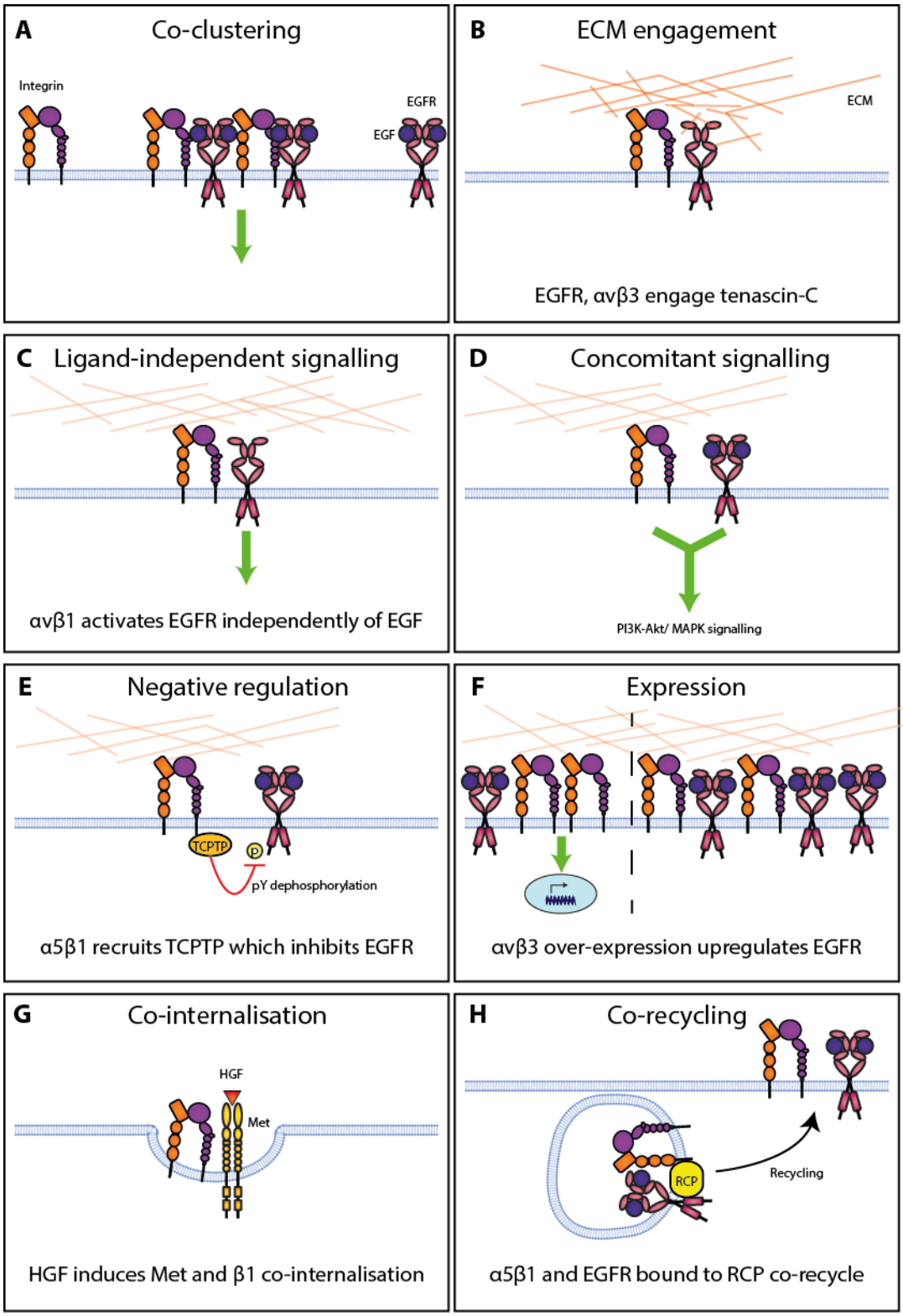

Figure 1.5 Integrin and growth factor receptor crosstalk. Examples of mechanisms of crosstalk, with published examples where appropriate that have are detailed in the text of section 1.9 (Ivaska and Heino, 2011). Green arrows represent signalling. (A) Integrins and growth factors can co-cluster which positively regulates their signalling. (B) Integrins and GFRs can be bridges by ECM proteins. (C) Integrins can stimulate EGFR signalling in an EGFR ligand-independent manner. (D) Integrins and GFRs can activate common signalling pathways. (E) Integrins can negatively regulate GFR signalling. (F) Integrins can upregulate the expression of GFRs. (G) Integrins and GFRs can be co-internalised (H) and co-recycled.

Integrins also negatively regulate GFR activity, by mechanisms such as recruiting phosphatases. One example of this is the recruitment of the phosphatase TCPTP (T-cell protein tyrosine phosphatase) by integrin α1β1 (Mattila et al., 2005). Binding to collagen promotes an interaction between the integrin α1 cytoplasmic domain and TCPTP, activating TCPTP potentially by interfering with autoinhibitory interactions. TCPTP dephosphorylates EGFR, resulting in reduced EGFR phosphorylation after EGF stimulation, inhibiting EGF induced cell proliferation (Mattila et al., 2005). TCPTP has also been shown to dephosphorylate VEGF receptor 2, which is the receptor type primarily responsive to VEGF (Mattila et al., 2008).

Integrins and GFRs can affect the expression and surface levels of one another (Ivaska and Heino, 2011). For example overexpression of αVβ3 upregulates EGFR expression (Lossner et al., 2008), and sustained stimulation with HGF increases integrin α2 levels. Integrins can also indirectly affect GFR activity through interacting with their ligands. The best characterised example of this is integrin-mediated activation of the growth factor TGFβ through mechanical force or proteases (Worthington et al., 2011). Integrins are also able to bind some growth factors, such as αVβ3 which can bind insulin-like growth factor-1 (IGF-1) and angiopoietin-2 (Saegusa et al., 2009; Thomas et al., 2010). Integrin binding to growth factors can promote the signalling of the corresponding GFR, suggesting integrins could be involved in introducing the growth factor to the GFR (Ivaska and Heino, 2011).

Integrin and GFR mediated crosstalk therefore has important consequences for regulating the activity of both receptor families, in a positive or negative manner. Crosstalk can be mediated indirectly of both receptors for example by a divalent ECM ligand, through permissive mechanisms such as influencing receptor expression and clustering, and by direct mechanisms such as the recruitment of phosphatases to directly control receptor activity.

1.9.2 Concomitant Signalling

In addition to promoting GFR signalling in a collaborative manner integrins can independently activate common signalling pathways, enhancing signalling concomitantly (Ivaska and Heino, 2011). Key shared pathways are Ras-MAPK, PI3K-Akt, and the downstream regulation of Rho family GTPases.

Integrin-mediated adhesion recruits FAK to adhesion sites, where it is then phosphorylated on multiple residues. FAK binds to β integrin cytoplasmic domains indirectly via paxillin and talin (Mitra et al., 2005). FAK autophosphorylation at Y397 (either in *cis* or *trans*) produces a binding site for SH2 domain containing proteins, including Src family kinases, Shc,

p120RasGAP and PI3K (Mitra et al., 2005). Phosphorylated Src Y397 is a high-affinity binding site for Src, and the 'FAK-Src' complex phosphorylates itself and a range of other signalling proteins, many of which are RTK signalling effectors (Mitra and Schlaepfer, 2006). FAK phosphorylation of bound PI3K stimulates PI3K-Akt survival pathway signalling (Xia et al., 2004). Src phosphorylation of FAK Y925 creates an SH2 binding site for Grb2, connecting FAK to Ras activation and the MAPK cascade (Mitra et al., 2005). Overexpression of FAK facilitates competitive sequestering of p120RasGAP away from active Ras, resulting in elevated Ras activity (Hecker et al., 2004). GFRs can activate FAK directly or indirectly via Src, and both are central nodes downstream of both integrin and GFR signalling (Ivaska and Heino, 2011).

Recently a role for EGFR and ErbB2 directly participating in integrin-mediated force sensation has been discovered (Saxena et al., 2017). During cell attachment and spreading cells produce actomyosin based 'contractile units' to sense ECM rigidity. Cells attached to rigid matrices (17.2 kPa) of FN coated pillars generate a greater number of contractile units than those on soft matrices (7.2 kPa). Inhibition of EGFR kinase activity under serum-free and EGF-free conditions, statistically significantly decreased cell area spreading and formation of contractile units on rigid substrates (Saxena et al., 2017). Inhibition of ErbB2 had no effect, however ErbB2 overexpression rescued the EGFR knockdown phenotype indicating potential compensation. The number of contractile units peaks 20 minutes after attachment, diminishing 10-fold after 5 hours. Stimulation with EGF after 6 hours of attachment stimulated lamellipodial protrusion and the formation of contractile units in extensions. An inhibitor of myosin-II ROCK-mediated activity (ROCK phosphorylates myosin-regulatory light chain, which promotes myosin-II contractility) abrogated the effects of EGF stimulation, indicating EGFR exerts its contractile function via myosin-II. EGFR has previously been shown to activate myosin-II contractility (Schneider et al., 2009), potentially indirectly via PKC (Chen et al., 2017).

Src is recruited to active EGFR, and both can phosphorylate each other stimulating their activity and signalling (Alberts et al., 2015). Src-mediated phosphorylation of EGFR was required for EGFR localisation to early adhesions, in a rigidity dependent manner (Saxena et al., 2017). Src is not recruited to adhesions in a force-dependent manner however, so is unlikely to be directly involved in recruiting EGFR (Chen et al., 2017). One likely candidate for this role is p130cas, which can be mechanically unfolded (Sawada et al., 2006) and is involved in EGFR localisation (Kang et al., 2011; Moro et al., 2002).

Shared signalling effectors downstream of integrins and GFRs results in collaborative signalling whereby both receptors independently activate the same pathways. Integrins and GFRs can additionally regulate downstream signalling of the reciprocal receptor family, controlling their associated functions.

1.9.3 Trafficking Crosstalk

Crosstalk between integrins and GFRs affects the endosomal trafficking of both receptor types. The receptor families have shared trafficking routes including those for internalisation, and recycling (Ivaska and Heino, 2011). Both demonstrate constitutive endocytosis with predominant membrane localisations (Bridgewater et al., 2012; Sorkin and Goh, 2008). They differ however in their ligand stimulated trafficking fates, with the traditional view being integrins are predominantly recycled, whereas GFRs are degraded (Wiley et al., 1991).

Integrins and GFRs can affect each other's internalisation. Expression of the constitutively active EGFR vIII mutant reduced surface levels of integrin α2 and cell spreading, which was reversed through inhibition of EGFR catalytic activity (Ning et al., 2007). EGF stimulation triggered internalisation of both EGFR and α2 through distinct pathways with different trafficking fates (Ning et al., 2007). HGF stimulation promotes co-internalisation and co-trafficking of Met and β1, promoting sustained signalling from internalised Met (Barrow-McGee et al., 2016). Integrin β1 may also co-internalise with bone morphogenic protein receptor 1A, as the receptors colocalised in internal compartments when β1 internalisation was triggered by culturing bone marrow mesenchymal stem cells on soft substrates (Bridgewater et al., 2012; Du et al., 2011). Co-internalisation of surface receptors is an important mechanism by which receptor surface bioavailability can be regulated in a co-ordinated and linked manner.

Receptor recycling is an important determinant of spatial and temporal control of bioavailability at the plasma membrane, which can be regulated by integrins and GFRs. Under serum-starved conditions integrin αVβ3 traffics through Rab4 positive early endosomes to Rab11 positive endosomes in the perinuclear recycling compartment and is recycled in a long-loop Rab11 dependent manner. PDGF stimulation diverts αVβ3 recycling to short-loop Rab4 dependent recycling, and directs αVβ3 to small puncta which later develop into focal complexes, implicating a role for PDGF in promoting cell-matrix adhesions (Roberts et al., 2001). Protein kinase D (PKD) signalling downstream of PDGF is potentially the mechanism behind this switch, promoting an interaction between the Rab5 effector rabaptin-5 and Rab4 (Christoforides et al., 2012). Integrins and GFRs can also directly associate and recycle in a

coordinated manner together. Inhibition of αVβ3 promotes the coordinated recycling of α5β1 and EGFR (Caswell et al., 2008; White et al., 2007). Rab-coupling protein (RCP) binds to β1 and EGFR, physically linking them. This results in fast rapid motility associated with α5β1, and elevated EGFR autophosphorylation and Akt signalling (Caswell et al., 2008). Regulation of receptor recycling has direct consequences for receptor surface bioavailability dynamics and levels, which influences receptor function.

The small GTP binding protein Arf6 has been implicated in controlling the recycling of both integrins and GFRs (Caswell et al., 2009). The Arf family regulate endocytic trafficking by recruiting cargo-sorting coat proteins, and modifying membrane lipid composition through recruiting phosphatidylinositol kinases, and interacting with the cytoskeleton (Donaldson and Jackson, 2011). The Arf family are activated by GEFs, and inactivated by GAPs that hydrolyse GTP which is crucial as Arfs have negligible intrinsic capacity to hydrolyse GTP (Donaldson and Jackson, 2011). EGFR signalling activates Arf6 through recruiting the Arf GEF GEP100 to phosphorylated EGFR Y1068 (Morishige et al., 2008). Activation of Arf6 in conjunction with a downstream effector AMAP1 promotes recycling of integrin β1, through indirect binding of AMAP1 to β1 via PKD (Onodera et al., 2012). HGF stimulation is also able to stimulate the recycling of β1, via a mechanism that requires Arf6 (Hongu et al., 2015). The Arf family GTPases therefore represent important regulators of integrin and GFR recycling and trafficking crosstalk.

1.10 Crosstalk between αVβ6 and EGFR

Integrin αVβ6 is involved in downstream signalling associated with EGFR. Treatment of Detroit 562 pharyngeal carcinoma cell xenografts with the clinical αVβ6 inhibitor 264RAD resulted in a dose-dependent inhibition of ERK phosphorylation levels, detected histologically (Eberlein et al., 2013). αVβ6 levels were also reduced, indicating these phenomena could be linked (Eberlein et al., 2013). Stimulation of OSCC cells with FN stimulated the activity of the Src family kinase Fyn. This effect was abrogated with αVβ6 inhibition, and Fyn was co-immunoprecipitated with αVβ6 indicating proximity and therefore a potentially direct mechanism (Li et al., 2003). Stimulation of Fyn activity could indirectly couple αVβ6 to the Ras-MAPK activity, through activity of a Fyn-FAK complex activating Shc (Li et al., 2003). The αVβ6 may associate with ERK2 via the β6 subunit and promote its activity, demonstrating a direct link between αVβ6 and Ras-MAPK pathway signalling (Ahmed et al., 2002a). The mechanisms by which αVβ6 effects GFR signalling is undefined and therefore requires further studying.

Crosstalk between αVβ6 and EGFR has been demonstrated to have global cellular consequences on migration and force application. Stimulation of three pancreatic cancer cell lines (Capan1, BxPC3 and Panc0403) with EGF statistically significantly increased migration towards the αVβ6 ligand LAP. This effect was abrogated with inhibition of αVβ6, demonstrating the migration induced by EGF was αVβ6 dependent (Tod et al., 2017). EGF stimulation promoted Rac1 activity, which was also dependent on αVβ6 (Tod et al., 2017). Unpublished data from our laboratory (Stephanie Mo, University of Liverpool) demonstrated EGF stimulation reduced the capacity of MDA-MB-468 cells to apply force to LAP coated matrices, measured by traction force microscopy (TFM). Modulating the ability of αVβ6 to transduce force would have physiological consequences as this is the mechanism by which αVβ6 activates TGFβ (Worthington et al., 2011). These data imply EGF stimulation may alter the composition of αVβ6 adhesions or downregulate αVβ6 at the plasma membrane by stimulating internalisation.

1.11 Thesis Aims

Integrin αVβ6 has been implicated as an attractive therapeutic target for a range of cancers, with inhibitory antibodies in clinical development. Unanticipated crosstalk mechanisms are a major concern behind integrin therapy failures. Preliminary evidence indicates crosstalk exists between integrin αVβ6 and EGFR, which may have implications for the therapeutic potential of these receptors.

The primary aim of this thesis was to elucidate αVβ6 crosstalk mechanisms with EGFR and generate a greater understanding of αVβ6. Trafficking crosstalk was investigated through stimulating receptor endocytosis and analysing changes in endosomal localisation and internalisation rates. Collaborative signalling was assessed by analysing downstream receptor signalling target activations statuses following receptor activation. Isolation and proteomic analysis of αVβ6-specific adhesions contributed to the characterisation of the αVβ6 adhesome and identify novel regulators. The adhesion isolation technique was adapted to identify novel regulators of integrin GFR crosstalk and led to the investigation into the function of the adaptor protein Eps8.

2. Materials and Methods

All reagents were obtained from Sigma-Aldrich (Poole,UK) unless otherwise stated.

2.1 General Buffers

DMEM 5: Dulbecco's Modified Eagle's Medium with 25 mM Hepes

Heat denatured BSA: 10 mg/ml > 98% pure BSA in PBS (-), heated to 85°C for 13 minutes, cooled, filtered through 0.45 µm pore Millex filter unit (Millipore)

Krebs Buffer: 118 mM NaCl, 25 mM $NaHCO_3$, 11 mM glucose, 4.8 mM KCl, 1.5 mM $CaCl_2$, 1.5 mM sodium pyruvate, 1.2 mM KH_2PO_4, 1.2 mM $MgSO_4$

PBS (-): Dulbecco's phosphate buffered saline without divalent cations (136.9 mM NaCl, 1.5 mM KH_2PO_4, 8.1 mM Na2HPO4, 2.7 mM KCl; pH 7.1 – 7.5)

PBS (+): Dulbecco's phosphate buffered saline with divalent cations Mg^{2+} [0.1 g/L] and Ca^{2+} [0.133 g/L]

PBST: PBS (-) containing 0.1% (v/v) Tween-20

5 x Sodium dodecyl sulfate (SDS) Sample Buffer: 50% (v/v) glycerol, 10% (w/v) SDS, 0.01% (w/v) bromophenol blue, 250 mM pH 6.8 Tris HCl; 15% (v/v) β-mercaptoethanol added fresh

TBST: 20 mM Tris base (Fisher Scientific), 150 mM NaCl (Fisher Scientific), 0.1% Tween-20 (v/v), pH 7.6

0.1/0.1 Buffer: 0.1% BSA (w/v), 0.1% sodium azide (v/v) in PBS (-)

2.2 Extracellular Matrix Proteins

All extracellular matrix proteins used as 2D coated ligands were diluted in PBS (+). Fibronectin (from bovine plasma) at 10 µg/ml, Collagen I (rat tail) (Corning) at 10 µg/ml and LAP at 0.5 µg/ml. Surfaces for coating were incubated with the protein solution rocking overnight at 4°C, washed three times with PBS (-) then blocked with heat denatured BSA for 30 minutes at room temperature. Surfaces were washed in PBS (-) followed by the appropriate media, and allowed to equilibrate. Coated surfaces were used for experiments immediately after equilibration.

2.3 Growth Factors and Ligands

Recombinant human EGF was reconstituted in molecular biology grade water to 0.1 mg/ml stock, and used at 10 ng/ml in DMEM with 25 mM Hepes (DMEM5). LAP was reconstituted in 0.22 µm-filtered PBS (-) containing 0.1% (w/v) >99% purity BSA, to 25 µg/ml stock, and used at 0.5 µg/ml in DMEM5.

2.4 Oligonucleotides

siRNA oligonucleotides were obtained from Dharmacon (GE healthcare). The siRNA lyophilised powder was reconstituted in siRNA buffer (Dharmacon) (75 mM KCl, 7.5 mM HEPES-pH 7.5, 0.25 mM $MgCl_2$) in RNAse-free water, and stored at – 20° C.

Target sequences are detailed below in table 2.1. AllStars negative control siRNA (Qiagen) was used as a negative control for all siRNA knockdown experiments. The negative control siRNA lyophilised powder was reconstituted in RNAse-free water (Qiagen) for a 20 µM solution, and stored at - 20° C.

Target	Target sequence	Catalogue number	Stock
Mouse Eps8	ACGACUUUGUGGCGAGGAA	J-045154-11-0050	50 µM
Mouse Eps8L2	UCGACUAUCUGUACGACAU	J-062758-10-0010	40 µM

Table 2.1: List of siRNA oligonucleotide target sequences

2.5 Antibodies

2.5.1 Immunoblotting Antibodies

Immunoblotting antibodies were diluted in either 1 x casein blocking buffer solution with 0.1% (v/v) Tween-20, 5% non-fat dry milk (Marvel) in PBST, or 5% BSA in TBST. Alexa fluor conjugated 680 and 790 secondary antibodies (Molecular Probes Invitrogen) were diluted to 1:10,000 in the same buffer as the corresponding primary antibody used.

Primary Antibody	Clone	Host Species	Supplier	Catalogue Number	Dilution	kDa	Buffer
α-actinin	BM-75.2,	Mouse mAb	Sigma Aldrich	A5044	1:1000	100	5% BSA (TBST)
Actin	AC-40	Mouse mAb	Sigma Aldrich	A3853	1:1000	42	1 x casein
Akt (pan)	C67E7	Rabbit mAb	CST	4691	1:1000	60	5% BSA (TBST)
Phospho-Akt (Ser473)	D9E	Rabbit mAb	CST	4060	1:1000	60	5% BSA (TBST)
BAK	D4E4	Rabbit pAb	CST	12105	1:1000	25	1 x casein
Clathrin heavy chain	23	Mouse mAb	BD Biosciences	610499	1:1000	180	5% BSA (TBST)
EGFR	D38B1	Rabbit mAb	CST	4267	1:1000	175	5% BSA (TBST)

Primary Antibody	Clone	Host Species	Supplier	Catalogue Number	Dilution	kDa	Buffer
EGFR	(1005)-G	Goat pAb	Santa Cruz	sc-03-G	1:1000	170	5% milk (PBST)
EGFR (pY1068)	D7A5	Rabbit mAb	CST	3777	1:1000	175	5% BSA (TBST)
Eps8	15/Eps8	Mouse mAb	BD Biosciences	610144	1:500	97	5% BSA (TBST)
Eps8L2		Rabbit pAb	Protein tech	20461-1-AP	1:500	81	5% BSA (TBST)
FAK	77/FAK	Mouse mAb	BD Biosciences	610088	1:1000	116-125	5% BSA (TBST)
Phospho-FAK pTyr397		Rabbit pAb	Invitrogen	44-624G	1:1000	125	5% BSA (TBST)
GAPDH	mAbcam 9484	Mouse mAb	Abcam	ab9484	1:1000	36	1 x casein
GEF-H1		Rabbit pAb	Fisher Scientific	PA5-32213	1:1000	111	5% BSA (TBST)
HER2/ErbB2	29D8	Rabbit mAb	CST	2165	1:1000	185	1 x casein
HSP70	JG1	Mouse mAb	Invitrogen	MA3-028	1:1000	70	1 x casein
HSP90α	CA1023	Mouse mAb	Merck Millipore	EMD17E7	1:1000	90	1 x casein
Integrin α5		Rabbit pAb	CST	4705	1:1000	150	1 x casein
Integrin αV	EPR16800	Rabbit mAb	Abcam	ab179475	1:1000	125, 135	1 x casein
Integrin αVβ6	c-19	Goat pAb	Santa Cruz	sc-6632	1:300	97	5% milk (PBST)
Integrin β1	EP1041Y	Rabbit mAb	Abcam	ab52971	1:1000	140-150	1 x casein
Integrin β3	D7X3P	Rabbit mAb	CST	13166	1:1000	100	1 x casein
Liprin α1	A-5	Mouse mAb	Santa Cruz	sc-376141	1:1000	134-136	5% BSA (TBST)
p44/42 MAPK (Erk1/2)	137f5	Rabbit mAb	CST	4695	1:1000	42, 44	5% BSA (TBST)
p44/42 MAPK (Erk1/2) (pT202/pY204)		Rabbit pAb	CST	9101	1:1000	42, 44	5% BSA (TBST)
Paxillin	349/ Paxillin	Mouse mAb	BD Biosciences	610051	1:500	68	5% BSA (TBST)
Paxillin (pY118)		Rabbit pAb	CST	2541	1:500	68	5% BSA (TBST)
Paxillin (pY31)	19/ Paxillin (Y31)	Mouse mAb	BD Biosciences	558356	1:500	68	5% BSA (TBST)
Rab8A	EPR14873	Rabbit mAb	Abcam	ab188574	1:2000	24	5% BSA (TBST)
Rap1A/Rap1B		Rabbit pAb	CST	4938	1:500	21	5% BSA (TBST)
Src		Rabbit pAb	CST	2108	1:1000	60	1 x casein

Primary Antibody	Clone	Host Species	Supplier	Catalogue Number	Dilution	kDa	Buffer
Src	GD11	Mouse mAb	Merck Millipore	05-184	1:1000	60	5% BSA (TBST)
Src Family Kinase (pY416)		Rabbit pAb	CST	2101	1:1000	60	5% BSA (TBST)
Src (pY527)		Rabbit pAb	CST	2105	1:500	60	5% BSA (TBST)
Talin	c-20	Goat pAb	Santa Cruz	sc-7534	1:1000	230	1 x casein
Tubulin	DM1A	Mouse mAb	Sigma Aldrich	T9026	1:1000	50	5% BSA (TBST)
Vinculin	hVIN-1	Mouse mAb	Abcam	ab11194	1:1000	123	1 x casein

Table 2.2 Primary antibodies used for immunoblotting. Antibody details, dilution factor, molecular weight of the protein recognised (kDa) and the appropriate blocking buffer. The supplier Cell Signalling Technologies is abbreviated to CST.

2.5.2 Immunofluorescence Antibodies

Immunofluorescence antibodies were diluted in 0.1/0.1 buffer. All fluorophore conjugated secondary antibodies (Alexa 488, Alexa 594 and Alexa 647) were obtained from Jackson ImmunoResearch (Philadelphia, USA) and conjugated Phalloidin from Molecular Probes Invitrogen. Secondary antibodies and Phalloidin stains were diluted 1:400 in 0.1/0.1 buffer.

Primary Antibody	Clone	Host Species	Supplier	Catalogue Number	Dilution
Caveolin		Rabbit pAb	BD Biosciences	610060	1:25
Clathrin Heavy Chain	23/Clathrin Heavy	Mouse mAb	BD Biosciences	610499	1:100
EEA1	14/EEA1	Mouse mAb	BD Biosciences	610456	1:500
EGFR	D38B1	Rabbit mAb	CST	4267	1:1000
EGFR	R-1	Mouse mAb	CRUK	n/a	1:2000
HRS	958/3	Rabbit pAb	Sylvie Urbé	n/a	1:1000
Integrin αVβ6	53A2	Rat pAb	John Marshall	n/a	1:137
LAMP2	H4B4	Mouse mAb	Abcam	ab119124	1:100

Table 2.3 Primary antibodies used in immunofluorescence. Anti-HRS 958/3 (Sachse et al., 2002), anti-integrin αVβ6 (Marsh et al., 2008).

2.5.3 Flow Cytometry Antibodies

Flow Cytometry antibodies were diluted in 0.1/0.1 buffer to 5 µg/µl. Fluorophore conjugated secondary antibodies (Alexa 488) were obtained from Jackson ImmunoResearch (Philadelphia, USA), and used diluted 1:400 in 0.1/0.1 buffer.

Primary Antibody	Clone	Host Species	Supplier	Catalogue Number	Concentration
Integrin α5	VC5	Mouse mAb	BD Biosciences	555651	5µg/µl
Integrin αV	272-17E6	Mouse mAb	Abcam	ab16821	5µg/µl

Primary Antibody	Clone	Host Species	Supplier	Catalogue Number	Concentration
Integrin αVβ3	LM609	Mouse mAb	Merck Millipore	MAB1976	5µg/µl
Integrin αVβ5	P1F6	Mouse mAb	Merck Millipore	MAB1961Z	5µg/µl
Integrin αVβ6	E7P6	Mouse mAb	Merck Millipore	MAB2074Z	5µg/µl
Integrin β1	K-20	Mouse mAb	Santa Cruz	sc-18887	5µg/µl
IgG1 kappa	11711	Mouse mAb	R&D Systems	MAB002	5µg/µl

Table 2.4 Primary antibodies used in flow cytometry

2.6 Immunoblotting

2.6.1 Sample Preparation

Cells ready for lysis were placed on ice and washed once in ice cold PBS (-). Cells were lysed in a modified RIPA lysis buffer (500 mM NaCl, 50 mM pH 7.2 Tris, 10 mM $MgCl_2$, 5 mM EGTA, 1% (v/v) Triton X-100, 0.5% (v/v) Igepal, 0.1% (v/v) SDS; protease inhibitors added fresh: 20 mM NaF, 2 mM Na_3VO_4, 50 µg/µl leupeptin, 50 µg/µl apoprotein, 0.5 mM AEBSF), and adherent cells were scraped off and transferred to a pre-cooled Eppendorf tube. Lysed cell suspensions were centrifuged at 13,000 x g for 10 minutes at 4°C. Supernatants were harvested and stored at – 20°C.

Sample protein concentration was measured using the Pierce™ BCA Protein Assay Kit (ThermoFisher), per the manufacturer's microplate procedure instructions (User guide MAN0011430 Rev. A). Samples were diluted for the assay 1:5 or 1:10, and all sample and standard curve samples were made in triplicate. Sample absorbance was measured at 562 nm on the Promega Golmax Multi Detection System.

Reducing 5 x SDS sample buffer was added to samples for a final 1 x concentration. Samples were heated at 95°C for 5 minutes to denature the protein.

2.6.2 Electrophoresis

Sample protein concentrations typically loaded ranged between 5 – 30 µg depending on the sample concentration and volume. Equal amounts of protein were used for samples electrophoresed on the same gel. Samples were electrophoresed and separated in 1 or 1.5 mm 4 – 12% Novex® NuPAGE™ gels (Invitrogen), in the Novex® Mini-cell XCell SureLock™ Electrophoresis tanks (Invitrogen). A constant 200 V for 45 minutes was used to resolve the samples. Precision Plus Protein™ All Blue Prestained Protein Standards (Bio-Rad) was used as the molecular weight marker. Novex® NuPAGE™ MES-SDS running buffer (Invitrogen) was used.

2.6.3 Transfer and Detection of Proteins

Proteins were transferred using the semi-dry XCell SureLock™ XCell II™ Blot Module (Fisher Scientific) onto Amersham™ Protran® Premium Western blotting nitrocellulose membrane (pore size 0.45 µm). The transfer buffer was 20% (v/v) methanol, 200 mM glycine, 25 mM tris base, 350 µM SDS. A constant 35 V for 90 minutes was used to transfer the protein.

Membranes were incubated in the appropriate blocking buffer corresponding to the primary antibody used (5% BSA in TBST, 5% non-fat dry milk in PBST or 1 x casein), for half an hour at room temperature on a rocker. Membranes were incubated with primary antibody solution overnight at 4°C on a rocker.

Membranes were washed three times in TBST for five minutes on a shaker (120 RPM), before incubation with the secondary antibody (Alexa fluor 680 or 790 conjugated, Molecular Probes Invitrogen) diluted to 1: 10,000 in the corresponding blocking solution that was used. Membranes were washed again in TBST as before, then visualised on the LI-COR Odyssey Sa imaging system. Band pixel intensities were quantified using the Image Studio Version 3.1 software.

2.7 Immunofluorescence

Cells were fixed with 4% (w/v) paraformaldehyde (PBS (-), pH 6.9) for 20 minutes at room temperature, then washed three times in PBS (-). Cells were then permeabilized for 3 – 4 minutes with 0.1% (v/v) Triton X-100 at room temperature followed by three 0.1/0.1 buffer washes. Primary antibody incubations were for 45 minutes at room temperature, followed by three washes in 0.1/0.1 buffer. Samples were incubated with secondary antibody, with or without phalloidin (1:400 in 0.1/0.1 buffer), for 45 minutes at room temperature protected from light. Samples were then washed twice in PBS (-) and once in Milli-Q water, before mounting with Prolong Gold anti-fade mountant (Molecular Probes Invitrogen) on glass Superfrost® Plus glass slides (Thermo Scientific).

Samples were imaged using the Zeiss 3i Marianas spinning disk confocal system using a 63x/1.4 oil objective. Downstream image processing was performed using Image J FIJI. Co-localisation analysis was assessed visually by eye.

2.8 Flow Cytometry

Cells were washed three times in PBS (-) and detached with trypsin. Cells were centrifuged at 280 x g for four minutes, then washed three times in cold 0.1/0.1 buffer. Cells were centrifuged again at 4°C and re-suspended in 100 µl primary antibody or isotype control (5

µg/ml in 0.1/0.1). Three negative controls were included: unstained cells re-suspended in 0.1/0.1 buffer only, secondary antibody only control re-suspended in 0.1/0.1 buffer only at this stage, and an IgG isotype control. Only one isotype control was required as all the primary antibodies used were mouse. Cells were incubated in primary antibody for 30 minutes on ice.

Cells were washed three times in 0.1/0.1 buffer, centrifuged (280 x g, 4 minutes, 4°C) and re-suspended in 100 µl secondary antibody (1:200 in 0.1/0.1) (Donkey anti-mouse 488, Jackson ImmunoResearch), excluding the unstained control that was re-suspended in 0.1/0.1 buffer. Cells were incubated with the secondary antibody for 30 minutes on ice. Cells were washed three times in 0.1/0.1 buffer, centrifuged and re-suspended in 1 ml of cold PBS (-) and kept on ice.

Cell surface fluorescence was measured using the FACSCanto II flow cytometer (BD Biosciences), with technical assistance from Carolyn Rainer from the University of Liverpool Technology Directorate Cell Sorting facility. Results were analysed using FlowJo® software.

2.9 Mammalian Cell Culture

The breast cancer cell lines MDA-MB-468, MCF-7, HER2-18, BT-474, pancreatic adenocarcinoma cell line BxPC3 (Tan et al., 1986), and fibroblast cell line TIFs (Telomerase-immortalised fibroblasts) were maintained in Dulbecco's Modified Eagle's Medium (high glucose), supplemented with 10% (v/v) fetal calf serum (FCS) (Gibco) at 37°C, 5% CO_2. The breast cancer cell line BT-20 (Lasfargues and Ozzello, 1958) was maintained in Minimum Essential Medium Eagle supplemented with 10% (v/v) fetal calf serum (FCS) (Gibco), at 37°C, 5% CO_2. Immortalised mouse embryonic fibroblasts (Im^+ MEFs) (Jat et al., 1991) were maintained in Dulbecco's Modified Eagle's Medium (high glucose), supplemented with 10% (v/v) fetal calf serum (FCS) (Gibco) and 20 ng/ml interferon gamma (PeproTech, London, UK) at 33°C, 5% CO_2. MDA-MB-468 (Cailleau et al., 1978), BT-20 and HER2-18 (Benz et al., 1992) were a gift from John Marshall (Barts Cancer Institute), MCF-7 (Soule et al., 1973) from Viki Allan (University of Manchester), BT-474 (Lasfargues et al., 1978) from Ian MacDonald (University of Nottingham), and TIFs (Bodnar et al., 1998) from Jim Norman (The Beatson Institute).

2.9.1 Sub-cultivation

Cells were washed three times with PBS (-) and detached from the culture flask using trypsin-EDTA (0.5 g/l porcine trypsin, 0.2 g/l EDTA•4Na in Hank's Balanced Salt Solution (5.4 mM KCl, 4.4 mM KH_2PO_4, 4.3 mM $NaHCO_3$, 136.9 mM NaCl, 335.7 µM $Na_2HPO_4 \cdot 7H2O$, 5.6 mM

$C_6H_{12}O_6$, 28.2 µM Phenol red sodium salt ($C_{19}H_{13}NaO_5S$))) at 37°C. Cell suspensions were centrifuged at 280 x g for 4 minutes, before re-suspension in medium and re-plating appropriately.

2.9.2 Cryopreservation

Cells were washed three times with PBS (-) and detached from the culture flask using trypsin-EDTA at 37°C. Cell suspensions were centrifuged at 280 x g for 4 minutes, before washing once in PBS (-), then re-suspending in FCS with 10% (v/v) DMSO. Cell suspensions in cryovials were frozen at -80°C before transferral to liquid nitrogen for long term storage.

2.10 siRNA Transfection

Im^+ MEFs were transfected using the Lonza MEF 2 Nucleofector® Kit using the A-023 programme on the Amaxa biostystems Nucleofector™ II (Lonza) machine, per the manufacturer's instructions. Cells were 50 – 60% density before nucleofection. 2 x 10^6 cells and 3 µg of the oligonucleotide were used per reaction. A second round of transfection was performed 48 hours later, and the cells were used for the assay 48 hours after this.

2.11 Generation of Cell-derived Matrices

Cell-derived matrices were produced by stimulating TIF fibroblasts to produce extracellular matrix, and subsequently removing the cellular material leaving the intact structure (Beacham et al., 2007). Fibroblasts were cultured over time on pre-treated 13 mm coverslips (VWR) in a 24 well plate format.

Coverslips were washed three times in PBS (-) then incubated with 0.2% sterile gelatin (from porcine skin) for one hour at 37°C. Coverslips were again washed in PBS (-), cross linked with 1% (v/v) sterile glutaralydehyde in PBS (-) for 30 minutes at room temperature. After another PBS (-) wash, the crosslinker was then quenched with 1 M sterile glycine in PBS (-) for 20 minutes at room temperature. The coverslips were then washed with PBS (-) and left to equilibrate in the appropriate culture medium (DMEM, 10% (v/v) FCS) at 37°C, prior to cell seeding.

TIFs were detached with 1 x trypsin-EDTA as described and seeded at a concentration of 5 x 10^4 cells per well on the pre-treated coverslips. Cells were then cultured overnight at 37°C 8% CO_2. If cells were sub-confluent at this stage, they were cultured longer until they reached confluence. The medium on confluent cells was changed to the same medium, supplemented with 50 µg/ml ascorbic acid. The ascorbic acid supplemented media was replaced every other day, until denudation. Ascorbic acid stimulates collagen production and stabilises the matrix.

Cells were cultured at 37°C, 8% CO_2 for 8 days from the first ascorbic acid stimulation, prior to denudation.

On the day of denudation, medium was removed and cells were washed with PBS (-), before adding pre-warmed (37°C) extraction buffer (20 mM NH_4OH, 0.5% (v/v) Triton X-100 in PBS (-)). Cells were lysed for 2 minutes, by which point no intact cells were visible. Extraction buffer was removed, and cells washed in PBS (+). Residual DNA was digested with 10 µg/ml DNase I (Roche) in PBS (+) for 30 minutes at 37°C, 5% CO_2. The DNase solution was removed, followed by two PBS (+) washes. At this point the cell-derived matrices were ready for use or stored at 4°C in PBS (+) supplemented with 1 x antibiotic antimycotic solution (100 x stock: 10,000 units penicillin, 10 mg streptomycin, 25 µg/ml amphotericin B, Sigma), for up to a month.

Prior to use, cell-derived matrices were washed twice in PBS (+) before blocking in heat-denatured BSA for 30 minutes at room temperature. Matrices were then washed in PBS (+) and equilibrated in the appropriate medium for the assay.

2.12 Cell Protrusion Assay

Im+ MEFs were transfected with control, Eps8 or Eps8L2 siRNA, as detailed in section 2.10. The second transfection however was a co-transfection, containing 4 µg of LifeAct-GFP (Thistle Scientific) in addition to the siRNA oligonucleotides. LifeAct stains filamentous (F-actin) without interfering with actin dynamics (Riedl et al., 2008).

The next day cell-derived matrices were washed in PBS (-), then blocked in heat denatured BSA for 30 minutes at room temperature. Matrices were then washed again in PBS (-), then in phenol red free reduced serum Opti-MEM™ (Fisher Scientific) and left to equilibrate at 37°C. Transfected Im+ MEFs were seeded at a density of 5 x 10^3 per compartment in a 35mm diameter 4 compartment CELLview™ glass bottom cell culture dish (Greiner Bio-One).

16 hours later the media in each compartment was replenished, and cells were imaged using a Zeiss 3i Spinning disk confocal microscope Marianas™ SDC live cell imaging system, using a 63x/1.4 aperture oil objective. Images were captured at 40 second intervals. After an hour of imaging, cells were stimulated with EGF (10 ng/ml), and then imaged after a brief interval (2 – 3 minutes) required for capture focusing, for another hour.

Cellular protrusive activity and motility was quantified using the QuimP software set of plug-ins for ImageJ (Till Bretschneider, University of Warwick) (Dormann et al., 2002).

2.13 Growth Factor Stimulation

Prior to growth factor stimulation cells were washed twice in PBS (-) and twice in DMEM5. Cells were then serum starved in DMEM5 at 37°C, 5% CO_2 for a minimum of four hours. Growth factor was added diluted in pre-equilibrated DMEM5 in a bolus 10% of the volume of DMEM5 on the cells.

2.13.1 Inhibition of EGFR

Cells were pre-incubated with gefitinib at 1 µM for one hour to inhibit EGFR prior to assays. Gefitinib stock concentration (20 mg/ml) was in DMSO, so a corresponding fold diluted DMSO vehicle control condition was included in all assays. Gefitinib is a potent selective inhibitor of EGFR that binds to the kinase domain of the receptor.

2.14 Inhibition of Protein Degradation

Folimycin (Calbiochem) was used as a lysosomal inhibitor, as it is a potent and selective inhibitor of the vacuolar-type H+-ATPase that prevents acidification of the lysosome. Epoxomicin (Calbiochem) was used as a proteasomal inhibitor, as it is a potent and selective inhibitor of the peptide hydrolysing activities of the proteasome. Serum starved cells were incubated in 100 nM concentrations of both folimycin and epoxomicin for 6 hours, before EGF or LAP stimulation (Eccles et al., 2016). Inhibitor stocks were reconstituted in DMSO (1 mg/ml) therefore control conditions included a DMSO vehicle control.

2.15 Surface Receptor Internalisation Assay

Cells were seeded at a 60% density in 10 cm dishes (three per condition) for 8 hours, before serum starvation overnight, by washing three times in PBS (-) then incubating in DMEM5 solution. High binding half area 96 well ELISA (Enzyme Linked Immunosorbent Assay) immunoassay plates (Corning) were coated overnight at 4°C on a rocker with 5 µg/ml primary antibody (620W7 anti-integrin αVβ6, rat polyclonal, in-house supplied by John Marshall, Barts Cancer Institute, London (Morgan et al., 2011); or EGFR.1 anti-EGFR, mouse polyclonal (BD Biosciences, cat# 555996)) diluted in 0.05 M $NaCO_3$ pH 9.6. The 96 well plates were washed four times in PBST, then blocked in 5% BSA at room temperature for a minimum of 1 hour. All wash steps with cells during the assay were done on ice with ice cold buffers, unless otherwise stated.

Cells were washed twice in Krebs, before labelling with EZ-Link™ Sulfo-NHS-SS-Biotin (Thermo Scientific) (220 µM in PBS (-)) at 4°C on a gentle rocker (7 RPM). Unbound biotin was removed by washing three times in Krebs. 'Total' positive control cell plates were returned

to 4°C to show maximal surface biotinylated receptor signal. 'Blank' negative control plates were also returned to 4°C to show the efficiency of surface biotin removal without internalisation. Equilibrated warm medium alone or with LAP (0.5 µg/ml) or EGF (10 ng/ml) was added to plates, before immediate transferral to 37°C to allow surface receptor internalisation for either 4, 7, 15 or 30 minutes.

After internalisation plates were immediately returned to ice and washed twice with PBS (-) and once with pH 8.6 buffer (100 mM NaCl, 50 mM Tris pH 7.5, pH 8.6 at 4°C). pH 8.6 buffer supplemented with 22.84 mM Sodium 2-mercaptoethanesulfonate (MesNa) (Fluka Analytical) and 0.22 mM NaOH was then added to the blank and internalised plates, before incubation for 30 minutes at 4°C on a gentle rocker. The incubation with the reducing agent MesNa removes surface biotin by cleaving the reducible disulphide bond in the biotin reagent. Biotin bound to internalised surface receptors is unaffected, as MesNa is cell-impermeant (Rainero et al., 2013).

Plates are then washed twice in PBS (-) then lysed in lysis buffer (200 mM NaCl, 75 mM Tris, 7.5 mM EDTA, 7.5 mM EGTA, 1.5% (v/v) Triton X-100, 0.75% (v/v) Igepal CA-630, 15 mM NaF, 1.5 mM Na_3VO_4, 50 µg/µl leupeptin, 50 µg/µl apoprotein, 1 mM AEBSF). Lysates were spun at 13,000 x g for 10 minutes at 4°C. The blocking buffer was removed from the 96 well plate which was washed four times in PBST, before the lysate supernatant was added into each corresponding well. Plates were incubated with the lysate overnight at 4°C.

Unbound material was removed with four PBST washes. Wells were then incubated with streptavidin-conjugated horseradish peroxidase (1:500) in PBST containing 1% BSA, for 1 hour at room temperature. The plate was then washed again four times in PBST, before incubation with an ABTS substrate solution (ABTS buffer: 0.1 M sodium acetate, 0.05 NaH_2PO_4 pH 5, with 2 mM ABTS, 2.5 mM H_2O_2). The resultant colourimetric change was measured at 405 nm absorbance on a Thermo Labsystem Multiskan Spectrum plate reader. Readings were taken across multiple time points ranging from 30 minutes to 24 hours, depending on the rate of development.

2.16 Isolation of 2D Cell-matrix Adhesions

The protocol for isolating 2D cell-matrix adhesions is based on the published methodology with some outlined modifications (Jones et al., 2015). Tissue culture 10 cm dishes were coated with either fibronectin, LAP or collagen I ligands overnight at 4°C on a rocker. Dishes were then washed twice in PBS (-), blocked using heat inactivated BSA for 30 minutes at room

temperature on a rocker. Plates were then washed twice in PBS (-), once in DMEM5, then incubated with 9 ml of DMEM5 to equilibrate at 37°C, 5% CO_2.

Cells were washed in PBS (-), harvested by trypsinisation and centrifuged at 280 x g for 4 minutes. Cell pellets were then re-suspended in DMEM5 and incubated in 40 ml DMEM5 at 37°C for 30 minutes. The cell suspension was centrifuged and re-suspended in DMEM5 sufficient to plate 1 ml of cell suspension per prepared 10 cm dish. Cells were seeded at 5 x 10^6 per ml and allowed to adhere to ligand for 2 hours 30 minutes at 37°C, 5% CO_2.

Cells were then cross-linked with the cell-permeable crosslinker DTBP (dimethyl 3,3'-dithiobispropionimidate, Thermo Fisher), which stabilises protein interactions. DMEM5 was then removed and replaced with 5 ml per plate of pre-warmed (37°C) 3 mM DTBP in DMEM5. Plates are incubated at 37°C for 30 minutes to permit cross-linking.

Cells were then washed twice in ice cold PBS (-) and incubated with 20 mM pH 8.0 Tris for 5 minutes at room temperature, to quench the crosslinker activity. Plates were then washed twice in ice cold PBS (-) and transferred to ice packs.

Immediately prior to sonication, cells were washed once and filled with cold extraction buffer (20 mM NH_4OH, 0.5% (v/v) Triton X-100 in PBS (-)). Cells were sonicated submerged in extraction buffer, using the SONICS Vibra cell™ sonicator at 20% amplitude for approximately 2 minutes per plate. After sonication plates were washed three times in cold extraction buffer, and three times in cold PBS (-).

PBS (-) was then thoroughly removed from the plates, and plates were dried. Remaining adhesion complexes were harvested by scraping in 2 x concentrated reducing Sodium dodecyl sulfate (SDS) sample buffer. Harvested material was collected in an Eppendorf and incubated at 95°C for 5 minutes. A proportion of the sample was then immunoblotted to assess the quality and specificity of the adhesion isolation. The remaining sample was then processed for MS.

2.17 Mass Spectrometry

2.17.1 Protein Gel Preparation

Samples from 2D cell-matrix adhesion isolation preparation were resolved by polyacrylamide gel electrophoresis (PAGE), in 1.5 mm 10 well 4 – 12% Novex® NuPAGE™ gels (Invitrogen), in the Novex® Mini-cell XCell SureLock™ Electrophoresis tanks (Invitrogen). A constant 160 V

was used to resolve the samples. Novex® NuPAGE™ MES-SDS running buffer (Invitrogen) was used.

Protein in the gels was stained by incubating the gel in Instant Blue™ (Expedion) colloidal Coomassie protein stain, for one hour at room temperature on the rocker. Gels were then de-stained with five five-minute washes in MilliQ water, on the rocker. Gels were then washed further in MilliQ for one hour on the rocker, before storing in MilliQ overnight at 4°C.

2.17.2 Peptide Digestion

Gel bands were excised with sterile scalpel blades on a clean tile. Gel bands were then cut into ~1 mm^3 pieces and transferred into a single corresponding well of a 96-well perforated plate (Glygen Corp). The gel was kept moist throughout excision with MilliQ water. Gel pieces were then destained by incubation in 100 µl 50% (v/v) acetonitrile (ACN) / 50% (v/v) NH_4HCO_3 for 30 minutes at room temperature, before removing the supernatant (wash) by centrifugation (96-well-plate rotor, 1,500 RPM, 2 minutes). This step was repeated until all the stain was removed from the gel pieces, leaving them transparent (usually four washes were required).

Gel pieces were then dehydrated twice by incubating with 50 µl 100% ACN for 5 minutes, removing the supernatant following centrifugation each time. Gel pieces were then dried by vacuum centrifugation for 20 minutes using the Christ VWR RVC 2-25 Speed vacuum, then incubated in 50 µl 10 Mm Dithiothreitol (DTT) for one hour at 56°C, to reduce the proteins in the sample. DTT was then removed following centrifugation, and proteins then alkylated by incubating the gel pieces in 50 µl 55 mM Iodoacetamide (IA) for 45 minutes at room temperature, in the dark.

IA was then removed, and gel pieces were then sequentially washed then dehydrated twice, by incubating in 50 µl 25 mM NH_4HCO_3 for 10 minutes, then 50 µl ACN for 5 minutes at room temperature, removing each solution after incubation following centrifugation. The gel pieces were then dried by vacuum centrifugation for 20 minutes.

A fresh collection plate (microplate u-shaped well bottom, Thermo Scientific) was then placed under the perforated plate, for peptide collection. Gel pieces were then incubated with 1.25 ng/µl trypsin gold (Promega) in 25 mM NH_4HCO_3 for 45 minutes at 4°C to allow even penetration into the gel without proteolytic activity. Proteins in gel pieces were then incubated in the trypsin solution overnight at 37°C for protein digestion.

2.17.3 Peptide Extraction

Tryptic peptides were collected by centrifugation. Additional peptides were extracted by incubating the gel pieces in 50 µl 99.8% (v/v) ACN/ 0.2% (v/v) formic acid (FA) for 30 minutes at room temperature, centrifugation, followed by incubating with 50 µl 50% (v/v) ACN/ 0.1% (v/v) FA for 30 minutes at room temperature. These additional extracted peptides were collected by centrifugation then pooled with the initial supernatant and evaporated to dryness in the collection plate by vacuum centrifugation for approximately two hours, monitoring every 20 minutes after the initial hour to ensure peptides were not over-dried.

Dried peptides were then re-suspended in 20 µl 5% (v/v) ACN in 0.1% FA and transferred into 12 x 32 mm glass screw neck vials (Waters). Peptides were then stored at –20°C until analysis.

2.17.4 Mass Spectrometry

5 µl of each digest was injected onto a Nanoacquity™ (Waters) Ultra Performance Liquid Chromatography (UPLC) column, coupled to an LTQ-Orbitrap XL (Thermo Fisher) equipped with a nanoelectrospray source (Proxeon). Samples were separated on a 1 – 85% ACN gradient, 0.300 µl/min flow rate, with an 80-minute retention time. Dynamic exclusion was enabled for a repeat count of 1 for a duration of 30.00 s. MS spectra were acquired by the LTQ-Orbitrap at a resolution of 30,000 and MS/MS was performed on the top 12 most intense ions in the LTQ ion trap.

2.17.5 Peptide Identification

Raw peptide MS data were converted into peak lists and searched against a reviewed H. Sapiens UniProt database (containing 149,633 sequences; 47,132,354 residues) using Mascot Daemon (version 2.3.2) software. The initial precursor and fragment ion maximum mass deviations in the database search were set to 5 ppm and 0.6 Da, respectively, which is optimal for linear ion trap data. One missed cleavage by the enzyme trypsin was allowed. Cysteine carbamidomethylation (C) was set as a fixed modification, whereas oxidation (M, K, P), and phosphorylation (S, T, Y) were considered as variable modifications.

The database search results were processed and statistically evaluated within Scaffold (version 4) The false discovery rate (FDR) for the peptides and proteins were set to 0.01 and 0.4 respectively, to ensure the worst peptide/protein identifications had a 1% or 4% probability of being a false identification, respectively. The imported data was also searched with the X!Tandem (The Global Proteome Machine Organization), and the results from both were combined to increase protein identification confidence.

2.17.6 Proteomic Analysis

Data was imported into Cytoscape (v3.4.0) for visualization of protein-protein interactions mapped using the Protein Interaction Network Analysis (PINA) interactome database (release date 21/05/2014) (Wu et al., 2009) supplemented with a literature curated database of IAC proteins (Robertson et al., 2015; Zaidel-Bar et al., 2007). Three proteins could not be mapped (E9PAV3, NACA; Q9BQ48, MRPL34; E9PRG8, c11orf98) as these were not present in the PPI database.

Over-representation of gene ontology (GO) term analysis was performed using the Cytoscape plug-in ClueGO (version 2.3.3), with KEGG (Kyoto Encyclopedia of Genes and Genomes) and Reactome pathway terms. GO term grouping was used to combine related terms into groups, with a designated leading term.

2.18 Statistics

Pair-wise comparisons of continuous data were tested using Student's two-tailed t-test for parametric data, or Rank sums test for non-parametric data where the equal variance test (Brown-Forsythe) failed. Comparisons between more than two groups were tested using the analysis of variance (ANOVA) with the appropriate *post-hoc* test for multiple test correction. Statistical tests were performed using either SigmaPlot 13.0 statistical software, or within the 'Quantitative Analysis' section of Scaffold 4.8 (Proteome Software).

3. Crosstalk between αVβ6 and EGFR

3.1 Introduction

Integrin αVβ6 is normally expressed at very low or undetectable levels and is upregulated during processes that require epithelial remodelling such as wound healing (Breuss et al., 1995). A key function of αVβ6 is the local activation of TGFβ, which is thought to be achieved through the application of mechanical force to LAP, releasing TGFβ from its inactive complex (Tod et al., 2017; Worthington et al., 2011). Integrin αVβ6 is therefore intimately linked with functions downstream of TGFβ signalling including epithelial repair, ECM deposition and EMT. Upregulation of αVβ6 is observed in a range of cancers such as breast, pancreatic, oral squamous cell and colon carcinomas, and usually correlates with poor survival (Bates et al., 2005; Li et al., 2016; Moore et al., 2014; Thomas et al., 2001b). Expression of αVβ6 can be elevated at the invasive front of tumours and is associated with increased incidence of metastatic lesions (Cantor et al., 2015; Moore et al., 2014; Yang et al., 2008). These observations suggest αVβ6 promotes local invasion and distant metastases, linking it to higher mortality rates caused by metastases (Chaffer and Weinberg, 2011).

Integrin αVβ6 is shown to drive cellular invasion, and therefore can be described as a pro-invasive integrin. Knockout or inhibition of αVβ6 decreases cell invasion *in vitro* in transwell and organotypic assays (Moore et al., 2014; Morgan et al., 2011; Thomas et al., 2001b). Local invasion can be facilitated through αVβ6 promoted expression, secretion and activation of proteinases including uPa and MMPs which degrade ECM that can otherwise be a physical barrier to cell migration (Dalvi et al., 2004; Morgan et al., 2004). Invasion can also be increased through αVβ6 dependent induction of EMT via activation of TGFβ, which causes a switch from collective to single cell motility (Lee et al., 2014).

Integrin αVβ6 is an independent predictor for breast cancer survival, with statistically significant lower survival rates in patients with high αVβ6 expression in cohort studies (Moore et al., 2014). Patients with ErbB2 positive breast cancer and high levels of αVβ6 also had a statistically significant worse survival prognosis compared to those with low αVβ6 expression (Moore et al., 2014). Inhibition of αVβ6 abrogated ErbB2-dependent invasion in response to the ErbB2/ErbB3 ligand Heregulin β1 (HRGβ), suggesting ErbB2 invasion was αVβ6 dependent, leading to the study of the complex relationship between the two receptors (Moore et al., 2014). Monotherapy with the clinical αVβ6 inhibitor 264RAD or the ErbB2 inhibitor trastuzumab slowed tumour growth in ErbB2 positive breast cancer

xenografts, however a combination of the two therapies effectively stopped tumour growth even in a trastuzumab resistant xenograft model (Moore et al., 2014). These data demonstrated potential for 264RAD as either a mono or combination therapy in ErbB2 positive breast cancer, and indicated crosstalk between αVβ6 and ErbB2 may be clinically important.

High expression of αVβ6 is associated with very poor survival in triple-negative breast cancer (TNBC) (HR = 1.71, 95% CI = 1.06 to 2.77, P = 0.026) (personal correspondence, Louise Jones, Barts Cancer Institute QMUL). TNBC is a highly aggressive sub-category representing 15% of breast cancer, defined by the absence of the oestrogen receptor (ER), progesterone receptor (PG) and absence or lack of amplification or overexpression of ErbB2 (Andreopoulou et al., 2017; Denkert et al., 2017). TNBC typically has a poor prognosis and rapid onset of metastasis (Denkert et al., 2017). There are no specific targeted therapies against TNBC, and chemotherapy is the mainline treatment (Harbeck and Gnant, 2017). Few therapeutic targets are identified in TNBC aside from the BRCA1/2 mutation and androgen receptor (Denkert et al., 2017; Harbeck and Gnant, 2017). EGFR is overexpressed in the majority of TNBC and associated with a worse prognosis (Livasy et al., 2006; Nielsen et al., 2004); however, despite this, anti-EGFR therapeutics have been unsuccessful in clinical trials (Andreopoulou et al., 2017). There is therefore a great clinical need for identification of therapeutic targets for the treatment of TNBC.

Unanticipated receptor crosstalk is an important feature behind clinical trial failures, which has been particularly problematic in the development of integrin targeting agents (Raab-Westphal et al., 2017). The relationship between αVβ6 and ErbB2 has been demonstrated to be therapeutically relevant in ErbB2 positive breast cancer (Moore et al., 2014). This project aims to investigate crosstalk between αVβ6 and EGFR, which are both associated with poor prognosis in TNBC and have been reported to exhibit crosstalk (Ahmed et al., 2002a; Eberlein et al., 2013; Tod et al., 2017).

An appropriate cell line model will be established, based on expression and sub-cellular distribution of αVβ6 and EGFR. Trafficking of the receptors will be examined with ligand-induced stimulation, to determine if this can concomitantly affect the endocytosis and trafficking routes of the reciprocal receptor. Collaborative signalling downstream of the receptors will be assessed by investigating activation status of relevant signalling cascades following ligand stimulation of either receptor.

3.2 Results

3.2.1 Cell line characterisation

An appropriate cell line for use in this study needed to be established. The key criteria were expression of αVβ6 and EGFR without ErbB2 to allow the dissection of EGFR specific effects that do not rely on its dimerisation with ErbB2. The TIF fibroblast cell line was used as a negative control for αVβ6 expression, as αVβ6 expression is restricted to epidermal cells. The breast cancer cell lines MCF-7 and HER2-18 were used as negative and positive controls for αVβ6 respectively. The HER2-18 cell line was created by overexpressing ErbB2 in MCF-7 cells (Benz et al., 1992). HER2-18 cells exhibit *de novo* expression of αVβ6 (Moore et al., 2014), however it is unknown if this is a consequence of ErbB2 overexpression or a result of clonal selection. BT-474 were used as an additional positive control for αVβ6 and ErbB2 expression (Holliday and Speirs, 2011; Moore et al., 2014). The TNBC cell lines MDA-MB-468 and BT-20 were identified as potentially relevant models as both have documented EGFR expression (Grigoriadis et al., 2012). The pancreatic cancer cell line BxPC3 was also assessed as a potential model as αVβ6 EGFR crosstalk may also be therapeutically relevant in pancreatic cancer (Li et al., 2016).

Total expression levels of integrins, EGFR and HER2 were assessed by immunoblotting (Figure 3.1 A). All cell lines were positive for integrin αV and β1, which can form heterodimers with multiple other subunits. HER2-18, BT-474, MDA-MB-468, BT-20 and BxPC3 cell lines were positive for β6 subunit expression. HER2-18, MCF-7, BxPC3 and TIF were positive for α5, which can dimerise with β1 and bind the RGD motif. All cell lines except MCF-7 expressed EGFR, with particularly high levels observed in MDA-MB-468. EGFR expressed in BT-474 cells is a slightly higher molecular weight than in the other cell lines, suggesting that the protein may have undergone post-translational modifications. The positive controls HER2-18 and BT-474 expressed high levels of ErBb2, whereas TIF and BT-20 cells expressed low levels. Protein loading was not very equal in these experiments (see GAPDH in Figure 3.1 A) therefore only broad conclusions regarding protein expression levels can be made.

Surface expression of a panel of integrins was assessed by flow cytometry for MDA-MB-468, BT-20 and BxPC3 cell lines (Figure 3.1 B). In agreement with the immunoblotting data, all cell lines were positive for αVβ6 (detected by a heterodimer specific antibody) and β1. BxPC3 cells had low surface levels of β1 in contrast to the high total protein levels observed by immunoblotting, suggesting the cellular pool of β1 is not entirely at the cell surface. BT-20

and BxPC3 but not MDA-MB-468 were positive for α5. All cell lines were negative for αVβ3, and BT-20 was the only cell line positive for αVβ5.

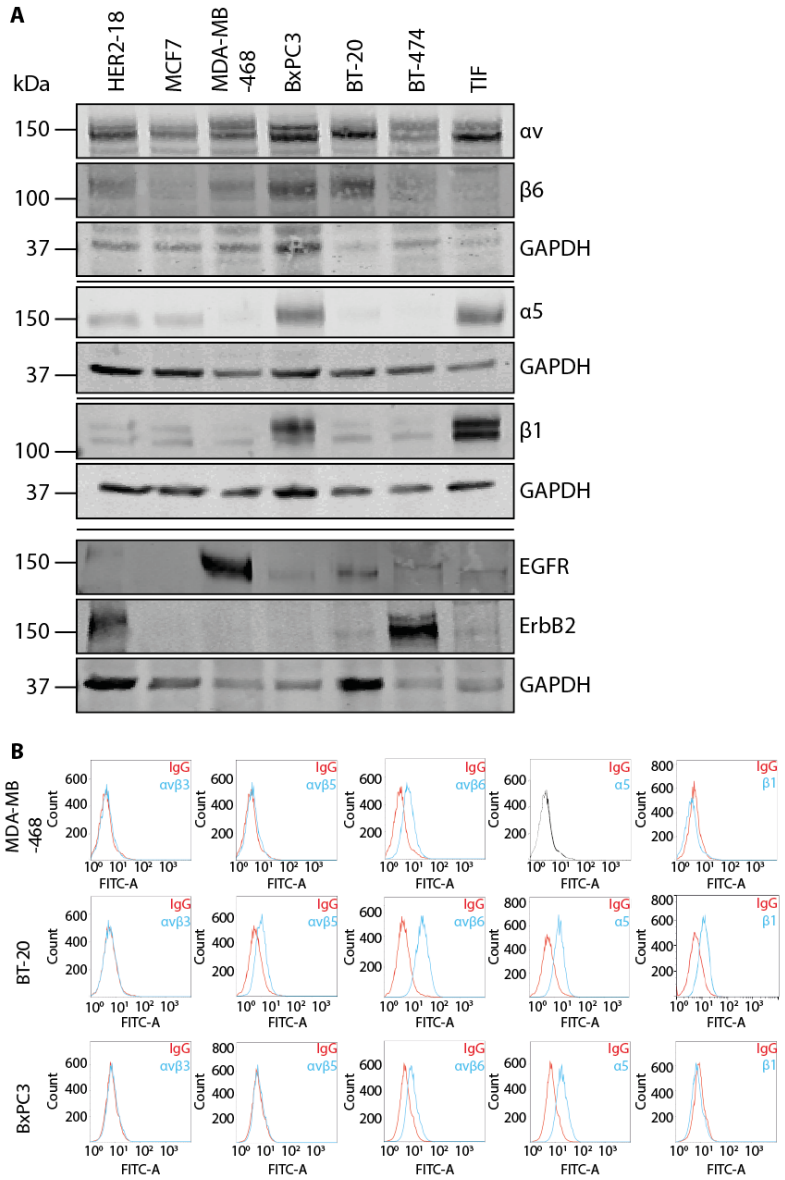

Figure 3.1 Integrin, EGFR and ErbB2 expression in a panel of cell lines. (A) Western blotting of integrin, EGFR and ErbB2 protein expression levels in Her2-18, MCF-7, MDA-MB-468, BxPC3, BT-20, BT-474 and TIF total cell lysates. N=3 for integrin, and N=1 for EGFR and ErbB receptor immunoblotting (B) Flow cytometry surface expression of integrin αvβ3, αvβ5, αvβ6, α5, β1 in MDA-MB-468, BT-20 and BxPC3 cell lines. N=1

MDA-MB-468, BT-20 and BxPC3 were all characterised as potentially suitable cell line models. This project aimed to investigate αVβ6-specific processes, using LAP as a key ligand, therefore a lack of alternative LAP binding integrins facilitates the use of LAP as an αVβ6-specific ligand. Integrins αVβ3 and αVβ5 bind the RGD motif present in ligands including LAP. MDA-MB-468s were chosen as the primary cell line model for study due to the high level of αVβ6 and EGFR expression. BT-20s were identified as a complementary cell line with a similar αVβ6 expression profile but a lower level of EGFR. BT-20s have surface expression of αVβ5 and α5 whereas MDA-MB-468s do not. Work was not continued with the BxPC3 cell line to concentrate focus on molecular processes associated with TNBC.

Having identified MDA-MB-468s as the primary cell line model, the subcellular distribution of αVβ6 and EGFR was then investigated by co-staining for both receptors by immunofluorescence (Figure 3.2). Cells were plated either in the presence of 10% serum, or on coverslips coated with FN or LAP ligands in the absence of serum. Serum contains ECM molecules and therefore represents a mixed ligand environment (Zheng et al., 2006). Serum-free conditions were used for FN and LAP ligand conditions to ensure cells specifically engaged the coated ligand rather than alternative serum-derived ligands, as FCS contains a mixture of ECM proteins and growth factors.

Preliminary data showed cells plated in serum, or bound to FN, had αVβ6 positive adhesions and actin stress fibres, clearly visible in juxtamembrane z-sections (Figure 3.2). Few αVβ6 adhesions were observable on LAP, and cells had a more rounded morphology without clear stress fibres. It is likely cells on LAP were not forming focal adhesions which are dependent on mechanical force application associated with actin stress fibres, as opposed to the alternative scenario that cells were forming focal adhesions lacking αVβ6. Integrin αVβ6 present across the ventral surface of the cell is likely to be engaging ligands regardless of aggregation into mature adhesions, as it is at the site of the cell-matrix interface. EGFR was distributed throughout the cell at the surface and intracellularly (Figure 3.2). Integrin αVβ6 and EGFR co-localised in the ventral cell surface plane proximal to αVβ6-dependent adhesions and at intracellular structures reminiscent of trafficking vesicles, most evident in juxtabasal z-sections towards the middle of the cell. Co-localisation between αVβ6 and EGFR was seen across all three ligand conditions at the membrane and in vesicles, although appeared most pronounced in the presence of serum (Figure 3.2). A key difference between the serum containing condition compared to the FN and LAP ligand conditions is that cells were serum-starved for 2.5 hours during adherence and spreading to facilitate engagement of specific ligands. The presence of soluble growth factors and ECM ligands in serum could

potentially engage both αVβ6 and EGFR and stimulate receptor internalisation, resulting in an altered subcellular distribution.

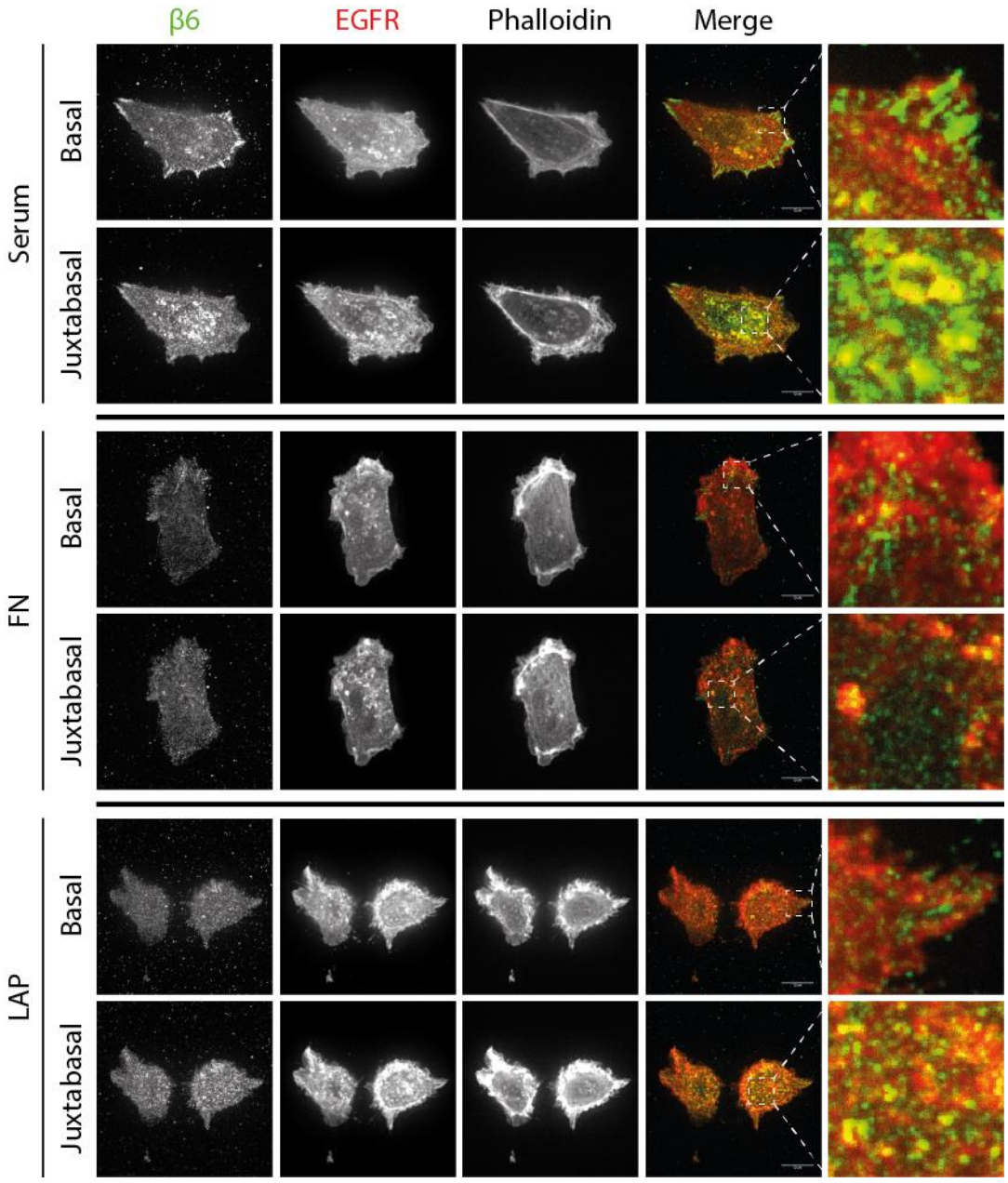

Figure 3.2 β6 and EGFR subcellular distribution in MDA-MB-468 cells on different ligands. MDA-MB-468 cells adhered and spread on glass coverslips in the presence of 10% FBS, or under serum free conditions on glass coverslips coated with FN or LAP, over the course of 2.5 hours. Single z sections are displayed for basal and juxtramembrane sections of the cell, 1 µm, 0.8 µm and 0.6µm above for serum, FN and LAP images, respectively. β6; green and EGFR (R-1); red. Scale bar = 10µm. N=1

3.2.2 αVβ6 and EGFR traffic concomitantly

Internal structures of overlapping αVβ6 and EGFR were reminiscent of endosomes. To determine the nature of these structures MDA-MB-468 cells were co-stained by immunofluorescence for αVβ6 and EGFR, and the trafficking compartment markers EEA1 (early endosomal antigen 1), HRS (hepatocyte growth factor-regulated tyrosine kinase substrate) or LAMP2 (lysosome-associated membrane protein 2). EEA1 is a marker of early endosomes, and is recruited to their membrane during their formation shortly after endocytosis (Sorkin and von Zastrow, 2009). HRS is classed as a later trafficking marker, as it is a major component of ESCRT-0 which predominantly localises to MVBs (Raiborg and Stenmark, 2009). LAMP2 is a marker of the lysosome, which cargo can be trafficked to from the late endosome (Luzio et al., 2007).

MDA-MB-468 cells were seeded onto coverslips in DMEM in the presence of 10% FBS and allowed to adhere and spread, then serum-starved prior to stimulation with EGF or LAP to promote the internalisation of αVβ6 and EGFR. LAP stimulation was hypothesised to trigger endocytosis of αVβ6, as ligand stimulation is known to trigger integrin internalisation (Bridgewater et al., 2012). For LAMP2 co-localisation assays, lysosomal and proteasomal inhibition was achieved by pre-incubating cells with the inhibitors folimycin and epoxomicin (Eccles et al., 2016). Co-localisation of αVβ6, EGFR and endosomal markers was analysed by eye.

Under serum-starved conditions αVβ6 and EGFR colocalise with each other but not EEA1, HRS or LAMP2 (20/20 cells) (Figure 3.3 and Figure 3.4). The receptor distribution with respect to EEA1 is unchanged after 5 minutes EGF stimulation (17/17 cells) (Figure 3.3 A). After 10 minutes cells exhibit one of three phenotypes; 1) αVβ6 and EGFR co-localisation with (6/18 cells) or 2) without low levels of EEA1 overlap (6/18 cells), and 3) EGFR EEA1 co-localisation with little αVβ6 co-localisation (6/18 cells). The predominant subcellular distribution after 15 minutes of EGF is weak co-localisation of αVβ6, EGFR and EEA1 (16/16 cells). This distribution persists until 30 minutes (9/13 cells), however there is a shift towards weak co-localisation between EGFR and EEA1 only in some cells (4/13 cells). This is followed by a return to αVβ6 and EGFR co-localisation without EEA1 in vesicles at 60 minutes (10/15 cells), although some infrequent EGFR EEA1 colocalising cells persist (5/15 cells).

EGF stimulation triggers endocytosis of EGFR, therefore it was expected that stimulation with EGF would increase co-localisation of EGFR with the early endosomal marker EEA1. EGF stimulation also causes αVβ6 to weakly colocalise with EEA1, proximal to EGFR. These data

demonstrate that EGF induces re-distribution of αVβ6 in a manner consistent with internalisation. This preliminary data showing weak co-localisation of αVβ6 and EGFR in the same EEA1 positive endosomes suggests these receptors could have co-internalised together.

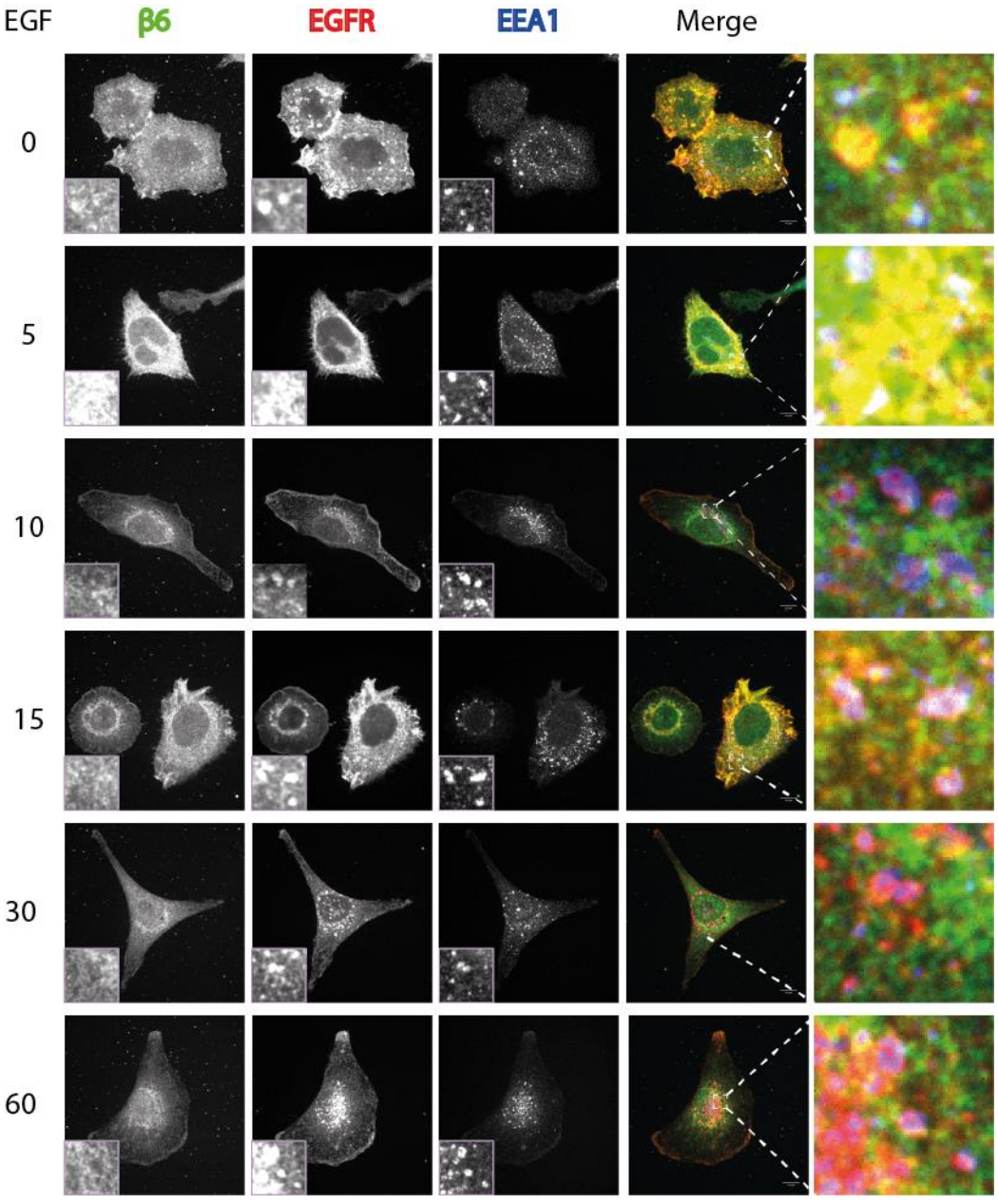

Figure 3.3 A EGF stimulation induces colocalisation of β6 and EGFR with EEA1. MDA-MB-468 cells, co-stained for β6, EGFR (D38B1) and EEA1. Single z slice shown for a juxtamembrane section of the cell. EGF stimulation is shown in minutes. EGFR is shown at 50 – 15000 for 0, 5 and 15 minutes and 100 - 2000 for 10, 30 and 60 minutes, intensity arbitrary units. Scale bar = 10 µm. N= 2, n= 13 - 20 cells per timepoint.

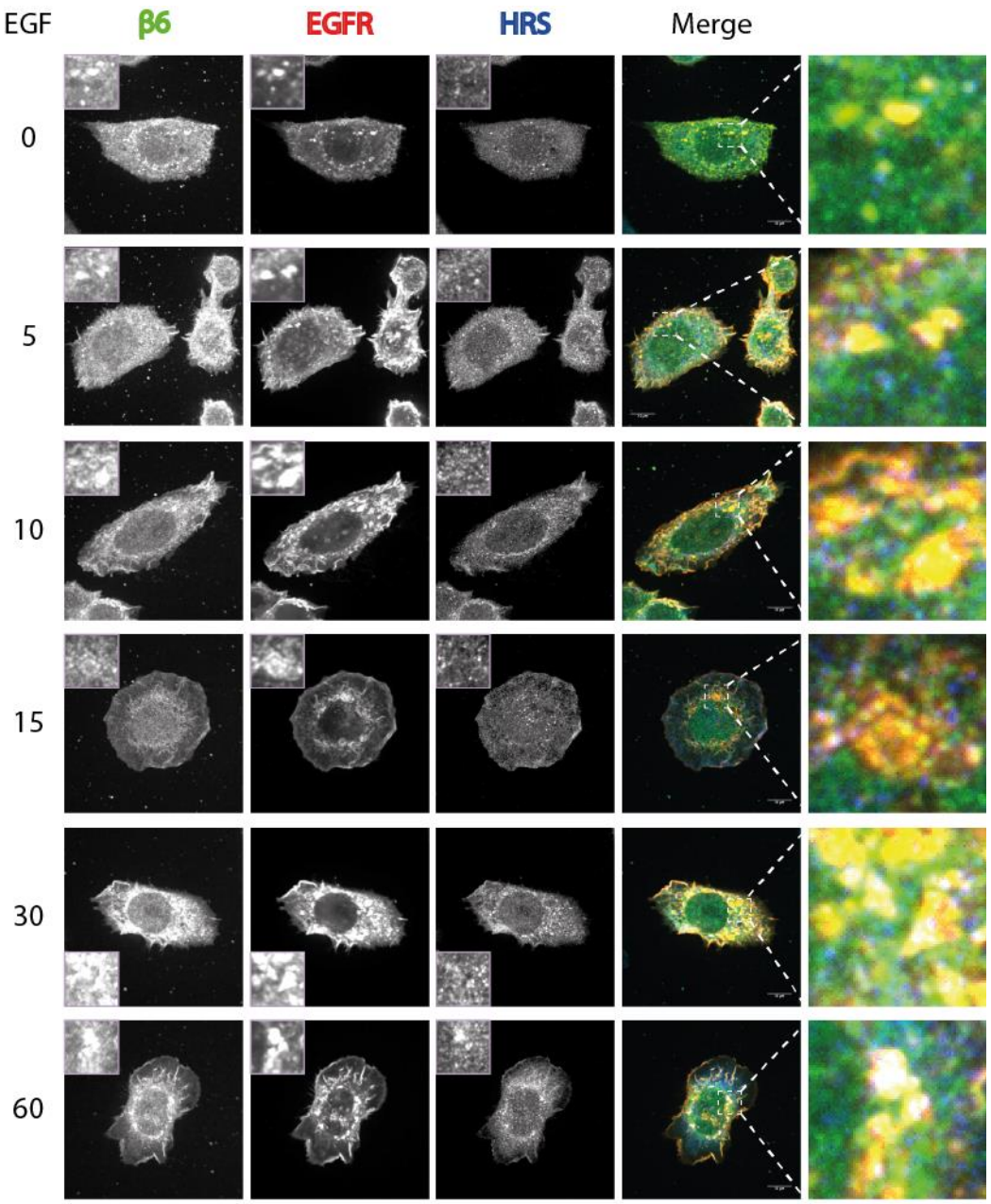

Figure 3.3 B EGF stimulation induces colocalisation of β6 and EGFR with HRS. MDA-MB-468 cells, co-stained for β6, EGFR (R-1) and HRS. Single z slice shown for a juxtamembrane section of the cell. EGF stimulation shown in minutes. Scale bar = 10 µm. N= 2, n= 16 – 18 cells per timepoint.

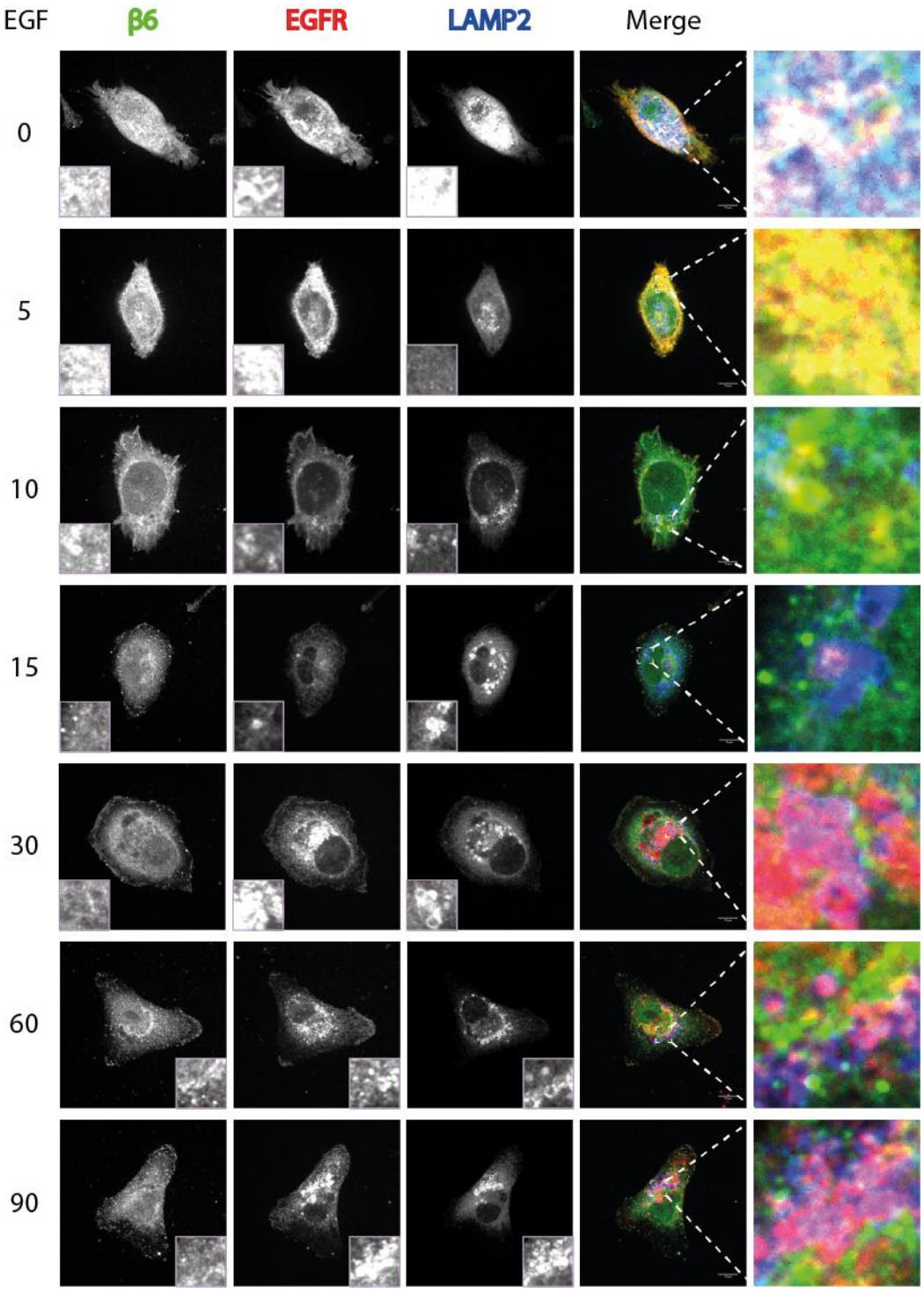

Figure 3.3 C EGF stimulation induces colocalisation of EGFR with LAMP2. MDA-MB-468 cells, co-stained for β6, EGFR (D38B1) and LAMP2. Cells were pre-incubated with the lysosomal and proteasomal inhibitors folimycin and epoxomicin, respectively. Single z-slice shown for a juxtamembrane section of the cell. EGF stimulation shown in minutes. EGFR is shown at 100 - 19000 for 0 - 10 minutes and 100 - 2600 for 15 - 90 minutes, intensity arbitary units. Scale bar = 10 µm. N=1, n= 15 - 20 cells per timepoint.

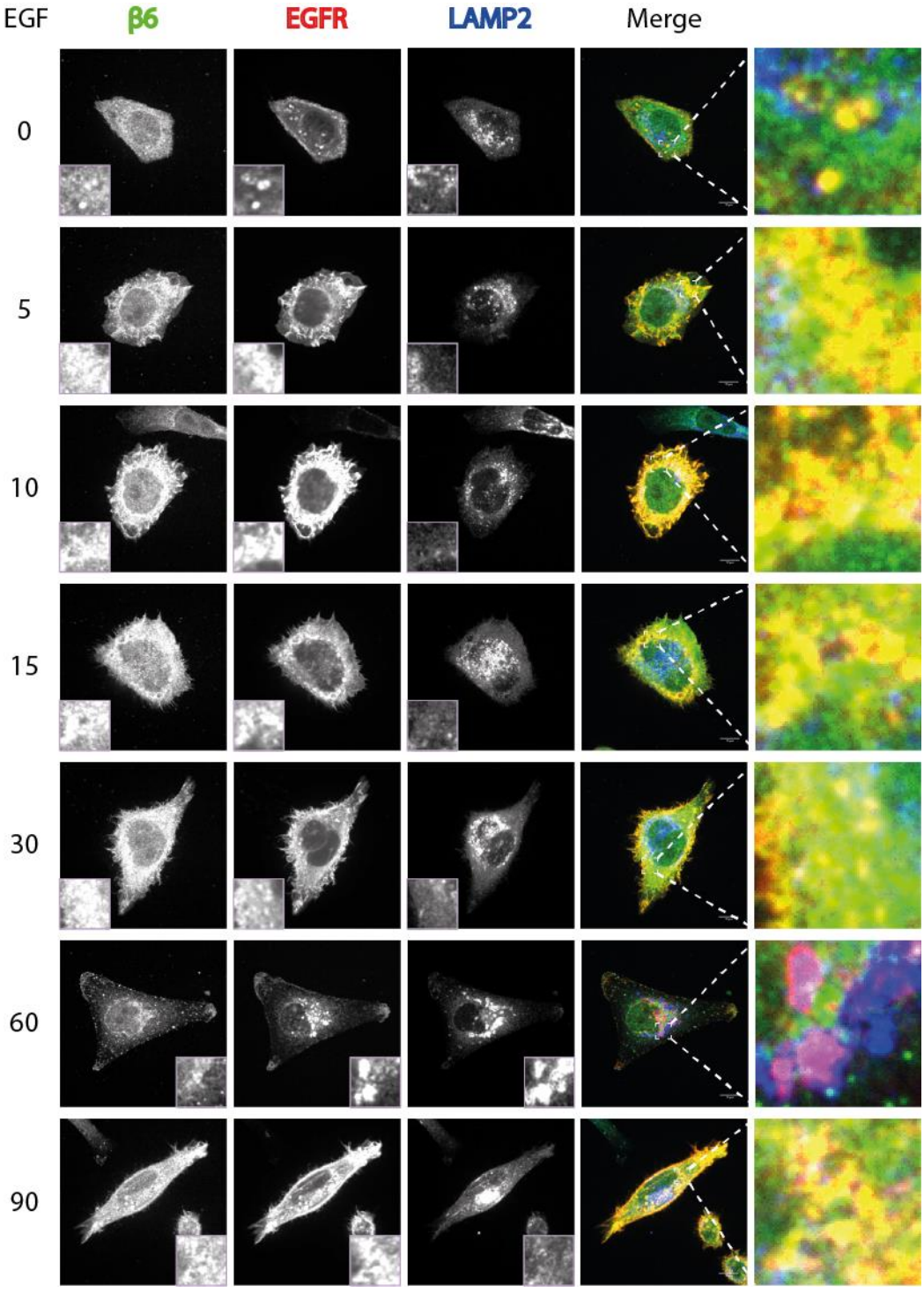

Figure 3.3 D: EGF stimulation induces colocalisation of EGFR with LAMP2. MDA-MB-468 cells, co-stained for β6, EGFR (D38B1) and LAMP2. DMSO vehicle control for folimycin and epoxomicin lysosomal and proteasomal inhibitors. Single z slice shown for a juxtamembrane section of the cell. EGF stimulation shown in minutes. EGFR is shown at 100 - 19000 for 0 - 30 and 90 minutes and 100 - 2600 for 60 minutes, intensity arbitrary units. Scale bar = 10 µm. N=1, n= 8 - 24 cells per timepoint.

All cells at 5 minutes (16/16 cells), and most cells at 10 minutes (10/16 cells) of EGF stimulation, had some weak co-localisation between EGFR and αVβ6 but not HRS (Figure 3.3 B). Approximately one-third of cells (5/16 cells) at 10 minutes have some co-localisation between both αVβ6 and EGFR with HRS. After 15 minutes the majority of cells have some weak co-localisation between EGFR and αVβ6 in HRS positive endosomes (14/18 cells), whilst a remaining quarter of cells have EGFR and αVβ6 co-localisation without HRS overlap (4/18). Some punctae of co-localisation was observed between both receptors and HRS at 30 (11/16 cells) and 60 minutes (18/18 cells) EGF stimulation. This preliminary data indicates some co-localisation of EGFR and αVβ6 with HRS positive endosomes, which could suggest the receptors remain proximal whilst HRS is recruited to early endosomes and in the formation of the MVB.

Without lysosomal and proteasomal inhibition, no co-localisation was observed between either αVβ6 or EGFR and LAMP2, except at 60 minutes where EGFR colocalised with LAMP2 in approximately one-quarter of cells (6/23 cells) (Figure 3.3 D). In the presence of inhibitors, EGFR and LAMP2 co-localised initially after 15 minutes of EGF stimulation (8/17 cells), prior to which co-localisation was between EGFR and αVβ6 only (Figure 3.3 C). EGFR/LAMP2 co-localisation increased further with EGF stimulation time (30 minutes 7/15, 60 minutes 13/20 cells. Integrin αVβ6 is excluded from sites of EGFR and LAMP2 co-localisation. Preliminary data showing co-localisation of EGFR with LAMP2 indicates EGFR is trafficked to the lysosome for degradation. The absence of αVβ6 in LAMP2 positive structures indicates it may follow an alternative trafficking route following EGF stimulation, likely recycling. These fates for EGFR and αVβ6 agree with the canonical view that EGFR is targeted for lysosomal degradation, and integrins are predominantly recycled (Bridgewater et al., 2012; Wiley et al., 1991). Increasing EGFR and LAMP2 co-localisation with EGF stimulation time is likely influenced by accumulation of EGFR in lysosomes, as the lysosomal inhibitor Folimycin inhibits lysosomal acidification therefore preventing enzymatic degradation of its contents.

A reciprocal experiment with LAP stimulation was also performed to test the hypothesis that soluble LAP stimulates αVβ6 endocytosis, and if so, if αVβ6 internalisation affects the distribution of EGFR. Most cells show co-localisation between αVβ6 and EGFR after 5 minutes of stimulation, without co-localisation with EEA1 (4/7 cells). However, some cells exhibited weak co-localisation of αVβ6 and EGFR in EEA1 positive endosomes (3/7 cells) (Figure 3.4 A). All cells at 10 minutes LAP stimulation had a degree of co-localisation between αVβ6, EGFR and EEA1 (5/5 cells). No co-localisation was observed between αVβ6 and EEA1 between 15

to 60 minutes LAP stimulation. Cells at 60 minutes have αVβ6 positive focal adhesions indicating a large proportion of receptor at the cell membrane.

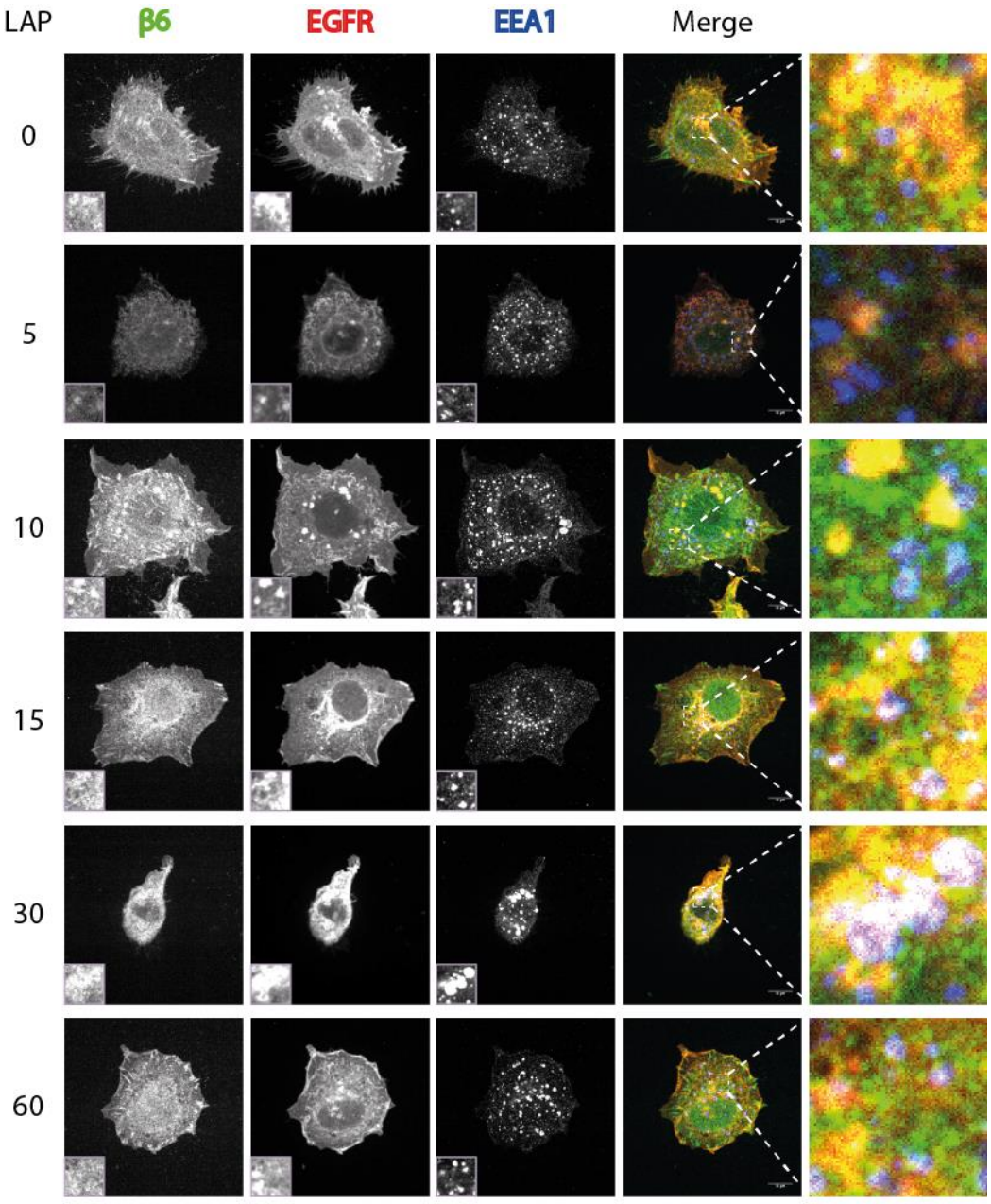

Figure 3.4 A LAP stimulation induces colocalisation of β6 and EGFR with EEA1. MDA-MB-468 cells, co-stained for β6 (620W7), EGFR (D38B1) and EEA1. Single z slice shown for a juxtamembrane section of the cell. LAP stimulation is shown in minutes. Scale bar = 10 µm. N=2, n= 13 - 20 cells per timepoint.

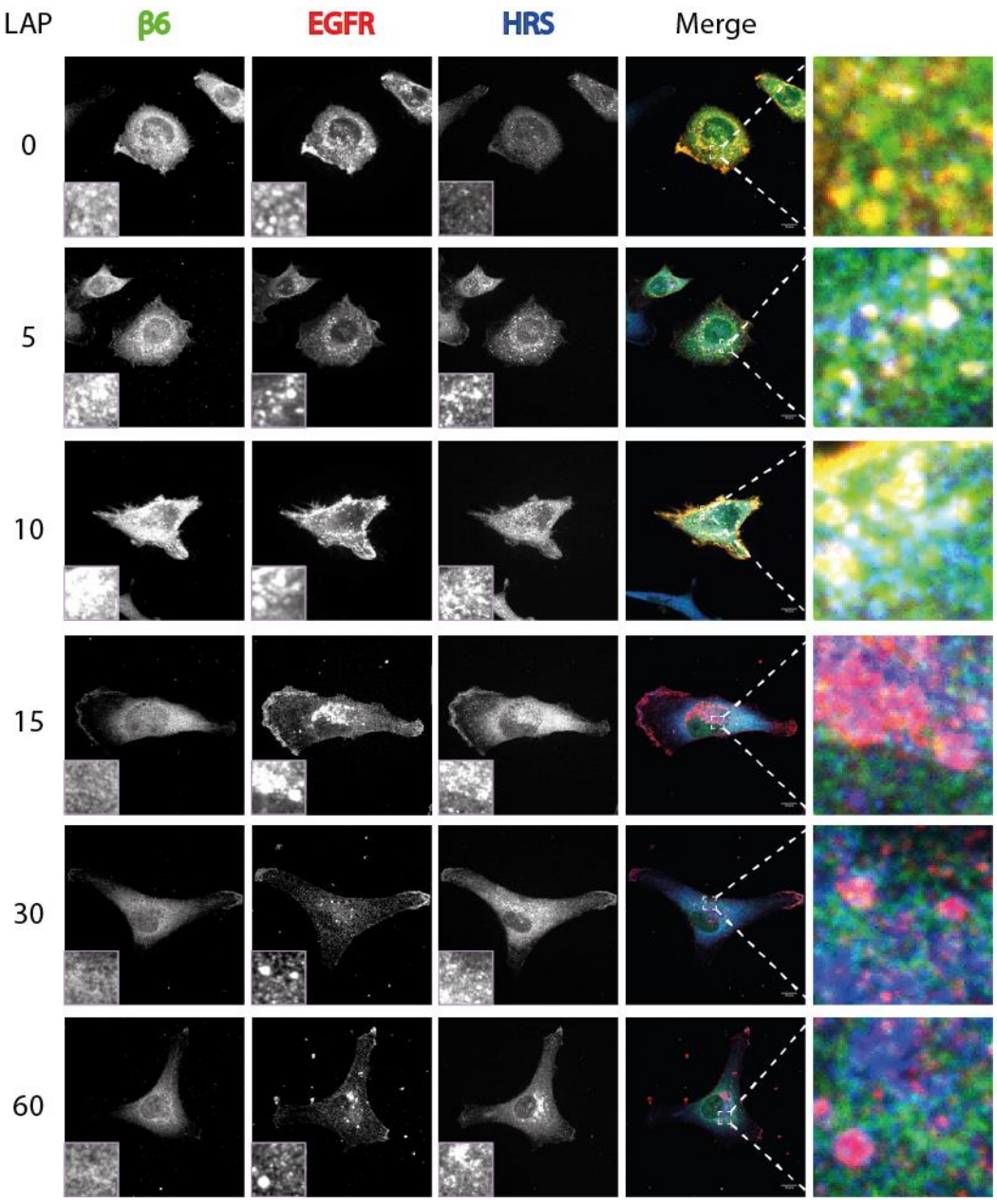

Figure 3.4 B LAP stimulation induces colocalisation of β6 and EGFR with HRS. MDA-MB-468 cells, co-stained for β6, EGFR (D38B1) and HRS. Single z slice shown for a juxtamembrane section of the cell. LAP stimulation is shown in minutes. EGFR is shown at 100 - 14000 for 0, 5 and 10 minutes and 120 - 500 for 15, 30 and- 60 minutes, intensity arbitrary units. Scale bar = 10 µm. N=2, n= 13 - 19 cells per condition.

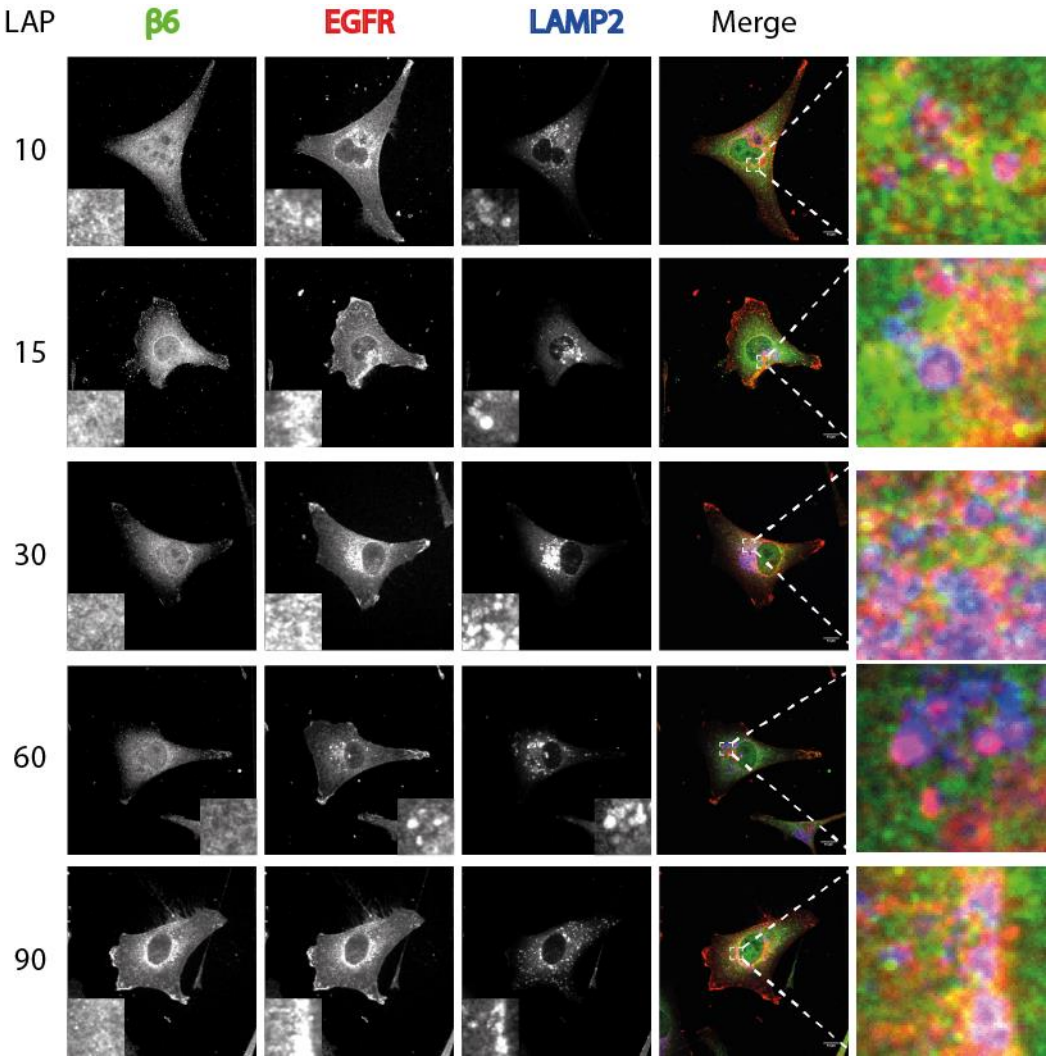

Figure 3.4 C LAP stimulation induces colocalisation of EGFR with LAMP2. MDA-MB-468 cells, co-stained for β6, EGFR (D38B1) and LAMP2. Cells were pre-incubated with the lysosomal and proteasomal inhibitors folimycin and epoxomicin, respectively. Single z slice shown for a juxtamembrane section of the cell. LAP is stimulation shown in minutes. EGFR is shown at 160-3700 intensity arbitrary units. Scale bar = 10 µm. N=1, n =12 - 15 cells per condition.

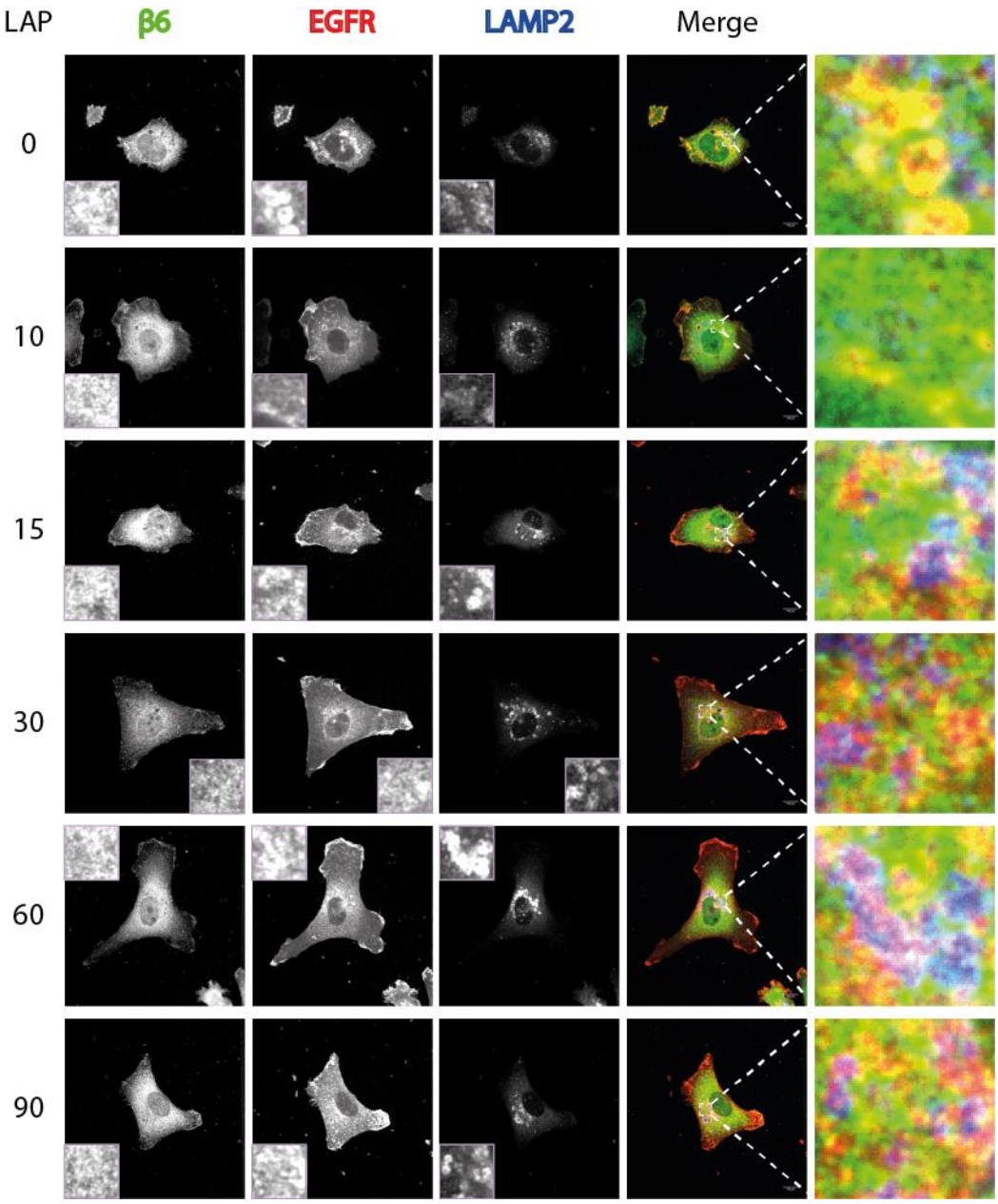

Figure 3.4 D LAP stimulation induces colocalisation of EGFR with LAMP2. MDA-MB-468 cells, co-stained for β6, EGFR (D38B1) and LAMP2. DMSO vehicle control for folimycin and epoxomicin lysosomal and proteasomal inhibitors. Single z slice shown for a juxtamembrane section of the cell. LAP stimulation shown in minutes. EGFR is shown at 160 - 47000 for 10 minutes and 160 - 3700 for 15, 30, 60 and 90 minutes, intensity arbitrary units. Scale bar = 10 µm. N=1, n= 15-17 cells per condition.

Preliminary data indicating an induction of αVβ6 co-localisation with EEA1 demonstrates stimulation with soluble LAP causes αVβ6 internalisation, supporting our earlier hypothesis. A change in EGFR distribution with αVβ6 to EEA1 positive endosomes following LAP stimulation, would suggest αVβ6 triggers co-internalisation of EGFR.

Most cells had αVβ6 and EGFR co-localisation after 5 minutes LAP stimulation (11/15 cells), many of which also had HRS co-localisation (7/15 cells) (Figure 3.4 B). Co-localisation between αVβ6, EGFR and HRS was not observed between 10 and 60 minutes. Preliminary data suggests co-localisation between αVβ6, EGFR and HRS which, if proven, would indicate these receptors are proximal on early endosomes and the MVB.

As with EGF stimulation, little co-localisation was observed between either receptor and LAMP2 without lysosomal and proteasomal inhibition, except after 60 minutes of LAP stimulation where EGFR colocalised with LAMP2 in approximately one-third of cells (7/17) (Figure 3.4 D). In the presence of lysosomal and proteasomal inhibitors, co-localisation of EGFR with LAMP2 was first observed after 30 minutes of LAP stimulation (4/15 cells) (Figure 3.4 C). The highest co-localisation between EGFR and LAMP2 was at 60 minutes, with almost all cells (13/15 cells) displaying this phenotype. This was still the predominant phenotype at 90 minutes (11/14 cells). In common with EGF stimulated trafficking, preliminary data shows αVβ6 did not colocalise with LAMP2 and is presumably targeted to alternative recycling trafficking routes. Co-localisation of EGFR and LAMP2 would indicate that despite αVβ6 engagement during EGFR internalisation rather than EGF, EGFR was still targeted for lysosomal degradation in agreement with its canonical trafficking route.

Together these preliminary data indicate that stimulation of MDA-MB-468 cells with EGF or LAP triggers the internalisation of αVβ6 and EGFR, which potentially traffic together to the MVB. Following this, EGFR is likely targeted for lysosomal degradation and αVβ6 potentially could be recycled. This suggests mutual and reciprocally-regulated trafficking mechanisms for αVβ6 and EGFR.

Preliminary immunofluorescence data indicated stimulation with either EGF or LAP triggered the endocytosis of both EGFR and αVβ6. To confirm this result, the rate of receptor internalisation was measured using a biotinylation receptor internalisation assay.

The rate of EGFR internalisation was unaffected by either EGF or LAP stimulation (Figure 3.5 A). This was unexpected as EGF stimulation canonically stimulates EGFR endocytosis. The unstimulated rate of EGFR internalisation was quite high however, suggesting any further

increase may not be measurable. Conclusions therefore cannot be made on the effect of LAP on EGFR internalisation in this experiment. Internalisation of αVβ6 was statistically significantly increased with EGF stimulation compared to the control (4 minutes: EGF mean= 4.06, SD= 2.63; control mean= 0.532, SD = 2.41; p= 0.021. 30 minutes: EGF mean= 12.84, SD= 6.97; control mean= 5.04, SD= 3.87; p= 0.016) (Figure 3.5 B), confirming the immunofluorescence trafficking results. By contrast, LAP stimulation had no effect on αVβ6 internalisation rates.

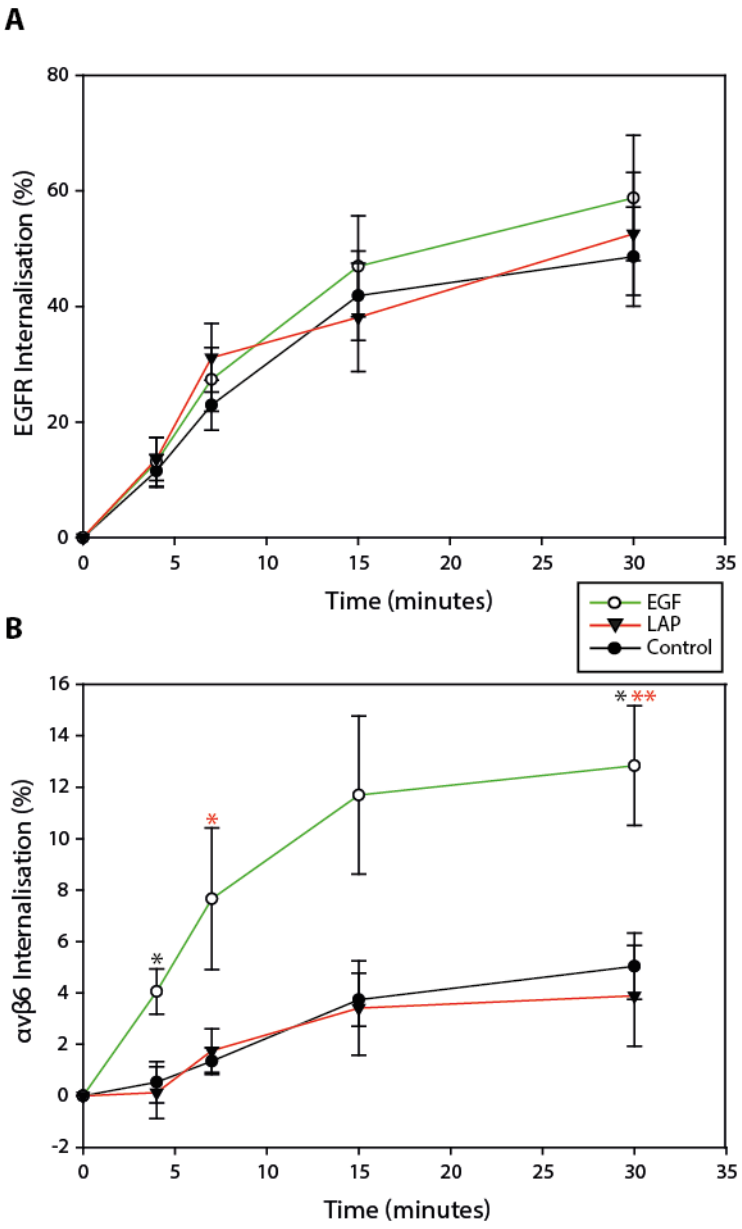

Figure 3.5 EGF increases rate of αvβ6 internalisation. Surface receptor internalisation assay percentage receptor internalisation of (A) EGFR (EGFR.1) and (B) αvβ6 (620W7) at 4, 7, 15 and 30 minutes with EGF (10 ng/ml) or LAP (0.5 µg/ml) stimulation. Receptor internalisation is expressed as a percentage of the total surface levels from unstimulated cells. Mean and SEM of data points is plotted. One-way ANOVA * = p< 0.05 EGF Vs control, ** = p< 0.01 EGF Vs LAP. N = 3.

Concomitant trafficking observed between EGFR and αVβ6 by immunofluorescence prompted the study of receptor dynamics with the anti-β6 clinical inhibitory antibody 264RAD (Eberlein et al., 2013). Inhibitory anti-αVβ6 antibodies can differentially affect its trafficking, for example constraining it at the cell surface, or stimulating endocytosis (Weinreb et al., 2004). BT-20 cells were seeded onto glass dishes in DMEM in the presence of 10% FBS and allowed to adhere and spread for four hours. Cells were then serum-starved for four-hours, prior to incubation with 10 μg/ml 264RAD. Cells were co-stained for αVβ6 and EGFR by immunofluorescence.

Receptor distribution was assessed using an arbitrary visual scale (Figure 3.6 A) of predominantly surface to internal distributions. Images were blinded for analysis, and αVβ6 and EGFR distribution was defined a value 0 – 4 using the scale for each cell. 264RAD incubation caused a more internal receptor distribution of both αVβ6 and EGFR (Figure 3.6B, C). This preliminary data suggests 264RAD stimulates the internalisation of both receptors, which could be an important consideration in its development as a αVβ6-targeting therapeutic.

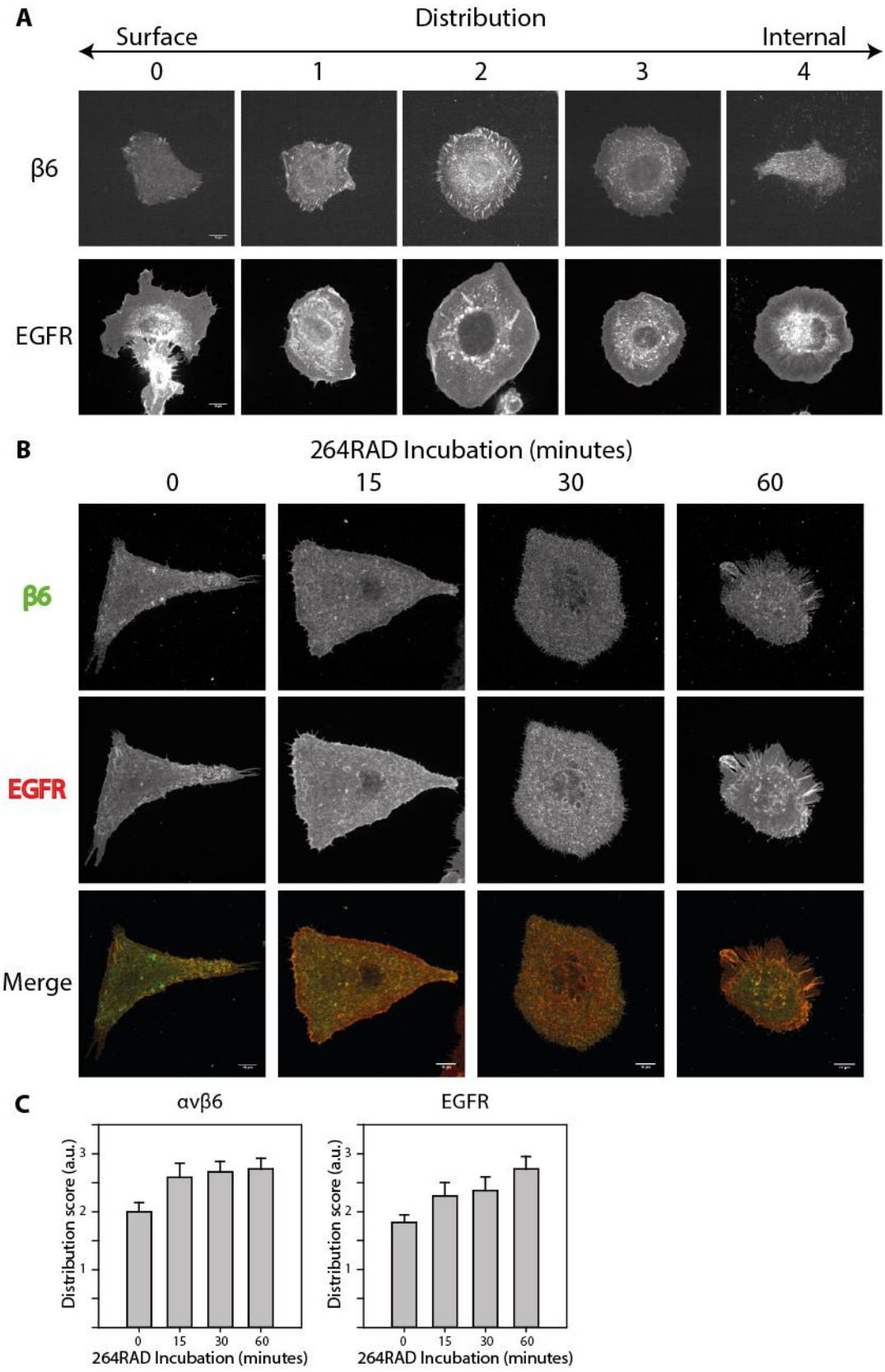

Figure 3.6 264RAD promotes a more intracellular subcellular distribution of integrin β6 and EGFR (D38B1) in BT-20s. (A) Arbitrary scale of predominantly surface to internal receptor distributions for β6 and EGFR (D38B1). (B) Representative images of β6 and EGFR with β6 inhibitor 264RAD incubation. Scale bar = 10μm. (C) Quantitation of distribution scale score for β6 and EGFR with 264RAD incubation. N=1, n= 10 - 15 cells per timepoint.

3.2.3 Collaborative signalling crosstalk

Response to the ligand EGF and the EGFR tyrosine kinase inhibitor gefitinib was assessed by measuring EGFR and ERK phosphorylation, to determine the appropriate concentrations to use experimentally. EGFR phosphorylation at tyrosine residue 1068 (Y1068) increased with EGF concentration (Figure 3.7 A). The residue Y1068 is auto-phosphorylated by EGFR upon ligand stimulated activation in a concentration dependent manner, below saturation (Tanaka et al., 2018). EGFR Y1068 phosphorylation does not plateau, indicating the saturation point is either between 30 – 100 ng/ml EGF or greater than 100 ng/ml EGF. EGFR Y1068 was phosphorylated post-serum starvation in the absence of EGF (Figure 3.7 A). Basal activation of EGFR occurs in ligand-independent activation mutants, however the cell line MDA-MB-468 has no documented mutations in EGFR (Forbes et al., 2017; Purba et al., 2017). ERK phosphorylation was increased with EGF stimulation in a concentration dependent manner (Figure 3.7 A). ERK is phosphorylated as part of the MAPK cascade that is activated downstream of EGFR phosphorylation. The optimal concentration of EGF concluded to use was 10 ng/ml, as this was below the point of EGFR and ERK phosphorylation saturation and is frequently used in the literature (Waterman and Yarden, 2001).

Gefitinib is a potent and selective EGFR inhibitor (Ki = 0.4 nM, www.kinasenet.ca) produced by AstraZeneca. Gefitinib suppressed EGFR Y1068 phosphorylation in a concentration dependent manner in the presence of EGF (Figure 3.7 B). Phosphorylation of ERK was not notably reduced at the concentrations trialled however. The maximum concentration AstraZeneca recommend gefitinib *in vitro* use is 1 µM, above which off-target effects due to inhibition of other tyrosine kinases may occur. The optimal concentration of gefitinib chosen based on data in figure 3.7 and commercial recommendations was 1 µM, to achieve maximal inhibition of EGFR and its downstream signalling.

Integrins and GFRs can signal collaboratively, activating common signalling pathways (Ivaska and Heino, 2011). To investigate if a signalling crosstalk mechanism exists between EGFR and αVβ6, both receptors were stimulated individually, and a panel of downstream signalling proteins were assessed for activation status.

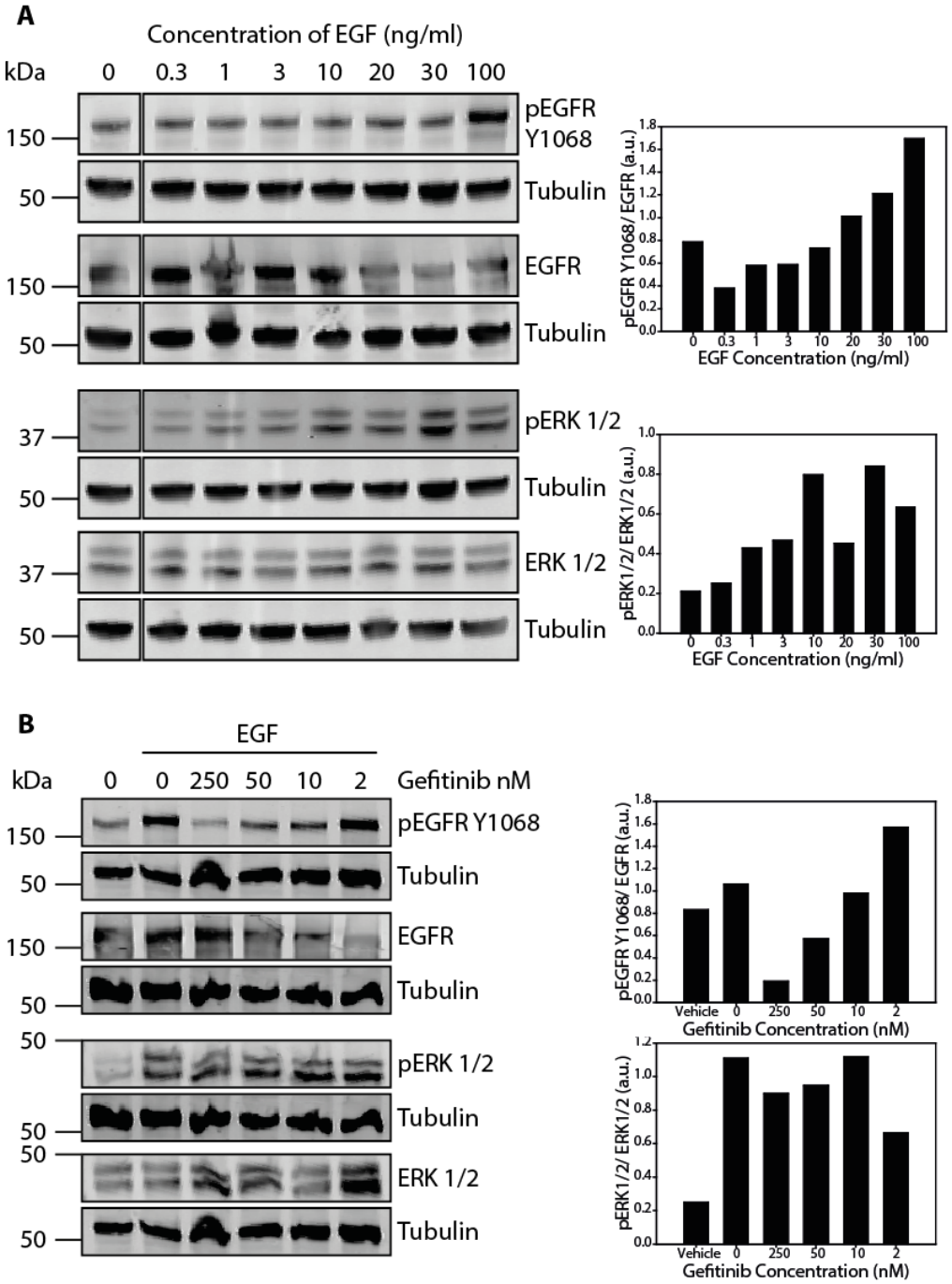

Figure 3.7 EGF and Gefitinib concentration titration. (A) Stimulation of serum starved MDA-MB-468 cells with 0.3 - 100 ng/ml EGF for 10 minutes. (B) Stimulation of serum starved MDA-MB-468 cells with 10 ng/ml EGF for 10 minutes after one-hour pre-incubation with a DMSO vehicle control or 2 - 250 nM of the EGFR kinase inhibitor gefitinib. Western blot of EGFR and ERK1/2 phosphorylation with accompanying quantification. N=1.

Signalling associated with EGFR stimulation was assessed by phosphorylation of EGFR, ERK, and Akt. ERK and Akt are phosphorylated and activated in the MAPK and PI3K-Akt signalling pathways respectively, which are canonically activated downstream of EGFR. Preliminary data showed stimulation with EGF triggered phosphorylation of EGFR, ERK and Akt (Figure 3.8 A, B). Stimulation with LAP triggered phosphorylation of ERK, however EGFR and Akt were unaffected (Figure 3.8 A, C). EGFR inhibition with gefitinib may partially inhibit LAP-mediated ERK phosphorylation however this is unclear due to variability.

Signalling associated with integrin adhesions was assessed by phosphorylation of paxillin, FAK and Src. The adaptor protein paxillin, and the kinases FAK and Src are canonical adhesion components, that are recruited to and phosphorylated at sites of integrin-mediated adhesions (Horton et al., 2015a). Their phosphorylation status can also be regulated by growth factor stimulation, including EGF (Eberwein et al., 2015). LAP is an endogenous ligand for αVβ6 and is likely to engage with primed integrin at the surface and stimulate the formation of adhesions. Preliminary data showed differences in paxillin, Src or FAK phosphorylation levels observed with EGF or LAP stimulation were not statistically significant, suggesting that engagement of αVβ6 to soluble LAP may not affect the overall dynamics of integrin-mediated adhesions in the cell (Figure 3.9).

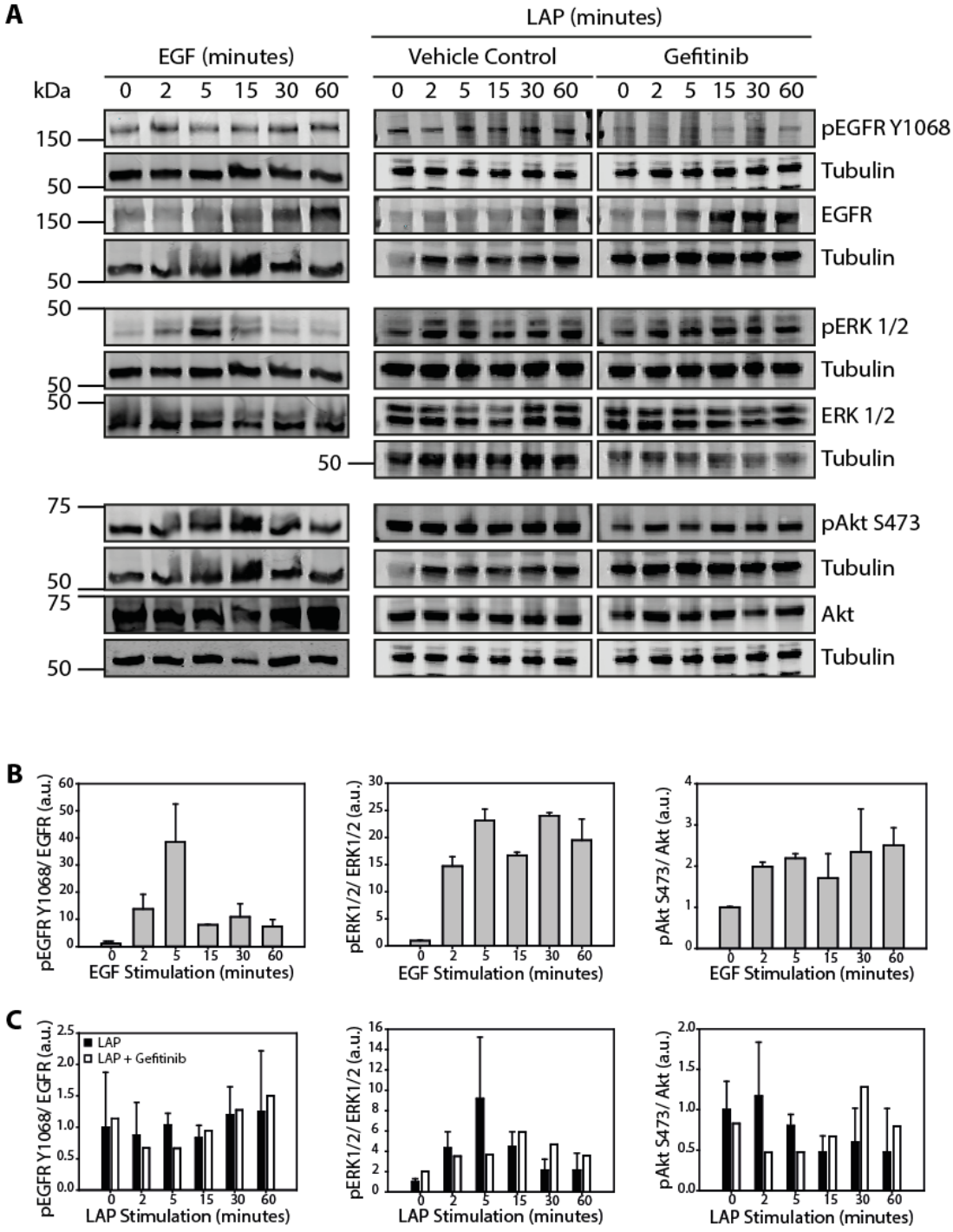

Figure 3.8 Effect of EGF and LAP stimulation on EGFR, ERK1/2 and Akt activity. (A) Stimulation of MDA-MB-468 cells with 10 ng/ml EGF; or 0.5 µg/ml LAP with DMSO vehicle control or 1 µM gefitinib (EGFR inhibitor). Western blots of phosphorylated and total levels of EGFR, ERK 1/2 and Akt. Quantification of phosphorylation relative to total protein levels with EGF (B) and LAP (C) stimulation. EGF stimulation N=2, LAP Stimulation N=2, LAP + Gefitinib N=1. Error bars = standard deviation. Black bar = LAP Stimulation, white bar = LAP + gefitinib

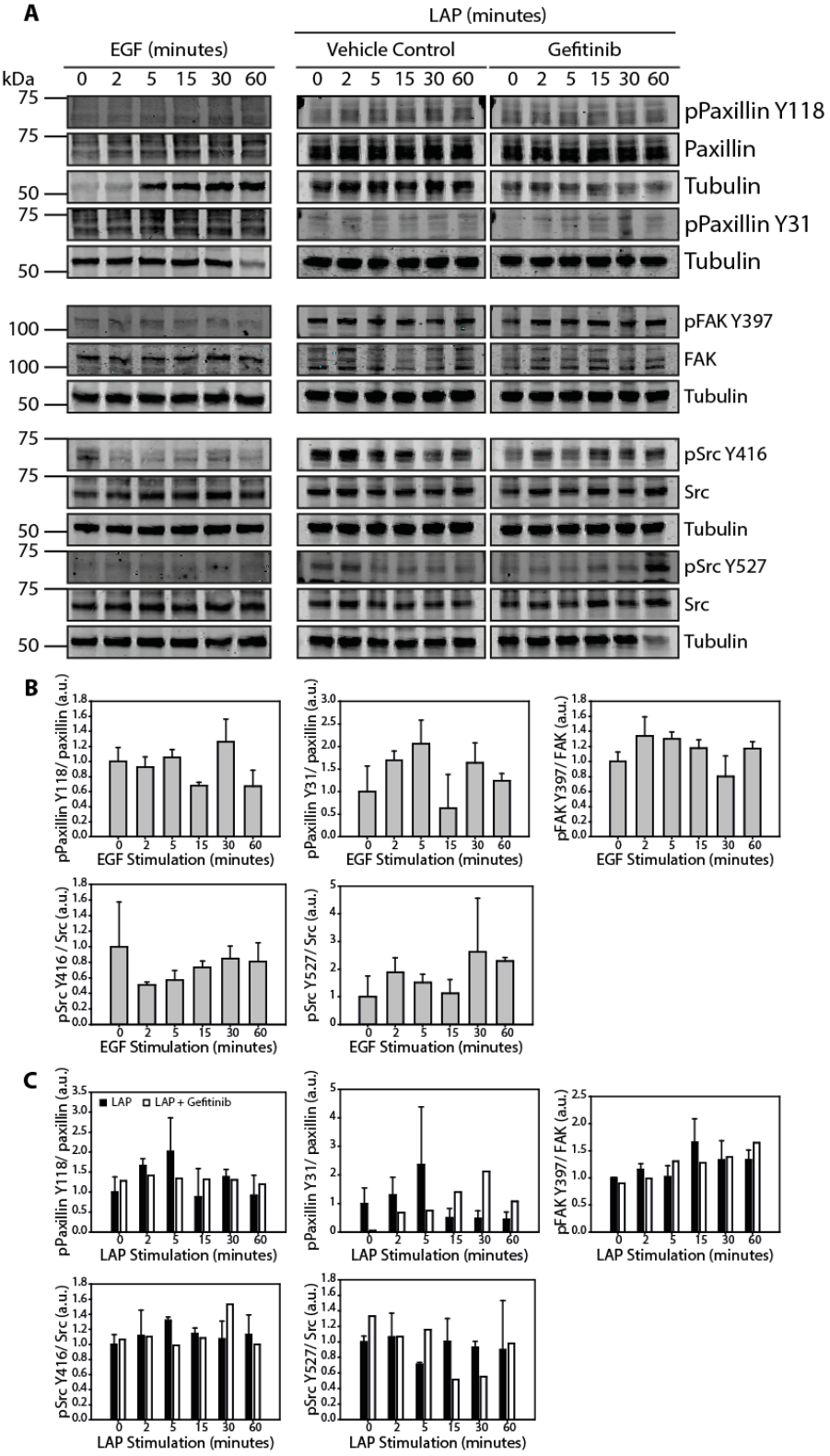

Figure 3.9 Effect of EGF and LAP stimulation on paxillin, FAK and Src activity. (A) Stimulation of MDA-MB-468 cells with 10 ng/ml EGF; or 0.5 µg/ml LAP with DMSO vehicle control or 1 µM gefitinib (EGFR inhibitor). Western blots of phosphorylated and total levels of paxillin, FAK and Src. Quantification of phosphorylation relative to total protein levels with EGF (B) and LAP (C) stimulation. EGF stimulation

N=2, LAP Stimulation N=2, LAP + gefitinib N=1. Error bars = standard deviation. Black bar = LAP Stimulation, white bar = LAP + gefitinib.

3.3 Discussion

The sub-cellular distribution of αVβ6 and EGFR was investigated in the TNBC cell line MDA-MB-468, and points of co-localisation were identified between αVβ6 and EGFR at sites of αVβ6-mediated ECM engagement, and in intracellular structures reminiscent of endosomes. Ligand stimulation experiments were combined with co-staining of endosomal markers to identify the nature of the internal structures that αVβ6 and EGFR co-localised at, and if ligand stimulation altered the distribution and trafficking of αVβ6 and EGFR. Stimulation with EGF and LAP caused the internalisation of both receptors, which co-localised at EEA1 and HRS positive endosomes. EGFR co-localisation was observed with the lysosome during later stimulation timepoints, suggesting EGFR is degraded. Signalling crosstalk was investigated by examining the phosphorylation status of signalling effectors downstream of integrin and EGFR signalling. These data revealed LAP stimulation causes the phosphorylation of ERK, which could potentially be mediated either directly downstream of αVβ6 or indirectly via ligand-independent stimulation of EGFR.

3.3.1 Cell line model

The cell line MDA-MB-468 was selected as the primary model for study, due to its TNBC status, and high expression of αVβ6 and EGFR. The EGFR gene is amplified in MDA-MB-468 cells (copy number 14, COSMIC database), therefore these cells represent a subset of TNBC that may be driven by EGFR amplification that could be more likely to respond to EGFR therapeutics (Chavez et al., 2010; Forbes et al., 2017). Cells can engage the ligand LAP via integrins αVβ6, αVβ1, αVβ8, αVβ3 and αVβ5 (Humphries et al., 2006; Worthington et al., 2011). MDA-MB-468 cells are positive for αVβ6, and possibly αVβ1, and negative for αVβ3 and αVβ5 expression. Expression of αVβ8 was not assessed, however has been reported (Meyer et al., 1998). The same research article also reports MDA-MB-468s are positive for αVβ5, which is in direct conflict our with flow cytometry data (Figure 3.1); however, highlighting differences in total and surface integrin expression, and potential variability in cell lines between laboratories and with passaging. The ligand LAP can therefore theoretically be engaged via αVβ6, αVβ1 and αVβ8 in MDA-MB-468s, meaning LAP is an αVβ6-selective but not αVβ6-specific ligand. However antibody-mediated functional blockade of αVβ6 in MDA-MB-468 cells reduces attachment to FN by 80%, indicating this is the primary integrin mediating FN binding (Singh et al., 2018).

3.3.2 Co-operation between αVβ6 and EGFR endocytosis

Preliminary data suggested stimulation with either EGF or LAP ligand triggered endocytosis of both αVβ6 and EGFR concomitantly. Different dynamics were observed for each receptor's endocytosis with EGF stimulation. EGFR co-localisation was observed with EEA1 prior to overlap with αVβ6 and persisted after αVβ6 had left EEA1 positive endosomes; indicating EGFR initially internalises before αVβ6 and continues endocytosing for longer. Cells overexpressing EGFR have slower rates of EGFR turnover, likely due to saturation of internalisation and degradation processes in trafficking (Sorkin and Goh, 2009). Saturation of clathrin-mediated endocytosis can result in a switch to slower non-clathrin-mediated endocytosis (Sorkin and Goh, 2009). Thus, it is possible that initial EGFR endocytosis could be clathrin-mediated, followed by slower non-clathrin-mediated mechanisms. Surface EGFR could continue endocytosing throughout the time-course, as cells are maintained in the presence of EGF throughout the experiment. Unlike EGFR, αVβ6 is not overexpressed in MDA-MB-468s therefore internalisation may be from a smaller finite pool that is endocytosed faster. Receptor dynamics were also different for HRS co-localisation with LAP stimulation. EGFR remained co-localised with HRS for longer than αVβ6. This indicates EGFR remains in the MVB whereas αVβ6 trafficking progresses onwards.

Under both ligand stimulations, EGFR appears to traffic to LAMP2 positive lysosomes however αVβ6 does not. Integrins are predominantly recycled, therefore it is likely that αVβ6 is in recycling endosomes or returned to the plasma membrane (De Franceschi et al., 2015). Internalisation and recycling rates reported for integrins are consistent with the plasma membrane pool of integrins trafficking through the endosomal system and returning to the plasma membrane in 30 minutes (Caswell and Norman, 2006). Whilst we have not analysed recycling dynamics for αVβ6, it is conceivable that the internalised pool of αVβ6 could be recycled within the time-course of these experiments. Integrin αVβ6 may also traffic to the trans-golgi network, as recycling integrins can also progress via this compartment (Mana et al., 2016; Riggs et al., 2012). Trafficking integrins have also been reported to be degraded in a proteasomal-dependent manner, although this is not thought to be a predominant mechanism indicating it is an unlikely fate for αVβ6 (Liu et al., 2011b). A proportion of EGFR may also be recycled or degraded at the proteasome, however the canonical fate for EGFR is lysosomal degradation (Sorkin and von Zastrow, 2009).

Preliminary immunofluorescence data indicated stimulation with EGF and LAP induced the internalisation of αVβ6 and EGFR. Biochemical internalisation assays confirmed EGF stimulation statistically significantly increases αVβ6 internalisation. However, conflictingly

stimulation with LAP did not affect the rate of αVβ6 internalisation measured in these assays. Soluble LAP has not previously been demonstrated to stimulate the internalisation of integrins and nothing is known about the likely magnitude of response. It is possible an effect would be seen at higher concentrations of LAP. Due to the nature of the assays, the biochemical approach measures an average global population of internalised receptor, whereas immunofluorescence identifies smaller internal pools and subcellular distributions. The effect of LAP on αVβ6 distribution could have been too subtle to be detected biochemically. The rate of receptor internalisation could also be underestimated due to receptor recycling, which was not inhibited in these assays (Rainero et al., 2013). Differences between the experimental set-ups could also have affected the results, such as the thermal cycling of cells between 4°C and 37°C in the biochemical assay, which can affect the microtubule network and was not employed in the immunofluorescence experiments (Rainero et al., 2013).

No effect was seen with either EGF or LAP on the rate of EGFR internalisation. This was unexpected as ligand-stimulated endocytosis is a well-defined mechanism for EGFR internalisation (Sorkin and Goh, 2008). The baseline unstimulated rate of EGFR internalisation was very high, potentially masking any differences with EGF or LAP stimulated conditions. This high baseline indicates EGFR is undergoing constitutive endo-exocytic cycling in the absence of ligand. EGFR can undergo constitutive endocytosis; however ligand-stimulation is thought to be the predominant mechanism of EGFR internalisation (Goh and Sorkin, 2013). Basal phosphorylation of EGFR at Y1068 observed in MDA-MB-468 cells (Figure 3.7) could potentially result in higher levels of constitutive endocytosis. The adaptor protein Grb2 which is recruited to active EGFR by binding to phosphorylated Y1068 and Y1086 is essential for EGF-stimulated EGFR internalisation (Huang and Sorkin, 2005). Basal phosphorylated Y1068 could recruit Grb2 and promote EGFR endocytosis. Conflicting evidence in the literature has shown a kinase dead EGFR mutant was internalised at the same rate as wild-type EGFR following EGF stimulation, leading to the conclusion that dimerisation of EGFR following EGF stimulation was more crucial than kinase domain activation for internalisation (Wang et al., 2005). Overexpression of EGFR in MDA-MB-468 cells could increase the chance of spontaneous dimer formation due to higher receptor concentration on the surface, which may promote constitutive endocytosis.

Incubation of BT-20 cells with the clinical αVβ6 inhibitory antibody 264RAD caused the internalisation of αVβ6 and EGFR. This is the first demonstration of the effect of 264RAD on αVβ6 subcellular distribution. Xenograft studies show treatment with 264RAD decreases

αVβ6 protein level in the tumours, although the mechanism for this is unclear (Eberlein et al., 2013; Moore et al., 2014). It is likely due to the statistically significant decrease in tumour volume that the loss of αVβ6 protein levels is due to selective targeting of αVβ6-positive tumour cells. Stimulation of αVβ6 internalisation provides an additional hypothesis for the loss of αVβ6 protein levels, as this could potentially result in protein degradation if αVβ6 is sorted towards degradative pathways. Stimulation of EGFR internalisation with 264RAD could also result in decreased EGFR levels, especially as endocytosed EGFR is predominantly degraded.

3.3.3 Signalling Crosstalk

Preliminary data showed stimulation of MDA-MB-468 cells with LAP caused phosphorylation of ERK. This phosphorylation is likely mediated downstream of αVβ6 either directly, or indirectly via GFRs such as EGFR. Grb2 can be recruited to phosphorylated FAK at Y925, activating ERK directly downstream of integrin-mediated adhesions (Schlaepfer et al., 1994). Integrin-mediated activation of ERK has been postulated to be a more important mechanism if growth factor supply is limited (Giancotti and Ruoslahti, 1999). Integrins can also activate GFR signalling pathways indirectly, for example by promoting GFR activity or influencing GFR trafficking (Ivaska and Heino, 2011).

Stimulation with LAP did not affect EGFR pY1068 or Akt S473 phosphorylation, indicating a mechanism specific to the Ras-MAPK signalling pathway. Incubation of cells with the EGFR inhibitor gefitinib did not statistically significantly prevent LAP-mediated ERK phosphorylation. This could suggest crosstalk between LAP stimulated αVβ6 and EGFR signalling is unlikely to directly affect EGFR. It is important to note however MDA-MB-468 cells are resistant to gefitinib (IC_{50} = 6.8 μM) (Normanno et al., 2006), and treatment with gefitinib in our experiments did not suppress ERK phosphorylation, indicating PI3K-MAPK pathway activity. Unpublished data from Professor John Marshall, Barts Cancer Institute London, has demonstrated LAP-mediated ERK phosphorylation was reduced with 1 μM gefitinib in BT-20 cells indicating this mechanism could be via EGFR. Expression of αVβ6 is reported to be required for ERK phosphorylation, as siRNA-mediated knockdown reduced EGF stimulated ERK phosphorylation three-fold (Ahmed et al., 2002a). This strengthens the hypothesis that αVβ6-mediated ERK phosphorylation is due to crosstalk between αVβ6 and EGFR signalling pathways.

No changes were observed in phosphorylation of paxillin, FAK or Src in response to EGF or LAP stimulation. Paxillin, FAK and Src become phosphorylated during adhesion formation and

can be dynamically regulated in adhesions (Robertson et al., 2015). Soluble LAP is a ligand for αVβ6 and therefore will engage αVβ6 at the cell surface initiating adhesions. A critical step in the progression from early nascent to more mature focal adhesions is the binding of talin and application of force, strengthening the adhesion and recruiting additional components (Wolfenson et al., 2013). The fact LAP is added as a soluble ligand means that force cannot be generated at these adhesions, as traction cannot be generated without anchoring of the ligand. Consequently paxillin, FAK and Src may not be recruited to these adhesions and phosphorylated, and therefore no changes would be observed. Additionally, most adhesions are likely to have been formed prior to stimulation, as cells were incubated to adhere and spread; therefore, small changes may not be detected.

Trafficking and signalling crosstalk demonstrated between αVβ6 and EGFR is likely to regulate cellular processes controlled by αVβ6 and EGFR. Trafficking is an important mechanism by which receptor dynamics is regulated, which impacts processes mediated by their ligand engagement such as signalling and engagement of the ECM. Signalling crosstalk demonstrates αVβ6 influences signalling downstream of EGFR, which could for example promote the stimulation of cell proliferation mediated by the MAPK pathway. These processes are likely to have potential clinical relevance to cancer, as they contribute to the pro-invasive and pro-mitogenic functions of αVβ6 and EGFR, respectively. Localisation of EGFR at sites of αVβ6-mediated LAP engagement indicates EGFR is a component of αVβ6-mediated adhesions. If so, other proteins associated with αVβ6 adhesions may have a role in mediating crosstalk between αVβ6 and EGFR, for example by facilitating their co-internalisation in response to ligand engagement. Unbiased proteomic analysis of αVβ6-mediated adhesions formed on the ligand LAP will aim to elucidate this.

4. The αVβ6-specific adhesome

4.1 Introduction

Integrin engagement of ECM ligands triggers recruitment of proteins to the integrin cytoplasmic domains. Integrins have no intrinsic catalytic activity or actin binding capacity and therefore rely on cytoplasmic adaptors and enzymatic proteins to exert their functions. Classically integrin-mediated adhesions can be sub-divided into nascent adhesions, focal complexes, focal adhesions and fibrillar adhesions (Wolfenson et al., 2013). These adhesions form sequentially and mature with the application of mechanical force. The canonical view of adhesion assembly is that integrin binding triggers rapid recruitment of paxillin and FAK, followed by talin and vinculin which provide a mechanical link to the actin cytoskeleton (Lawson and Schlaepfer, 2012). Integrin adhesion complexes (IACs) have been described as having three functionally distinct layers: 1) a membrane-proximal integrin signalling layer with integrin cytoplasmic domains, paxillin and FAK; 2) an intermediate force-transduction layer with talin and vinculin, and 3) a distal actin-regulatory layer with zyxin, VASP and α-actinin (Kanchanawong et al., 2010). Talin spans all three layers, orientated with its head domain directly binding integrin cytoplasmic domains, and tail domain binding actin (Kanchanawong et al., 2010). Temporal changes during adhesion assembly and disassembly support the hierarchical distribution theory that the first proteins to be recruited are the last to be removed, with integrins remaining most stable throughout disassembly (Horton et al., 2015a).

IACs contain core structural and force-transducing proteins, and non-canonical proteins that are differentially recruited in response to environmental factors. Fluorescence recovery after photobleaching (FRAP) studies have demonstrated the dynamic exchange of proteins at adhesion sites (Carisey et al., 2013; Rossier et al., 2012). The core of adhesions complexes can be described as 'meta-stable' as it is robust, yet dynamic, as it undergoes turnover (Humphries et al., 2015). The integrin adhesome is defined as a set of proteins that localise to and regulate integrin-mediated adhesions (Humphries et al., 2015). Previously knowledge of the adhesome was based on the 'literature-curated adhesome', which estimated the network consisted of more than 200 proteins (Winograd-Katz et al., 2014). More recently adhesion isolation techniques combined with non-biased MS analyses have identified a more complex larger network of proteins (Horton et al., 2015a).

Multiple proteomic datasets of enriched IACs have been integrated to identify a canonical (proteins identified in ≥ five of the seven datasets) and meta (proteins identified in ≥ one

dataset) adhesome (Horton et al., 2015a). The canonical adhesome is 60 proteins that are consistently recruited to IACs and are likely to represent core adhesion machinery. The non-canonical meta-adhesome is 2,352 proteins that are more variably recruited. Proteins identified in few datasets are likely to be context specific, low-abundance or difficult to detect by MS. Protein-protein interaction (PPI) network analysis revealed the consensus adhesome clustered into four signalling networks based on ILK–PINCH–kindlin, FAK–paxillin, talin–vinculin and α-actinin–zyxin–VASP (Horton et al., 2015a).

Unbiased protocols were developed to analyse isolated IACs by MS to circumvent the bias of candidate-driven techniques such as immunoblotting immunoprecipitations (Humphries et al., 2015). This enabled global analysis of adhesion signalling networks and revealed complexity that exceeded candidate-driven approaches. These techniques yielded proteins previously known to be canonical components of IACs as expected, with additional new components not previously isolated or identified. Components could be sub-divided into those with known functions relating to adhesion biology, proteins with domains in common with characterised adhesion proteins, and those with previously unlinked roles (Humphries et al., 2015).

Proteomic analysis and downstream validation have led to the discovery of novel components with previously unknown roles (Humphries et al., 2009). Proteomic analysis can also determine IAC compositional distinctions between different ECM ligands and heterodimers. Analysis of IACs formed via α5β1 or α4β1 revealed common and specific components, despite the shared β1 subunit (Humphries et al., 2009). Complexes specific to αV and β1 have also been analysed by generating pan-integrin-null cell lines and re-expressing subunits (Schiller et al., 2013).

The two main IAC isolation methods involve the use of ECM or antibody coated micro-beads or 2D surfaces. These protocols enrich for integrin-mediated adhesions with their local plasma membrane and cytosolic environments (Jones et al., 2015). The first method developed was micro-bead isolation (Humphries et al., 2009). Cells were incubated in suspension with magnetic micro-beads coated with ECM ligand or antibody. Adhesions were stabilised and the cell body was removed by sonication, followed by separation of the beads with bound adhesion complexes. Proteins were then eluted from the beads. This method had disadvantages as some canonical adhesion components were absent from the isolates, and some cell types routinely engulfed the beads during their incubation (Jones et al., 2015). This lead to the development of the IAC enrichment protocol, from cells plated on 2D cell culture

surfaces coated with ECM ligands, this allows cells to form load-bearing adhesion structures prior to DTBP cross-linking (Figure 4.1). Cell bodies are then removed to isolate ventral membrane preparations enriched for IACs, either by hydrodynamic force or sonication. The remaining IACs adherent to the 2D-surface are collected by scraping (Jones et al., 2015). The hydrodynamic force method is advantageous for assessing temporal changes in adhesion complexes, such as with the addition of an external stimulus. The sonication method is more time-consuming, but is easier to standardise, more stringent and results in fewer contaminants.

IAC MS datasets differ between cell types, ligands and integrin heterodimers. This was highlighted in the meta-adhesome database, where over half of the proteins were unique to a single dataset (Horton et al., 2015a). Targeted approaches can elucidate IACs recruited to specific integrin subunits or heterodimers, which can give functional insight. Integrin αVβ6 is pro-invasive and linked to a poor prognosis in a range of cancers (Raab-Westphal et al., 2017). Despite this αVβ6 is a relatively under-studied integrin and little is known about its cancer-associated functions and interactome. Thus αVβ6 IACs was studied in the TNBC cell line MDA-MB-468s, as αVβ6 is linked to a poor prognosis in TNBC (Unpublished data, Louise Jones, Barts Cancer Institute, London), and TNBC is an aggressive form of breast cancer that particularly affects younger women (< 50 years) with no current targeted therapies (Jitariu et al., 2017). The implication of αVβ6 as a potential therapeutic target for TNBC is novel and driven by our unpublished data in collaboration with the Marshall and Jones labs. The αVβ6-associated IAC was characterised to give insight into proteins that were differentially recruited to αVβ6 IACs, which provided insight into its functions and mechanisms by which αVβ6 promotes cell invasion.

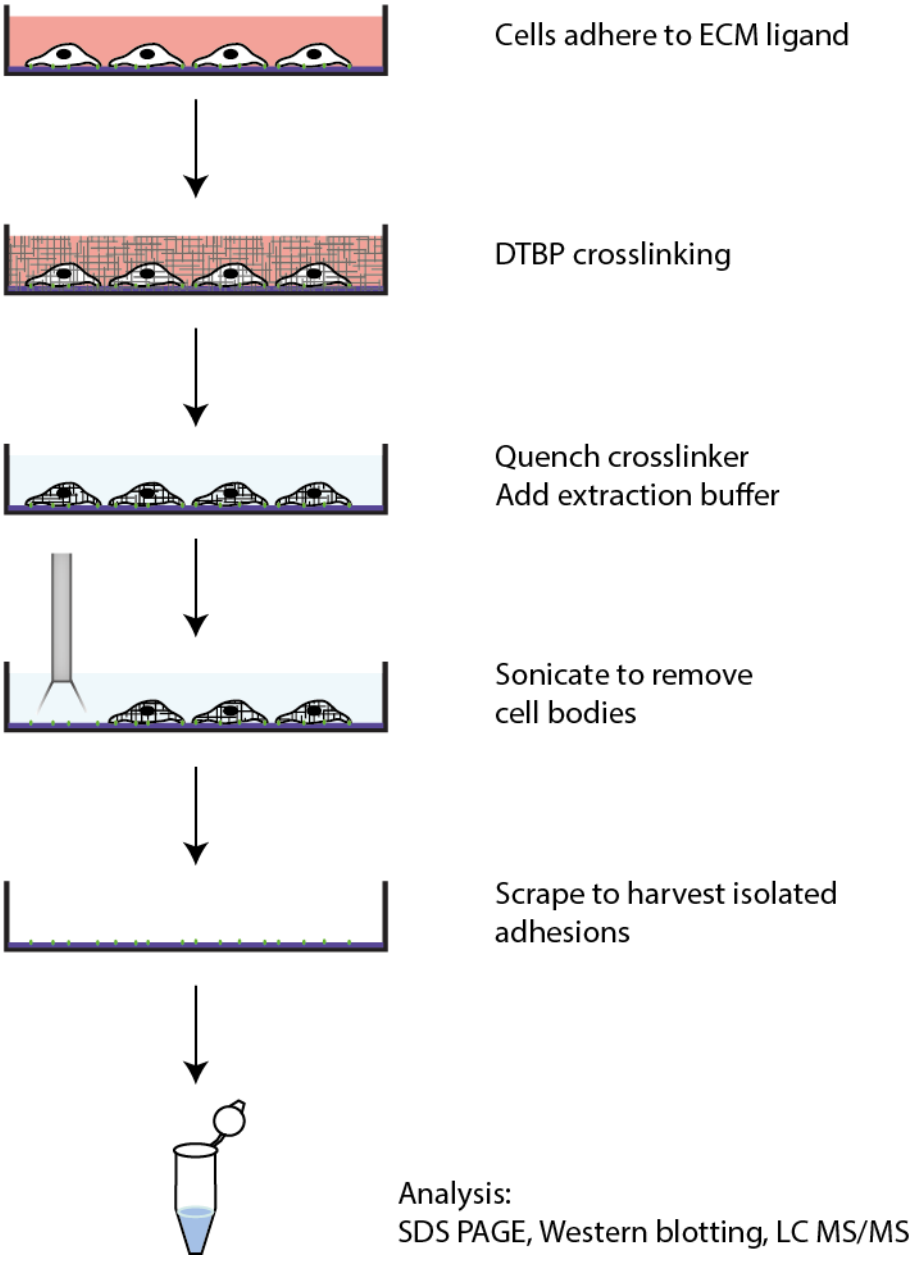

Figure 4.1 Schematic of integrin associated complex adhesion isolation protocol. Cells are allowed to spread and adhere onto plates coated with an ECM ligand. Protein interactions are then stabilised with the cell permeable crosslinker DTBP. The crosslinker is then quenched and extraction buffer is added to the cells. Sonication is used to remove the cell body, leaving isolated adhesion complexes, which are then harvested by scarping. Composition of the samples can then be analysed by western blotting or LC MS/MS.

4.2 Results

4.2.1 αVβ6 adhesions

Three ECM ligands were used for pairwise comparisons to elucidate proteins selectively recruited to αVβ6-mediated IACs. IACs were isolated from MDA-MB-468 cells plated on 2D plastic coated with either FN, LAP or Collagen I ECM ligands. Collagen I was used as a negative control, as this cannot be engaged by αVβ6. FN and LAP ligands will be used to compare a mixed integrin environment of RGD and LDV binding integrins including αVβ6, and an αVβ6-selective environment of LAP binding integrins, respectively.

Initial validation of isolated IAC samples, prior to MS analysis, was achieved by immunoblotting for constituents of the samples. Focal adhesion components were probed for to confirm their presence, and negative controls that localise to other sub-cellular compartments were used to indicate their enrichment in IACs relative to the TCL.

LAP-associated IACs were enriched in integrin β6, αV, vinculin and talin (Figure 4.2). Integrin β6 was enriched on LAP compared to FN, and absent on collagen, confirming LAP is β6-selective. Integrin β1 was detected in the TCL but not in the IAC samples. While Src was not detected by immunoblotting in the experiment presented in figure 4.2, Src was identified in all IACs from replicates 2 and 3 (Figure S6 and S7). The negative controls GAPDH (cytoplasmic), BAK (mitochondrial) HSP70 and HSP90 (endoplasmic reticulum) were absent or substantially lower than the TCL in the IAC samples, indicating purity of the isolation.

Interestingly, EGFR was observed specifically on LAP isolated IACs (Figure 4.2). EGFR was probed for as previous data demonstrated colocalisation of EGFR with αVβ6 at points of matrix engagement (Figure 3.2), and EGF stimulation induced endocytosis of αVβ6, indicating EGFR may have a role in αVβ6 adhesion dynamics (Figure 3.5).

Canonical adhesion components appeared most abundant in the LAP condition, this is possibly due to enrichment, however could also be due to a higher concentration of the sample. Protein concentration of the IAC samples cannot be estimated as the composition of the reducing sample buffer used to harvest the samples does not permit measurement by standard methods such as the BCA or Bradford assays (Jones et al., 2015). This was not an issue however for proteomic analyses, as total peptide abundance is considered during data normalisation.

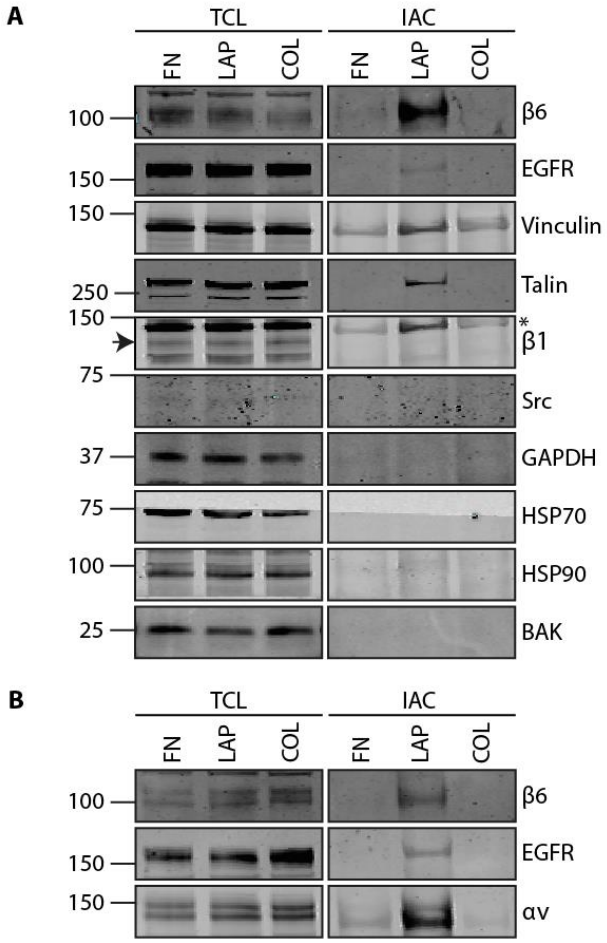

Figure 4.2 Validation of integrin-associated complex enrichment. Western blotting in total cell lysate (TCL) and isolated integrin-associated complexes (IAC) for the adhesome components integrin β6, β1, vinculin, talin, Src (GD11), EGFR (sc-03), and negative control proteins GAPDH, HSP70, HSP90 and BAK from other subcellular compartments. (A) Representative blots of N1 that was analysed subsequently by mass spectrometry. Arrow indicates detection of β1 integrin, asterisk indicates detection of vinculin from previous probe. (B) β6, EGFR and αv from replicate N3 demonstrating αv recruitment to FN and LAP IACs. Full N3 panel in figure S7.

4.2.2 Dataset quality and trends

IAC samples were processed and analysed by MS to identify a αVβ6-associated network in an unbiased way. Reproducibility across the dataset between three biological replicates was assessed using pairwise scatter plots (Figure 4.3). Pearson correlation coefficient values for the normalized spectral abundance factor (NSAF) values were all ≥ 0.85, indicating good reproducibility between biological replicates.

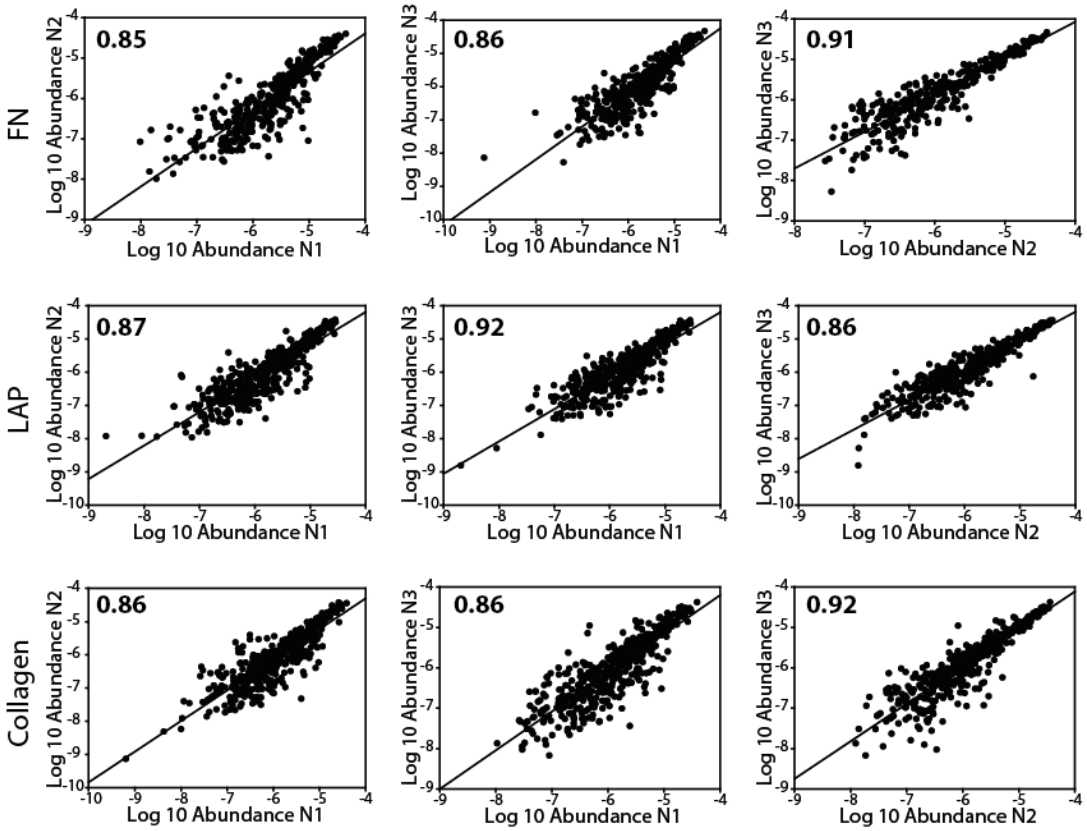

Figure 4.3: Scatter plots with regression lines. Pairwise comparison of log 10 transformed protein abundance normalized spectral abundance factor (NSAF) values between replicates for fibronectin, LAP and collagen ligand samples. Pearsson correlation coefficient value is indicated in the top left of each graph.

Unique proteins were not included in the scatterplot analysis, but were included in Venn diagram representations (Figure 4.4 A). The first biological replicate identified the greatest number of proteins, which is reflected in the fact it has the most unique proteins. Out of the total number of proteins identified (790), 505 were common between all replicates, indicating reasonable consistency. Venn diagrams were also constructed to indicate the shared and unique proteins identified on each ligand (Figure 4.4 B). A similar number of proteins were identified on each ligand, indicating a similar level of total protein isolated. The majority of proteins (581) were shared across all ligands, which is a similar order of

magnitude to other published proteomic datasets analysing different cell types and integrin heterodimers (Horton et al., 2015a; Schiller et al., 2013).

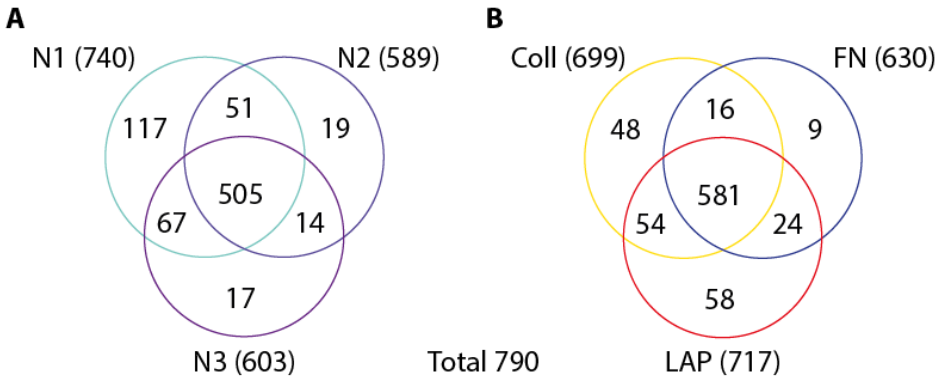

Figure 4.4 Venn Diagrams demonstrating the degree of shared and unique proteins between replicates (A) and ligands (B). Replicates indicate the total number of proteins pooled from all three ligands from each biological replicate. Ligands indicate the total number of proteins isolated from adhesions on each ligand from all three biological replicates. Total proteins identified = 790.

Thresholds for protein identification were applied to the dataset. The peptide threshold was > 4 peptide counts and identified in ≥ 2 biological replicate. Thresholds used in previous adhesome studies for IAC MS analysis are typically ≥ 4 spectral counts and/or ≥ 2 unique peptides, which is a comparative level of stringency to our thresholds (Horton et al., 2015a). Proteins which were unreviewed in the UniProtKB database were also removed as these are computer-annotated entries derived from the translation of coding sequences (Consortium, 2011). Pairwise analysis of protein-normalised intensity values (intensity values normalised to total protein amount) were made between LAP and Collagen, and LAP and FN (Figure 4.5). Most proteins were < two-fold different between ligands (57.5% LAP/collagen, 64.5% LAP/FN); indicating the majority are not differentially recruited to different integrin-mediated IACs. Fewer proteins were ≥ two-fold different between LAP/FN than LAP/collagen, indicating the IACs are more similar between LAP and FN than LAP and collagen (Figure 4.5 A). This was expected as αVβ6 binds both LAP and FN, there are more common integrin subunits that are bind LAP and non-LAP RGD ligand binding, than collagen. A greater number of proteins are enriched on LAP (122 proteins) compared to FN (33 proteins) (Figure 4.5 B). This is in agreement with data suggesting αVβ6 is the predominant integrin engaged on FN (Singh et al., 2018), as the majority of proteins isolated from FN IACs are likely to be present and enriched on LAP as this represents an αVβ6-selective environment.

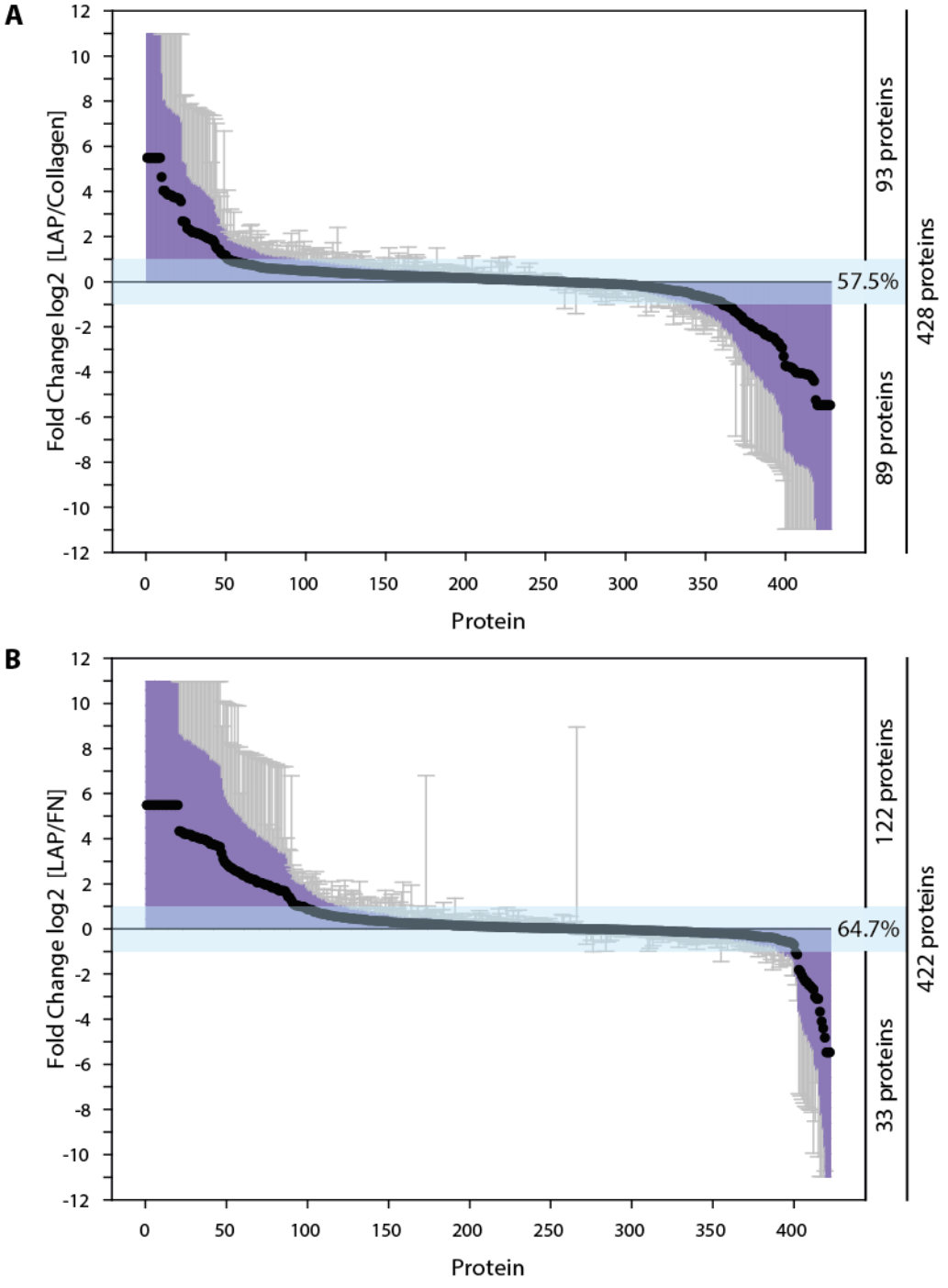

Figure 4.5 Fold change of proteins between ligand conditions. Low abundance (fewer than 5 peptides and/or unique to one N) and unreviewed UniProt proteins were removed from the dataset, yielding a total of 428 proteins. Graphs show ratios of normalised intensity values for log2 (A) [LAP/Collagen] and (B) [LAP Vs FN], mean ± SEM, N = 3 for each protein. Light blue shading corresponds to ≤ two-fold change. (A) LAP Vs Collagen, 428 proteins in total, 57.5% of dataset (93 and 89 proteins increased and decreased, respectively). (B) LAP Vs FN, 422 proteins in total, 64.7% of dataset (122 and 33 proteins increased and decreased, respectively).

4.2.3 Comparison to the literature-curated adhesome

The un-thresholded dataset (unreviewed proteins removed, without peptide threshold) was compared with the curated consensus- and meta-adhesome to determine which proteins from these datasets were identified (Horton et al., 2015a). Coverage of both the consensus (35%, 21 proteins) and meta-adhesome (20%, 468 proteins) was achieved (Figure 4.6). The coverage of the consensus adhesome is comparatively low, as these proteins were detected in ≥ five of the seven MS datasets used to curate the adhesome, and thus represent canonically recruited proteins. This divergence is interesting as it could represent novel IAC composition in αVβ6-mediated adhesions, TNBC cells, and adhesions formed on LAP ligands; all of which were previously unknown.

The consensus adhesome contains four clustered modules based on known interactions and signalling axes (Horton et al., 2015a). Our dataset contains all the high evidence direct integrin interactors in the networks (α-actinin, talin, tensin, kindlin and filamin) (Horton et al., 2015a) (See figure S8 for a visual representation). However, except for four proteins (TGM2, ANXA1, IQGAP and VCL), no other connected network proteins were detected. Of the reported consensus adhesome, 16 proteins were unconnected to the main network and had no known adhesive functions. Eleven of these were present in our dataset (ALYREF, BRIX1, DDX18, DDX27, DIMT1, DNAJB1, FEN1, H1FX, POLDIP3, RPL23A and SYNCRIP), all of which have roles in DNA or RNA regulation.

Whilst protein translation typically occurs in the endoplasmic reticulum or cytosol, proteins with roles in translation can localise to different subcellular structures. This can facilitate spatial compartmentalisation of translation that may be energetically favourable (Humphries et al., 2015). Local translation has also been demonstrated as a mechanism of controlling protein localisation to cell protrusions in migration (Mardakheh et al., 2015). Questions remain in the field about the relevance of these proteins at adhesions despite growing evidence, as many RNA binding proteins are common contaminants (Humphries et al., 2015; Mellacheruvu et al., 2013).

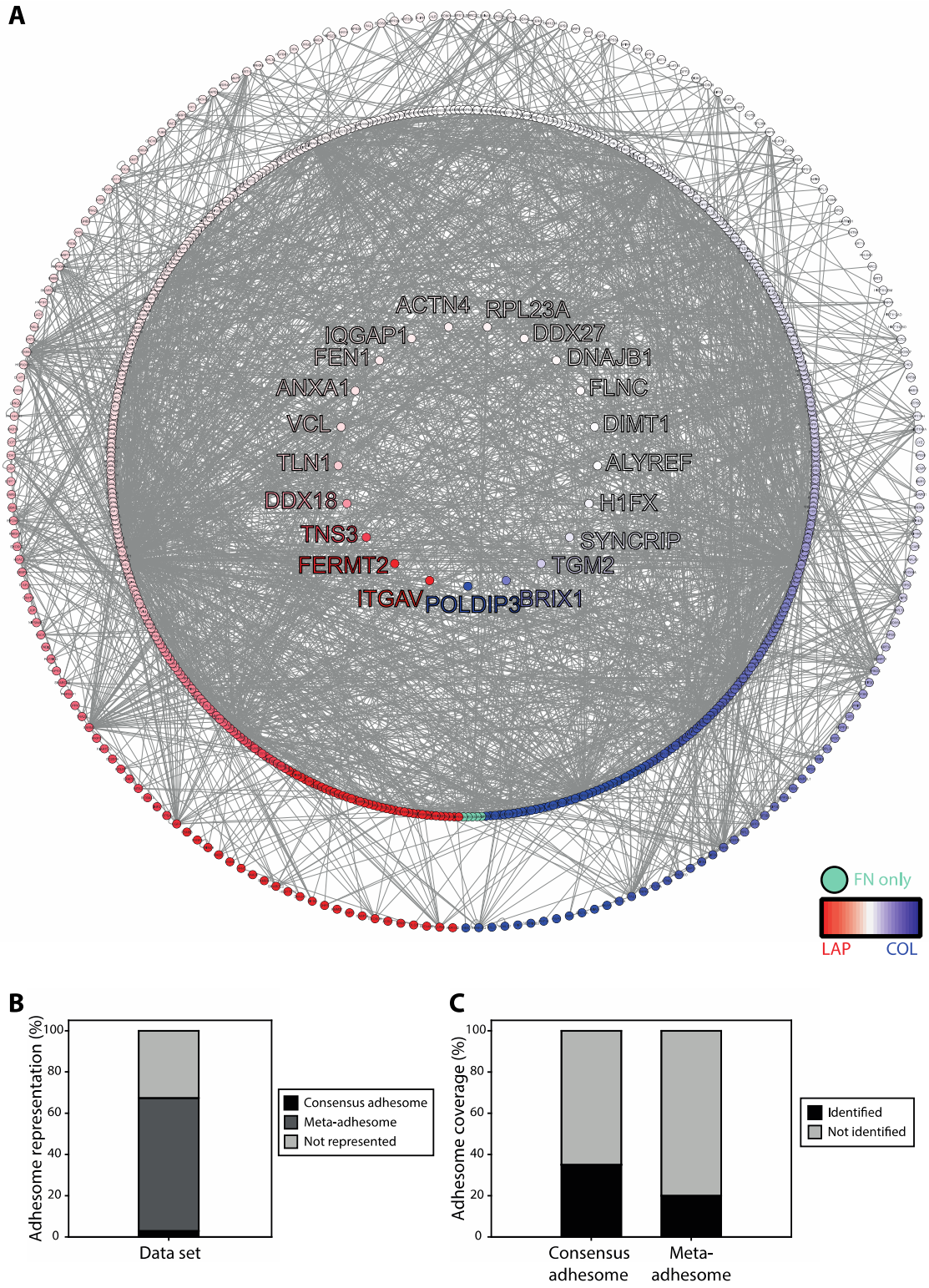

Figure 4.6 Representation of consensus and meta adhesome dataset coverage. 35% of the consensus adhesome (21 proteins), inner ring; 20% of the meta adhesome (468 proteins), middle ring. Proteins in the outer ring were not reported in the consensus or meta adhesome (219 proteins). Total number of proteins = 726. Nodes represent proteins and edges are known interactions. Node colour red to blue gradient = log2 fold enrichment on LAP versus collagen. Green = FN specific proteins. (B) Percent of the IAC dataset represented by the consensus adhesome (3%) and meta-adhesome (62%). (C) Percent of the consensus adhesome (35%) and meta-adhesome (20%) identified in the IAC dataset.

30% of the dataset was not represented in either the consensus or meta-adhesome. Considerable divergence between this dataset and the curated adhesome is likely to be due to differences in experimental conditions. Five out of the seven datasets that comprised the adhesome were isolated from fibroblasts, and none used the ligands collagen or LAP (Horton et al., 2015a). Fibroblasts do not normally express αVβ6, so it is unlikely any proteins specifically recruited to αVβ6 IACs were identified. Adhesions formed on collagen and LAP will recruit different combinations of integrin heterodimers and therefore different IACs that consequently may recruit different novel signalling proteins.

Our dataset was also compared to the literature-curated adhesome database from www.adhesome.org, which is divided into intrinsic and associated proteins (Winograd-Katz et al., 2014; Zaidel-Bar et al., 2007) (Table 4.1). Our dataset had 8% (19 proteins) of the total literature-curated adhesome database, consisting of 11% (16 proteins) of the intrinsic and 4% (3 proteins) of the associated proteins. Our database has a lower percentage coverage of the associated proteins, as these are less robustly recruited to IACs. Whereas our dataset has a higher percentage coverage of the consensus adhesome, which reflects the similarity in the protocols of isolation and identification.

Literature-curated Adhesome (150)						Both				Consensus Adhesome (60)					
CFL1	CORO1B	CORO2A	CTTN	ENAH	FLNA	ACTN1	LASP1	VASP		ACTN4	ANXA1	CALD1	CNN2	FHL3	Actin regulation
KEAP1	MACF1	MYH9	NEXN	SVIL						FLNC	IQGAP1	LIMD1	PALLD	PDLIM1	
										PDLIM5	PDLIM7	PLS3	RSU1	SIPA1	
										TNS3					
ACTB	BCAR1	CASS4	CAV1	CRK	CRKL	FHL2	FBLIM1	FERMT2	LIMS1						Adaptors
EZR	FERMT1	FERMT3	GAB1	GNB2L1	GRB2	LPP	PARVA	PXN	SORBS3						
GRB7	HAX1	ITGB1BP1	JUB	LDB3	LIMS2	TES	TLN1	TRIP6	VCL						
LPXN	MSN	NCK2	NDEL1	NEDD9	NF2	ZYX									
NUDT16L1	OSTF1	PALLD	PARVB	PPFIA1	RDX										
SDCBP	SH2B1	SH3KBP1	SMPX	SORBS2	SYNM										
TENC1	TGFB1I1	TNS1	ZFYVE21												
CD151	ITGA1	ITGA10	ITGA11	ITGA2	ITGA3	ITGA5	ITGAV	ITGB1	ITGB3						Adhesion Receptor
ITGA4	ITGA6	ITGA7	ITGA8	ITGA9	ITGAD										
ITGAE	ITGAL	ITGAM	ITGAW	ITGAX	ITGB2										
ITGB4	ITGB5	ITGB6	ITGB7	ITGB8	KTN1										
LRP1	NRP1	NRP2	PVR	SDC4	SLC3A2										
AGAP2	ARHGAP24	ARHGAP26	ARHGEF6	ASAP2	ASAP3	ARHGEF7	GIT2								GTPase
DDEF1	DEF6	DLC1	DNM2	DOCK1	ELMO1										
GIT1	GRLF1	RASA1	RHOU	STARD13											
ABL1	PAK1	PDPK1	PEAK1	PRKCA	PTK2B	CSK	ILK	PTK2							Kinase
SRC															
INPP5D	INPPL1	PPM1F	PPM1M	PPP2CA	PTPN11										Phosphatase
PTPN12	PTPN6	PTPRA	PTPRF												

Literature-curated Adhesome (150)	Both	Consensus Adhesome (60)	
ITGB3BP **RAVER1** STAT3		ALYREF BRIX1 **DDX18** **DDX27** DIMT1 DNAJB1 FAU FEN1 H1FX HP1BP3 MRTO4 POLDIP3 PPIB RPL23A SYNCRIP	DNA or RNA
CALR PDE4D PKD1 PLCG1 PRNP SPTLC1 TGFB1I1 TRPM7		P4HB **TGM2**	Various

Table 4.1: Dataset mapping onto the literature-curated and MS derived consensus adhesome. The literature-curated adhesome consists of 232 proteins from the database at www.adhesome.org. Only 'intrinsic proteins' rather than 'associated proteins' were used in these analyses. The consensus adhesome refers to the curated MS dataset of 60 proteins, defined by Horton et al. Proteins are grouped according to their annotation in the www.adhesome.org database. The group 'GTPase' contains GTPases and regulators, and the group 'DNA or RNA' includes all proteins with functions associated with DNA and RNA. The following proteins were listed under 'various' as their groups were formed of ≤ two proteins: PDE4D, PKD1, TRPM7, CALR, PLCG1, SPTLC1, PRNP, TGFB1I1, P4HB, TGM2. Of these, only TGM2 was present in our dataset. 19/232 (8.2%) of the total adhesome dataset, 16/150 (10.7%) of the intrinsic proteins, 3/82 (3.7%) associated proteins were present in our dataset. 21/60 (35%) of the consensus adhesome proteins were present in our dataset. Proteins in our dataset are shown in red. Proteins that were ≥ two-fold enriched on the ligand LAP are shown in bold and underlined.

4.2.4 Global analysis

To characterise the αVβ6-associated adhesome by identifying compositional changes in IAC proteomes formed on different ligands, fold change of protein detection was compared between LAP and collagen, and LAP and FN conditions. Protein-protein interaction (PPI) networks were constructed in Cytoscape (version 3.6.1) and interactions were mapped using the Protein Interaction Network Analysis (PINA) interactome database (release date 21/05/2014) (Wu et al., 2009) supplemented with a literature curated database of IAC proteins (Robertson et al., 2015; Zaidel-Bar et al., 2007). Three proteins could not be mapped (E9PAV3, NACA; Q9BQ48, MRPL34; E9PRG8, c11orf98) as these were not present in the PPI with matrisome component database. Networks were constructed for proteins that were ≥ 1.5, 2 and 5-fold different. On LAP versus collagen 183 proteins were ≥ 2-fold different (Figure 4.7), 256 were ≥ 1.5-fold different (Figure S9) and 113 were ≥ 5-fold different (Figure S10). On LAP versus FN 154 proteins were ≥ 2-fold different (Figure 4.8), 201 were ≥ 1.5-fold different (Figure S11) and 110 were ≥ 5-fold different (Figure S12). A ≥ two-fold change threshold was chosen for analysis as it has been used consistently in the literature and identifies differences without compromising network connectivity (Horton et al., 2016b).

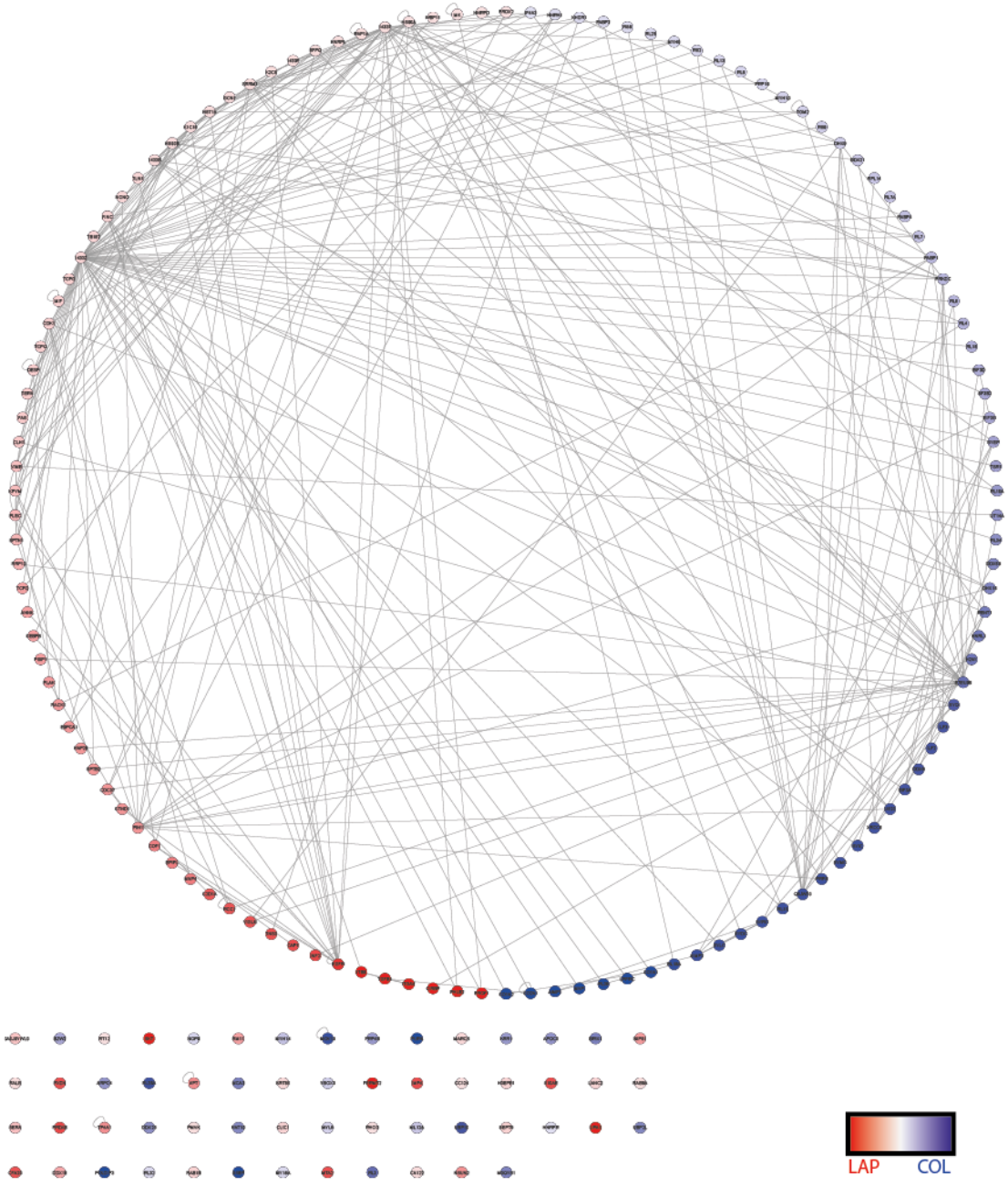

Figure 4.7 ≥ two-fold different proteins on LAP versus collagen. Total number of proteins = 183. Nodes represent proteins and edges are known interactions. Node colour red to blue gradient = log2 fold enrichment LAP/collagen.

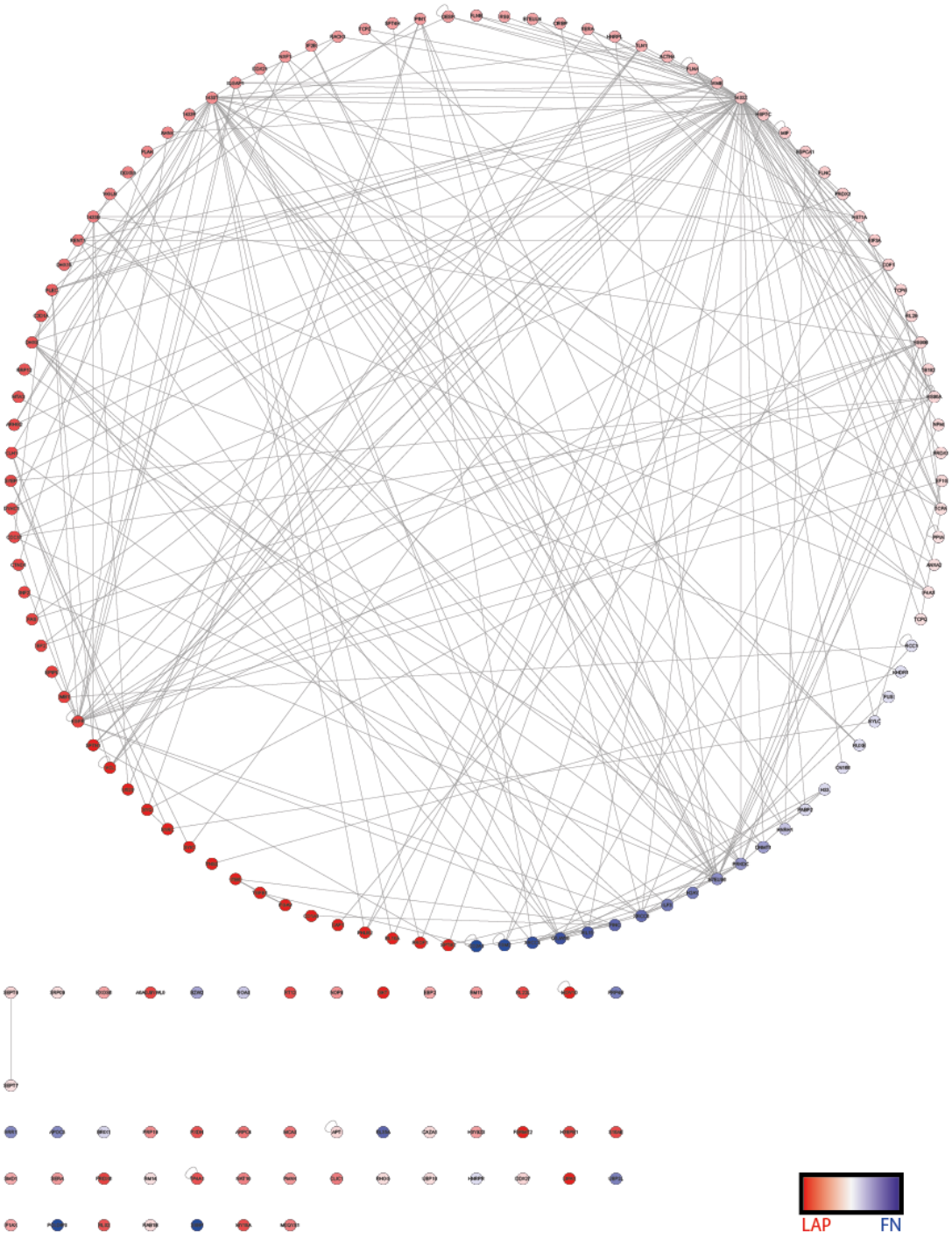

Figure 4.8: ≥ two-fold different proteins on LAP versus fibronectin. Total number of proteins = 154. Nodes represent proteins and edges are known interactions. Node colour red to blue gradient = log2 fold enrichment LAP/FN.

To provide additional stringency to the two-fold change threshold, statistical significance of protein NSAF value between ligands was assessed. Proteins that were statistically significantly different between ligands (p=<0.05) were mapped according to log_2 fold enrichment to LAP (LAP/FN, LAP/collagen) (Figure 4.9). Proteins with p values < 0.01 are presented with individual labelling in supplementary figure S13. De-enrichment of proteins on LAP relative to FN or collagen, suggests exclusion from αVβ6-mediated IACs. Proteins significantly enriched on LAP in either or both comparisons indicate these are likely to be enriched in αVβ6-mediated IACs.

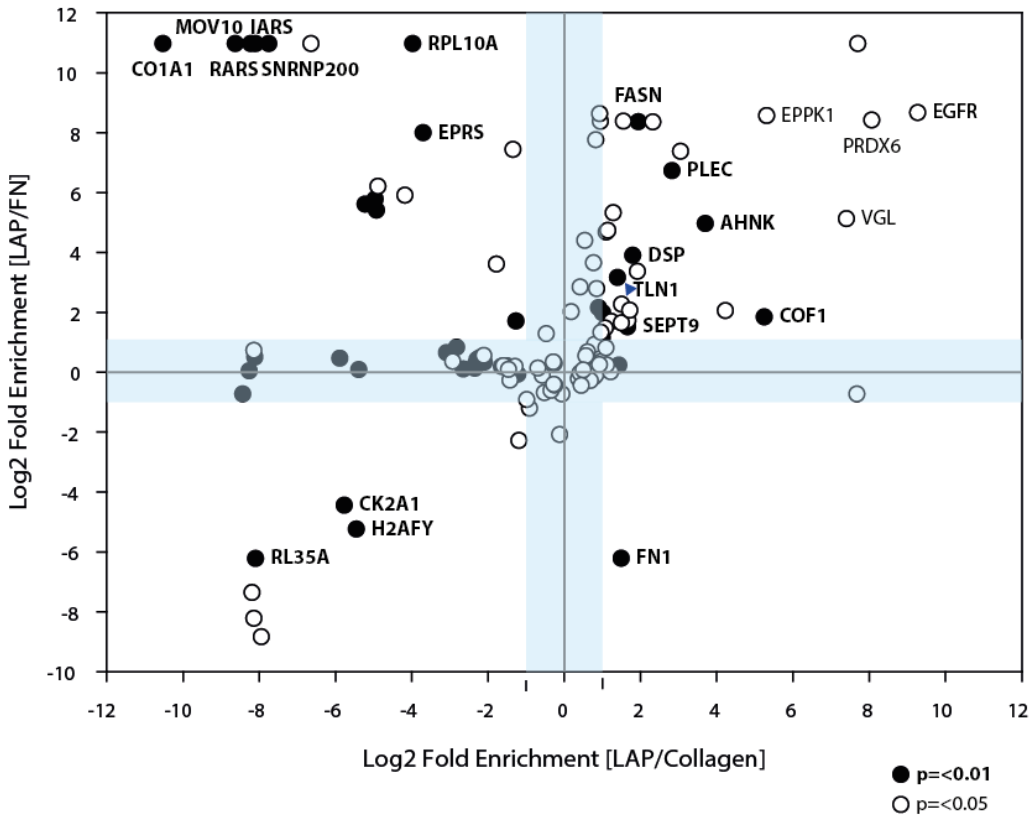

Figure 4.9: Statistically significantly different proteins between ligands. Analysis of variance (ANOVA) between LAP, FN and collagen ligands normalized spectral abundance factor (NSAF) values. Statistical analysis was performed in Scaffold (version 4). Statistically significantly different proteins (p=<0.05) were mapped by log2 fold enrichment of LAP/ FN and LAP/collagen. Light blue shading corresponds to ≤ two-fold change. Black and white circles correspond to a significance value of p=<0.01 and <0.05, respectively. Gene names of key proteins are indicated in bold or regular text for p=<0.01 and p=<0.05, respectively. Blue arrow head indicates datapoint for TLN1.

A protein-protein interaction network was constructed for statistically significantly different proteins that were enriched on both LAP/FN and LAP/FN, LAP/FN only and LAP/Collagen only (represented by the top right, top left and bottom right quadrants in Figure 4.9), arranged in

a hierarchical ring network (Figure 4.10). Of these proteins, 48% were unconnected by interaction to any others in the network, however the remaining clustered together in an interconnected ring. As expected, integrin β6 was clustered interacting with integrin αV, TGFβ1 and talin, forming the core of an αVβ6 adhesion. Peptide analysis revealed that TGFβ identification corresponded to the uncleaved precursor form of TGFβ that is bound to LAP. Therefore, here TGFβ represents the experimental ligand LAP used during the IAC isolation.

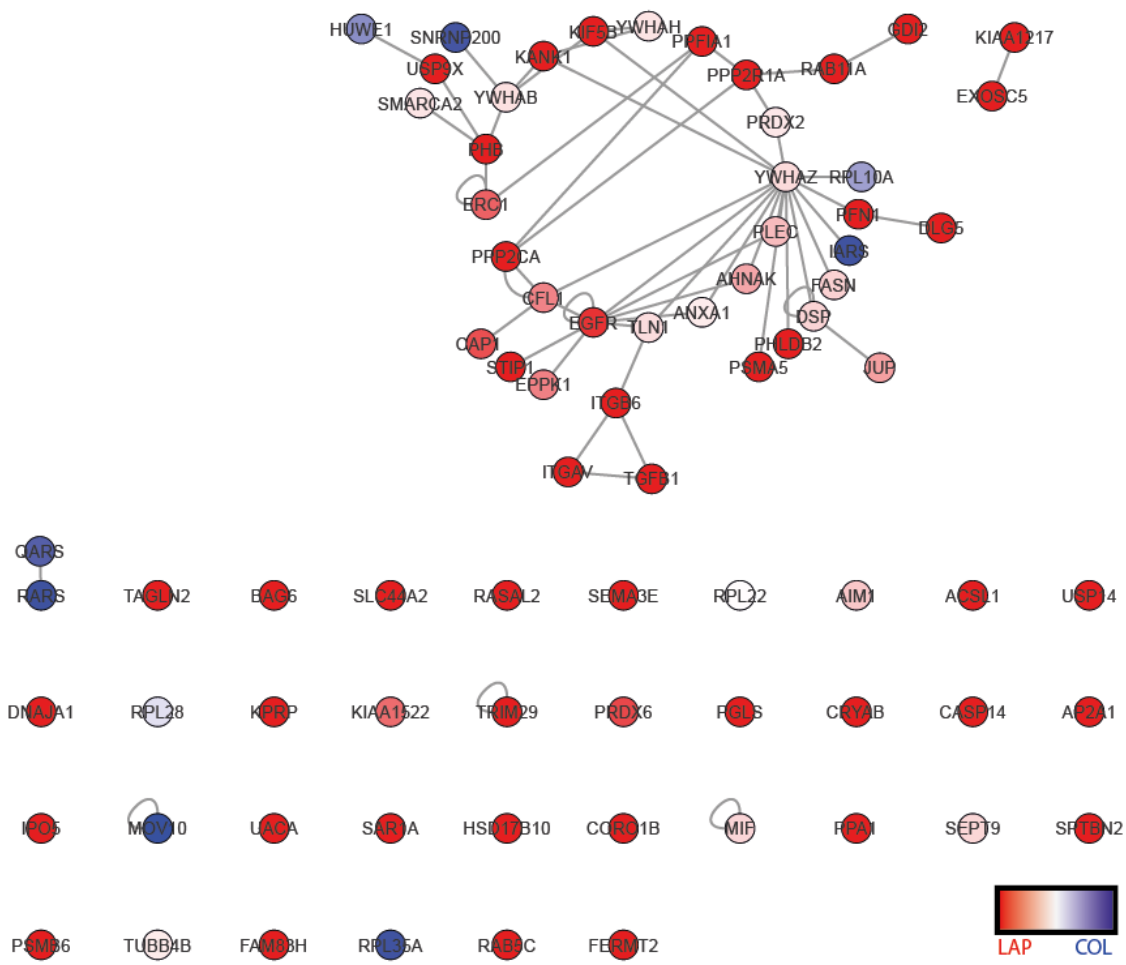

Figure 4.10: Interaction network of proteins statistically significantly different between ligands and enriched on LAP. Proteins arranged in a hierarchical ring network. Nodes represent proteins, and edges are known interactions. Node colour red to blue gradient = log2 fold enrichment LAP/collagen. Proteins that are enriched on collagen compared to LAP (represented in blue) are positively enriched on LAP compared to FN.

Functional enrichment analysis was performed on proteins statistically significantly different and enriched on LAP. Over-representation of gene ontology (GO) term analysis was performed with KEGG (Kyoto Encyclopedia of Genes and Genomes) and Reactome pathway terms. GO term grouping was used to combine related terms into groups. KEGG term analysis identified enrichment of proteins associated with ErbB signalling, cytokine-cytokine receptor

interactions, Hippo pathway signalling, arrhythmogenic right ventricular cardiomyopathy (ARVC), MAPK signalling, fatty acid biosynthesis and endocytosis (Figure 4.11, Table 4.2).

This identifies EGFR signalling as a key component of αVβ6 IACs, as ErbB signalling was the highest represented term. Interestingly, based on these analyses, ErbB signalling is more over-represented than adhesion signalling related terms, indicating it is highly prominent. Over-representation of Hippo pathway signalling, and fatty acid biosynthesis also suggests a potential role for αVβ6 in these processes. Reactome pathway analysis also identified ErbB signalling as an overrepresented term, represented by the RAF/MAPK cascade group (Figure 4.12).

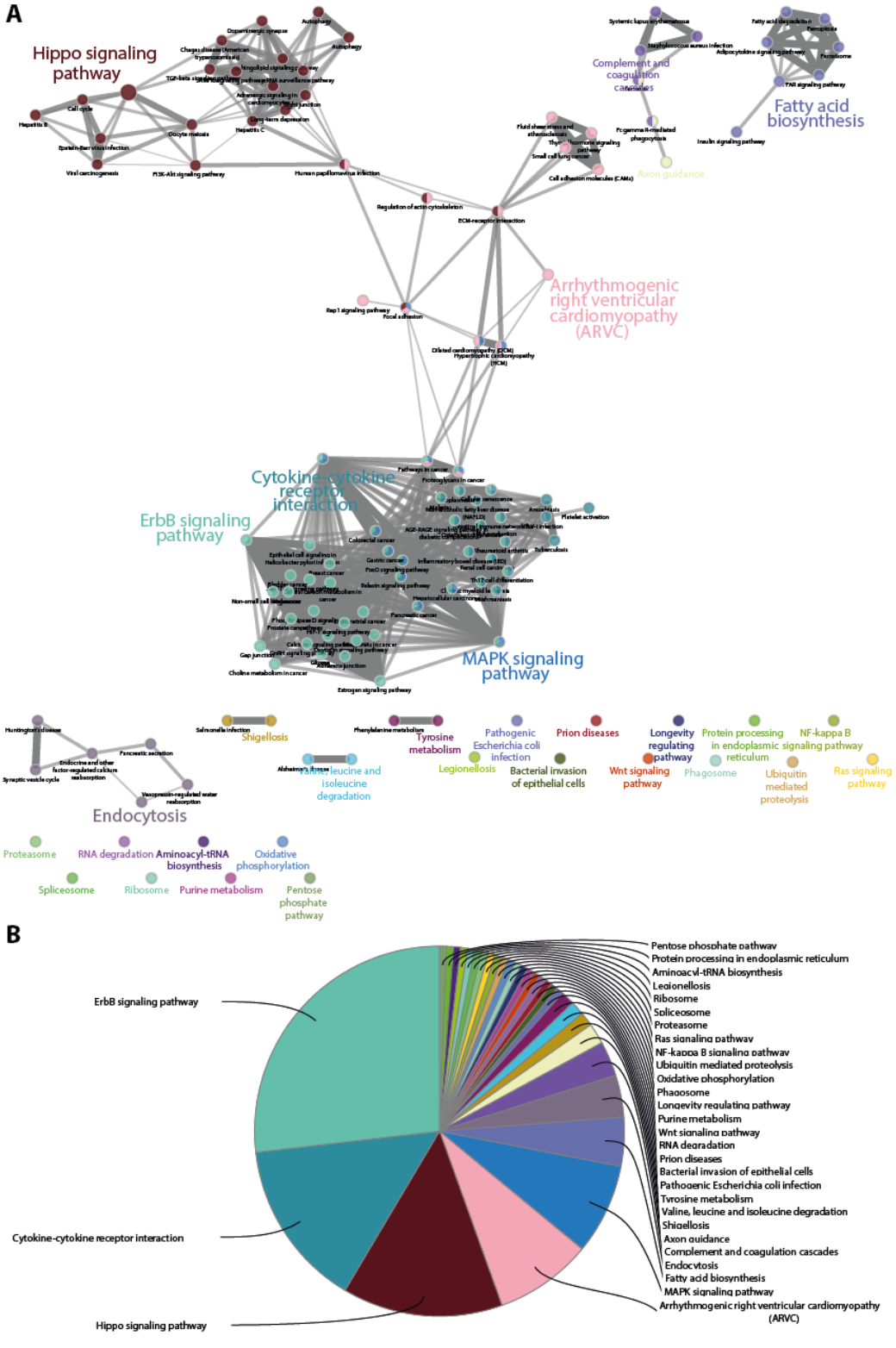

Figure 4.11: ClueGO KEGG Pathway term hierarchical clustering. (A) ClueGO hierarchical layout of represented KEGG terms. Node colour corresponds to grouping, with the lead term in corresponding coloured text. Nodes with split colours belong to multiple groups. Nodes represent individual KEGG pathway terms. (B) Pie-chart organised by the % of genes per term. Analysis parameters: minimum 1 gene per cluster, GO term/pathway network connectivity (Kappa score) =1; Statistical test Enrichment/Depletion (Two-sided hypergeometric test), Bonferroni p value correction, no p value threshold applied; GO term grouping based on kappa score, 50% of genes for group merge, 50% terms for group merge. Leading group term based on % gene/term.

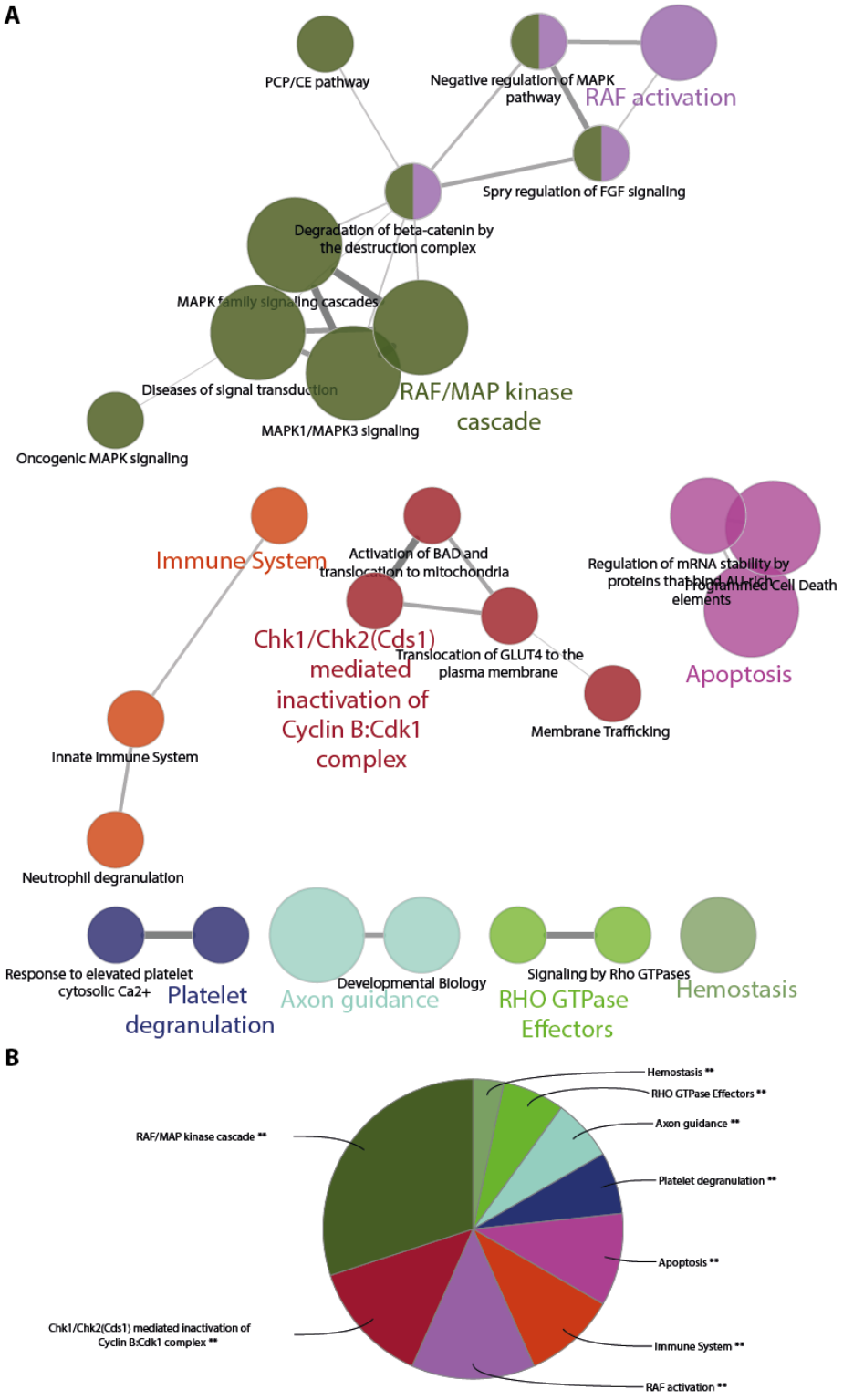

Figure 4.12: ClueGO Reactome Pathway term hierarchical clustering. (A) ClueGO hierarchical layout of represented KEGG terms. Node colour corresponds to grouping, with the lead term in corresponding coloured text. Nodes with split colours belong to multiple groups. Nodes represent individual KEGG pathway terms. (B) Pie-chart organised by the % of genes per term. Analysis parameters: minimum 1 gene per cluster, GO term/pathway network connectivity (Kappa score) =1; Statistical test Enrichment/Depletion (Two-sided hypergeometric test), Bonferroni p value correction, p value threshold <0.05 applied; GO term grouping based on kappa score, 50% of genes for group merge, 50% terms for group merge. Leading group term based on %gene/term.

Leading Group Term	Unique ID	Group p value	Bonferroni	Group Genes	All Term genes
ErbB signalling pathway	KEGG:04012	0.011	0.278	EGFR, ITGAV, SLC44A2, SMARCC2, TGFB1, TUBB2B.	EGFR, PAK4
Cytokine-cytokine receptor interaction	KEGG:04060	0.033	0.789	EGFR, RAB5C, TGFB1, TLN1	EGFR, FASN, TGFB1
Hippo signalling pathway	KEGG:04390	0.503	1.000	CFL1, EGFR, FASN, ITGAV, ITGB6, KIF5B, PFN1, PPP2CA, PPP2R1A, TGFB1, TLN1, YWHAB, YWHAH, YWHAZ	ACTB, PPP1CA, PPP2CA, PPP2R1A, PRKCI, TGFB1, YWHAB, YWHAH, YWHAQ, YWHAZ
Arrhythmogenic right ventricular cardiomyopathy (ARVC)	KEGG:05412	0.347	1.000	CFL1, DSG2, DSP, EGFR, ITGAV, ITGB6, PFN1, PPP2CA, PPP2R1A, TGFB1, TLN1	ACTB, DSP, ITGA2, ITGAV, ITGB6, JUP, LMNA
MAPK signalling pathway	KEGG:04010	0.451	1.000	EGFR, ITGAV, ITGB6, SMARCC2, TGFB1, TLN1	CDC42, EGFR, FASN, FLNA, FLNB, FLNC, GNG12, HSPA1A, HSPA8, HSPB1, RAC1, RAC2, RAP1A, TGFB1, TP53
Fatty acid biosynthesis	KEGG:00061	1.000	1.000	ACSL1, FASN	ACSL1, FASN
Endocytosis	KEGG:04144	0.608	1.000	AP2A1, EGFR, KIF5B, RAB11A, RAB5C	AP2A1, ARF6, ARPC3, ARPC4, CAPZA1, CDC42, CHMP4B, CHMP5, CHMP6, CLTC, EGFR, HSPA1A, HSPA8, KIF5B, PRKCI, RAB11A, RAB5C, RAB8A, RHOA

Table 4.2: KEGG GO Term analysis. Top group leading terms and their unique GO term ID. Statistical p values for each group, and the Bonferroni step-down corrected p value. Group genes lists all the genes within the group. All term genes list all genes that are associated with the group leading term, that are present in the entire MS dataset.

4.2.5 Key subnetworks

Having identified the GO terms over-represented by proteins statistically significantly enriched on LAP, proteomic analysis was widened to the entire dataset to identify functionally linked proteins that did not meet the criteria of statistical significance or enrichment on LAP. All proteins associated with the leading group KEGG term were identified in the dataset, regardless of enrichment profile (Table 4.2). Protein-protein interaction networks were constructed for these proteins combined with the list of genes associated with the KEGG term group, and their one-hop protein interactors present in the dataset. Clustering was performed on these networks using the Cytoscape plug-in 'clusterMaker2' using the Community Clustering (GLay) algorithm, to identify functionally related nodes. The

group ‘Cytokine-cytokine receptor interaction’ was not further analysed as the predominant proteins related to the term were EGFR and TGFβ1. TGFβ1 represents the experimental ligand LAP, and EGFR is well represented across the other over-represented groups including ErbB signalling and MAPK signalling, making this analysis redundant. Experimental ligands fibronectin and collagen where identified in the one-hop neighbourhood of the networks were discounted from clustering analysis.

4.2.6 ErbB and MAPK Signalling

ErbB signalling and the related term MAPK signalling were overrepresented in the LAP enriched dataset. Four clusters were identified for the ErbB signalling pathway, named by a key protein chosen by a high level of enrichment, and close functional link to the term (Figure 4.13). The EGFR-centric cluster contains LanC-like protein 2 (LANCL2), AP-2 complex subunit alpha-1 (AP2A1) and catenin delta-1 (CTNND1). LANCL2 is commonly amplified with EGFR in breast cancer (Eley et al., 2002), and may confer sensitivity to chemotherapy (Park and James, 2003). AP2A1 is a subunit of AP2 which is involved in clathrin-mediated endocytosis, which is the predominant mechanism of internalisation for EGFR (Goh et al., 2010). Delta-catenin inhibits EGFR degradation and promotes ERK1/2 signalling, potentially due to higher EGFR levels (He et al., 2016).

The EGFR-associated cluster contains receptor of activated protein C kinase 1 (RACK1) and Arf6. The canonical function of RACK1 is to bind to and stabilise active PKC, promoting PKC-mediated phosphorylation. RACK1 over-expression is associated with metastasis and poor clinical outcome, which has hypothesised to be due to an associated increase in EGFR, ErbB2 and MMP protein level (Li et al., 2012). Arf6 is often overexpressed in breast cancer and is activated by EGFR signalling (Morishige et al., 2008). The other three clusters include the DUB Probable ubiquitin carboxyl-terminal hydrolase FAF-X (USP9X), the actin regulator cofilin (CFL), and the serine/threonine-protein kinase PAK 4.

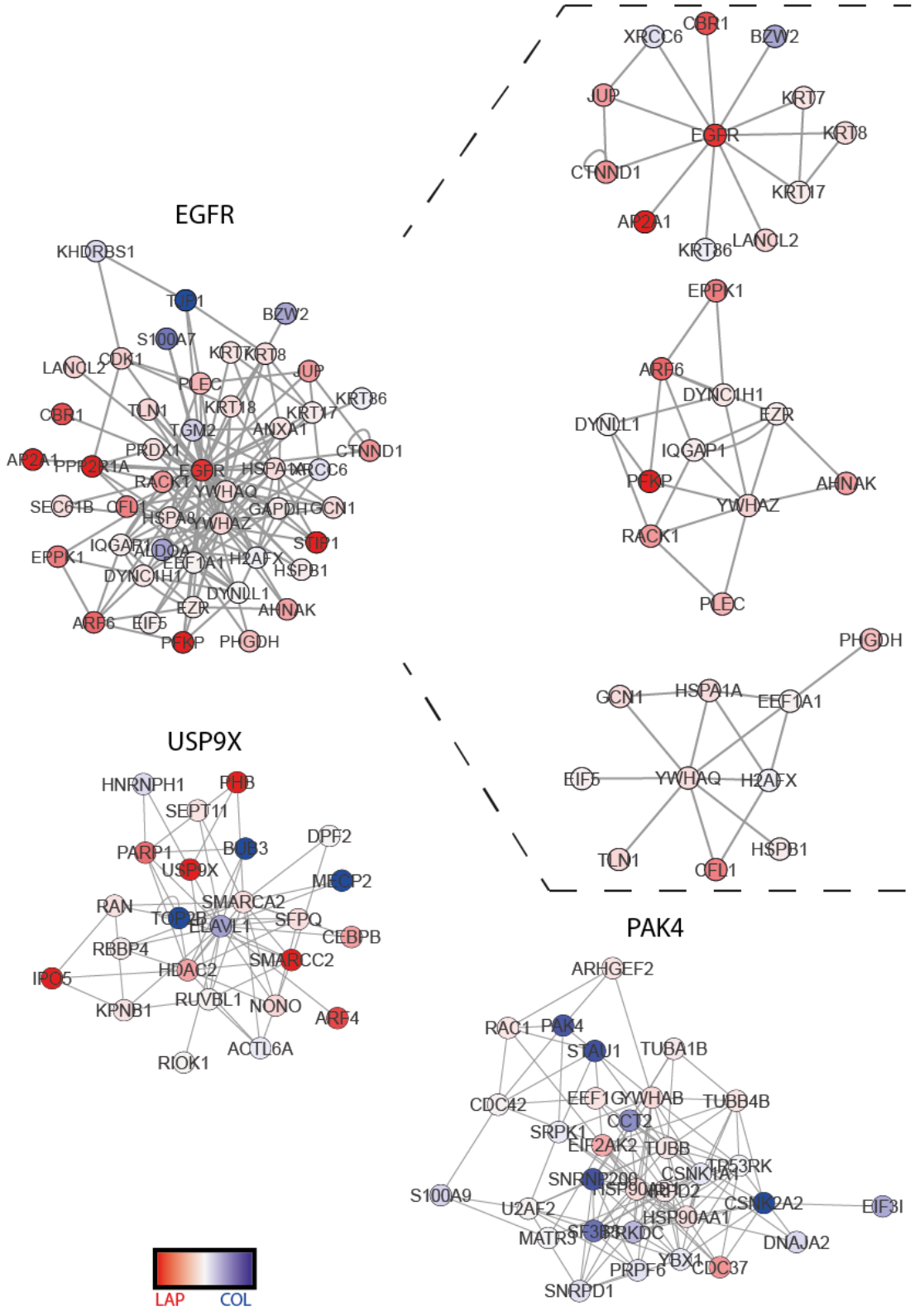

Figure 4.13: ErbB signalling pathway term subnetwork clusters. Selected key clusters from proteins associated with the ErbB signalling pathway KEGG term group and their one-hop interactors. Dashed lines from the EGFR cluster represent sub-clusters from within the large cluster. Clusters are named according to key proteins. Inter-cluster interactions are not shown. Nodes represent proteins, and edges are known interactions. Node colour red to blue gradient = log2 fold enrichment LAP/collagen.

The MAPK signalling pathway is canonically activated downstream of EGFR, and therefore is linked to ErbB signalling. The main clusters identified within the MAPK signalling pathway term were EGFR, Ras family GTPases, and three Rho family GTPase actin regulatory clusters centred on CDC42, RhoA and Rac1 (Figure 4.14). IQGAP within the EGFR cluster is a scaffold protein that binds to MEK and ERK2 and regulates their activity (Roy et al., 2005). The Ras family GTPase cluster contains isoforms of Rap1 and Ral which together with the three Ras isoforms (HRAS, KRAS, NRAS) comprise the Ras family (Mott and Owen, 2015).

The Rho family GTPases also have roles in MAPK signalling. Elevated levels of RhoA-GTP are observed in Ras-transformed cells which inhibits expression of the cell cycle inhibitor p21/Waf, promoting proliferation (Sahai et al., 2001). Filamin A is also within the RhoA cluster and can enhance MAPK signalling by binding to β-Arrestin scaffolding proteins, promoting the formation of a β-Arrestin-ERK complex and ERK activation (Scott et al., 2006). Rac1 and CDC42 can both bind and activate PAK1, PAK2 and PAK3 kinases, which phosphorylate Raf and MEK promoting their signal transduction to ERK (Schwartz, 2004).

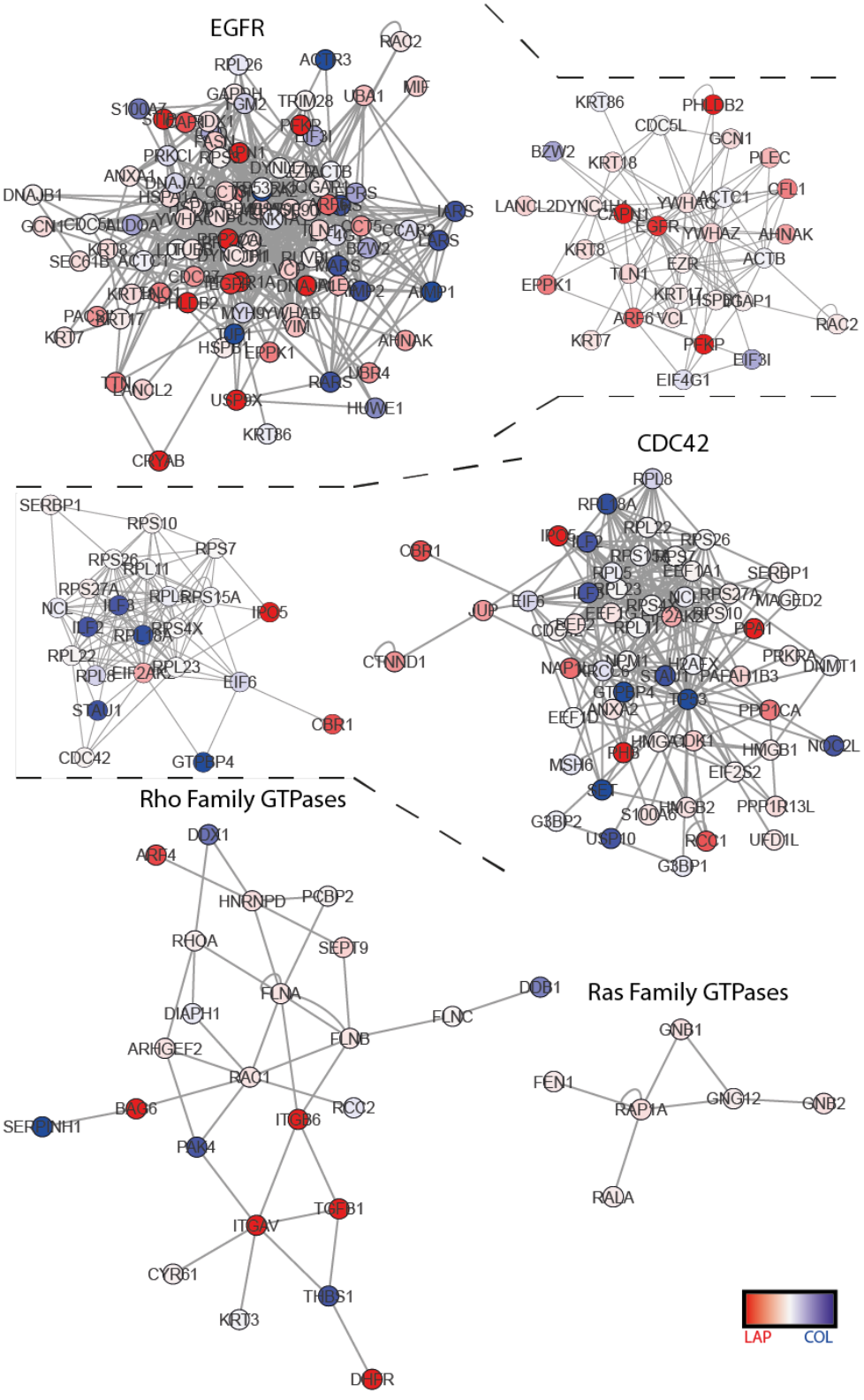

Figure 4.14: MAPK signalling pathway term subnetwork clusters. Selected key clusters from proteins associated with the MAPK signalling pathway KEGG term group and their one-hop interactors. Dashed lines from the EGFR and CDC42 clusters represent sub-clusters from within the large cluster. Clusters are named according to key proteins. Inter-cluster interactions are not shown. Nodes represent proteins, and edges are known interactions. Node colour red to blue gradient = log2 fold enrichment LAP/collagen.

4.2.7 Adhesion components

The leading group term ARVC refers to an inherited cardiac myopathy, characterised by defects in cell-cell adhesion proteins (Indik and Marcus, 2018). As a result, this group contains proteins involved in cell-cell and cell-ECM adhesion. Talin and vinculin are present in the same cluster amongst other predominantly cadherin binding proteins (Figure 4.15). Talin binding links integrin β-subunit cytoplasmic domains to actin. Vinculin strengthens this interaction by binding talin and actin. The three proteins most highly enriched on LAP proteins in this cluster are profilin, S100A11 and plakophilin-3. Profilin binds to the barbed end of actin monomers, preventing actin polymerisation (Pollard, 2017). S100A11 and its one-hop interactor annexin A1 (ANXA1) are calcium regulated proteins that can bind cadherin. Interestingly an annexin A1 complex with S100A11 is involved in formation of intraluminal vesicles in the MVB that sequester internalised EGFR from the limiting membrane, promoting its lysosomal targeting and degradation (Poeter et al., 2013). Plakophilin-3 (PKP3) is predominantly a structural protein that stabilises desmosome cell-cell adhesions (Hatzfeld, 2007).

Integrins αVβ6 and α2, which are enriched on LAP and collagen respectively, cluster together with the ECM proteins pro-TGFβ, CYR61 and thrombospondin-1 (THBS1). CYR61 is a matricellular protein secreted into the ECM that has a regulatory rather than structural role and can be engaged by select integrins via a non-canonical non-RGD binding site (Lau, 2011). CYR61 has opposing effects on tumourigenesis, promoting angiogenesis, tumour growth and invasion when bound to αVβ3; and promoting apoptosis and senescence when bound to α6β1 (Lau, 2011).

Two clusters focus on actin binding proteins, with one centred around actin isoforms, and the other including filamins. The most strongly enriched on LAP proteins are TAGLN2, CFL1, CAP1, CAPN1 and PHB. Transglein-2 (TAGLN2) stabilises actin filaments and acts as both a tumour promoter and suppressor (Dvorakova et al., 2014). Cofilin preferentially severs old GDP-bound actin filaments, promoting actin turnover which is critical for polarised growth of the actin network (Bravo-Cordero et al., 2013). CAP1 is an actin regulator that binds and sequesters G-actin monomers and also facilitates cofilin activity (Bertling et al., 2004). CAP1 may also have a role in IACs, as CAP1 depletion results in increased FAK activity and cell spreading (Zhang et al., 2013). Calpain 1 (CAPN1) is a calcium-dependent protease that cleaves a range of substrates including focal adhesion and actin regulatory proteins, and can therefore affect cell adhesion and the cytoskeleton (Lebart and Benyamin, 2006). Prohibitin (PHB) is a DNA synthesis inhibitor that is reported to bind actin (Sripathi et al., 2016).

Actin cross-linking proteins are contained in both actin-related clusters. Spectrin alpha-chain, non-erythrocytic 1 (SPTAN1) and Spectrin beta-chain, non-erythrocytic 2 (SPTBN2) are the alpha and beta chains of spectrin, and filamin A (FLNA) and filamin B (FLNB) are isoforms of filamin. Although not represented in these clusters the actin cross-linking protein α-actinin-4 is also enriched on LAP. Actin cross-linking proteins have two actin-binding domains and enabling them to link actin filaments. The distance between actin-binding domains varies considerably between actin cross-linking proteins (Pollard, 2016). Filamin has widely spaced actin-binding domains and forms a loose network of actin such as those in lamellipodia (Pollard, 2016). α-actinin has closely spaced actin-binding domains and forms bundles of actin such as those in filopodia (Sjoblom et al., 2008). Spectrin is a long flexible protein with distant actin-binding sites which forms a web-like actin network that it links to the plasma membrane to provide mechanical support (Machnicka et al., 2014).

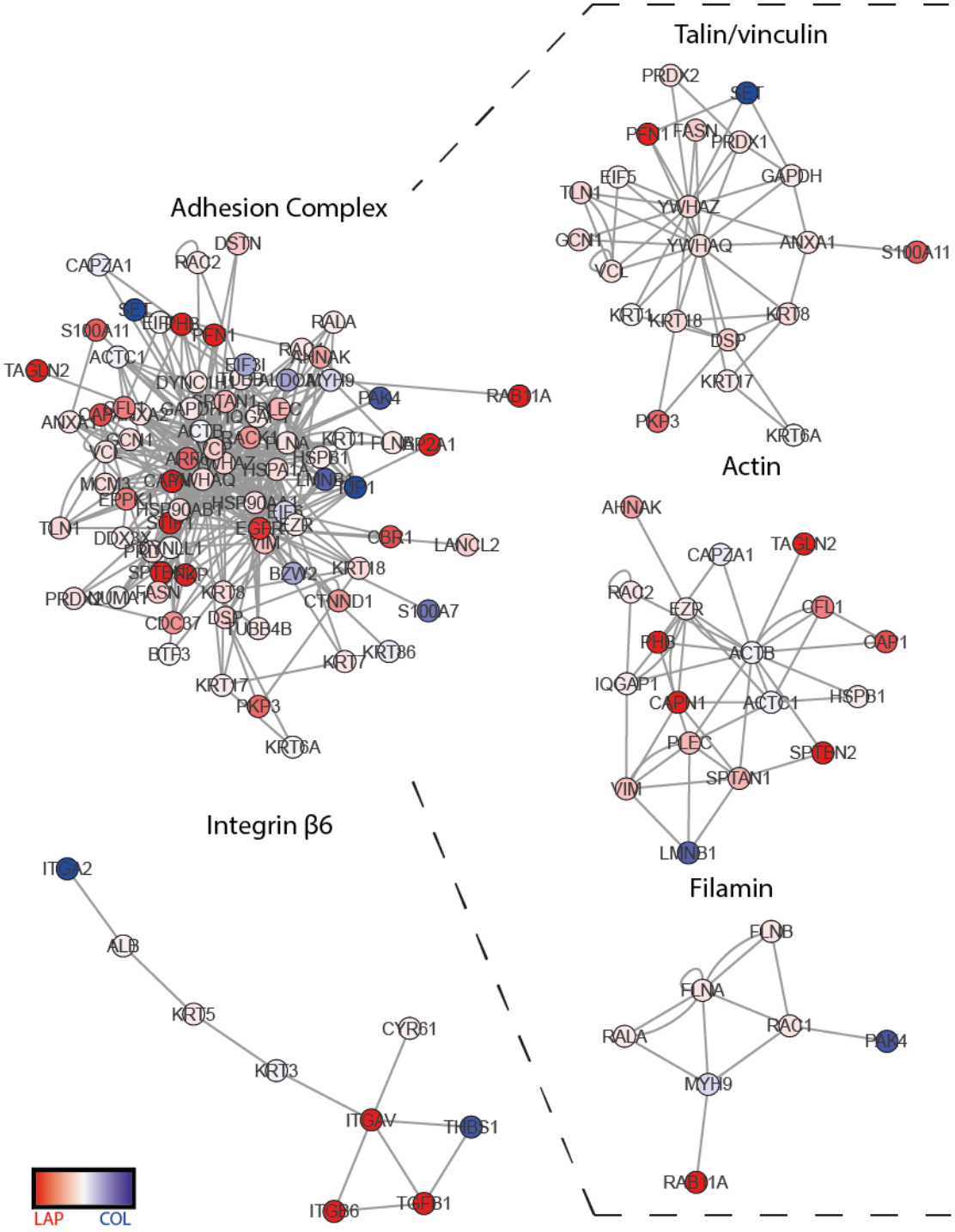

Figure 4.15: Arrhythmogenic right ventricular cardiomyopathy (ARVC) term subnetwork clusters. Selected key clusters from proteins associated with the ARVC KEGG term group and their one-hop interactors. Dashed lines from the adhesion complex cluster represent sub-clusters from within the large cluster. Clusters are named according to key proteins. Inter-cluster interactions are not shown. Nodes represent proteins, and edges are known interactions. Node colour red to blue gradient = log2 fold enrichment LAP/collagen.

4.2.8 Endocytosis

Clustering of proteins associated with the endocytosis KEGG term identified related groups that were divided by function broadly into internalisation, trafficking, and actin regulation (Figure 4.16). The internalisation and proteasomal clusters contain Rab5c, AP2A1 (AP2 complex subunit alpha-1) and CLTC (clathrin heavy chain 1), which all have roles in clathrin-mediated endocytosis (Merrifield and Kaksonen, 2014). The adaptor protein AP2 forms the inner coat of clathrin-coated vesicles and is involved in cargo selection. Clathrin assembles to form the curved outer coat and is recruited by adaptors such as AP2 (Merrifield and Kaksonen, 2014). Clathrin-mediated endocytosis is the predominant mechanism of internalisation for both EGFR and integrin αVβ6 (Goh et al., 2010; Ramsay et al., 2007). Rab5 has been implicated in EGFR and integrin endocytosis, although this has only been demonstrated for the Rab5a isoform (Barbieri et al., 2000; Pellinen et al., 2006). Rab5 has been shown to associate directly with integrins and promotes focal adhesion disassembly (Mendoza et al., 2013; Pellinen et al., 2006). KIF5B (kinesin-1 heavy chain) is a component of the motor protein kinesin-1, which transports cargo anterograde along microtubules, away from the cell body. KIF5B clusters with its one-hop interactors PSMA5 and PSMB6 which are alpha type-5 and beta type-6 subunits of the proteasome catalytic core (Figure 4.16, proteasomal cluster). Kinesin-1 has been shown to transport the proteasome for efficient degradation in neurons, therefore could be postulated to have a similar function at adhesion sites (Otero et al., 2014).

The vesicle recycling regulator Arf6 was clustered with USP9X (Probable ubiquitin carboxyl-terminal hydrolase FAF-X), GDI2 (Rab GDP dissociation inhibitor beta), Rab8a and Rab1b; and Rab11a clustered with Rap1A and RalA (Figure 4.16, trafficking cluster). These regulators have roles in receptor endocytosis and at additional steps in the trafficking pathways. Three ESCRT-III subunits CHMP6, CHMP5 and CHMP4B were also clustered together and enriched on LAP (CHMP5 AND CHMP4B were positively enriched on LAP/FN). ESCRT-III is conventionally associated with the MVB, however novel functions have been identified for ESCRT-III in the maintenance of membranes (Stoten and Carlton, 2018).

Many actin regulators were also present in the endocytosis group clusters, including the Arp2/3 complex subunits ARPC3 and ARPC4; CAPZA1 (F-actin-capping protein subunit alpha-1) and the ERM family proteins MSN (moesin) and EZR (ezrin); CFL1 (cofilin), Rac1, Rac2 and CDC42; and the Rho GEF ARHGEF2. Actin is required for endocytosis in the formation of the membrane invagination structures, and is also central to vesicle motility (Smythe and Ayscough, 2006).

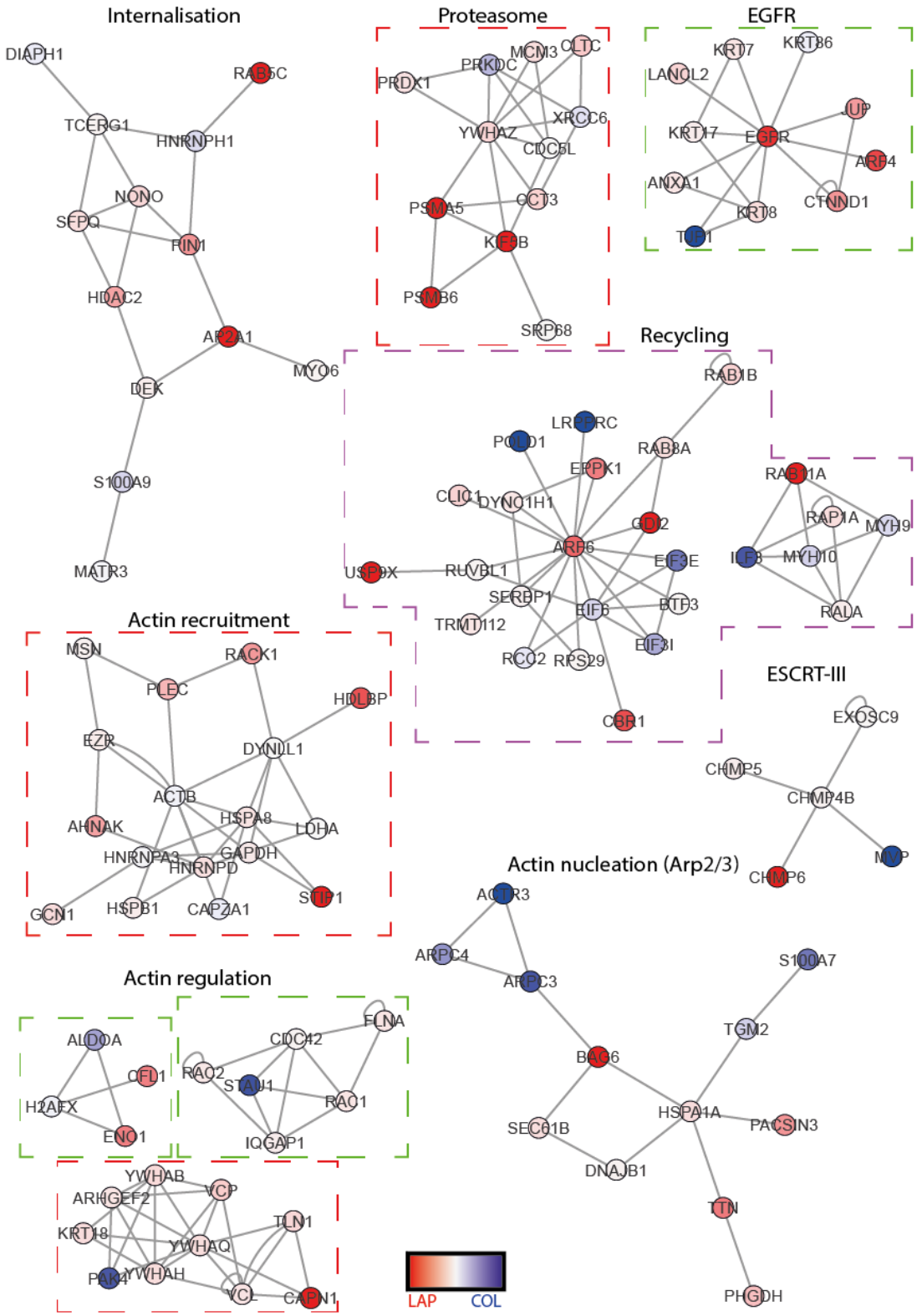

Figure 4.16: Endocytosis term subnetwork clusters. Selected key clusters from proteins associated with the endocytosis KEGG term group and their one-hop interactors. Clusters with dashed outlines are sub-clusters derived from larger clusters that are represented in the corresponding colour in figure S14. Clusters are named according to a key function or protein. Inter-cluster interactions are not shown. Nodes represent proteins, and edges are known interactions. Node colour red to blue gradient = log2 fold enrichment LAP/collagen.

Psoriasin (S100A7) is represented in the actin nucleation cluster as positively enriched on collagen compared to LAP. Psoriasin binds directly to the cytoplasmic domain of β6 and is required for αVβ6-mediated invasion (Morgan et al., 2011). The profile of psoriasin was inconsistent between IAC MS replicates however, as psoriasin was equal between LAP and collagen in replicate 1, and unique to FN and collagen in replicates 2 and 3, respectively. This indicates a potential issue with biological replicate consistency for psoriasin. Psoriasin binding to collagen engaging integrins is theoretically possible as this has not been investigated, however these integrins lack the cytoplasmic motif in integrin β6 that mediates psoriasin binding (Morgan et al., 2011). Alternatively, psoriasin may bind β6 in subcellular compartments distinct from IACs, in which case it would not be detected in these assays.

4.2.9 Hippo Pathway Signalling

The Hippo signalling pathway phosphorylates and inhibits the transcriptional activators YAP and TAZ, preventing their translocation to the nucleus and subsequent stimulation of proliferative and anti-apoptotic gene transcription (Badouel and McNeill, 2011). The key proteins identified in the Hippo pathway signalling cluster were two subunits of protein phosphatase 2 A (PP2A) (PPP2CA, catalytic subunit alpha isoform; PPP2R1A, PR65 subunit), 14-3-3 proteins (YWHAB, YWAH, YWHAQ, YWHAZ; beta/alpha, eta, theta and zeta, respectively), and a subunit of protein phosphatase 1 (PP1) (PPP1CA, alpha catalytic subunit) (Figure 4.17).

PP2A is a negative regulator of the Hippo pathway, and thus promotes the nuclear translocation of YAP and TAZ. PP2A dephosphorylates MST1/2 (Mammalian STE20-like protein kinase 1/2), inhibiting its downstream activity activating LATS1/2 (Serine/threonine-protein kinase LATS1/2) which phosphorylates YAP/TAZ (Guo et al., 2011) (Ribeiro et al., 2010). 14-3-3 proteins are also negative regulators of YAP/TAZ. Phosphorylation of YAP/TAZ creates a binding site for 14-3-3 proteins, which when bound constrain YAP/TAZ in the cytoplasm (Lei et al., 2008; Zhao et al., 2007). PP1 dephosphorylates YAP/TAZ and therefore promotes their activity (Liu et al., 2011a; Wang et al., 2011b).

Although not represented in the clustering, the DUB USP9X is enriched in αVβ6-mediated IACs on LAP (Figure 4.10) and contributes to Hippo signalling pathway regulation. USP9X has been shown to deubiquitinate both YAP and LATS2, stabilising them by inhibiting ubiquitin-mediated degradation (Li et al., 2018). USP9X can therefore be both a positive and negative regulator of YAP/TAZ activity.

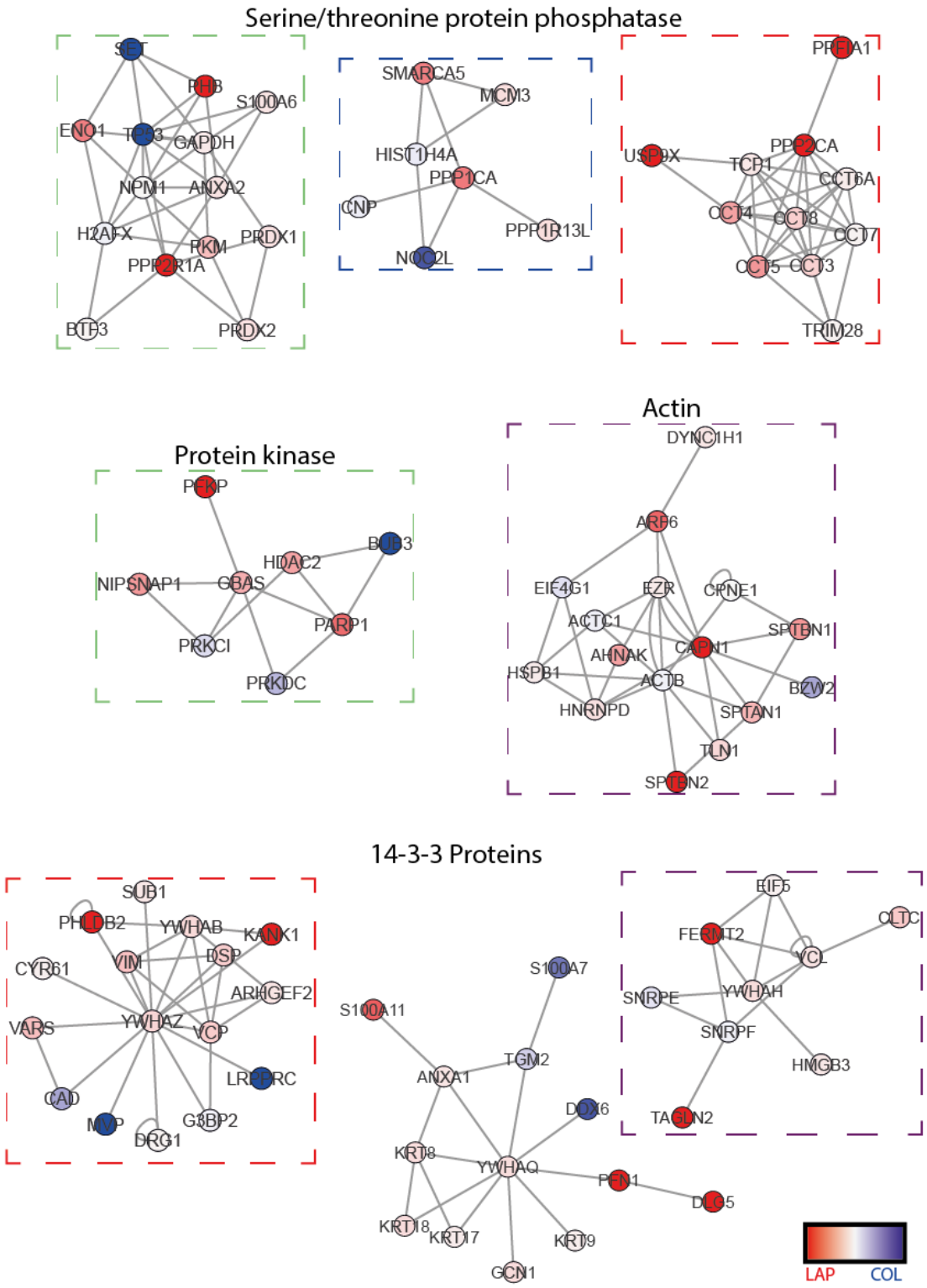

Figure 4.17: Hippo signalling pathway term subnetwork clusters. Selected key clusters from proteins associated with the hippo signalling pathway KEGG term group and their one-hop interactors. Clusters with dashed outlines are sub-clusters derived from larger clusters that are represented in the corresponding colour in figure S15. Clusters are named according to key proteins. Inter-cluster interactions are not shown. Nodes represent proteins, and edges are known interactions. Node colour red to blue gradient = log2 fold enrichment LAP/collagen.

Mechanical force from the cellular microenvironment is another major regulator of YAP/TAZ (Dupont et al., 2011). Key elements of this regulatory mechanism are the ECM, cell-cell and cell-ECM contacts and cytoskeletal dynamics. Integrin-mediated adhesions transmit mechanical force intracellularly by generating acto-myosin contractility. To determine if any actin regulators are differentially recruited to αVβ6-mediated IACs formed on LAP, proteins associated with actin binding and actin regulatory GO terms were identified within our dataset, that were ≥ two-fold different on LAP (Table 4.3). The majority of these proteins were positively enriched on LAP (26/30) and were predominantly non-actin binding regulators or actin crosslinkers. Proteins that were negatively enriched on LAP were predominantly myosins; possibly suggesting downregulated actomyosin contractility.

Name	Gene	Function	Log2 Fold Change			>Two-Fold Change		
			LAP vs FN	LAP vs Coll	FN vs Coll	LAP vs FN	LAP vs Coll	FN vs Coll
Alpha-actinin-4	ACTN4	Cross-linking	2.85	0.42	-2.43	**TRUE**	FALSE	**TRUE**
Arf6	ARF6	Actin regulator	-0.35	6.53	6.77	FALSE	**TRUE**	**TRUE**
Actin-related protein 2/3 complex subunit 4	ARPC4	Nucleation	5.91	-4.18	-7.83	**TRUE**	**TRUE**	**TRUE**
Adenylyl cyclase-associated protein	CAP1	Stabilising	10.97	7.7	-10.97	**TRUE**	**TRUE**	**TRUE**
F-actin-capping protein subunit alpha-1	CAPZA1	Stabilising	1.29	-0.47	-1.76	**TRUE**	FALSE	**TRUE**
Cofilin-1	CFL1	Severing	1.85	5.25	3.99	**TRUE**	**TRUE**	**TRUE**
Elongation factor 2	EEF2		8.37	0.95	-7.86	**TRUE**	FALSE	**TRUE**
EGFR	EGFR		8.66	9.27	1.83	**TRUE**	**TRUE**	**TRUE**
Filamin-A	FLNA	Cross-linking	2.79	0.85	-1.94	**TRUE**	FALSE	**TRUE**
Filamin-B	FLNB	Cross-linking	3.65	0.77	-2.88	**TRUE**	FALSE	**TRUE**
Filamin-C	FLNC	Cross-linking	2.02	0.18	-1.83	**TRUE**	FALSE	**TRUE**
Inverted Formin-2	INF2	Nucleation	8.2	8.07	0	**TRUE**	**TRUE**	FALSE
Microtubule-actin cross-linking factor 1	MACF1	Cytoskeletal linker	8.38	1.56	-7.67	**TRUE**	**TRUE**	**TRUE**
Myristoylated alanine-rich C-kinase substrate	MARCKS	Cross-linking	0.24	1.43	1.2	FALSE	**TRUE**	**TRUE**
Unconventional myosin-XVIIIa	MYO18A	Motor protein	7.79	-1.35	-7.89	**TRUE**	**TRUE**	**TRUE**
Profilin-1	PFN1	Elongation	10.97	10.97	ND	**TRUE**	**TRUE**	**FALSE**
Pleckstrin homology-like domain family B member 2	PHLDB2	Actin regulator	10.97	10.97	ND	**TRUE**	**TRUE**	FALSE
Plectin	PLEC	Cytoskeletal linker	6.73	2.83	-5.39	**TRUE**	**TRUE**	**TRUE**
Liprin-alpha	PPFIA1	Actin regulator	10.97	10.97	ND	**TRUE**	**TRUE**	FALSE
RhoG	RHOG	Actin regulator	1.15	1	-0.15	**TRUE**	**TRUE**	FALSE
Spectrin alpha chain, non-erythrocytic 1	SPTAN1	Cross-linking	10.97	2.88	-10.97	**TRUE**	**TRUE**	**TRUE**
Spectrin beta chain, non-erythrocytic 1	SPTBN1	Cross-linking	10.97	4.26	-10.97	**TRUE**	**TRUE**	**TRUE**
Pro-TGFβ1	TGFB1	Actin regulator	10.97	10.97	ND	**TRUE**	**TRUE**	**FALSE**
Talin	TLN1	Focal Adhesion	3.16	1.4	-1.76	**TRUE**	**TRUE**	**TRUE**
Vinculin	VCL	Focal Adhesion	10.97	0.95	-10.97	**TRUE**	FALSE	**TRUE**

Name	Gene	Function	Log2 Fold Change			>Two-Fold Change		
			LAP vs FN	LAP vs Coll	FN vs Coll	LAP vs FN	LAP vs Coll	FN vs Coll
14-3-3 Eta	YWHAH		4.73	1.14	-3.94	**TRUE**	**TRUE**	**TRUE**
Myosin-9	MYH9	Motor protein	0.19	-1.29	-1.48	FALSE	**TRUE**	**TRUE**
Myosin-10	MYH10	Motor protein	0.22	-1.6	-1.81	FALSE	**TRUE**	**TRUE**
Myosin-14	MYH14	Motor protein	0.42	-2.29	-2.71	FALSE	**TRUE**	**TRUE**
Leucine-rich PPR motif-containing protein, mitochondrial	LRPPRC		ND	-10.97	-10.97	FALSE	**TRUE**	**TRUE**

Table 4.3: Actin binding/regulating proteins. Proteins associated with the GO MF term' actin binding' (GO:0003779) and GO BP term 'regulation of actin cytoskeleton organisation' (GO:0032956). All proteins are ≥ two-fold different on the ligand LAP in the dataset and satisfy peptide cut-off values. Function annotation is manually curated as the dominant canonical function. Proteins without function listed have complex or ill-defined functions relating to actin. All proteins are positively enriched on LAP, except row myosin-9,10,14 and LRPPRC, highlighted in red/white are negatively enriched on LAP.

4.2.10 Fatty Acid Biosynthesis

The key genes within the fatty acid biosynthesis cluster are fatty acid synthase (FASN) and long-chain-fatty-acid--CoA ligase 1 (ACSL1) (Figure 4.18). FASN synthesises the fatty acid palmitate from acetyl-CoA and malonyl-CoA (Buckley et al., 2017). Palmitate is added to cysteine residues of proteins, by a process known as palmitoylation. Palmitoylation affects 12% of the human proteome, and enables the reversible association of proteins with membranes, and can also modulate the behaviour within membranes of integral membrane proteins (Daniotti et al., 2017). FASN mainly localises to the cytoplasm but can be recruited to lipid rafts in the plasma membrane in association with caveolin-1 (Di Vizio et al., 2008). FASN expression and activity is associated with a poor prognosis in various cancers including breast, as tumour cells become 'addicted' to *de novo* synthesis of fatty acids opposed to dietary uptake (Buckley et al., 2017).

ACSL1 is involved in the cellular uptake and degradation of fatty acids preferentially palmitoleate, oleate and linoleate, to acetyl CoA in the mitochondria (Zhan et al., 2012). ACSL1 co-localisation with a fatty acid transporter has been observed at the plasma membrane, however ACSL1 localisation is thought to be predominantly mitochondrial (Gargiulo et al., 1999).

Palmitoylation is important in regulating membrane localisation of proteins, therefore proteins in our dataset were assessed to see if they are palmitoylated suggesting functional relevance of this modification. Our dataset was compared to the SwissPalm database on protein palmitoylation (Database release: 2 (2018-02-18) (www.swisspalm.org) (Blanc et al., 2015). Of the 734 reviewed proteins in our dataset, 505 were observed in at least one

palmitome, and 220 were observed in ≥ three (Supplementary table 2). Just over half (111 proteins) of the proteins observed in ≥ three palmitomes were ≥ two-fold enriched on LAP, and of these half (49 proteins) were enriched on LAP relative to FN and collagen. Fewer proteins were enriched on FN or collagen compared to LAP (70), and a similar number were unchanged (65). This indicates FASN which is enriched on LAP, may function to recruit palmitoylatable proteins to αVβ6 IACs, or may be locally regulating palmitoylation at sites of αVβ6 engagement.

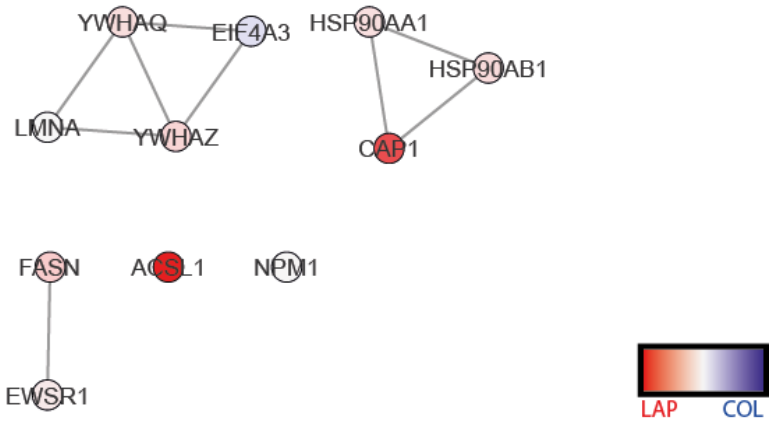

Figure 4.18: Fatty acid biosynthesis term subnetwork clusters. Clusters from proteins associated with the fatty acid biosynthesis KEGG term group and their one-hop interactors. Inter-cluster interactions are not shown. Nodes represent proteins, and edges are known interactions. Node colour red to blue gradient = log2 fold enrichment LAP/collagen.

4.2.11 Candidate Validation

Having identified over-represented functional clusters and enriched proteins, we wanted to determine if these were increased in LAP-isolated IACs by immunoblotting in addition to MS. Integrin β6, EGFR and liprin α1 were unique to LAP IACs by immunoblotting (Figure 4.19 A). Clathrin, Rab8A, α-actinin, ARHGEF2 and Rap1A were observed in IACs on all three ligands, however were strongest in LAP-dependent IACs. Rap1a is present in all IACs but is strongest in FN and weakest in collagen. The immunoblotting data confirms the MS data for β6, EGFR, liprin α1, Rab8A and GEF-H1 (Figure 4.19 B). Clathrin and α-actinin were detected at higher levels on collagen than LAP by MS which was not reflected by immunoblotting, however they were all enriched on LAP compared to FN. Rap1A was detected at similar levels on FN (86%) and LAP and at half the amount on collagen (48%) by MS. This was confirmed by immunoblotting that showed similar levels of Rap1A in FN and LAP, and less in collagen IACs.

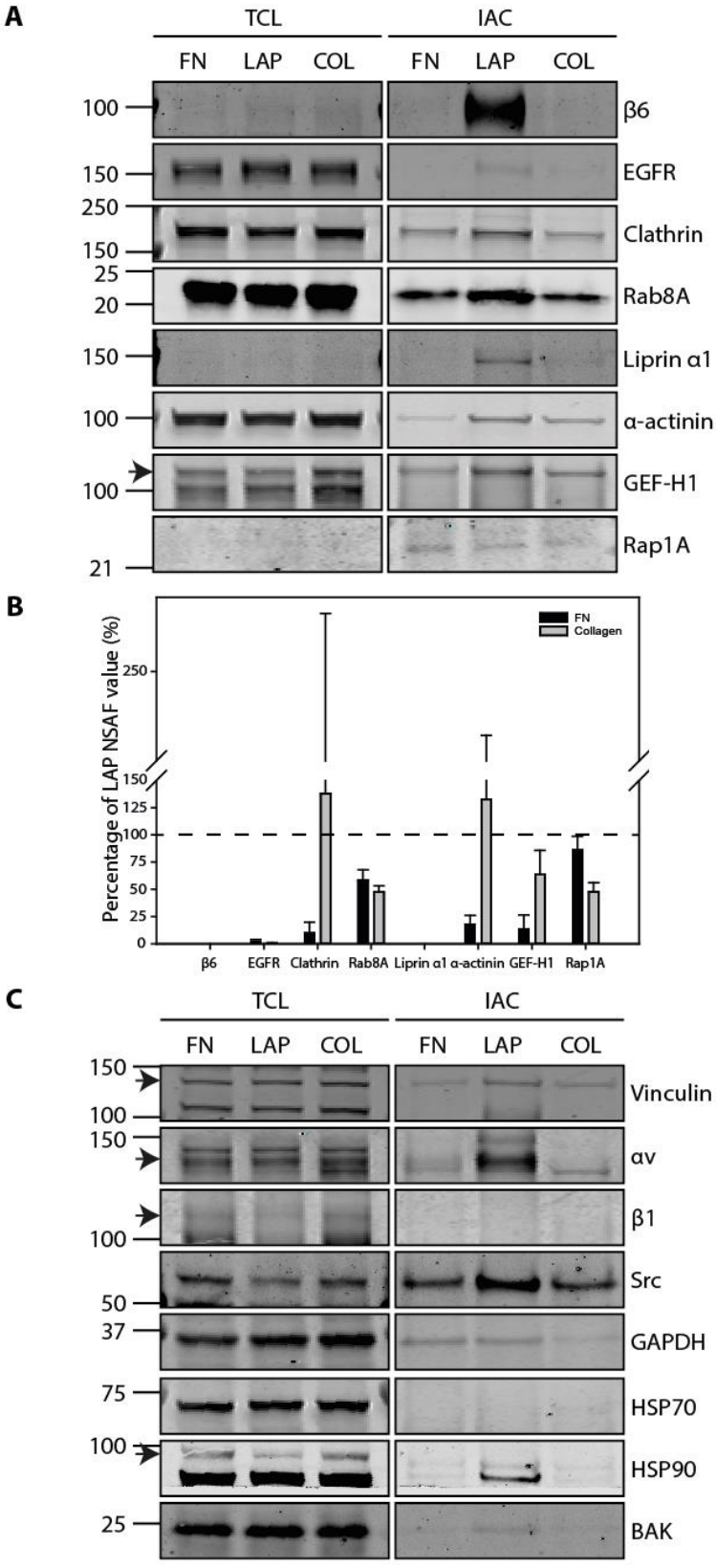

Figure 4.19: Proteomic candidate Validation. (A) Candidates statistically significantly enriched on LAP were validated by western blotting to verify their presence and distribution profile across the three different IAC isolation ligands. (B) MS NSAF abundance values of the candidates expressed as a percentage of LAP, for FN (black) and Collagen (grey) isolated IACs. Error bars = SEM of three replicates. (C) Validation of IAC isolation enrichment. Arrows indicate band of interest where ambiguous.

4.3 Discussion

Multiple signalling pathways have been identified that are over-represented at αVβ6 IACs and are likely to feed into αVβ6-mediated invasion and poor cancer prognosis. The LAP based IAC isolation approach successfully enriched for integrin β6 and isolated proteins likely to be associated with αVβ6 function. Integrin αVβ6 IAC composition diverges from the experimentally defined consensus adhesome and literature-curated adhesome.

4.3.1 EGFR Signalling

ErbB and MAPK signalling are over-represented in αVβ6 IACs, and many of the enriched proteins within these terms are positive regulators of EGFR signalling. This demonstrates αVβ6 adhesions are likely to be sites of collaborative EGFR signalling. ErbB and MAPK signalling is most likely to be mediated by EGFR in MDA-MB-468s, as no other ErbB receptors were detected in IACs. MDA-MB-468s are negative for ErbB2 expression (Figure 3.1) and are reported to be ErbB4 negative but ErbB3 positive (Jeong et al., 2014). ErbB3 can heterodimerise with EGFR when its preferential partner ErbB2 is not present (Graus-Porta et al., 1997). EGFR is highly overexpressed in MDA-MB-468s, therefore EGFR ErbB3 heterodimers if present are likely to account for a minority of the EGFR dimers (Forbes et al., 2017). ErbB3 cannot signal as a homodimer due to its truncated catalytic domain (Citri et al., 2003).

Endocytosis of active EGFR is required for full EGFR, ERK and PI3K phosphorylation (Murphy et al., 2009; Vieira et al., 1996). The DUB USP9X increases the rate of EGFR endocytosis, however does not appear to affect the phosphorylation levels of Akt and the MAPK Raf in response to EGF, although only one relevant timepoint was assessed (Savio et al., 2016). USP9X is essential for TGFβ signalling however and is required for TGFβ-mediated cell migration (Dupont et al., 2009). USP9X could therefore promote the autocrine response to local integrin αVβ6-mediated activation of TGFβ.

The small GTPase Arf6 is activated by EGFR via the Arf6 GEF GEP100 (Morishige et al., 2008). Arf6 is part of the Arf family of Ras superfamily of small GTPases, and localises to the plasma membrane and endosomes where it controls vesicle trafficking (D'Souza-Schorey and Chavrier, 2006). EGFR-mediated activation of Arf6 increases breast cancer cell motility and invasion by promoting recycling of integrin β1 via Arf6-mediated trafficking (Onodera et al., 2012). Arf6 is also involved in the trafficking of αV integrins and promotes recycling of αVβ3 (Morgan et al., 2013).

EGFR signalling can also influence activity of the actin-severing protein cofilin, which promotes actin turnover by preferentially severing GDP-bound actin filaments (Pollard, 2017). EGFR activates cofilin by releasing it from its inhibitory interaction with PIP2 at the plasma membrane, by activating PLCγ which hydrolyses PIP2 (Mouneimne et al., 2004). Cofilin is active when dephosphorylated, therefore its activity is dictated by its phosphorylation status controlled by LIM kinase (LIMK) and slingshot (SHH) phosphatase. EGFR can also inhibit cofilin by signalling via PI3K which stimulates the activity of LIMK which phosphorylates cofilin resulting in inactivation (Wang et al., 2007). The kinase PAK4 can also negatively regulate cofilin activity by phosphorylating and inactivating the slingshot (SSH) phosphatase, reducing cofilin dephosphorylation (Soosairajah et al., 2005). PAK4 and many of the interactors it clusters with are enriched on collagen compared to LAP IACs, suggesting exclusion from αVβ6-mediated IACs.

The MAPK signalling term contained Ras and Rho family GTPases. Ras is activated in response to EGFR signalling, and triggers the MAPK cascade resulting in sequential recruitment and phosphorylation of the kinases Raf (MAPKKK), Mek (MAPKK), and Erk (MAPK). Ras was not detected in IACs, however the Ras related proteins Rap1a and RalA were identified, that can positively influence the MAPK signalling pathway. Rap1a is similar to Ras however does not efficiently activate the same effectors, and instead has distinct functions predominantly relating to cell adhesion, such as integrin activation (Lee et al., 2009; Simanshu et al., 2017). Rap1a has been shown to activate the MAPK pathway by binding Raf and potentiating downstream ERK signalling (Takahashi et al., 2017).

RalA also has distinct effectors such as Sec5 and filamin, allowing it to regulate processes such as exocytosis and actin organisation through these interactions (Simanshu et al., 2017). Stimuli that activate Ras such as EGF stimulation also activate RalA through a Ras-dependent manner, mediated by the RalGDS (Ral guanine nucleotide dissociation stimulator) family that can bridge Ras and Ral and activate Ral (Ferro and Trabalzini, 2010). RalGEFs and RalA have also been implicated as important for Ras-mediated tumourigenic growth (Lim et al., 2005).

4.3.2 YAP/TAZ nuclear localisation

Mechanical stimulation is an important mediator of YAP/TAZ nuclear translocation and can override the Hippo signalling pathway (Dupont et al., 2011). YAP/TAZ can be described as sensors and active mediators of mechanical cues. YAP/TAZ accumulate in the nucleus in response to mechanical inputs such as stiff ECM and cytoskeletal tension, and relay these signals by activating transcription of target genes (Piccolo et al., 2014). Integrin β6 and β8

have a unique ability to activate TGFβ by applying force to induce a conformational change in LAP, thus releasing active TGFβ from its inhibitory complex (Sheppard, 2005). Both integrins have evolutionarily conserved specialisations for this force application and support cytoskeletal tensile force transmission (Dong et al., 2017). In addition, αVβ6 expression has been shown to enhance the ability of cells to sense and apply mechanical force (Oria et al., 2017).

Adaptations to transmit force to an extracellular ligand may also have relevance to the intracellular transmission of force. Unpublished data from our laboratory (Mark Morgan, University of Liverpool) has shown that inhibition of αVβ6, or stimulation with EGF, reduces YAP nuclear localisation in both 2D and 3D substrates of different rigidities. This demonstrates αVβ6 is a positive regulator of YAP nuclear localisation. These experiments suggest EGFR is a negative regulator of YAP/TAZ, however these data are consistent with EGF-mediated induction of αVβ6 endocytosis (Figure 3.5). Reduction of YAP nuclear localisation in response to αVβ6 inhibition is likely mediated by force transmission, as inhibition of αVβ6 results in lower force application in TFM (Tod et al., 2017) and EGF stimulation reduces αVβ6 -mediated force transmission in TFM (unpublished data from our laboratory, Stephanie Mo, University of Liverpool).

Nuclear translocation of YAP/TAZ leads to the transcription of genes associated with a poor clinical outcome in a range of cancers including breast (Piccolo et al., 2014). YAP/TAZ expression may underlie some key hallmarks of cancer such as uncontrolled proliferation and evasion of apoptosis (Piccolo et al., 2014). YAP/TAZ activity correlates with histological grade and metastases of breast cancer (Cordenonsi et al., 2011) TAZ nuclear expression is strongly associated with TNBC in comparison to ER/PG receptor-positive and ErbB2-positive breast cancer, and correlates with poorer clinical outcomes of recurrence and overall survival (Diaz-Martin et al., 2015). Integrin αVβ6 and EGFR-mediated positive regulation of YAP/TAZ nuclear localisation therefore has direct clinical relevance to TNBC.

4.3.3 Receptor trafficking and adhesion turnover

Proteins associated with receptor endocytosis and endosomal trafficking were identified in αVβ6-IACs. Both integrins and EGFR can signal from endosomes, therefore endocytosis is unlikely to result in immediate signal termination (Alanko et al., 2015; Vieira et al., 1996). Indeed, endocytosis is actually required for the complete signalling response downstream of integrins and EGFR (Alanko and Ivaska, 2016; Tomas et al., 2014). Integrin adhesion turnover is co-ordinated by integrin endocytosis, as adhesion disassembly involves integrin

internalisation. Efficient adhesion turnover is important for co-ordinated and persistent cell migration. The Rho GTPase RhoG and the scaffold protein liprin α1 are both statistically significantly enriched on LAP IACs and are involved in adhesion turnover. Activation of RhoG induces β1 integrin endocytosis and is required for persistent cell migration (Bass et al., 2011). Interestingly EGF-mediated activation of RhoG also increases the rate of EGFR internalisation (Samson et al., 2010).

Liprin α1 localises to focal adhesions and forms a complex with ELKS/Rab6-interacting/CAST family member 1 (ERC1), Pleckstrin homology-like domain family B member 1 (PHLDB1) and PHLDB2 (Astro et al., 2014) which are all strongly enriched on LAP-IACs (Figure 4.10) except PHLDB1 which was not identified. This complex promotes internalisation of integrin β1 which is required for adhesion turnover at the migratory leading edge and stabilises lamellipodial protrusions (Astro et al., 2014; Astro et al., 2016). Liprin α1 also drives recycling of active FN-bound integrin α5β1, controlling its polarised localisation in endothelial cells (Mana et al., 2016). Liprin α1 is amplified in 15% of breast cancers (Dancau et al., 2010), and is associated with a poor prognosis and the formation of metastases (Chiaretti et al., 2016). Liprin α1 is required for TNBC cell invasion through promoting cell migration, lamellipodia stability and ECM degradation (Astro et al., 2011). Localisation of the liprin α1-ERC1-PHLDB2 complex at αVβ6-IACs is therefore potentially relevant for αVβ6-mediated invasion. Endocytosis of αVβ6 is required for αVβ6-mediated migration and invasion (Ramsay et al., 2007), and therefore is highly relevant to αVβ6-positive cancer prognoses.

4.3.4 Palmitoylation

Metabolic reprogramming is a hallmark of cancer that allows cells to grow and proliferate intensively (Jozwiak et al., 2014). FASN is normally expressed at very low levels in adult tissues, however is often upregulated in cancer, where cells favour *de novo* lipogenesis opposed to uptake (Buckley et al., 2017; Flavin et al., 2010). FASN expression is associated with a poor prognosis in a range of a cancers, including breast (Flavin et al., 2010).

Inhibition or knockdown of FASN decreases cell proliferation and migration (Gong et al., 2017; Sokolowska et al., 2017). Unpublished data from Claire Wells (Kings College London) shows FASN inhibition reduces cell invasion and area spreading, and increases adhesion to Matrigel®, which collectively indicate an adhesion disassembly defect. These effects were rescued with palmitate, demonstrating the availability of palmitate drives the phenotype. Further unpublished data from Claire Wells indicates the effects of FASN on cell-ECM

adhesions may be mediated by the non-canonical Rho GTPase RhoU, which is regulated by palmitoylation (Ory et al., 2007).

The post-translational modification palmitoylation is important for the membrane localisation cytosolic proteins, and the movement of transmembrane proteins which promotes the formation of signalling clusters (Daniotti et al., 2017). Palmitoylation positively mediates membrane localisation of H-Ras and N-Ras isoforms, but not K-Ras which does not undergo this modification (Eisenberg et al., 2013). Palmitoylation is reversible and de-palmitoylation redistributes N-Ras to the Golgi complex and decreases short-term plasma membrane ERK signalling (Eisenberg et al., 2011).

These analyses of αVβ6-IACs have generated novel insight into the functions of αVβ6-dependent and clinically-relevant pathways. EGFR-related signalling is highly represented at αVβ6-IACs, strengthening our hypothesis and data demonstrating that crosstalk with EGFR is an important consideration for αVβ6 biology. Endocytic and trafficking regulators identified are interesting mediators of crosstalk between αVβ6 and EGFR, as the activity of cell surface receptors is controlled by their trafficking. Recruitment of FASN to αVβ6-IACs suggests palmitoylation could influence the dynamics of αVβ6-mediated adhesions, which may influence their composition and therefore function. Identification of Hippo pathway regulators at αVβ6-IACs provided the rationale for experiments that have demonstrated αVβ6 is a positive regulator of YAP nuclear localisation which has direct clinical relevance. Further investigation of functionally important candidate proteins aims to further elucidate αVβ6 biology.

5. Eps8 is a convergence point integrating EGFR and integrin crosstalk

5.1 Introduction

Biologically significant crosstalk exists between integrins and GFRs, mediated by a diverse range of mechanisms affecting receptor expression levels, activity, signalling and trafficking (introduction section 1.9) (Ivaska and Heino, 2011). Integration of crosstalk can be very complex, therefore there is a drive to understand it and identify potential mediators. Previous work in our laboratory employed proteomic, ontological and network analyses to determine the effect of acute EGF stimulation on adhesion signalling networks. To facilitate identification of crosstalk mediators, Nikki Paul (Humphries/Streuli labs, University of Manchester) used the hydrodynamic force-mediated IAC isolation protocol (Jones et al., 2015), coupled with MS, to identify changes in IAC composition following 5 mins EGF stimulation. Downstream network and ontological analyses revealed a substantial decrease in the abundance of adhesion regulatory proteins and co-ordinators of endocytosis within 5 minutes of EGF stimulation (Figure 5.1A and data not shown). Together these data suggested a mechanism of EGF-induced receptor endocytosis and adhesion complex turnover.

Combinatorial interrogation of the networks allowed a global and dynamic view of adhesion and GFR crosstalk to be assembled. By interrogating network topology, Eps8 (Epidermal growth factor receptor kinase substrate 8) was identified as a putative node integrating α5β1 integrin and EGFR functions (Figure 5.1 B). Eps8 was identified in α5β1-positive IACs and Eps8 levels at IACs decreased in response to EGF stimulation. Importantly, Eps8 is a direct interactor of both EGFR and integrin β1 (Figure 5.1 A, B) (Calderwood et al., 2003; Castagnino et al., 1995). In addition, Eps8 interactors including Abi1 (Abl interactor 1) and RN-tre (USP6NL) were also de-enriched at IACs in response to EGF (Figure 5.1 C).

The related Eps8-family member, Eps8-like 2 (Eps8L2), was also identified in IACs and exhibited a similar level of de-enrichment, however, Eps8L2 was only identified in the 2-hop intersect of α5β1 integrin and EGFR interactors and was not as inter-connected within the network as Eps8. Based on the EGF-dependent localisation of Eps8 at adhesion sites, identification of endocytosis by gene ontological analysis as a key EGF-dependent biological process at IACs, and the regulatory functions of Eps8 (outlined below); Eps8, and to a limited extent Eps8L2, were identified as putative regulators of EGFR and integrin crosstalk for further study.

Eps8 has been identified as a putative regulator of crosstalk between EGFR and integrins. Eps8 was originally identified as a substrate for EGFR that enhanced mitogenic responsiveness (Fazioli et al., 1993). Eps8 can directly bind the juxtamembrane region of EGFR (Castagnino et al., 1995), and is tyrosine phosphorylated in response to EGF (Matoskova et al., 1995). Eps8 has four human isoforms Eps8-like 1 (Eps8L1), Eps8L2 and Eps8-like 3 (Eps8L3) which are homologous and have a conserved C-terminal "effector" domain (Tocchetti et al., 2003). A lack of phenotype in the Eps8 -/- mouse indicates redundancy in the Eps8 family (Scita et al., 1999). Eps8, Eps8L1 and Eps8L2 can activate Sos1 and bind actin, and Eps8 and Eps8L2 have overlapping expression profiles (Offenhauser et al., 2004). Eps8 coordinates multiple signalling pathways and functions differently depending on its interactions to co-ordinate actin dynamics, GTPase activity and receptor trafficking (Di Fiore and Scita, 2002).

Eps8 can regulate actin dynamics in a complex with Abi1 and Sos1. Abi1 functions as a scaffold, linking Eps8 to the bifunctional Ras/Rac-GEF Sos1 (Lanzetti et al., 2000). Eps8 association promotes Sos1 activity, and the tri-complex exhibits Rac-specific GEF activity (Scita et al., 1999). The Eps8-Abi1-Sos1 complex is regulated by RTK downstream signalling. PI3K is recruited to active RTKs and activated by Ras, to produce PIP3, which in turn activates Rac-GEFs including Sos1 (Vanhaesebroeck et al., 2001). Tri-complex-dependent Rac1 activity induces the formation of membrane ruffles and lamellipodia (Scita et al., 1999).

Eps8 binds to actin directly and has actin capping and bundling capabilities (Scita et al., 2001). Eps8 actin-binding is also involved in establishing appropriate localisation of the Eps8-Abi1-Sos1 complex to sites of actin re-modelling (Scita et al., 2001). Eps8 binds to the fast-growing barbed end of actin filaments, preventing addition of actin monomers and filament elongation (Disanza et al., 2004). Actin capping limits filament length and promotes actin branching which results in stiffer mesh-like networks, and aids polarisation by localising actin polymerisation (Disanza et al., 2004). Eps8 can also bind and sequester monomeric actin, preventing its incorporation into filaments (Hertzog et al., 2010). Eps8 is additionally capable of binding to the side of actin filaments and bundling actin, likely by forming homodimers or heterodimers with the CDC42 regulated actin-bundler IRSp53 (Hertzog et al., 2010; Vaggi et al., 2011).

Eps8 can inhibit endocytosis in a complex with the Rab5-GAP RN-tre (Lanzetti et al., 2000). Rab5 is involved in receptor endocytosis. EGF stimulation activates Rab5 and downmodulates the activity of RN-tre. Eps8 binding to RN-tre recruits the complex to EGFR, enabling RN-tre

to inactivate Rab5, inhibiting endocytosis. Eps8 binds RN-tre and Abi1 via the same SH3 domain, therefore RN-tre and Abi1 compete for binding and can therefore divert Eps8 function (Lanzetti et al., 2000). Eps8 binding to actin is mediated by a different site, however this cannot occur for the monomeric form of Eps8 and is positively influenced by Abi1 binding to Eps8 (Disanza et al., 2004; Hertzog et al., 2010).

The EGF regulated recruitment of Eps8 to IACs, its interconnectivity within the proteomic network indicate Eps8 could have functional relevance in integrating growth factor-mediated adhesion responses. Eps8 will therefore be examined as a potential mediator of EGFR and integrin crosstalk. Eps8 regulates EGFR endocytosis, therefore adhesion turnover and integrin receptor internalisation will be investigated. The effect of the diverse functions of Eps8 on the actin cytoskeleton will also be assessed by measuring cell membrane dynamics.

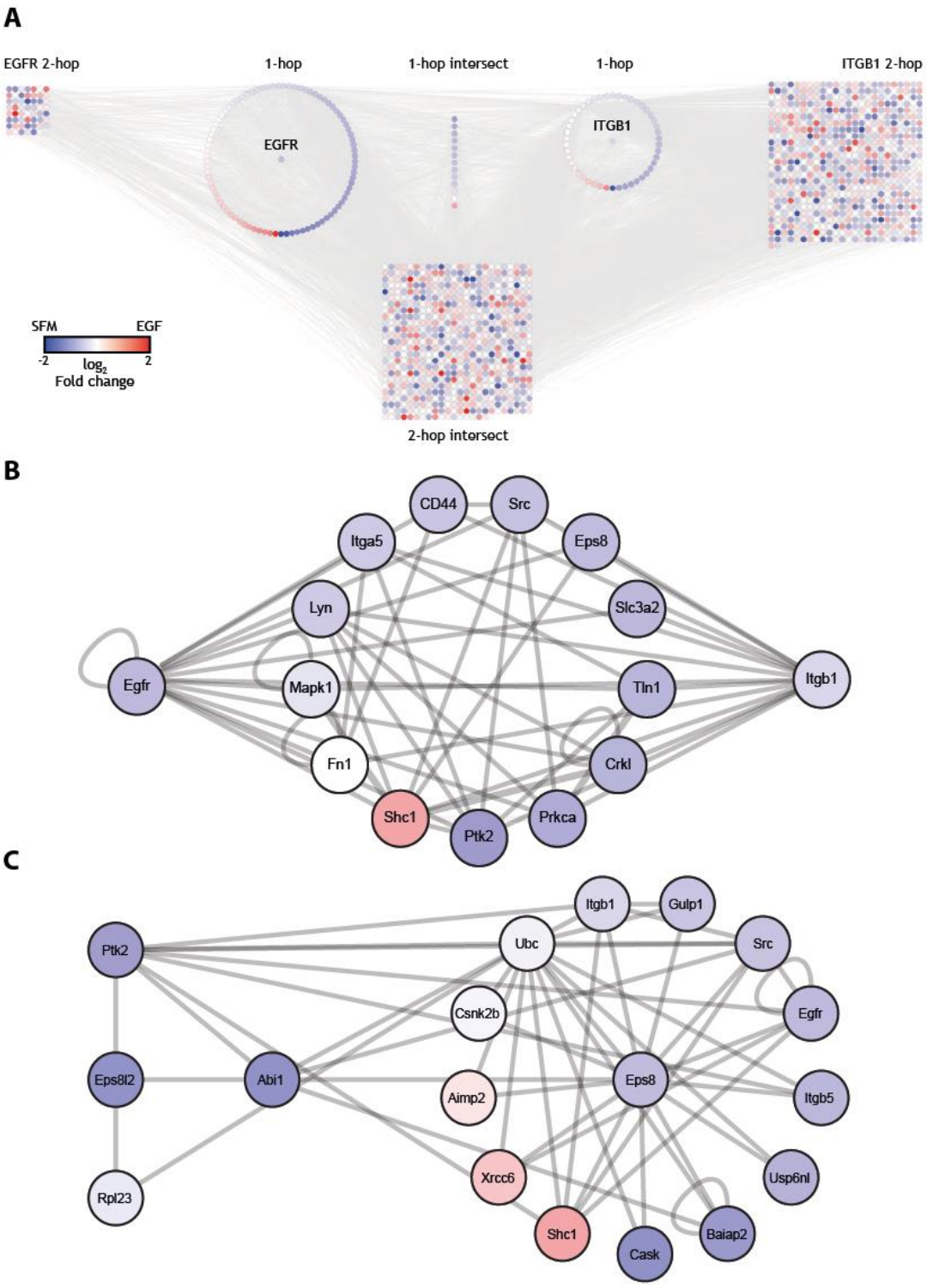

Figure 5.1: Network analysis of adhesion receptor-growth factor receptor crosstalk identified Eps8 as a putative node of signal interaction. MS dataset of IACs isolated from Eph4 cells plated on collagen initially, then cultured overnight with cells secreting ECM resulting in a mixed matrix environment. IACs were isolated under serum-free conditions or after 5 minutes EGF stimulation. Node colour red to blue gradient = log2 fold enrichment EGF/serum-free. (A) One and two-hop interactors of EGFR and integrin β1. (B) EGFR, integrin β1 and their one-hop intersect common interactors. (C) One and two-hop interactions of Eps8 and Eps8L2.

5.2 Results

5.2.1 Eps8 localises to focal adhesions

To investigate subcellular distribution of Eps8, cells were co-stained with Eps8, the canonical adhesion complex protein talin and phalloidin to determine if Eps8 localises to focal adhesions and actin, respectively. The Im+ MEF fibroblast cell line was used in addition to Eph4 mammary epithelial cells, as fibroblasts form robust load-bearing adhesion structures. Co-localisation between Eps8 and talin was observed in both Eph4 and Im+ MEF cell lines (Figure 5.2, Mark Morgan, unpublished data), confirming the results of the MS. Eps8 co-localisation with actin was observed in Eph4 but not Im+ MEF cells. The cytoskeletal organisation differs between the two cell lines, which may account for this difference. The distribution of Eps8L2 was also investigated, as it was also isolated from Eph4 IACs. Eps8 co-localised with Eps8L2 to a degree, however Eps8L2 was notably absent from talin positive focal adhesion structures (Figure 5.2 B). This observation was consistent with the reduced connectivity of Eps8L2 in enriched IACs and suggested that Eps8 may have more direct adhesion regulatory functions than Eps8L2.

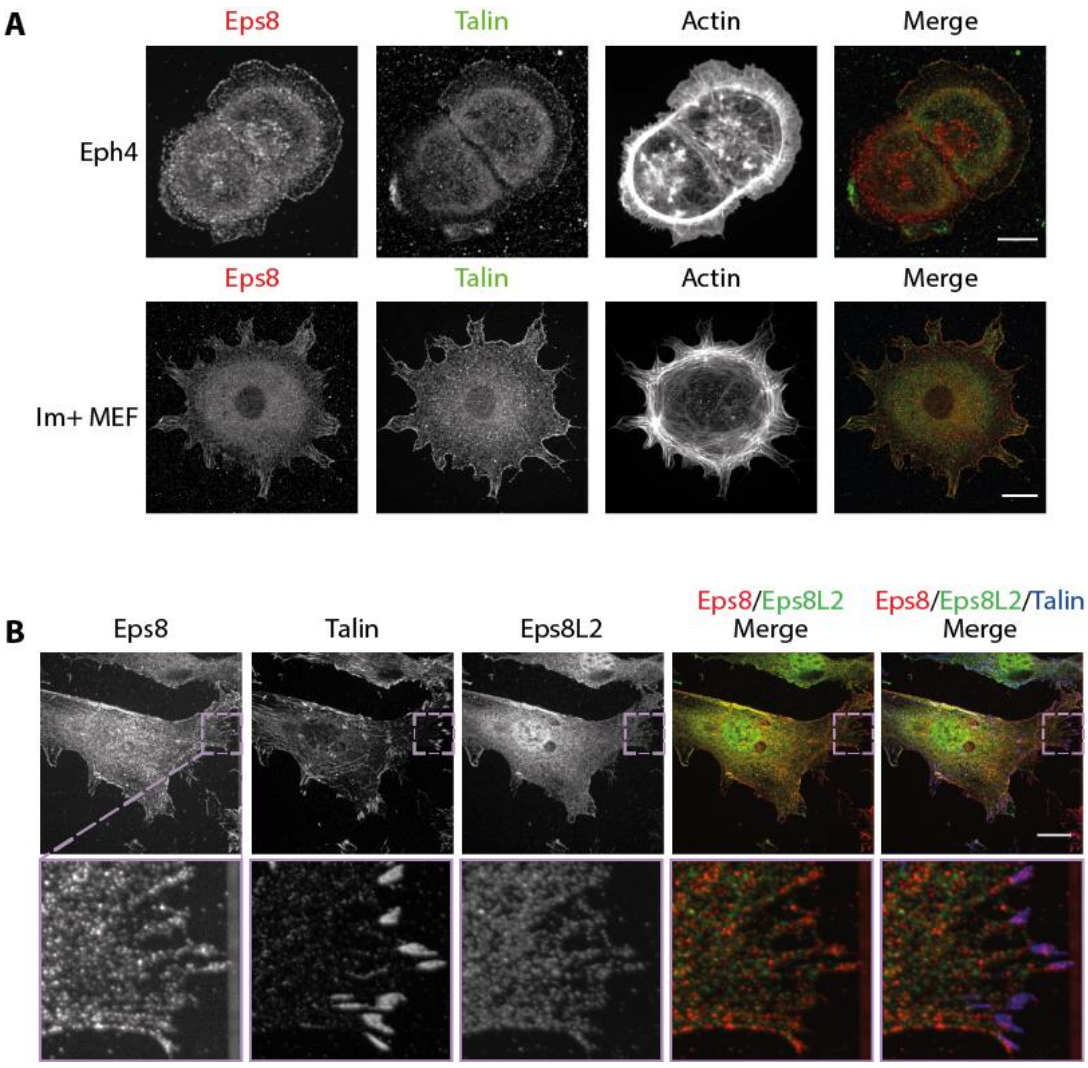

Figure 5.2: Eps8 localises to integrin-associated adhesion complexes. (A) Eps8 co-localises with talin in Eph4 and Im+ MEF cells. Scale bar = 10 µm for Eph4 and 20 µm for Im+ MEFs. (B) Eps8 co-localises with talin at focal adhesions whereas Eps8L2 does not in Im+ MEF cells. Lower panel are higher amplification image insets. Scale bar = 20 µm. All images are maximum z-slice projections. Representative cells from three replicates.

5.2.2 Eps8 constrains EGFR and α5β1 integrin internalisation

Ontological analysis suggested that endocytosis was a key biological process differentially regulated at IACs by EGF stimulation. While the effect of Eps8 on internalisation of integrins has never been determined, Eps8, in complex with RN-tre is known to inhibit Rab5 and suppress endocytosis of EGFR (Lanzetti et al., 2000). The detection of both Eps8 and RN-tre in isolated IACs, and the role that RN-tre plays in Rab5-dependent heterodimer-specific integrin endocytosis (Lanzetti et al., 2007; Palamidessi et al., 2013) led us to analyse whether Eps8 and Eps8L2 regulate integrin and/or EGFR trafficking. The EGF-dependent de-enrichment of α5β1 in IACs, and the connectivity of α5β1 to Eps8 and RN-tre in the proteomic networks indicates this complex may have a role in α5β1 endocytosis. To determine the effect of Eps8 on EGFR and integrin endocytosis, constitutive and EGF ligand-stimulated internalisation rates of EGFR and integrin α5β1 were assessed by biochemical endocytosis assays in control, Eps8 and Eps8L2 knockdown Im+ MEFs.

Under unstimulated conditions control knockdown Im+ MEFs exhibited low levels of constitutive endocytosis of both α5β1 and EGFR (Figure 5.3, Mark Morgan, unpublished data). Stimulation with EGF statistically significantly increased the rate of EGFR endocytosis (7.5 minutes p= 0.004; 15 minutes p= 0.005), and trended towards an increase in α5β1 endocytosis, suggesting a level of crosstalk between EGFR and integrin α5. However, in the absence of EGF-stimulation, knockdown of Eps8 increased the rate of constitutive endocytosis in comparison to control cells of both α5β1 (7.5 minutes p= 0.023, 15 minutes p= 0.033) and EGFR (7.5 minutes p = 0.001, 15 minutes p= 0.017), to levels comparable to EGF stimulation of control cells. Stimulation with EGF in Eps8 knock-down cells slightly increased the rate of α5β1 and EGFR endocytosis relative to unstimulated Eps8 knock-down cells, which was statistically significant at 7.5 minutes for EGFR internalisation rates (7.5 minutes Eps8 KD EGF stimulated compared to Eps8 KD nil p= 0.003). By contrast, Eps8L2 knockdown did not statistically significantly affect either constitutive or ligand stimulated of α5 or EGFR endocytosis (Figure 5.3 B). Together these data show that Eps8 functions to constrain the endocytosis of both α5β1 and EGFR.

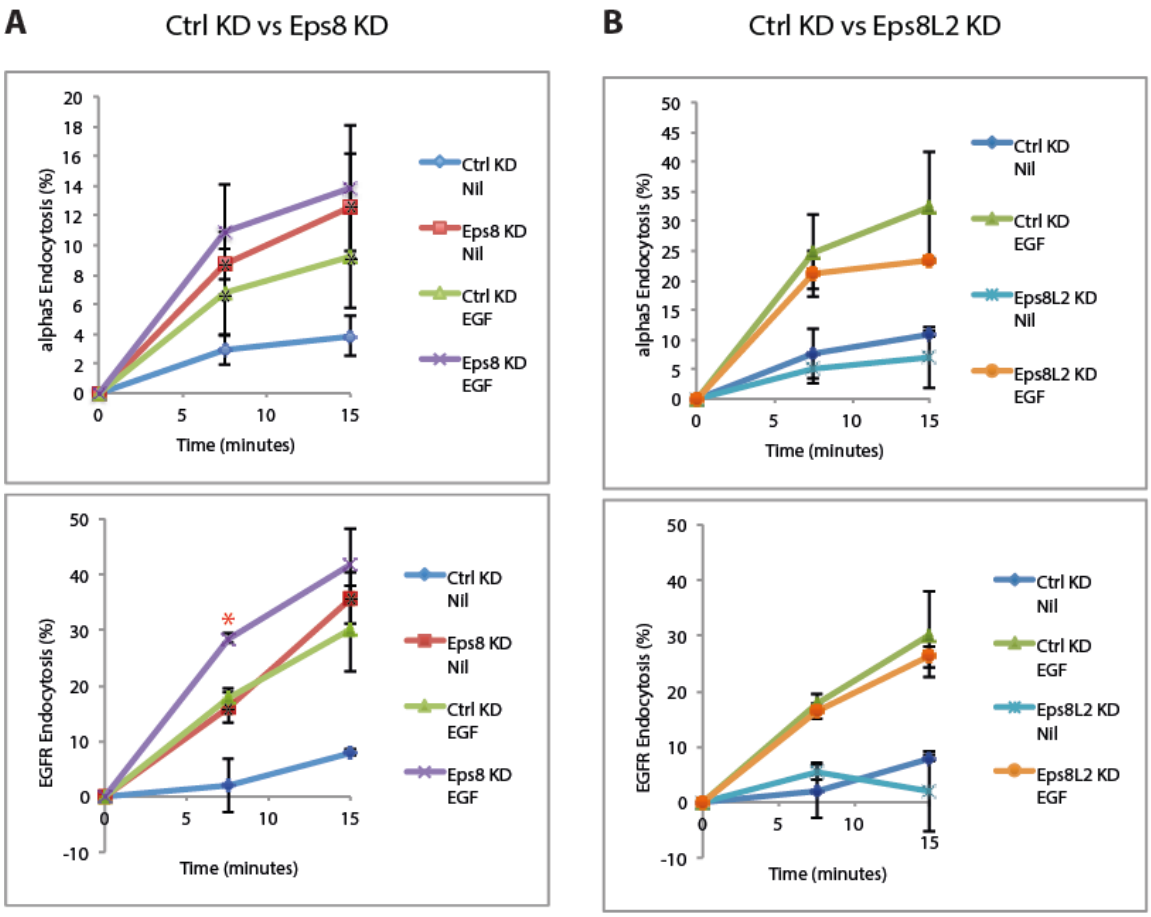

Figure 5.3: Eps8 constrains integrin α5β1 and EGFR endocytosis. EGF Stimulation increases endocytosis of both α5β1 and EGFR. (A) Eps8 knock down increases unstimulated constitutive and EGF stimulated endocytosis of α5β1 and EGFR. (B) Eps8L2 knock down does not statistically significantly affect α5β1 or EGFR endocytosis. Biochemical internalisation assay in Im+ MEFs. N = 3, data points plotted as means with SEM error bars. Statistical test = two-tailed t-test assuming unequal variance. * = p< 0.05 in comparison to the control KD nil. * = p< 0.05 in comparison to the Eps8 KD nil.

5.2.3 Eps8 is involved in EGF-mediated adhesion disassembly

Adhesion disassembly is closely linked to endocytosis, as dissociation of integrin-associated cytoskeletal components is required to permit assembly of endocytic complexes and internalisation of integrins and associated proteins from the cell membrane (Ezratty et al., 2009). As Eps8 constrains integrin α5β1 and EGFR internalisation, we assessed whether Eps8 has a role in regulating the disassembly or remodelling of adhesions. Adhesion complex organisation was therefore assessed by immunofluorescence under basal and EGF-stimulated conditions with Eps8 knockdown. (Figure 5.4, Mark Morgan, unpublished data).

Under steady-state serum-containing conditions, α5β1 distribution is similar in control and Eps8 knockdown cells, however after serum-starvation α5β1 is organised in fibrillar-like adhesion structures in control cells, whereas in Eps8 KD cells α5β1 adhesive structures are disorganised (Figure 5.4). In control knockdown cells, EGF stimulation causes rapid disassembly of α5β1 adhesion complexes which is most evident at 15 minutes, prior to re-assembly that is initiated from 30 minutes. However, in Eps8 knockdown cells α5β1 adhesions do not disassemble in response to acute EGF stimulation and remain disorganised. Together these data indicate Eps8 is required for the organisation and EGF-mediated disassembly of adhesion complexes, which is likely related to Eps8-mediated regulation of α5β1 endocytosis.

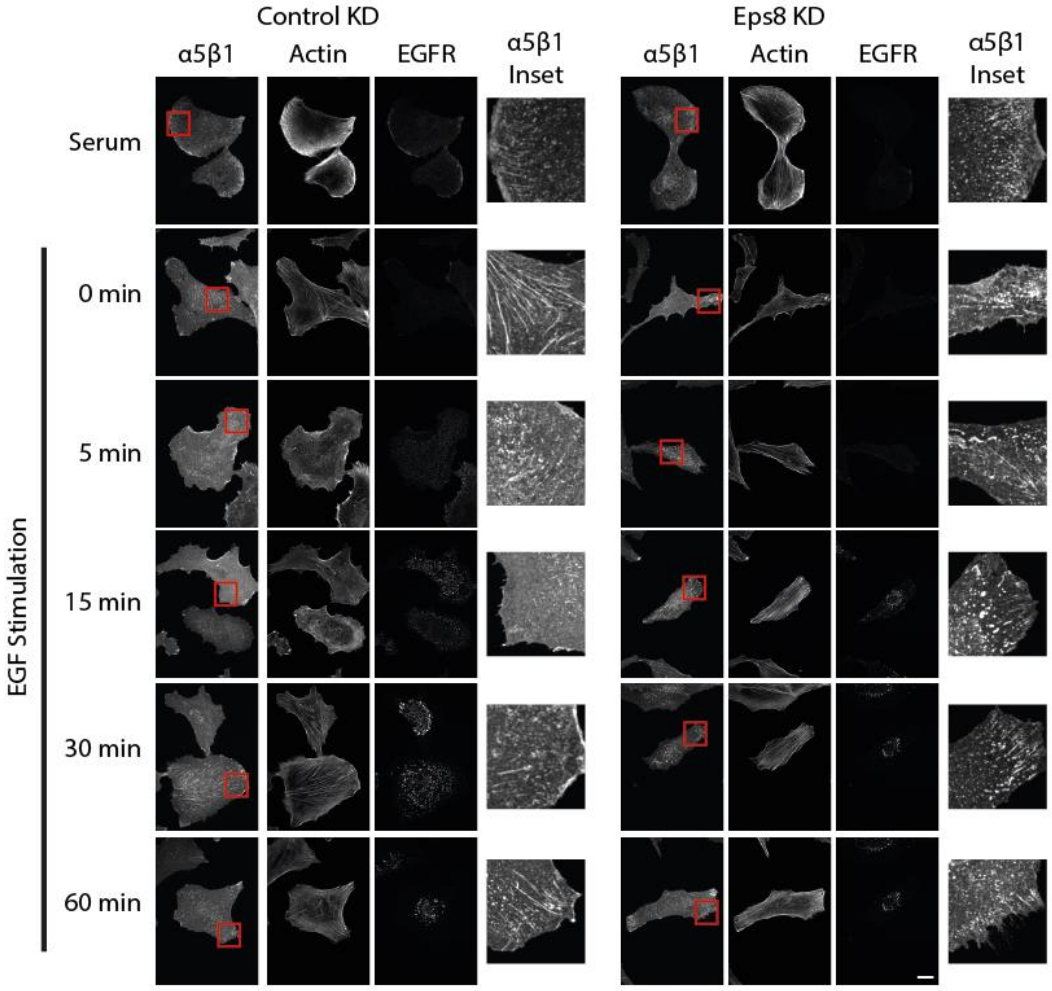

Figure 5.4: Eps8 regulates adhesion complex disassembly. Eps8 is required for maintenance of adhesion complex organisation, and EGF-dependent adhesion complex disassembly. TIF cells were serum starved then stimulated with 10 ng/ml EGF. Images are maximum z-slice projections. Representative cells from three replicates. Scale bar = 30 µm

5.2.4 Effect of Eps8 on EGFR and integrin signalling

Eps8 has been linked to EGFR signalling, as overexpression of Eps8 increases cell proliferation in response to EGF (Fazioli et al., 1993). Eps8 may also affect EGFR and integrin signalling by affecting their trafficking and consequent surface bioavailability and subcellular distribution. To determine the role of Eps8 in EGFR and integrin signalling, phosphorylation of canonical downstream signalling effectors was assessed in response to EGF with Eps8 or Eps8L2 knockdown. No statistically significant effect was observed on the phosphorylation of EGFR or its downstream targets ERK or Akt in response to EGF (Figure 5.5).

The phosphorylation of paxillin, FAK and Src which are canonically phosphorylated at IACs was also largely unchanged with Eps8 or Eps8L2 knockdown (Figure 5.6). Phosphorylation levels of Src at Y527 was statistically significantly lower in Eps8 knock-down cells compared to control knock-down cells at 5 minutes EGF stimulation (Eps8 KD mean= 0.14, SD= 0.04; control KD mean= 0.21, SD= 0.01; p= 0.04), and significantly higher in Eps8 knock-down cells compared to control knock-down cells at 60 minutes EGF stimulation (Eps8 KD mean= 0.28, SD= 0.05; control KD mean= 0.18, SD= 0.02; p= 0.03). This trend was not observed at any other timepoints and therefore is unlikely to have great biological significance. These data indicate Eps8 and Eps8L2 do not seem to have a direct role in regulating EGFR or α5β1 signalling.

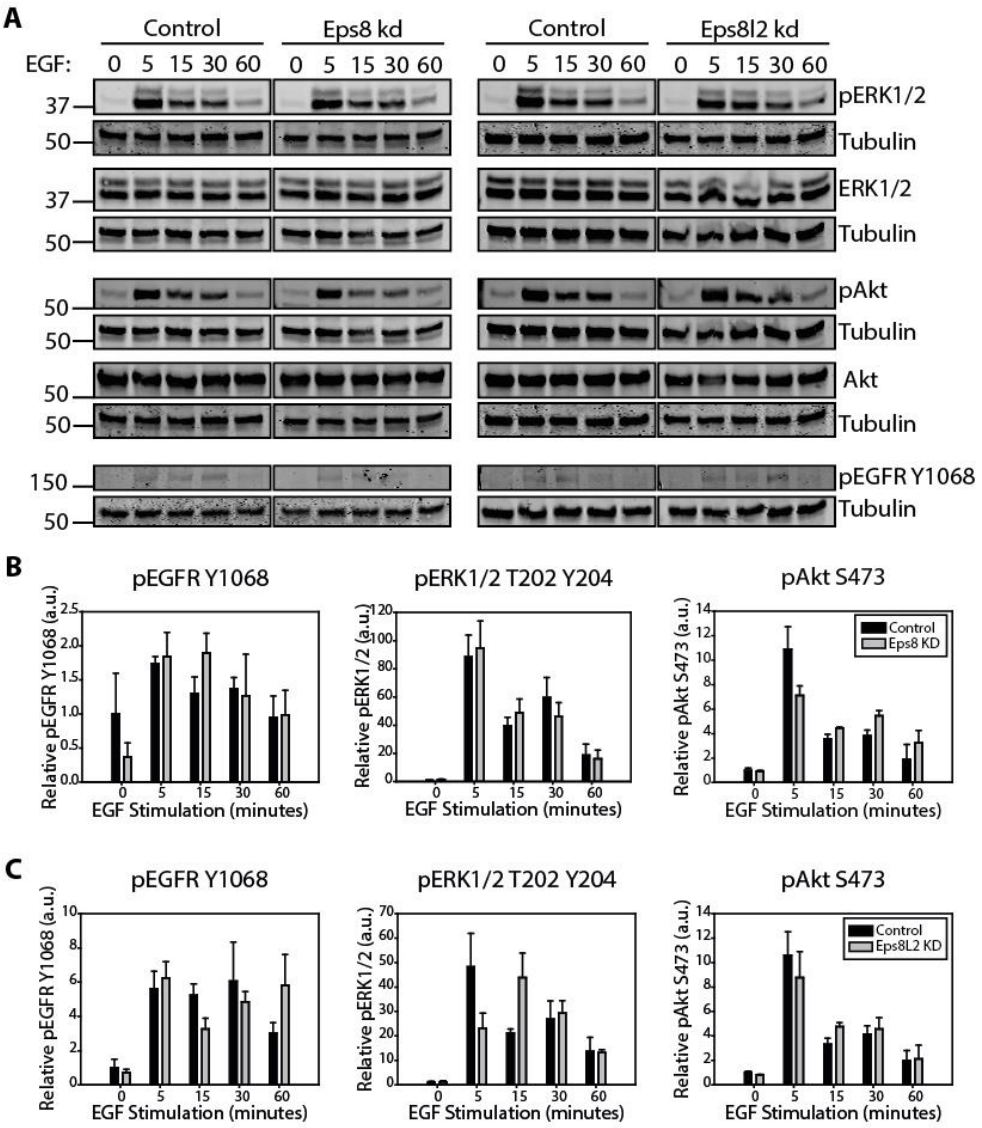

Figure 5.5: Eps8 knock down does not statistically significantly affect EGFR signalling. (A) Stimulation of Im+ MEF cells with 10 ng/ml EGF. Western blots of phosphorylated and total levels of EGFR, ERK1/2, Akt. Total EGFR is normalised to tubulin due to poor staining of total EGFR. Quantification of phosphorylation relative to total protein levels or tubulin normalised to unstimulated control in Eps8 KD (B) or Eps8L2 KD cells (C). N=3, error bars = SEM. Black bar = control siRNA, grey bar = Eps8 or Eps8L2 KD condition.

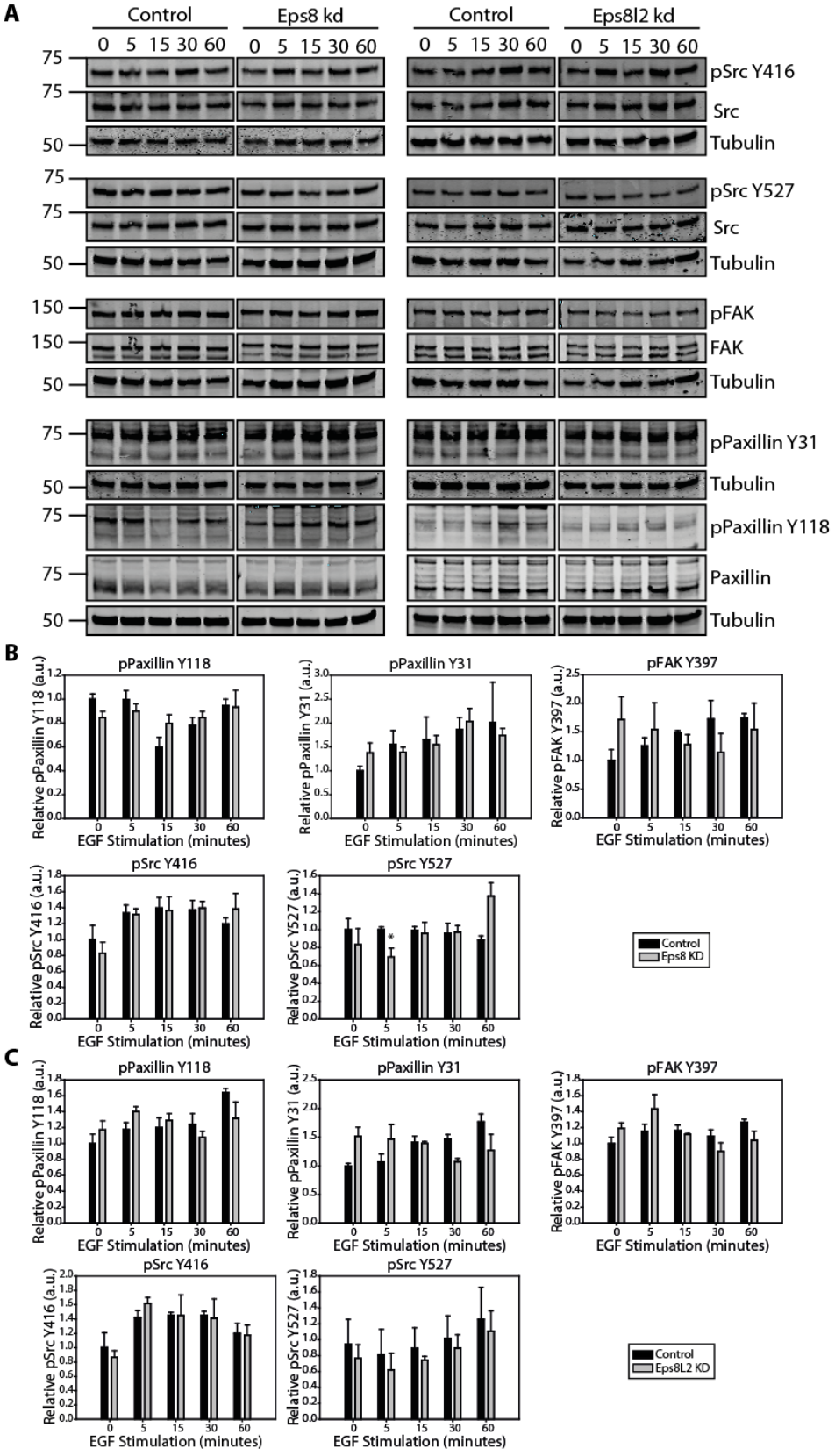

Figure 5.6: Eps8 knock down does not statistically significantly affect integrin signalling. A) Stimulation of Im+ MEF cells with 10 ng/ml EGF. Western blots of phosphorylated and total levels of paxillin, Src and FAK. Quantification of phosphorylation relative to total protein levels normalised to unstimulated control in Eps8 KD (B) or Eps8L2 KD cells (C). N=3, error bars = SEM. Black bar = control siRNA, grey bar = Eps8 or Eps8L2 KD condition. * = $p < 0.05$.

5.2.5 Effect of Eps8 on cell membrane protrusion

Eps8 is required for efficient cell migration, and influences membrane protrusion by promoting Rac1 activity in complex with Abi1 and Sos1, and capping or bundling actin (Disanza et al., 2004; Disanza et al., 2006; Scita et al., 1999). Our data have identified a key role for Eps8 in the regulation of α5β1 and EGFR endocytosis and EGF-dependent adhesion turnover. Coordinated integrin endocytosis and recycling is required for the spatio-temporal control of integrin-mediated adhesions and cytoskeletal dynamics, which is essential for membrane protrusion and retraction in cell migration (Paul et al., 2015). We therefore assessed the role of Eps8 on EGF-dependent cytoskeletal dynamics. Membrane protrusion and retraction were quantitatively analysed in cells on CDMs under serum-starved and EGF-stimulated conditions with Eps8 and Eps8L2 knockdown.

Control cells were contractile under serum-starved conditions, and EGF stimulation induced a suppression of contractility (Figure 5.7). No changes were observed in the non-directional membrane motility data (Figure 5.7 B), demonstrating overall dynamics were unchanged and only directionality was influenced. By contrast, Eps8 knockdown cells were less contractile than unstimulated control cells and did not respond to EGF stimulation. Serum-starved Eps8L2 knockdown cells exhibited similar levels of contractility to control cells, and also respond positively to EGF stimulation (although to a lesser degree than control knockdown). Thus, Eps8 is required to sustain membrane contractility in the absence of EGF and for the EGF-mediated stimulation of protrusion; whereas Eps8L2 is not essential for a protrusive response to EGF as this is only partially ameliorated with Eps8L2 knockdown. Collectively our data show Eps8 is required to constrain cellular functions that are stimulated by EGF, when Eps8 is displaced from IACs.

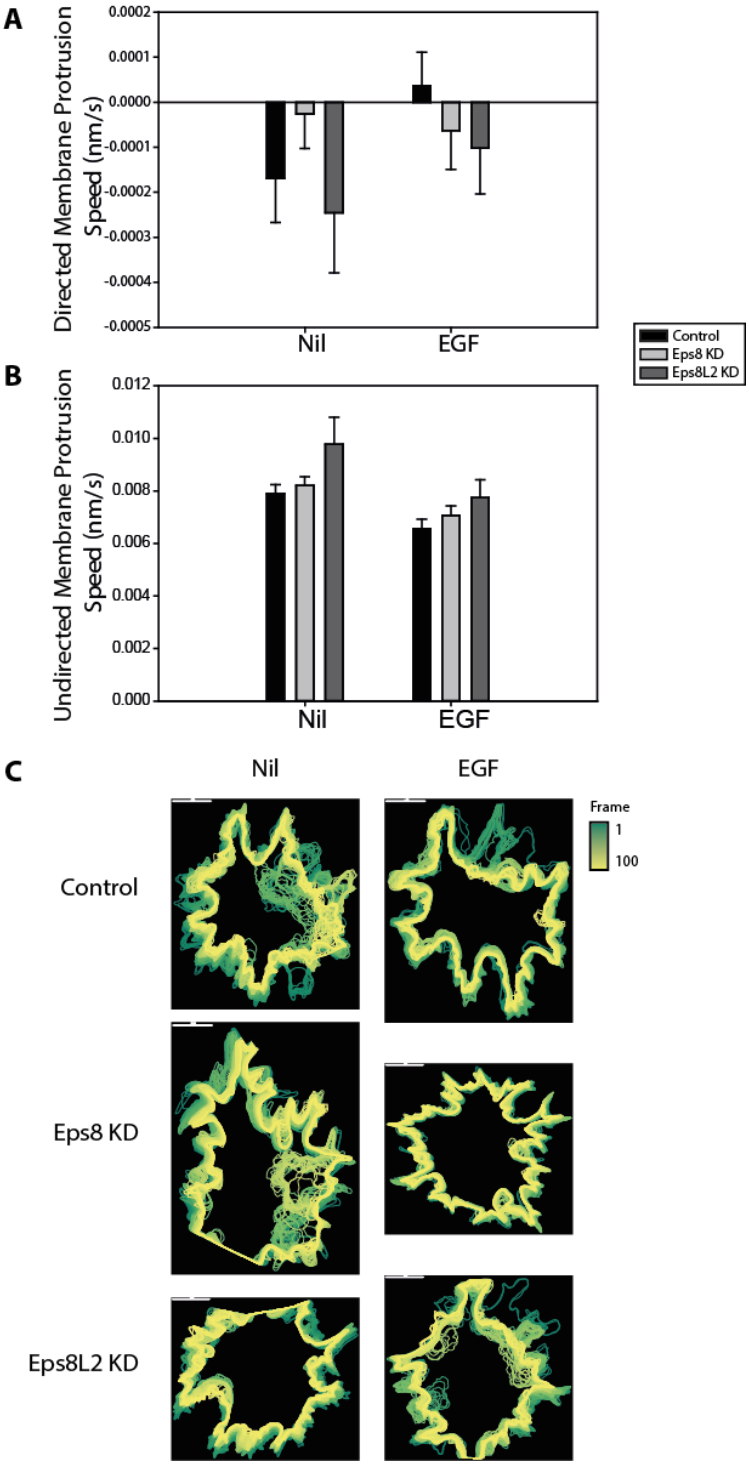

Figure 5.7: Effect of Eps8 KD on membrane protrusion and contractility. LifeAct transfected Im+ MEF cells were imaged on cell-derived matrices for one hour prior and post stimulation with 10 ng/ml EGF. Imaging was resumed approximately 10 minutes after EGF stimulation. Cell membrane tracking analysis was performed using the QuimP (V 17.10.02) plug-in for Image J. Directed (A) and undirected (B) membrane protrusion speed (nm/s) for control (black), Eps8 KD (light grey) and Eps8L2 KD (dark grey) cells under serum-starved and EGF stimulated conditions. Positive and negative values indicate membrane protrusion and contraction, respectively. Data was not statistically significant ($p<0.05$) by a two-way t-test. N =3 for control and Eps8 KD, N = 2 for Eps8L2 KD. Error bars = SEM. (C) Cell tracks for representative single cells in which all cell outlines are overlaid and coloured according to frame number. Corresponding movies are supplementary information on the accompanying CD. Scale bar = 10 μm.

5.3 Discussion

Eps8 has been identified as a novel mediator of GFR and integrin crosstalk, with previously undescribed roles in integrin regulation. Eps8 localises to integrin-mediated adhesion complexes and is required for α5β1-mediated adhesion structural organisation. EGF stimulation causes de-enrichment of Eps8 and α5β1 from IACs, and results in α5β1 adhesion disassembly. Eps8 does not alter immediate signalling from α5β1 or EGFR, however alters receptor dynamics by constraining them at the cell surface. Eps8 contributes to the regulation of cell contractility, which is normally released by EGF signalling. We propose that during tissue morphogenesis and repair, Eps8 functions to spatially and temporally constrain endocytosis, and engagement, of α5β1 and EGFR in order to precisely co-ordinate adhesion disassembly, cytoskeletal dynamics and cell migration.

It is not yet known how Eps8 is recruited to α5β1-mediated IACs. However, Eps8 can bind EGFR directly and therefore could be recruited via this interaction (Castagnino et al., 1995), as EGFR is present in the same IACs (Figure 5.1). Eps8 could also theoretically bind α5β1, as the isolated PTB domain of Eps8 binds the NPxY motif of integrin β1, β3 and β5 (Calderwood et al., 2003). Importantly, the EGFR binding region of Eps8 is separate from its PTB binding domain, therefore Eps8 would have the potential to bind both receptors simultaneously (Di Fiore and Scita, 2002). Localisation of the Eps8 binding partner RN-tre has been demonstrated at integrin-mediated adhesions and therefore RN-tre could also have a role in recruiting Eps8 (Palamidessi et al., 2013).

Adhesions formed via α5β1 are disorganised in Eps8 knockdown cells, and do not form fibrillar structures that are evident in control cells (Figure 5.4). Adhesion disorganisation is likely linked to the increased rate of constitutive α5β1 endocytosis, as this would disrupt adhesion maturation into fibrillar adhesions. Adhesion organisation would also be impacted by Eps8-dependent changes in actin dynamics, as actomyosin-dependent contractility is essential for the translocation of α5β1 during fibrillar adhesion formation (Wolanska and Morgan, 2015). Importantly, the disorganised α5β1 adhesion structures in Eps8 knockdown cells do not undergo EGF-mediated disassembly, indicating Eps8 is required to functionally link EGF responses and adhesion disassembly.

Eps8-dependent regulation of α5β1 endocytosis and adhesion organisation is likely to directly influence the ECM, as α5β1 has a major role in FN fibrillogenesis and remodelling (Wolanska and Morgan, 2015). Endocytosed active FN-bound α5β1 is trafficked to the lysosome where FN is degraded, resulting in matrix turnover (Shi and Sottile, 2008; Sottile

and Chandler, 2005). Unlike FN, α5β1 is recycled from the lysosome and perinuclear recycling compartment to the plasma membrane (Arjonen et al., 2012; Dozynkiewicz et al., 2012). Changes in ECM composition and structure can directly influence cellular functions.

Eps8 and Eps8L2 knockdown did not affect phosphorylation of signalling targets downstream of EGFR or integrins under basal or EGF-stimulated conditions (Figure 5.5 and 5.6). Eps8 is a positive regulator of EGF-mediated mitogenic signals (Fazioli et al., 1993), however Eps8 knockdown has been shown to have no effect on the level of ERK phosphorylation in response to EGF (Lanzetti et al., 2000). This is in agreement with our results, which suggest that positive regulation of cell proliferation in response to EGF by Eps8 is not due to a direct influence on phosphorylation of downstream effectors. Eps8 suppresses constitutive, and to some extent EGF-stimulated, EGFR endocytosis, which if it impacted surface-levels and bioavailability of EGFR, could potentially affect its signalling. However, recycling rates of EGFR and α5β1 have not been assessed, which if balanced with endocytosis would result in no net change in surface receptor levels.

Membrane protrusion/retraction analysis demonstrated Eps8 is required for cell contractility in the absence of EGF (Figure 5.7). Control cells responded to EGF by decreasing contractility. This could be mediated by Rac1 which is activated downstream of EGFR-PI3K signalling which promotes the activity of the Abi1-Eps8-Sos1 complex which acts as a Rac-GEF, stimulating the formation of membrane ruffle protrusions (Offenhauser et al., 2004). Protrusive activity in Eps8 knockdown cells is unchanged with EGF stimulation, indicating the Abi1-Eps8-Sos1 complex is required for EGF-mediated changes in cell protrusion.

Eps8L2 knockdown cells exhibit similar levels of basal contractility as control cells. Moreover, Eps8L2 knockdown cells respond to EGF stimulation in a similar manner to control cells but to a lesser extent. This suggests that Eps8L2 does not function to supress contractility in the absence of EGF stimulation. However, Eps8 and Eps8L2 display the greatest protein homology within the Eps8 family of proteins (Offenhauser et al., 2004), so an alternative possibility is that the function of Eps8L2 may be compensated for by Eps8. If this were the case, our data suggest that Eps8 could possibly compensate for Eps8L2 knockdown, but not vice versa. Considerable redundancy is thought to exist within the Eps8 family, due to the highly conserved protein structure and apparent lack of phenotype in the Eps8 knockout mouse (Offenhauser et al., 2004; Scita et al., 1999). Eps8 and Eps8L2 bind and activate Sos1 with similar kinetics, and ectopic expression of Eps8L2 can restore membrane ruffles in response to EGF in Eps8 knockdown cells (Offenhauser et al., 2004). However, while Eps8 and

Eps8L2 share 60% homology within their SH3 domains (Offenhauser et al., 2004), little is known about the ability of Eps8L2 to associate with RN-tre, so it is possible that Eps8 and Eps8L2 have differential abilities to modulate receptor trafficking.

Eps8 knockdown cells under unstimulated conditions are less contractile than the control. Eps8 stimulates Rac1 activity downstream of PI3K activity, however knockdown of Eps8 has no effect on basal Rac1 activity levels (Scita et al., 1999). Unpublished data from our laboratory (Katarzyna Wolanska, University of Liverpool) also suggests Eps8 does not modulate Rac1 activity levels in MEFs. Therefore, it is likely that Eps8-dependent contractility is a function of the actin regulatory and/or receptor trafficking regulatory roles of Eps8.

Eps8 can function as a barbed-end actin capping protein, inhibiting filament elongation (Disanza et al., 2004). Actin capping proteins limit actin filament length, promoting the formation of a branched actin network and preventing inappropriate actin polymerisation (Pollard and Cooper, 2009). Loss of Eps8-mediated actin capping could result in an increase in uncoordinated protrusions and a less established actin-network that could be less contractile. In addition, the higher rate of α5β1 internalisation following Eps8 knockdown could limit cell contractility, as there would be fewer load-bearing cell-ECM interactions with the capacity to establish robust stress fibres in order to apply mechanical force. In conclusion, we have shown the multifunctional roles of Eps8 are likely to contribute to the regulation of integrin biology in an EGFR-influenced manner.

6. Discussion

We have shown that integrin αVβ6 and EGFR exhibit functionally-relevant crosstalk in TNBC cell lines. EGFR co-localises with points of αVβ6-mediated cell-ECM adhesions, which was indicated by both immunofluorescence and proteomic analysis of αVβ6-IACs. Integrin αVβ6 and EGFR crosstalk may modulate trafficking dynamics, as preliminary data suggested stimulation of either receptor induces co-internalisation and co-trafficking of both. Crosstalk also influences receptor signalling, as preliminary data showed stimulation of αVβ6 induces the phosphorylation of ERK which is canonically downstream of EGFR signalling.

Unbiased interrogation of αVβ6 IAC proteomic networks revealed the composition of αVβ6-associated adhesions and identified endocytosis and ErbB signalling as over-represented terms, highlighting relevant candidate proteins that may potentially regulate αVβ6-EGFR crosstalk. Using different cellular systems, proteomic analysis of EGF-regulated IAC composition identified Eps8 as a novel regulator of α5β1 and EGFR crosstalk, with roles affecting receptor trafficking, adhesion organisation and membrane dynamics. The potential for the novel functions of Eps8, revealed by these analyses, to have wider implications for other integrins, including αVβ6, will be considered below.

6.1 Co-trafficking of αVβ6 and EGFR co-ordinates functional receptor crosstalk

Integrin αVβ6 and EGFR co-localise at cell-ECM adhesion sites. Immunofluorescence data and αVβ6-IAC composition analysis indicates αVβ6 and EGFR are proximal, however it is unknown if the two interact. Co-immunoprecipitation of integrins and GFRs including EGFR has been reported (Borges et al., 2000; Yu et al., 2000), however direct interactions have not been robustly proven.

Indirect interactions between integrins and GFRs can be mediated by other transmembrane proteins, such as syndecans and tetraspanins (Afratis et al., 2017; Byron et al., 2010; Charrin et al., 2014). Syndecan-4 can simultaneously bind EGFR and α6β4 integrin to form a trimolecular complex which is required for EGF-mediated motility (Wang et al., 2015). Syndecan-1 is required for the interaction between insulin-like growth factor-1 (IGF-1) and αVβ3 and mediates their crosstalk (Beauvais and Rapraeger, 2010). Tetraspanins can bind both EGFR and integrins (Odintsova et al., 2003). The interaction between some tetraspanins and integrins can be positively regulated by palmitoylation (Yang et al., 2004), which could be especially relevant for αVβ6, as FASN which produces palmitate is recruited to αVβ6-IACs.

Some ECM molecules can also function as bridges between integrins and GFRs, such as tenascin-C which can be bound by both EGFR and αVβ3 (Jones et al., 1997b; Swindle et al., 2001). Cytoplasmic interactions may also influence association between αVβ6 and EGFR. Eps8 could also potentially mediate an interaction between EGFR and integrins, as Eps8 can bind both EGFR and integrin β-subunit cytoplasmic domain NPxY motifs, via separate domains (Calderwood et al., 2003; Castagnino et al., 1995). Proximity without interaction is also possible, and could be mediated by aggregation of integrins causing GFR co-clustering (Yamada and Even-Ram, 2002).

Stimulation of either EGFR or αVβ6 triggers the endocytosis of both receptors, which then co-traffic to HRS-positive endosomes. Co-internalisation of these receptors is likely to affect the functions of both receptors both their functions. EGF stimulation reduced αVβ6-dependent force application (Stephanie Mo, University of Liverpool), which is likely to be caused by EGF-mediated internalisation of αVβ6 reducing surface αVβ6 levels and therefore αVβ6-mediated adhesions. Reduced αVβ6-mediated force application reduces TGFβ activity, as αVβ6 cannot efficiently apply mechanical force to LAP (Tod et al., 2017). Thus, it is likely that trafficking-mediated αVβ6 and EGFR directly impacts TGFβ activation. Perturbation of αVβ6 and EGFR during ligand-stimulated endocytosis is required to investigate the influence of receptor crosstalk on trafficking. The use of super-resolution microscopy and advanced imaging techniques including photoactivatable EGFR and αVβ6 constructs would provide better spatial and temporal resolution of receptor trafficking dynamics, to enable further elucidation of αVβ6 and EGFR co-trafficking. Perturbation of key trafficking regulators identified in chapter 4 such as liprin α1 and Arf6 would allow us to dissect the mechanisms controlling αVβ6 and EGFR trafficking crosstalk.

The effect of EGF and LAP stimulation on receptor recycling and overall surface levels of EGFR and αVβ6 is currently unknown. Imbalance in the rate of endocytosis and recycling would result in changes in receptor surface bioavailability. EGFR traffics to the lysosome following LAP-mediated internalisation, where it is likely degraded which could reduce total EGFR protein levels. αVβ6 does not co-localise with lysosomal markers and therefore is likely to be recycled back to the plasma membrane. Whilst this has not been yet been tested experimentally, EGFR-αVβ6 crosstalk could induce changes in plasma membrane bioavailability of receptors, which would be likely to influence EGFR and αVβ6-mediated cell migration and invasion. Importantly, the clinical αVβ6 inhibitor 264RAD stimulated the internalisation of both αVβ6 and EGFR in TNBC cells. Therefore, the impact of αVβ6 and EGFR co-trafficking is potentially relevant clinically as it may modulate the effect of therapeutically

targeting αVβ6. If this were the case, the EGFR status of tumours could be an important consideration for treatment stratification. The potential for αVβ6 and EGFR crosstalk to influence the response to targeted molecular therapeutics are the subject of ongoing studies in the Morgan and Marshall Laboratories.

6.2 αVβ6 promotes EGFR functions

Preliminary data showed LAP stimulation induced ERK phosphorylation, which was only partially ameliorated by EGFR inhibition (gefitinib treatment) in MDA-MB-468 cells, indicating that the process could be a consequence of ligand-independent stimulation of EGFR signalling or that αVβ6 directly regulated MAPK activity. Unpublished phospho-proteomics KSEA (Kinase Substrate Enrichment Analysis) data from our collaborators (Caroline Sproat, Marshall laboratory, Barts Cancer Institute; analysed by Mark Morgan, University of Liverpool), and candidate follow-up by immunoblotting, also demonstrates upregulation of MAPK signalling in response to LAP stimulation (Sproat, 2017). Moreover, in BT-20 TNBC cells, LAP-induced induction of MAPK signalling was inhibited by gefitinib, suggesting that αVβ6-dependent MAPK signalling is, at least in part, EGFR-dependent. Together these data, when considered with the fact that MDA-MB-468 cells are resistant to gefitinib (IC_{50} = 6.8 μM) (Normanno et al., 2006), suggest that LAP-induced endocytosis of αVβ6 triggers EGFR-dependent MAPK activation. However, it is important to note that αVβ6 has been reported to bind, and activate ERK, so it is possible that LAP-stimulation could directly contribute to ERK activation (Ahmed et al., 2002a). This study did not consider however the potential of crosstalk mechanisms with GFRs.

Positive regulation of ERK signalling by αVβ6-EGFR crosstalk is a potential mechanism by which αVβ6 expression may result in a poor prognosis in cancer, as ERK signalling elicits mitogenic responses which could be linked to hallmarks of cancer such as dysregulated proliferation and anoikis. EGFR is linked to a poor prognosis in a range of cancers, and the expression of αVβ6 could function to exacerbate this, resulting in a worse prognosis with co-expression of the both receptors.

Unpublished data from our collaborators (Kate Moore, John Marshall laboratory, Barts Cancer Institute) has demonstrated that αVβ6 mediates EGFR-dependent invasion. Knockdown of αVβ6 or EGFR in a panel of TNBC cells (MDA-MB-468, SUM-159, BT-20) statistically significantly decreases cell invasion, indicating invasion is αVβ6- and EGFR-dependent. Moreover, under control conditions stimulation with EGF statistically significantly increases invasion, whereas knockdown of αVβ6 completely abrogates this

response, suggesting αVβ6 is required for EGFR-dependent invasion. Together these data indicate αVβ6 has an important function in promoting and mediating EGFR-dependent functions with potential consequences for tumour growth and invasion.

6.3 Novel aspects of αVβ6 biology

Integrin αVβ6 has been relatively under-studied compared to many other integrins, and little is known about its function. It is clear that αVβ6 is associated with a poor prognosis in a range of carcinomas, which is likely to be mediated at least in part by its pro-invasive functions. Integrin αVβ6 is known to stimulate invasion through upregulating the expression and activity of proteases such as MMPs, promoting cell migration, by activating TGFβ and by promoting TGFβ-mediated EMT (Margadant and Sonnenberg, 2010; Morgan et al., 2004; Tod et al., 2017).

Characterisation of αVβ6-IACs validated initial co-localisation data and revealed potential mechanisms of αVβ6-EGFR crosstalk co-ordination. Analysis has identified putative roles for αVβ6 in EGFR signalling, endocytosis, regulation of YAP/TAZ nuclear localisation, palmitoylation and adhesion turnover. All these processes could potentially contribute to αVβ6-mediated invasion. Proteins recruited to αVβ6-IACs and identified as functionally relevant currently being investigated further regarding their role to αVβ6 function.

The identification of Hippo pathway over-representation at αVβ6-IACs provided the rationale for experiments investigating the role of αVβ6 in YAP/TAZ nuclear localisation. Translocation of YAP/TAZ to the nucleus is mediated by mechanical force, which is influenced by ECM rigidity which is often elevated in breast cancer (Dupont, 2016). YAP/TAZ regulate gene transcription, therefore elevated nuclear localisation of YAP/TAZ can lead to transcriptional programming of breast cancer that leads to a worse prognosis (Diaz-Martin et al., 2015). Inhibition of αVβ6 reduced YAP nuclear shuttling across a range of substrate rigidities, in 2D and 3D (unpublished data, Mark Morgan, University of Liverpool). Inhibition of αVβ6 also decreased RhoA activity and myosin-light chain phosphorylation (unpublished data, Mark Morgan, University of Liverpool). Together, these data suggest that αVβ6 blockade suppresses force-transmission and dysregulates YAP localisation and transcriptional reprogramming. Importantly, EGF stimulation also reduced nuclear YAP localisation, which could be a consequence of triggering αVβ6 endocytosis and limiting αVβ6 levels at the cell-matrix interface. Although, to date, we cannot discount that the effect of EGF on YAP distribution is independent of αVβ6 function.

IAC analysis identified endocytic regulators recruited to αVβ6 IACs including a liprin-α1-associated sub-network, that are likely to regulate αVβ6 endocytosis and adhesion turnover and therefore contribute to a pro-invasive phenotype in a similar manner to Hax-1 which is required for αVβ6 endocytosis (Ramsay et al., 2007) (Astro et al., 2014). This is the first comprehensive unbiased analysis of αVβ6 signalling networks and it is anticipated that the dataset of proteins recruited to αVβ6-mediated IACs will be a useful resource for many labs attempting to understand of αVβ6 biology.

6.4 Eps8 is a novel mediator of integrin and growth factor receptor crosstalk

A novel role for Eps8 has been identified in the regulation of basal and EGF-stimulated integrin endocytosis, adhesion organisation and membrane dynamics. While these studies were performed in non-tumour cell lines (Eph4, Im+ MEF & TIF), these newly identified functions of Eps8 are also likely to contribute to the mechanism by which Eps8 promotes cell migration and a poor prognosis in cancer (Cattaneo et al., 2012; Chen et al., 2015; Disanza et al., 2004). To follow up on these studies, it would be interesting to investigate if Eps8 is involved in integrin regulation and trafficking in the absence of EGFR, or in the absence of EGFR-coupling/binding, to determine if EGFR-mediated crosstalk is an essential requirement.

Eps8 is reported to bind integrin β1, β3 and β5 subunits via the NPxY motif which is conserved across all integrin β-subunits (Calderwood et al., 2003). Eps8 binding to β6, β8 and β4 has not been investigated but is theoretically possible. Eps8 regulates the function of αVβ6 (Tod et al., 2017) therefore it is conceivable Eps8 binding to β6 could be a mechanism for this. Eps8 stimulates αVβ6-dependent migration and inhibits αVβ6 force-application and TGFβ activation (Tod et al., 2017). Over-expression of Eps8 in αVβ6-positive tumours could contribute to a worse prognosis if it enhanced αVβ6-mediated invasion. Pro-invasive functions of αVβ6 have been near impossible to separate from indirect effects mediated via TGFβ, so the perturbation of Eps8 could provide a relevant mechanism to explore direct activity of αVβ6. Differentiation between αVβ6 functions is therapeutically important in cancers where inhibition of αVβ6 is contraindicated as TGFβ can function as a tumour suppressor (Thomas et al., 2006).

6.5 The future of αVβ6 cancer therapy

Therapeutic targeting of αVβ6 holds exciting opportunities for the treatment of TNBC which is in desperate need of molecular targets. 25% of TNBCs have high levels of αVβ6, and treatment with the αVβ6 inhibitor statistically significantly reduces tumour growth in *in vivo*

xenografts (Unpublished data, Kate Moore, John Marshall lab, Barts Cancer Institute). Combination of 264RAD with the EGFR inhibitor gefitinib statistically significantly further decreased tumour growth in the same assays, indicating co-targeting of αVβ6 and EGFR could be of therapeutic benefit.

Crosstalk between αVβ6 and EGFR is likely to directly impact the consequences of αVβ6 therapeutic inhibition. Data from this study, and other work in the Morgan Lab, indicates a complex relationship where αVβ6 promotes EGFR signalling and is required for EGF-mediated invasion (Kate Moore, Marshall Lab), and EGF-mediated internalisation of αVβ6 inhibits αVβ6-mediated force-application and YAP nuclear translocation. Thus, one might speculate that therapeutic targeting of EGFR would be contraindicated in αVβ6 positive tumours. However, this conflicts with the overall outcome demonstrated in *in vivo* xenografts. However, there are limitations to the clinical relevance of xenograft models and in the longer term it will be necessary to determine the impact of αVβ6- and EGFR-targeting in genetically-engineered mouse models, or patient-derived xenografts, of TNBC. It will also be important to assess the impact of αVβ6- and EGFR-dependent transcriptional control in TNBC patient tissue.

Ultimately, the success of an αVβ6 therapeutic is likely to be highly-dependent on patient stratification. As an example, TGFβ can function as either a tumour suppressor or promoter in cancer. Inhibition of αVβ6 promoted tumour growth in a PDAC mouse model, however this adverse effect was abrogated in a Smad4-null version of the model (Hezel et al., 2012). Thus, mutations in Smad4, which is essential for TGFβ signalling, are likely to be good criteria for predicting αVβ6 therapy success. However, to fully predict patient responses to αVβ6-targeting drugs, and combination therapies, it will be necessary to employ single-cell next generation sequencing with systems-level analyses to understand the impact of key regulatory mechanisms on the proteomic, phospho-proteomic and transcriptional landscapes of both tumour and stromal cells.

Bibliography

Afratis, N.A., D. Nikitovic, H.A. Multhaupt, A.D. Theocharis, J.R. Couchman, and N.K. Karamanos. 2017. Syndecans - key regulators of cell signaling and biological functions. *FEBS J*. 284:27-41.

Agrez, M., A. Chen, R.I. Cone, R. Pytela, and D. Sheppard. 1994. The alpha v beta 6 integrin promotes proliferation of colon carcinoma cells through a unique region of the beta 6 cytoplasmic domain. *J Cell Biol*. 127:547-556.

Ahmed, N., J. Niu, D.J. Dorahy, X. Gu, S. Andrews, C.J. Meldrum, R.J. Scott, M.S. Baker, I.G. Macreadie, and M.V. Agrez. 2002a. Direct integrin alphavbeta6-ERK binding: implications for tumour growth. *Oncogene*. 21:1370-1380.

Ahmed, N., F. Pansino, R. Clyde, P. Murthi, M.A. Quinn, G.E. Rice, M.V. Agrez, S. Mok, and M.S. Baker. 2002b. Overexpression of alpha(v)beta6 integrin in serous epithelial ovarian cancer regulates extracellular matrix degradation via the plasminogen activation cascade. *Carcinogenesis*. 23:237-244.

Alanko, J., and J. Ivaska. 2016. Endosomes: Emerging Platforms for Integrin-Mediated FAK Signalling. *Trends Cell Biol*. 26:391-398.

Alanko, J., A. Mai, G. Jacquemet, K. Schauer, R. Kaukonen, M. Saari, B. Goud, and J. Ivaska. 2015. Integrin endosomal signalling suppresses anoikis. *Nature cell biology*. 17:1412-1421.

Alberts, B., A. Johnson, J. Lewis, D. Morgan, M. Raff, K. Roberts, and P. Walter. 2015. Molecular Biology of the Cell. Garland Science, New York. 1342 pp.

Alexi, X., F. Berditchevski, and E. Odintsova. 2011. The effect of cell-ECM adhesion on signalling via the ErbB family of growth factor receptors. *Biochem Soc Trans*. 39:568-573.

Allen, M.D., J.F. Marshall, and J.L. Jones. 2014a. alphavbeta6 Expression in myoepithelial cells: a novel marker for predicting DCIS progression with therapeutic potential. *Cancer Res*. 74:5942-5947.

Allen, M.D., G.J. Thomas, S. Clark, M.M. Dawoud, S. Vallath, S.J. Payne, J.J. Gomm, S.A. Dreger, S. Dickinson, D.R. Edwards, C.J. Pennington, I. Sestak, J. Cuzick, J.F. Marshall, I.R. Hart, and J.L. Jones. 2014b. Altered microenvironment promotes progression of preinvasive breast cancer: myoepithelial expression of alphavbeta6 integrin in DCIS identifies high-risk patients and predicts recurrence. *Clin Cancer Res*. 20:344-357.

Aluwihare, P., Z. Mu, Z. Zhao, D. Yu, P.H. Weinreb, G.S. Horan, S.M. Violette, and J.S. Munger. 2009. Mice that lack activity of alphavbeta6- and alphavbeta8-integrins reproduce the abnormalities of Tgfb1- and Tgfb3-null mice. *Journal of cell science*. 122:227-232.

Andreopoulou, E., C.M. Kelly, and H.M. McDaid. 2017. Therapeutic Advances and New Directions for Triple-Negative Breast Cancer. *Breast Care (Basel)*. 12:21-28.

Annes, J.P., J.S. Munger, and D.B. Rifkin. 2003. Making sense of latent TGFbeta activation. *Journal of cell science*. 116:217-224.

Anthis, N.J., J.R. Haling, C.L. Oxley, M. Memo, K.L. Wegener, C.J. Lim, M.H. Ginsberg, and I.D. Campbell. 2009. Beta integrin tyrosine phosphorylation is a conserved mechanism for regulating talin-induced integrin activation. *J Biol Chem*. 284:36700-36710.

Arjonen, A., J. Alanko, S. Veltel, and J. Ivaska. 2012. Distinct recycling of active and inactive beta1 integrins. *Traffic*. 13:610-625.

Arora, N., D. Mainali, and E.A. Smith. 2012. Unraveling the role of membrane proteins Notch, Pvr, and EGFR in altering integrin diffusion and clustering. *Anal Bioanal Chem*. 404:2339-2348.

Askari, J.A., P.A. Buckley, A.P. Mould, and M.J. Humphries. 2009. Linking integrin conformation to function. *Journal of cell science*. 122:165-170.

Astro, V., C. Asperti, M.G. Cangi, C. Doglioni, and I. de Curtis. 2011. Liprin-alpha1 regulates breast cancer cell invasion by affecting cell motility, invadopodia and extracellular matrix degradation. *Oncogene*. 30:1841-1849.

Astro, V., S. Chiaretti, E. Magistrati, M. Fivaz, and I. de Curtis. 2014. Liprin-alpha1, ERC1 and LL5 define polarized and dynamic structures that are implicated in cell migration. *Journal of cell science*. 127:3862-3876.

Astro, V., D. Tonoli, S. Chiaretti, S. Badanai, K. Sala, M. Zerial, and I. de Curtis. 2016. Liprin-alpha1 and ERC1 control cell edge dynamics by promoting focal adhesion turnover. *Sci Rep*. 6:33653.

Atherton, P., and C. Ballestrem. 2017. Talin gets SHANKed in the fight for integrin activation. *Nature cell biology*. 19:265-267.

Avraham, R., and Y. Yarden. 2011. Feedback regulation of EGFR signalling: decision making by early and delayed loops. *Nat Rev Mol Cell Biol*. 12:104-117.

Bader, B.L., H. Rayburn, D. Crowley, and R.O. Hynes. 1998. Extensive vasculogenesis, angiogenesis, and organogenesis precede lethality in mice lacking all alpha v integrins. *Cell*. 95:507-519.

Badouel, C., and H. McNeill. 2011. SnapShot: The hippo signaling pathway. *Cell*. 145:484-484 e481.

Banno, A., and M.H. Ginsberg. 2008. Integrin activation. *Biochem Soc Trans*. 36:229-234.

Barbieri, M.A., R.L. Roberts, A. Gumusboga, H. Highfield, C. Alvarez-Dominguez, A. Wells, and P.D. Stahl. 2000. Epidermal growth factor and membrane trafficking. EGF receptor activation of endocytosis requires Rab5a. *J Cell Biol*. 151:539-550.

Barrow-McGee, R., N. Kishi, C. Joffre, L. Menard, A. Hervieu, B.A. Bakhouche, A.J. Noval, A. Mai, C. Guzman, L. Robert-Masson, X. Iturrioz, J. Hulit, C.H. Brennan, I.R. Hart, P.J. Parker, J. Ivaska, and S. Kermorgant. 2016. Beta 1-integrin-c-Met cooperation reveals an inside-in survival signalling on autophagy-related endomembranes. *Nature communications*. 7:11942.

Bass, M.D., R.C. Williamson, R.D. Nunan, J.D. Humphries, A. Byron, M.R. Morgan, P. Martin, and M.J. Humphries. 2011. A syndecan-4 hair trigger initiates wound healing through caveolin- and RhoG-regulated integrin endocytosis. *Dev Cell*. 21:681-693.

Bates, R.C., D.I. Bellovin, C. Brown, E. Maynard, B. Wu, H. Kawakatsu, D. Sheppard, P. Oettgen, and A.M. Mercurio. 2005. Transcriptional activation of integrin beta6 during the epithelial-mesenchymal transition defines a novel prognostic indicator of aggressive colon carcinoma. *J Clin Invest*. 115:339-347.

Beacham, D.A., M.D. Amatangelo, and E. Cukierman. 2007. Preparation of extracellular matrices produced by cultured and primary fibroblasts. *Curr Protoc Cell Biol*. Chapter 10:Unit 10 19.

Beauvais, D.M., and A.C. Rapraeger. 2010. Syndecan-1 couples the insulin-like growth factor-1 receptor to inside-out integrin activation. *Journal of cell science*. 123:3796-3807.

Benz, C.C., G.K. Scott, J.C. Sarup, R.M. Johnson, D. Tripathy, E. Coronado, H.M. Shepard, and C.K. Osborne. 1992. Estrogen-dependent, tamoxifen-resistant tumorigenic growth of MCF-7 cells transfected with HER2/neu. *Breast Cancer Res Treat*. 24:85-95.

Berryman, S., S. Clark, P. Monaghan, and T. Jackson. 2005. Early events in integrin alphavbeta6-mediated cell entry of foot-and-mouth disease virus. *J Virol*. 79:8519-8534.

Bertling, E., P. Hotulainen, P.K. Mattila, T. Matilainen, M. Salminen, and P. Lappalainen. 2004. Cyclase-associated protein 1 (CAP1) promotes cofilin-induced actin dynamics in mammalian nonmuscle cells. *Mol Biol Cell*. 15:2324-2334.

Bessman, N.J., A. Bagchi, K.M. Ferguson, and M.A. Lemmon. 2014. Complex relationship between ligand binding and dimerization in the epidermal growth factor receptor. *Cell Rep*. 9:1306-1317.

Blanc, M., F. David, L. Abrami, D. Migliozzi, F. Armand, J. Burgi, and F.G. van der Goot. 2015. SwissPalm: Protein Palmitoylation database. *F1000Res*. 4:261.

Bodnar, A.G., M. Ouellette, M. Frolkis, S.E. Holt, C.P. Chiu, G.B. Morin, C.B. Harley, J.W. Shay, S. Lichtsteiner, and W.E. Wright. 1998. Extension of life-span by introduction of telomerase into normal human cells. *Science*. 279:349-352.

Borges, E., Y. Jan, and E. Ruoslahti. 2000. Platelet-derived growth factor receptor beta and vascular endothelial growth factor receptor 2 bind to the beta 3 integrin through its extracellular domain. *J Biol Chem*. 275:39867-39873.

Bouvard, D., L. Vignoud, S. Dupe-Manet, N. Abed, H.N. Fournier, C. Vincent-Monegat, S.F. Retta, R. Fassler, and M.R. Block. 2003. Disruption of focal adhesions by integrin cytoplasmic domain-associated protein-1 alpha. *J Biol Chem*. 278:6567-6574.

Brankatschk, B., S.P. Wichert, S.D. Johnson, O. Schaad, M.J. Rossner, and J. Gruenberg. 2012. Regulation of the EGF transcriptional response by endocytic sorting. *Sci Signal*. 5:ra21.

Braulke, T., and J.S. Bonifacino. 2009. Sorting of lysosomal proteins. *Biochimica et biophysica acta*. 1793:605-614.

Bravo-Cordero, J.J., M.A. Magalhaes, R.J. Eddy, L. Hodgson, and J. Condeelis. 2013. Functions of cofilin in cell locomotion and invasion. *Nat Rev Mol Cell Biol*. 14:405-415.

Bretscher, M.S. 1989. Endocytosis and recycling of the fibronectin receptor in CHO cells. *EMBO J*. 8:1341-1348.

Bretscher, M.S. 1992. Circulating integrins: alpha 5 beta 1, alpha 6 beta 4 and Mac-1, but not alpha 3 beta 1, alpha 4 beta 1 or LFA-1. *EMBO J*. 11:405-410.

Breuss, J.M., J. Gallo, H.M. DeLisser, I.V. Klimanskaya, H.G. Folkesson, J.F. Pittet, S.L. Nishimura, K. Aldape, D.V. Landers, W. Carpenter, and et al. 1995. Expression of the beta 6 integrin subunit in development, neoplasia and tissue repair suggests a role in epithelial remodeling. *J Cell Sci*. 108 (Pt 6):2241-2251.

Bridgewater, R.E., J.C. Norman, and P.T. Caswell. 2012. Integrin trafficking at a glance. *Journal of cell science*. 125:3695-3701.

Brunton, V.G., V.J. Fincham, G.W. McLean, S.J. Winder, C. Paraskeva, J.F. Marshall, and M.C. Frame. 2001. The protrusive phase and full development of integrin-dependent adhesions in colon epithelial cells require FAK- and ERK-mediated actin spike formation: deregulation in cancer cells. *Neoplasia*. 3:215-226.

Buckley, D., G. Duke, T.S. Heuer, M. O'Farrell, A.S. Wagman, W. McCulloch, and G. Kemble. 2017. Fatty acid synthase - Modern tumor cell biology insights into a classical oncology target. *Pharmacol Ther*. 177:23-31.

Busk, M., R. Pytela, and D. Sheppard. 1992. Characterization of the integrin alpha v beta 6 as a fibronectin-binding protein. *J Biol Chem*. 267:5790-5796.

Byron, A., J.D. Humphries, J.A. Askari, S.E. Craig, A.P. Mould, and M.J. Humphries. 2009. Anti-integrin monoclonal antibodies. *J Cell Sci*. 122:4009-4011.

Byron, A., M.R. Morgan, and M.J. Humphries. 2010. Adhesion signalling complexes. *Curr Biol*. 20:R1063-1067.

Cailleau, R., M. Olive, and Q.V. Cruciger. 1978. Long-term human breast carcinoma cell lines of metastatic origin: preliminary characterization. *In Vitro*. 14:911-915.

Calderwood, D.A., Y. Fujioka, J.M. de Pereda, B. Garcia-Alvarez, T. Nakamoto, B. Margolis, C.J. McGlade, R.C. Liddington, and M.H. Ginsberg. 2003. Integrin beta cytoplasmic domain interactions with phosphotyrosine-binding domains: a structural prototype for diversity in integrin signaling. *Proc Natl Acad Sci U S A*. 100:2272-2277.

Campbell, I.D., and M.J. Humphries. 2011. Integrin structure, activation, and interactions. *Cold Spring Harb Perspect Biol*. 3.

Cantor, D.I., H.R. Cheruku, E.C. Nice, and M.S. Baker. 2015. Integrin alphavbeta6 sets the stage for colorectal cancer metastasis. *Cancer Metastasis Rev*. 34:715-734.

Carisey, A., R. Tsang, A.M. Greiner, N. Nijenhuis, N. Heath, A. Nazgiewicz, R. Kemkemer, B. Derby, J. Spatz, and C. Ballestrem. 2013. Vinculin regulates the recruitment and release of core focal adhesion proteins in a force-dependent manner. *Curr Biol*. 23:271-281.

Castagnino, P., Z. Biesova, W.T. Wong, F. Fazioli, G.N. Gill, and P.P. Di Fiore. 1995. Direct binding of eps8 to the juxtamembrane domain of EGFR is phosphotyrosine- and SH2-independent. *Oncogene*. 10:723-729.

Caswell, P.T., M. Chan, A.J. Lindsay, M.W. McCaffrey, D. Boettiger, and J.C. Norman. 2008. Rab-coupling protein coordinates recycling of alpha5beta1 integrin and EGFR1 to promote cell migration in 3D microenvironments. *J Cell Biol*. 183:143-155.

Caswell, P.T., and J.C. Norman. 2006. Integrin trafficking and the control of cell migration. *Traffic*. 7:14-21.

Caswell, P.T., S. Vadrevu, and J.C. Norman. 2009. Integrins: masters and slaves of endocytic transport. *Nat Rev Mol Cell Biol*. 10:843-853.

Cattaneo, M.G., E. Cappellini, and L.M. Vicentini. 2012. Silencing of Eps8 blocks migration and invasion in human glioblastoma cell lines. *Experimental cell research*. 318:1901-1912.

Caunt, C.J., and S.M. Keyse. 2013. Dual-specificity MAP kinase phosphatases (MKPs): shaping the outcome of MAP kinase signalling. *FEBS J*. 280:489-504.

Chaffer, C.L., and R.A. Weinberg. 2011. A perspective on cancer cell metastasis. *Science*. 331:1559-1564.

Charrin, S., S. Jouannet, C. Boucheix, and E. Rubinstein. 2014. Tetraspanins at a glance. *Journal of cell science*. 127:3641-3648.

Chavez, K.J., S.V. Garimella, and S. Lipkowitz. 2010. Triple negative breast cancer cell lines: one tool in the search for better treatment of triple negative breast cancer. *Breast Dis*. 32:35-48.

Chen, C., Z. Liang, W. Huang, X. Li, F. Zhou, X. Hu, M. Han, X. Ding, and S. Xiang. 2015. Eps8 regulates cellular proliferation and migration of breast cancer. *Int J Oncol*. 46:205-214.

Chen, Z., D. Oh, A.K. Dubey, M. Yao, B. Yang, J.T. Groves, and M. Sheetz. 2017. EGFR family and Src family kinase interactions: mechanics matters? *Current opinion in cell biology*. 51:97-102.

Chiaretti, S., V. Astro, E. Chiricozzi, and I. de Curtis. 2016. Effects of the scaffold proteins liprin-alpha1, beta1 and beta2 on invasion by breast cancer cells. *Biol Cell*. 108:65-75.

Cho, H.S., K. Mason, K.X. Ramyar, A.M. Stanley, S.B. Gabelli, D.W. Denney, Jr., and D.J. Leahy. 2003. Structure of the extracellular region of HER2 alone and in complex with the Herceptin Fab. *Nature*. 421:756-760.

Christoforides, C., E. Rainero, K.K. Brown, J.C. Norman, and A. Toker. 2012. PKD controls alphavbeta3 integrin recycling and tumor cell invasive migration through its substrate Rabaptin-5. *Dev Cell*. 23:560-572.

Citri, A., K.B. Skaria, and Y. Yarden. 2003. The deaf and the dumb: the biology of ErbB-2 and ErbB-3. *Experimental cell research*. 284:54-65.

Citri, A., and Y. Yarden. 2006. EGF-ERBB signalling: towards the systems level. *Nat Rev Mol Cell Biol*. 7:505-516.

Clague, M.J., H. Liu, and S. Urbe. 2012. Governance of endocytic trafficking and signaling by reversible ubiquitylation. *Dev Cell*. 23:457-467.

Cohen, M.H., J.R. Johnson, Y.F. Chen, R. Sridhara, and R. Pazdur. 2005. FDA drug approval summary: erlotinib (Tarceva) tablets. *Oncologist*. 10:461-466.

Cohen, M.H., G.A. Williams, R. Sridhara, G. Chen, and R. Pazdur. 2003. FDA drug approval summary: gefitinib (ZD1839) (Iressa) tablets. *Oncologist*. 8:303-306.

Coller, B.S., and S.J. Shattil. 2008. The GPIIb/IIIa (integrin alphaIIbbeta3) odyssey: a technology-driven saga of a receptor with twists, turns, and even a bend. *Blood*. 112:3011-3025.

Consortium, T.U. 2011. Ongoing and future developments at the Universal Protein Resource. *Nucleic Acids Research*. 39:D214–D219.

Cordenonsi, M., F. Zanconato, L. Azzolin, M. Forcato, A. Rosato, C. Frasson, M. Inui, M. Montagner, A.R. Parenti, A. Poletti, M.G. Daidone, S. Dupont, G. Basso, S. Bicciato, and S. Piccolo. 2011. The Hippo transducer TAZ confers cancer stem cell-related traits on breast cancer cells. *Cell*. 147:759-772.

Couchman, J.R., L. Chen, and A. Woods. 2001. Syndecans and cell adhesion. *Int Rev Cytol*. 207:113-150.

D'Souza-Schorey, C., and P. Chavrier. 2006. ARF proteins: roles in membrane traffic and beyond. *Nat Rev Mol Cell Biol*. 7:347-358.

Dalvi, N., G.J. Thomas, J.F. Marshall, M. Morgan, R. Bass, V. Ellis, P.M. Speight, and S.A. Whawell. 2004. Modulation of the urokinase-type plasminogen activator receptor by the beta6 integrin subunit. *Biochem Biophys Res Commun*. 317:92-99.

Dancau, A.M., L. Wuth, M. Waschow, F. Holst, A. Krohn, M. Choschzick, L. Terracciano, S. Politis, S. Kurtz, A. Lebeau, K. Friedrichs, K. Wencke, O. Monni, and R. Simon. 2010. PPFIA1 and CCND1 are frequently coamplified in breast cancer. *Genes, chromosomes & cancer*. 49:1-8.

Daniotti, J.L., M.P. Pedro, and J. Valdez Taubas. 2017. The role of S-acylation in protein trafficking. *Traffic*. 18:699-710.

De Franceschi, N., H. Hamidi, J. Alanko, P. Sahgal, and J. Ivaska. 2015. Integrin traffic - the update. *Journal of cell science*. 128:839-852.

Decker, L., W. Baron, and C. Ffrench-Constant. 2004. Lipid rafts: microenvironments for integrin-growth factor interactions in neural development. *Biochem Soc Trans*. 32:426-430.

Denkert, C., C. Liedtke, A. Tutt, and G. von Minckwitz. 2017. Molecular alterations in triple-negative breast cancer-the road to new treatment strategies. *Lancet*. 389:2430-2442.

Desai, K., M.G. Nair, J.S. Prabhu, A. Vinod, A. Korlimarla, S. Rajarajan, R. Aiyappa, R.S. Kaluve, A. Alexander, P.S. Hari, G. Mukherjee, R.V. Kumar, S. Manjunath, M. Correa, B.S. Srinath, S. Patil, M.S. Prasad, K.S. Gopinath, R.N. Rao, S.M. Violette, P.H. Weinreb, and T.S. Sridhar. 2016. High expression of integrin beta6 in association with the Rho-Rac pathway identifies a poor prognostic subgroup within HER2 amplified breast cancers. *Cancer Med*. 5:2000-2011.

Desgrosellier, J.S., and D.A. Cheresh. 2010. Integrins in cancer: biological implications and therapeutic opportunities. *Nat Rev Cancer*. 10:9-22.

Di Fiore, P.P., and G. Scita. 2002. Eps8 in the midst of GTPases. *Int J Biochem Cell Biol*. 34:1178-1183.

Di Vizio, D., R.M. Adam, J. Kim, R. Kim, F. Sotgia, T. Williams, F. Demichelis, K.R. Solomon, M. Loda, M.A. Rubin, M.P. Lisanti, and M.R. Freeman. 2008. Caveolin-1 interacts with a lipid raft-associated population of fatty acid synthase. *Cell Cycle*. 7:2257-2267.

Diaz-Martin, J., M.A. Lopez-Garcia, L. Romero-Perez, M.R. Atienza-Amores, M.L. Pecero, M.A. Castilla, M. Biscuola, A. Santon, and J. Palacios. 2015. Nuclear TAZ expression associates with the triple-negative phenotype in breast cancer. *Endocr Relat Cancer*. 22:443-454.

Dickson, M.C., J.S. Martin, F.M. Cousins, A.B. Kulkarni, S. Karlsson, and R.J. Akhurst. 1995. Defective haematopoiesis and vasculogenesis in transforming growth factor-beta 1 knock out mice. *Development*. 121:1845-1854.

Disanza, A., M.F. Carlier, T.E. Stradal, D. Didry, E. Frittoli, S. Confalonieri, A. Croce, J. Wehland, P.P. Di Fiore, and G. Scita. 2004. Eps8 controls actin-based motility by capping the barbed ends of actin filaments. *Nature cell biology*. 6:1180-1188.

Disanza, A., S. Mantoani, M. Hertzog, S. Gerboth, E. Frittoli, A. Steffen, K. Berhoerster, H.J. Kreienkamp, F. Milanesi, P.P. Di Fiore, A. Ciliberto, T.E. Stradal, and G. Scita. 2006. Regulation of cell shape by Cdc42 is mediated by the synergic actin-bundling activity of the Eps8-IRSp53 complex. *Nature cell biology*. 8:1337-1347.

Donaldson, J.G., and C.L. Jackson. 2011. ARF family G proteins and their regulators: roles in membrane transport, development and disease. *Nat Rev Mol Cell Biol*. 12:362-375.

Dong, X., B. Zhao, R.E. Iacob, J. Zhu, A.C. Koksal, C. Lu, J.R. Engen, and T.A. Springer. 2017. Force interacts with macromolecular structure in activation of TGF-beta. *Nature*. 542:55-59.

Dormann, D., T. Libotte, C.J. Weijer, and T. Bretschneider. 2002. Simultaneous quantification of cell motility and protein-membrane-association using active contours. *Cell Motil Cytoskeleton*. 52:221-230.

Dozynkiewicz, M.A., N.B. Jamieson, I. Macpherson, J. Grindlay, P.V. van den Berghe, A. von Thun, J.P. Morton, C. Gourley, P. Timpson, C. Nixon, C.J. McKay, R. Carter, D. Strachan, K. Anderson, O.J. Sansom, P.T. Caswell, and J.C. Norman. 2012. Rab25 and CLIC3 collaborate to promote integrin recycling from late endosomes/lysosomes and drive cancer progression. *Dev Cell*. 22:131-145.

Du, J., X. Chen, X. Liang, G. Zhang, J. Xu, L. He, Q. Zhan, X.Q. Feng, S. Chien, and C. Yang. 2011. Integrin activation and internalization on soft ECM as a mechanism of induction of stem cell differentiation by ECM elasticity. *Proc Natl Acad Sci U S A*. 108:9466-9471.

Dupont, S. 2016. Role of YAP/TAZ in cell-matrix adhesion-mediated signalling and mechanotransduction. *Experimental cell research*. 343:42-53.

Dupont, S., A. Mamidi, M. Cordenonsi, M. Montagner, L. Zacchigna, M. Adorno, G. Martello, M.J. Stinchfield, S. Soligo, L. Morsut, M. Inui, S. Moro, N. Modena, F. Argenton, S.J. Newfeld, and S. Piccolo. 2009. FAM/USP9x, a deubiquitinating enzyme essential for TGFbeta signaling, controls Smad4 monoubiquitination. *Cell*. 136:123-135.

Dupont, S., L. Morsut, M. Aragona, E. Enzo, S. Giulitti, M. Cordenonsi, F. Zanconato, J. Le Digabel, M. Forcato, S. Bicciato, N. Elvassore, and S. Piccolo. 2011. Role of YAP/TAZ in mechanotransduction. *Nature*. 474:179-183.

Dvorak, H.F. 2015. Tumors: wounds that do not heal-redux. *Cancer Immunol Res*. 3:1-11.

Dvorakova, M., R. Nenutil, and P. Bouchal. 2014. Transgelins, cytoskeletal proteins implicated in different aspects of cancer development. *Expert Rev Proteomics*. 11:149-165.

Eberlein, C., J. Kendrew, K. McDaid, A. Alfred, J.S. Kang, V.N. Jacobs, S.J. Ross, C. Rooney, N.R. Smith, J. Rinkenberger, A. Cao, A. Churchman, J.F. Marshall, H.M. Weir, V. Bedian, D.C. Blakey, I.N. Foltz, and S.T. Barry. 2013. A human monoclonal antibody 264RAD targeting alphavbeta6 integrin reduces tumour growth and metastasis, and modulates key biomarkers in vivo. *Oncogene*. 32:4406-4416.

Eberwein, P., D. Laird, S. Schulz, T. Reinhard, T. Steinberg, and P. Tomakidi. 2015. Modulation of focal adhesion constituents and their down-stream events by EGF: On the cross-talk of integrins and growth factor receptors. *Biochimica et biophysica acta*. 1853:2183-2198.

Eccles, R.L., M.T. Czajkowski, C. Barth, P.M. Muller, E. McShane, S. Grunwald, P. Beaudette, N. Mecklenburg, R. Volkmer, K. Zuhlke, G. Dittmar, M. Selbach, A. Hammes, O.

Daumke, E. Klussmann, S. Urbe, and O. Rocks. 2016. Bimodal antagonism of PKA signalling by ARHGAP36. *Nature communications*. 7:12963.

Eden, E.R., F. Huang, A. Sorkin, and C.E. Futter. 2012. The role of EGF receptor ubiquitination in regulating its intracellular traffic. *Traffic*. 13:329-337.

Eisenberg, S., A.J. Beckett, I.A. Prior, F.J. Dekker, C. Hedberg, H. Waldmann, M. Ehrlich, and Y.I. Henis. 2011. Raft protein clustering alters N-Ras membrane interactions and activation pattern. *Mol Cell Biol*. 31:3938-3952.

Eisenberg, S., A.J. Laude, A.J. Beckett, C.J. Mageean, V. Aran, M. Hernandez-Valladares, Y.I. Henis, and I.A. Prior. 2013. The role of palmitoylation in regulating Ras localization and function. *Biochem Soc Trans*. 41:79-83.

Elayadi, A.N., K.N. Samli, L. Prudkin, Y.H. Liu, A. Bian, X.J. Xie, Wistuba, II, J.A. Roth, M.J. McGuire, and K.C. Brown. 2007. A peptide selected by biopanning identifies the integrin alphavbeta6 as a prognostic biomarker for nonsmall cell lung cancer. *Cancer Res*. 67:5889-5895.

Eley, G.D., J.L. Reiter, A. Pandita, S. Park, R.B. Jenkins, N.J. Maihle, and C.D. James. 2002. A chromosomal region 7p11.2 transcript map: its development and application to the study of EGFR amplicons in glioblastoma. *Neuro Oncol*. 4:86-94.

Elez, E., I. Kocakova, T. Hohler, U.M. Martens, C. Bokemeyer, E. Van Cutsem, B. Melichar, M. Smakal, T. Csoszi, E. Topuzov, R. Orlova, S. Tjulandin, F. Rivera, J. Straub, R. Bruns, S. Quaratino, and J. Tabernero. 2015. Abituzumab combined with cetuximab plus irinotecan versus cetuximab plus irinotecan alone for patients with KRAS wild-type metastatic colorectal cancer: the randomised phase I/II POSEIDON trial. *Ann Oncol*. 26:132-140.

Engler, A.J., S. Sen, H.L. Sweeney, and D.E. Discher. 2006. Matrix elasticity directs stem cell lineage specification. *Cell*. 126:677-689.

Ezratty, E.J., C. Bertaux, E.E. Marcantonio, and G.G. Gundersen. 2009. Clathrin mediates integrin endocytosis for focal adhesion disassembly in migrating cells. *J Cell Biol*. 187:733-747.

Fassler, R., and M. Meyer. 1995. Consequences of lack of beta 1 integrin gene expression in mice. *Genes Dev*. 9:1896-1908.

Fazioli, F., L. Minichiello, V. Matoska, P. Castagnino, T. Miki, W.T. Wong, and P.P. Di Fiore. 1993. Eps8, a substrate for the epidermal growth factor receptor kinase, enhances EGF-dependent mitogenic signals. *EMBO J*. 12:3799-3808.

Ferguson, K.M., M.B. Berger, J.M. Mendrola, H.S. Cho, D.J. Leahy, and M.A. Lemmon. 2003. EGF activates its receptor by removing interactions that autoinhibit ectodomain dimerization. *Mol Cell*. 11:507-517.

Ferro, E., and L. Trabalzini. 2010. RalGDS family members couple Ras to Ral signalling and that's not all. *Cell Signal*. 22:1804-1810.

Flavin, R., S. Peluso, P.L. Nguyen, and M. Loda. 2010. Fatty acid synthase as a potential therapeutic target in cancer. *Future oncology*. 6:551-562.

Forbes, S.A., D. Beare, H. Boutselakis, S. Bamford, N. Bindal, J. Tate, C.G. Cole, S. Ward, E. Dawson, L. Ponting, R. Stefancsik, B. Harsha, C.Y. Kok, M. Jia, H. Jubb, Z. Sondka, S. Thompson, T. De, and P.J. Campbell. 2017. COSMIC: somatic cancer genetics at high-resolution. *Nucleic Acids Res*. 45:D777-D783.

Forman-Kay, J.D., and T. Pawson. 1999. Diversity in protein recognition by PTB domains. *Curr Opin Struct Biol*. 9:690-695.

Fortian, A., and A. Sorkin. 2014. Live-cell fluorescence imaging reveals high stoichiometry of Grb2 binding to the EGF receptor sustained during endocytosis. *Journal of cell science*. 127:432-444.

Fournier, A.K., L.E. Campbell, P. Castagnino, W.F. Liu, B.M. Chung, V.M. Weaver, C.S. Chen, and R.K. Assoian. 2008. Rac-dependent cyclin D1 gene expression regulated by cadherin- and integrin-mediated adhesion. *Journal of cell science*. 121:226-233.

Frantz, C., K.M. Stewart, and V.M. Weaver. 2010. The extracellular matrix at a glance. *Journal of cell science*. 123:4195-4200.

French, A.R., D.K. Tadaki, S.K. Niyogi, and D.A. Lauffenburger. 1995. Intracellular trafficking of epidermal growth factor family ligands is directly influenced by the pH sensitivity of the receptor/ligand interaction. *J Biol Chem*. 270:4334-4340.

Friedland, J.C., M.H. Lee, and D. Boettiger. 2009. Mechanically activated integrin switch controls alpha5beta1 function. *Science*. 323:642-644.

Gargiulo, C.E., S.M. Stuhlsatz-Krouper, and J.E. Schaffer. 1999. Localization of adipocyte long-chain fatty acyl-CoA synthetase at the plasma membrane. *J Lipid Res*. 40:881-892.

Garrett, T.P., N.M. McKern, M. Lou, T.C. Elleman, T.E. Adams, G.O. Lovrecz, H.J. Zhu, F. Walker, M.J. Frenkel, P.A. Hoyne, R.N. Jorissen, E.C. Nice, A.W. Burgess, and C.W. Ward. 2002. Crystal structure of a truncated epidermal growth factor receptor extracellular domain bound to transforming growth factor alpha. *Cell*. 110:763-773.

Giampieri, S., C. Manning, S. Hooper, L. Jones, C.S. Hill, and E. Sahai. 2009. Localized and reversible TGFbeta signalling switches breast cancer cells from cohesive to single cell motility. *Nature cell biology*. 11:1287-1296.

Giancotti, F.G., and E. Ruoslahti. 1999. Integrin signaling. *Science*. 285:1028-1032.

Goh, L.K., F. Huang, W. Kim, S. Gygi, and A. Sorkin. 2010. Multiple mechanisms collectively regulate clathrin-mediated endocytosis of the epidermal growth factor receptor. *J Cell Biol*. 189:871-883.

Goh, L.K., and A. Sorkin. 2013. Endocytosis of receptor tyrosine kinases. *Cold Spring Harb Perspect Biol*. 5:a017459.

Gong, J., S. Shen, Y. Yang, S. Qin, L. Huang, H. Zhang, L. Chen, Y. Chen, S. Li, S. She, M. Yang, H. Ren, and H. Hu. 2017. Inhibition of FASN suppresses migration, invasion and growth in hepatoma carcinoma cells by deregulating the HIF-1alpha/IGFBP1 pathway. *Int J Oncol*. 50:883-892.

Gonzalo, P., V. Moreno, B.G. Galvez, and A.G. Arroyo. 2010. MT1-MMP and integrins: Hand-to-hand in cell communication. *Biofactors*. 36:248-254.

Goodman, S.L., and M. Picard. 2012. Integrins as therapeutic targets. *Trends Pharmacol Sci*. 33:405-412.

Grandal, M.V., R. Zandi, M.W. Pedersen, B.M. Willumsen, B. van Deurs, and H.S. Poulsen. 2007. EGFRvIII escapes down-regulation due to impaired internalization and sorting to lysosomes. *Carcinogenesis*. 28:1408-1417.

Grant, B.D., and J.G. Donaldson. 2009. Pathways and mechanisms of endocytic recycling. *Nat Rev Mol Cell Biol*. 10:597-608.

Graus-Porta, D., R.R. Beerli, J.M. Daly, and N.E. Hynes. 1997. ErbB-2, the preferred heterodimerization partner of all ErbB receptors, is a mediator of lateral signaling. *EMBO J*. 16:1647-1655.

Griffin, M., R. Casadio, and C.M. Bergamini. 2002. Transglutaminases: nature's biological glues. *The Biochemical journal*. 368:377-396.

Grigoriadis, A., A. Mackay, E. Noel, P.J. Wu, R. Natrajan, J. Frankum, J.S. Reis-Filho, and A. Tutt. 2012. Molecular characterisation of cell line models for triple-negative breast cancers. *BMC Genomics*. 13:619.

Guo, C., X. Zhang, and G.P. Pfeifer. 2011. The tumor suppressor RASSF1A prevents dephosphorylation of the mammalian STE20-like kinases MST1 and MST2. *J Biol Chem*. 286:6253-6261.

Guo, L., C.J. Kozlosky, L.H. Ericsson, T.O. Daniel, D.P. Cerretti, and R.S. Johnson. 2003. Studies of ligand-induced site-specific phosphorylation of epidermal growth factor receptor. *J Am Soc Mass Spectrom*. 14:1022-1031.

Haapasalmi, K., K. Zhang, M. Tonnesen, J. Olerud, D. Sheppard, T. Salo, R. Kramer, R.A. Clark, V.J. Uitto, and H. Larjava. 1996. Keratinocytes in human wounds express alpha v beta 6 integrin. *The Journal of investigative dermatology*. 106:42-48.

Hager, A., S. Alexander, and P. Friedl. 2013. Cancer invasion and resistance. *EJC Suppl*. 11:291-293.

Hakkinen, L., L. Koivisto, H. Gardner, U. Saarialho-Kere, J.M. Carroll, M. Lakso, H. Rauvala, M. Laato, J. Heino, and H. Larjava. 2004. Increased expression of beta6-integrin in skin leads to spontaneous development of chronic wounds. *Am J Pathol*. 164:229-242.

Hamidi, H., M. Pietila, and J. Ivaska. 2016. The complexity of integrins in cancer and new scopes for therapeutic targeting. *British journal of cancer*. 115:1017-1023.

Han, W., T. Zhang, H. Yu, J.G. Foulke, and C.K. Tang. 2006. Hypophosphorylation of residue Y1045 leads to defective downregulation of EGFRvIII. *Cancer Biol Ther*. 5:1361-1368.

Harbeck, N., and M. Gnant. 2017. Breast cancer. *Lancet*. 389:1134-1150.

Harburger, D.S., and D.A. Calderwood. 2009. Integrin signalling at a glance. *Journal of cell science*. 122:159-163.

Hatzfeld, M. 2007. Plakophilins: Multifunctional proteins or just regulators of desmosomal adhesion? *Biochimica et biophysica acta*. 1773:69-77.

Hazelbag, S., G.G. Kenter, A. Gorter, E.J. Dreef, L.A. Koopman, S.M. Violette, P.H. Weinreb, and G.J. Fleuren. 2007. Overexpression of the alpha v beta 6 integrin in cervical squamous cell carcinoma is a prognostic factor for decreased survival. *J Pathol*. 212:316-324.

He, Y., T. Ryu, N. Shrestha, T. Yuan, H. Kim, H. Shrestha, Y.C. Cho, Y.W. Seo, W.K. Song, and K. Kim. 2016. Interaction of EGFR to delta-catenin leads to delta-catenin phosphorylation and enhances EGFR signaling. *Sci Rep*. 6:21207.

Hecker, T.P., Q. Ding, T.A. Rege, S.K. Hanks, and C.L. Gladson. 2004. Overexpression of FAK promotes Ras activity through the formation of a FAK/p120RasGAP complex in malignant astrocytoma cells. *Oncogene*. 23:3962-3971.

Hendriks, B.S., L.K. Opresko, H.S. Wiley, and D. Lauffenburger. 2003. Quantitative analysis of HER2-mediated effects on HER2 and epidermal growth factor receptor endocytosis: distribution of homo- and heterodimers depends on relative HER2 levels. *J Biol Chem*. 278:23343-23351.

Hertzog, M., F. Milanesi, L. Hazelwood, A. Disanza, H. Liu, E. Perlade, M.G. Malabarba, S. Pasqualato, A. Maiolica, S. Confalonieri, C. Le Clainche, N. Offenhauser, J. Block, K. Rottner, P.P. Di Fiore, M.F. Carlier, N. Volkmann, D. Hanein, and G. Scita. 2010. Molecular basis for the dual function of Eps8 on actin dynamics: bundling and capping. *PLoS Biol*. 8:e1000387.

Hetmanski, J.H., E. Zindy, J.M. Schwartz, and P.T. Caswell. 2016. A MAPK-Driven Feedback Loop Suppresses Rac Activity to Promote RhoA-Driven Cancer Cell Invasion. *PLoS Comput Biol*. 12:e1004909.

Hezel, A.F., V. Deshpande, S.M. Zimmerman, G. Contino, B. Alagesan, M.R. O'Dell, L.B. Rivera, J. Harper, S. Lonning, R.A. Brekken, and N. Bardeesy. 2012. TGF-beta and alphavbeta6 integrin act in a common pathway to suppress pancreatic cancer progression. *Cancer Res*. 72:4840-4845.

Holliday, D.L., and V. Speirs. 2011. Choosing the right cell line for breast cancer research. *Breast cancer research : BCR*. 13:215.

Hongu, T., Y. Funakoshi, S. Fukuhara, T. Suzuki, S. Sakimoto, N. Takakura, M. Ema, S. Takahashi, S. Itoh, M. Kato, H. Hasegawa, N. Mochizuki, and Y. Kanaho. 2015. Arf6 regulates tumour angiogenesis and growth through HGF-induced endothelial beta1 integrin recycling. *Nature communications*. 6:7925.

Horton, E.R., P. Astudillo, M.J. Humphries, and J.D. Humphries. 2016a. Mechanosensitivity of integrin adhesion complexes: role of the consensus adhesome. *Experimental cell research*. 343:7-13.

Horton, E.R., A. Byron, J.A. Askari, D.H. Ng, A. Millon-Fremillon, J. Robertson, E.J. Koper, N.R. Paul, S. Warwood, D. Knight, J.D. Humphries, and M.J. Humphries. 2015a. Definition of a consensus integrin adhesome and its dynamics during adhesion complex assembly and disassembly. *Nat Cell Biol*.

Horton, E.R., A. Byron, J.A. Askari, D.H.J. Ng, A. Millon-Fremillon, J. Robertson, E.J. Koper, N.R. Paul, S. Warwood, D. Knight, J.D. Humphries, and M.J. Humphries. 2015b. Definition of a consensus integrin adhesome and its dynamics during adhesion complex assembly and disassembly. *Nature cell biology*. 17:1577-1587.

Horton, E.R., J.D. Humphries, B. Stutchbury, G. Jacquemet, C. Ballestrem, S.T. Barry, and M.J. Humphries. 2016b. Modulation of FAK and Src adhesion signaling occurs independently of adhesion complex composition. *J Cell Biol*. 212:349-364.

Hoshino, A., B. Costa-Silva, T.L. Shen, G. Rodrigues, A. Hashimoto, M. Tesic Mark, H. Molina, S. Kohsaka, A. Di Giannatale, S. Ceder, S. Singh, C. Williams, N. Soplop, K. Uryu, L. Pharmer, T. King, L. Bojmar, A.E. Davies, Y. Ararso, T. Zhang, H. Zhang, J. Hernandez, J.M. Weiss, V.D. Dumont-Cole, K. Kramer, L.H. Wexler, A. Narendran, G.K. Schwartz, J.H. Healey, P. Sandstrom, K. Jorgen Labori, E.H. Kure, P.M. Grandgenett, M.A. Hollingsworth, M. de Sousa, S. Kaur, M. Jain, K. Mallya, S.K. Batra, W.R. Jarnagin, M.S. Brady, O. Fodstad, V. Muller, K. Pantel, A.J. Minn, M.J. Bissell, B.A. Garcia, Y. Kang, V.K. Rajasekhar, C.M. Ghajar, I. Matei, H. Peinado, J. Bromberg, and D. Lyden. 2015. Tumour exosome integrins determine organotropic metastasis. *Nature*.

Huang, F., L.K. Goh, and A. Sorkin. 2007. EGF receptor ubiquitination is not necessary for its internalization. *Proc Natl Acad Sci U S A*. 104:16904-16909.

Huang, F., and A. Sorkin. 2005. Growth factor receptor binding protein 2-mediated recruitment of the RING domain of Cbl to the epidermal growth factor receptor is essential and sufficient to support receptor endocytosis. *Mol Biol Cell*. 16:1268-1281.

Huang, F.T., D. Kirkpatrick, X.J. Jiang, S. Gygi, and A. Sorkin. 2006. Differential regulation of EGF receptor internalization and degradation by multiubiquitination within the kinase domain. *Molecular Cell*. 21:737-748.

Huang, X.Z., J.F. Wu, D. Cass, D.J. Erle, D. Corry, S.G. Young, R.V. Farese, Jr., and D. Sheppard. 1996. Inactivation of the integrin beta 6 subunit gene reveals a role of epithelial integrins in regulating inflammation in the lung and skin. *J Cell Biol*. 133:921-928.

Hughes, P.E., F. Diaz-Gonzalez, L. Leong, C. Wu, J.A. McDonald, S.J. Shattil, and M.H. Ginsberg. 1996. Breaking the integrin hinge. A defined structural constraint regulates integrin signaling. *J Biol Chem*. 271:6571-6574.

Humphrey, J.D., E.R. Dufresne, and M.A. Schwartz. 2014. Mechanotransduction and extracellular matrix homeostasis. *Nat Rev Mol Cell Biol*. 15:802-812.

Humphries, J.D., A. Byron, M.D. Bass, S.E. Craig, J.W. Pinney, D. Knight, and M.J. Humphries. 2009. Proteomic analysis of integrin-associated complexes identifies RCC2 as a dual regulator of Rac1 and Arf6. *Sci Signal*. 2:ra51.

Humphries, J.D., A. Byron, and M.J. Humphries. 2006. Integrin ligands at a glance. *Journal of cell science*. 119:3901-3903.

Humphries, J.D., N.R. Paul, M.J. Humphries, and M.R. Morgan. 2015. Emerging properties of adhesion complexes: what are they and what do they do? *Trends Cell Biol*. 25:388-397.

Humphries, M.J., P.A. McEwan, S.J. Barton, P.A. Buckley, J. Bella, and A.P. Mould. 2003a. Integrin structure: heady advances in ligand binding, but activation still makes the knees wobble. *Trends Biochem Sci*. 28:313-320.

Humphries, M.J., E.J. Symonds, and A.P. Mould. 2003b. Mapping functional residues onto integrin crystal structures. *Curr Opin Struct Biol*. 13:236-243.

Hynes, N.E., and G. MacDonald. 2009. ErbB receptors and signaling pathways in cancer. *Current opinion in cell biology*. 21:177-184.

Hynes, R.O. 2002. Integrins: bidirectional, allosteric signaling machines. *Cell*. 110:673-687.

Hynes, R.O. 2009. The extracellular matrix: not just pretty fibrils. *Science*. 326:1216-1219.

Hynes, R.O. 2014. Stretching the boundaries of extracellular matrix research. *Nat Rev Mol Cell Biol*. 15:761-763.

Indik, J.H., and F.I. Marcus. 2018. Chapter 21 - Arrhythmogenic Right Ventricular Cardiomyopathy. *In* Heart Failure in the Child and Young Adult. J.L. Jefferies, A.C. Chang, J.W. Rossano, R.E. Shaddy, and J.A. Towbin, editors. Academic Press, Boston. 291-296.

Ivaska, J., and J. Heino. 2011. Cooperation between integrins and growth factor receptors in signaling and endocytosis. *Annu Rev Cell Dev Biol*. 27:291-320.

Iwamoto, D.V., and D.A. Calderwood. 2015. Regulation of integrin-mediated adhesions. *Current opinion in cell biology*. 36:41-47.

Jansen, K.A., P. Atherton, and C. Ballestrem. 2017. Mechanotransduction at the cell-matrix interface. *Semin Cell Dev Biol*.

Jat, P.S., M.D. Noble, P. Ataliotis, Y. Tanaka, N. Yannoutsos, L. Larsen, and D. Kioussis. 1991. Direct derivation of conditionally immortal cell lines from an H-2Kb-tsA58 transgenic mouse. *Proc Natl Acad Sci U S A*. 88:5096-5100.

Jeong, H., J. Kim, Y. Lee, J.H. Seo, S.R. Hong, and A. Kim. 2014. Neuregulin-1 induces cancer stem cell characteristics in breast cancer cell lines. *Oncol Rep*. 32:1218-1224.

Jiang, X., F. Huang, A. Marusyk, and A. Sorkin. 2003. Grb2 regulates internalization of EGF receptors through clathrin-coated pits. *Mol Biol Cell*. 14:858-870.

Jitariu, A.A., A.M. Cimpean, D. Ribatti, and M. Raica. 2017. Triple negative breast cancer: the kiss of death. *Oncotarget*. 8:46652-46662.

Jones, J., F.M. Watt, and P.M. Speight. 1997a. Changes in the expression of alpha v integrins in oral squamous cell carcinomas. *Journal of oral pathology & medicine : official publication of the International Association of Oral Pathologists and the American Academy of Oral Pathology*. 26:63-68.

Jones, M.C., J.D. Humphries, A. Byron, A. Millon-Fremillon, J. Robertson, N.R. Paul, D.H. Ng, J.A. Askari, and M.J. Humphries. 2015. Isolation of integrin-based adhesion complexes. *Curr Protoc Cell Biol*. 66:9 8 1-9 8 15.

Jones, P.L., J. Crack, and M. Rabinovitch. 1997b. Regulation of tenascin-C, a vascular smooth muscle cell survival factor that interacts with the alpha v beta 3 integrin to promote epidermal growth factor receptor phosphorylation and growth. *J Cell Biol*. 139:279-293.

Jozwiak, P., E. Forma, M. Brys, and A. Krzeslak. 2014. O-GlcNAcylation and Metabolic Reprograming in Cancer. *Front Endocrinol (Lausanne)*. 5:145.

Kaartinen, V., J.W. Voncken, C. Shuler, D. Warburton, D. Bu, N. Heisterkamp, and J. Groffen. 1995. Abnormal lung development and cleft palate in mice lacking TGF-beta 3 indicates defects of epithelial-mesenchymal interaction. *Nat Genet*. 11:415-421.

Kanchanawong, P., G. Shtengel, A.M. Pasapera, E.B. Ramko, M.W. Davidson, H.F. Hess, and C.M. Waterman. 2010. Nanoscale architecture of integrin-based cell adhesions. *Nature*. 468:580-584.

Kang, Y.S., W. Kim, Y.H. Huh, J. Bae, J.S. Kim, and W.K. Song. 2011. P130Cas attenuates epidermal growth factor (EGF) receptor internalization by modulating EGF-triggered dynamin phosphorylation. *PLoS One*. 6:e20125.

Kaverina, I., O. Krylyshkina, and J.V. Small. 1999. Microtubule targeting of substrate contacts promotes their relaxation and dissociation. *J Cell Biol*. 146:1033-1044.

Khan, Z., and J.F. Marshall. 2016. The role of integrins in TGFbeta activation in the tumour stroma. *Cell Tissue Res*. 365:657-673.

Kiema, T., Y. Lad, P. Jiang, C.L. Oxley, M. Baldassarre, K.L. Wegener, I.D. Campbell, J. Ylanne, and D.A. Calderwood. 2006. The molecular basis of filamin binding to integrins and competition with talin. *Mol Cell*. 21:337-347.

Kong, F., A.J. Garcia, A.P. Mould, M.J. Humphries, and C. Zhu. 2009. Demonstration of catch bonds between an integrin and its ligand. *J Cell Biol*. 185:1275-1284.

Kong, F., Z. Li, W.M. Parks, D.W. Dumbauld, A.J. Garcia, A.P. Mould, M.J. Humphries, and C. Zhu. 2013. Cyclic mechanical reinforcement of integrin-ligand interactions. *Mol Cell*. 49:1060-1068.

Lanzetti, L., V. Margaria, F. Melander, L. Virgili, M.H. Lee, J. Bartek, and S. Jensen. 2007. Regulation of the Rab5 GTPase-activating protein RN-tre by the dual specificity phosphatase Cdc14A in human cells. *J Biol Chem*. 282:15258-15270.

Lanzetti, L., V. Rybin, M.G. Malabarba, S. Christoforidis, G. Scita, M. Zerial, and P.P. Di Fiore. 2000. The Eps8 protein coordinates EGF receptor signalling through Rac and trafficking through Rab5. *Nature*. 408:374-377.

Lasfargues, E.Y., W.G. Coutinho, and E.S. Redfield. 1978. Isolation of two human tumor epithelial cell lines from solid breast carcinomas. *J Natl Cancer Inst*. 61:967-978.

Lasfargues, E.Y., and L. Ozzello. 1958. Cultivation of human breast carcinomas. *J Natl Cancer Inst*. 21:1131-1147.

Lau, L.F. 2011. CCN1/CYR61: the very model of a modern matricellular protein. *Cell Mol Life Sci*. 68:3149-3163.

Lawson, C., and D.D. Schlaepfer. 2012. Integrin adhesions: who's on first? What's on second? Connections between FAK and talin. *Cell Adh Migr*. 6:302-306.

Lebart, M.C., and Y. Benyamin. 2006. Calpain involvement in the remodeling of cytoskeletal anchorage complexes. *FEBS J*. 273:3415-3426.

Lee, C., C. Lee, S. Lee, A. Siu, and D.M. Ramos. 2014. The cytoplasmic extension of the integrin beta6 subunit regulates epithelial-to-mesenchymal transition. *Anticancer Res*. 34:659-664.

Lee, H.S., C.J. Lim, W. Puzon-McLaughlin, S.J. Shattil, and M.H. Ginsberg. 2009. RIAM activates integrins by linking talin to ras GTPase membrane-targeting sequences. *J Biol Chem*. 284:5119-5127.

Lei, Q.Y., H. Zhang, B. Zhao, Z.Y. Zha, F. Bai, X.H. Pei, S. Zhao, Y. Xiong, and K.L. Guan. 2008. TAZ promotes cell proliferation and epithelial-mesenchymal transition and is inhibited by the hippo pathway. *Mol Cell Biol*. 28:2426-2436.

Lemmon, M.A. 2009. Ligand-induced ErbB receptor dimerization. *Experimental cell research*. 315:638-648.

Lemmon, M.A., and J. Schlessinger. 2010. Cell signaling by receptor tyrosine kinases. *Cell*. 141:1117-1134.

Levental, K.R., H. Yu, L. Kass, J.N. Lakins, M. Egeblad, J.T. Erler, S.F. Fong, K. Csiszar, A. Giaccia, W. Weninger, M. Yamauchi, D.L. Gasser, and V.M. Weaver. 2009. Matrix crosslinking forces tumor progression by enhancing integrin signaling. *Cell*. 139:891-906.

Li, J., Y. Guo, X. Feng, Z. Wang, Y. Wang, P. Deng, D. Zhang, R. Wang, L. Xie, X. Xu, Y. Zhou, N. Ji, J. Hu, M. Zhou, G. Liao, N. Geng, L. Jiang, Z. Wang, and Q. Chen. 2012. Receptor for activated C kinase 1 (RACK1): a regulator for migration and invasion in oral squamous cell carcinoma cells. *J Cancer Res Clin Oncol*. 138:563-571.

Li, L., T. Liu, Y. Li, C. Wu, K. Luo, Y. Yin, Y. Chen, S. Nowsheen, J. Wu, Z. Lou, and J. Yuan. 2018. The deubiquitinase USP9X promotes tumor cell survival and confers chemoresistance through YAP1 stabilization. *Oncogene*.

Li, W., B. Zhang, H. Li, C. Zhao, Y. Zhong, J. Sun, and S. Lv. 2014. TGF beta1 mediates epithelial mesenchymal transition via beta6 integrin signaling pathway in breast cancer. *Cancer Invest*. 32:409-415.

Li, X., Y. Yang, Y. Hu, D. Dang, J. Regezi, B.L. Schmidt, A. Atakilit, B. Chen, D. Ellis, and D.M. Ramos. 2003. Alphavbeta6-Fyn signaling promotes oral cancer progression. *J Biol Chem*. 278:41646-41653.

Li, Z., P. Lin, C. Gao, C. Peng, S. Liu, H. Gao, B. Wang, J. Wang, J. Niu, and W. Niu. 2016. Integrin beta6 acts as an unfavorable prognostic indicator and promotes cellular malignant behaviors via ERK-ETS1 pathway in pancreatic ductal adenocarcinoma (PDAC). *Tumour Biol*. 37:5117-5131.

Liddington, R.C. 2014. Structural aspects of integrins. *Adv Exp Med Biol*. 819:111-126.

Lilja, J., T. Zacharchenko, M. Georgiadou, G. Jacquemet, N. Franceschi, E. Peuhu, H. Hamidi, J. Pouwels, V. Martens, F.H. Nia, M. Beifuss, T. Boeckers, H.J. Kreienkamp, I.L. Barsukov, and J. Ivaska. 2017. SHANK proteins limit integrin activation by directly interacting with Rap1 and R-Ras. *Nature cell biology*.

Lim, K.H., A.T. Baines, J.J. Fiordalisi, M. Shipitsin, L.A. Feig, A.D. Cox, C.J. Der, and C.M. Counter. 2005. Activation of RalA is critical for Ras-induced tumorigenesis of human cells. *Cancer Cell*. 7:533-545.

Liotta, L.A., and E. Kohn. 2004. Anoikis: cancer and the homeless cell. *Nature*. 430:973-974.

Liu, C.Y., X. Lv, T. Li, Y. Xu, X. Zhou, S. Zhao, Y. Xiong, Q.Y. Lei, and K.L. Guan. 2011a. PP1 cooperates with ASPP2 to dephosphorylate and activate TAZ. *J Biol Chem*. 286:5558-5566.

Liu, J., X. He, Y. Qi, X. Tian, S.J. Monkley, D.R. Critchley, S.A. Corbett, S.F. Lowry, A.M. Graham, and S. Li. 2011b. Talin1 regulates integrin turnover to promote embryonic epithelial morphogenesis. *Mol Cell Biol*. 31:3366-3377.

Livasy, C.A., G. Karaca, R. Nanda, M.S. Tretiakova, O.I. Olopade, D.T. Moore, and C.M. Perou. 2006. Phenotypic evaluation of the basal-like subtype of invasive breast carcinoma. *Mod Pathol*. 19:264-271.

Longva, K.E., F.D. Blystad, E. Stang, A.M. Larsen, L.E. Johannessen, and I.H. Madshus. 2002. Ubiquitination and proteasomal activity is required for transport of the EGF receptor to inner membranes of multivesicular bodies. *J Cell Biol*. 156:843-854.

Lossner, D., C. Abou-Ajram, A. Benge, and U. Reuning. 2008. Integrin alphavbeta3 mediates upregulation of epidermal growth-factor receptor expression and activity in human ovarian cancer cells. *Int J Biochem Cell Biol*. 40:2746-2761.

Luetteke, N.C., T.H. Qiu, S.E. Fenton, K.L. Troyer, R.F. Riedel, A. Chang, and D.C. Lee. 1999. Targeted inactivation of the EGF and amphiregulin genes reveals distinct roles for EGF receptor ligands in mouse mammary gland development. *Development*. 126:2739-2750.

Luzio, J.P., P.R. Pryor, and N.A. Bright. 2007. Lysosomes: fusion and function. *Nat Rev Mol Cell Biol*. 8:622-632.

Machnicka, B., A. Czogalla, A. Hryniewicz-Jankowska, D.M. Boguslawska, R. Grochowalska, E. Heger, and A.F. Sikorski. 2014. Spectrins: a structural platform for stabilization and activation of membrane channels, receptors and transporters. *Biochimica et biophysica acta*. 1838:620-634.

Mai, A., S. Veltel, T. Pellinen, A. Padzik, E. Coffey, V. Marjomaki, and J. Ivaska. 2011. Competitive binding of Rab21 and p120RasGAP to integrins regulates receptor traffic and migration. *J Cell Biol*. 194:291-306.

Man, Y.K.S., J.A. Davies, L. Coughlan, C. Pantelidou, A. Blazquez-Moreno, J.F. Marshall, A.L. Parker, and G. Hallden. 2018. The Novel Oncolytic Adenoviral Mutant Ad5-3Delta-A20T Retargeted to alphavbeta6 Integrins Efficiently Eliminates Pancreatic Cancer Cells. *Mol Cancer Ther*.

Mana, G., F. Clapero, E. Panieri, V. Panero, R.T. Bottcher, H.Y. Tseng, F. Saltarin, E. Astanina, K.I. Wolanska, M.R. Morgan, M.J. Humphries, M.M. Santoro, G. Serini, and D. Valdembri. 2016. PPFIA1 drives active alpha5beta1 integrin recycling and controls fibronectin fibrillogenesis and vascular morphogenesis. *Nature communications*. 7:13546.

Mann, G.B., K.J. Fowler, A. Gabriel, E.C. Nice, R.L. Williams, and A.R. Dunn. 1993. Mice with a null mutation of the TGF alpha gene have abnormal skin architecture, wavy hair, and curly whiskers and often develop corneal inflammation. *Cell*. 73:249-261.

Mardakheh, F.K., A. Paul, S. Kumper, A. Sadok, H. Paterson, A. McCarthy, Y. Yuan, and C.J. Marshall. 2015. Global Analysis of mRNA, Translation, and Protein Localization: Local Translation Is a Key Regulator of Cell Protrusions. *Dev Cell*. 35:344-357.

Margadant, C., and A. Sonnenberg. 2010. Integrin-TGF-beta crosstalk in fibrosis, cancer and wound healing. *EMBO Rep*. 11:97-105.

Marsh, D., S. Dickinson, G.W. Neill, J.F. Marshall, I.R. Hart, and G.J. Thomas. 2008. alpha vbeta 6 Integrin promotes the invasion of morphoeic basal cell carcinoma through stromal modulation. *Cancer Res*. 68:3295-3303.

Massague, J. 2008. TGFbeta in Cancer. *Cell*. 134:215-230.

Matoskova, B., W.T. Wong, A.E. Salcini, P.G. Pelicci, and P.P. Di Fiore. 1995. Constitutive phosphorylation of eps8 in tumor cell lines: relevance to malignant transformation. *Mol Cell Biol*. 15:3805-3812.

Mattila, E., K. Auvinen, M. Salmi, and J. Ivaska. 2008. The protein tyrosine phosphatase TCPTP controls VEGFR2 signalling. *Journal of cell science*. 121:3570-3580.

Mattila, E., T. Pellinen, J. Nevo, K. Vuoriluoto, A. Arjonen, and J. Ivaska. 2005. Negative regulation of EGFR signalling through integrin-alpha1beta1-mediated activation of protein tyrosine phosphatase TCPTP. *Nature cell biology*. 7:78-85.

Mazza, V., and F. Cappuzzo. 2017. Treating EGFR mutation resistance in non-small cell lung cancer - role of osimertinib. *Appl Clin Genet*. 10:49-56.

McCullough, J., M.J. Clague, and S. Urbe. 2004. AMSH is an endosome-associated ubiquitin isopeptidase. *J Cell Biol*. 166:487-492.

Mehta, R.J., B. Diefenbach, A. Brown, E. Cullen, A. Jonczyk, D. Gussow, G.A. Luckenbach, and S.L. Goodman. 1998. Transmembrane-truncated alphavbeta3 integrin retains high affinity for ligand binding: evidence for an 'inside-out' suppressor? *The Biochemical journal*. 330 (Pt 2):861-869.

Mellacheruvu, D., Z. Wright, A.L. Couzens, J.P. Lambert, N.A. St-Denis, T. Li, Y.V. Miteva, S. Hauri, M.E. Sardiu, T.Y. Low, V.A. Halim, R.D. Bagshaw, N.C. Hubner, A. Al-Hakim, A. Bouchard, D. Faubert, D. Fermin, W.H. Dunham, M. Goudreault, Z.Y. Lin, B.G. Badillo, T. Pawson, D. Durocher, B. Coulombe, R. Aebersold, G. Superti-Furga, J. Colinge, A.J. Heck, H. Choi, M. Gstaiger, S. Mohammed, I.M. Cristea, K.L. Bennett, M.P. Washburn, B. Raught, R.M. Ewing, A.C. Gingras, and A.I. Nesvizhskii. 2013. The CRAPome: a contaminant repository for affinity purification-mass spectrometry data. *Nat Methods*. 10:730-736.

Mendoza, P., R. Ortiz, J. Diaz, A.F. Quest, L. Leyton, D. Stupack, and V.A. Torres. 2013. Rab5 activation promotes focal adhesion disassembly, migration and invasiveness in tumor cells. *Journal of cell science*. 126:3835-3847.

Mendrola, J.M., M.B. Berger, M.C. King, and M.A. Lemmon. 2002. The single transmembrane domains of ErbB receptors self-associate in cell membranes. *J Biol Chem*. 277:4704-4712.

Merrifield, C.J., and M. Kaksonen. 2014. Endocytic accessory factors and regulation of clathrin-mediated endocytosis. *Cold Spring Harb Perspect Biol*. 6:a016733.

Meyer, T., J.F. Marshall, and I.R. Hart. 1998. Expression of alphav integrins and vitronectin receptor identity in breast cancer cells. *British journal of cancer*. 77:530-536.

Micke, P., and A. Ostman. 2004. Tumour-stroma interaction: cancer-associated fibroblasts as novel targets in anti-cancer therapy? *Lung Cancer*. 45 Suppl 2:S163-175.

Miettinen, P.J., J.E. Berger, J. Meneses, Y. Phung, R.A. Pedersen, Z. Werb, and R. Derynck. 1995. Epithelial immaturity and multiorgan failure in mice lacking epidermal growth factor receptor. *Nature*. 376:337-341.

Millard, M., S. Odde, and N. Neamati. 2011. Integrin targeted therapeutics. *Theranostics*. 1:154-188.

Mitra, S.K., D.A. Hanson, and D.D. Schlaepfer. 2005. Focal adhesion kinase: in command and control of cell motility. *Nat Rev Mol Cell Biol*. 6:56-68.

Mitra, S.K., and D.D. Schlaepfer. 2006. Integrin-regulated FAK-Src signaling in normal and cancer cells. *Current opinion in cell biology*. 18:516-523.

Moore, K.M., G.J. Thomas, S.W. Duffy, J. Warwick, R. Gabe, P. Chou, I.O. Ellis, A.R. Green, S. Haider, K. Brouilette, A. Saha, S. Vallath, R. Bowen, C. Chelala, D. Eccles, W.J. Tapper, A.M. Thompson, P. Quinlan, L. Jordan, C. Gillett, A. Brentnall, S. Violette, P.H. Weinreb, J. Kendrew, S.T. Barry, I.R. Hart, J.L. Jones, and J.F. Marshall. 2014. Therapeutic targeting of integrin αvβ6 in breast cancer. *J Natl Cancer Inst*. 106.

Morgan, M.R., H. Hamidi, M.D. Bass, S. Warwood, C. Ballestrem, and M.J. Humphries. 2013. Syndecan-4 phosphorylation is a control point for integrin recycling. *Dev Cell*. 24:472-485.

Morgan, M.R., M.J. Humphries, and M.D. Bass. 2007. Synergistic control of cell adhesion by integrins and syndecans. *Nat Rev Mol Cell Biol*. 8:957-969.

Morgan, M.R., M. Jazayeri, A.G. Ramsay, G.J. Thomas, M.J. Boulanger, I.R. Hart, and J.F. Marshall. 2011. Psoriasin (S100A7) associates with integrin beta6 subunit and is required for alphavbeta6-dependent carcinoma cell invasion. *Oncogene*. 30:1422-1435.

Morgan, M.R., G.J. Thomas, A. Russell, I.R. Hart, and J.F. Marshall. 2004. The integrin cytoplasmic-tail motif EKQKVDLSTDC is sufficient to promote tumor cell invasion mediated by matrix metalloproteinase (MMP)-2 or MMP-9. *J Biol Chem*. 279:26533-26539.

Morishige, M., S. Hashimoto, E. Ogawa, Y. Toda, H. Kotani, M. Hirose, S. Wei, A. Hashimoto, A. Yamada, H. Yano, Y. Mazaki, H. Kodama, Y. Nio, T. Manabe, H. Wada, H. Kobayashi, and H. Sabe. 2008. GEP100 links epidermal growth factor receptor signalling to Arf6 activation to induce breast cancer invasion. *Nature cell biology*. 10:85-92.

Moro, L., L. Dolce, S. Cabodi, E. Bergatto, E. Boeri Erba, M. Smeriglio, E. Turco, S.F. Retta, M.G. Giuffrida, M. Venturino, J. Godovac-Zimmermann, A. Conti, E. Schaefer, L. Beguinot, C. Tacchetti, P. Gaggini, L. Silengo, G. Tarone, and P. Defilippi. 2002. Integrin-induced epidermal growth factor (EGF) receptor activation requires c-Src and p130Cas and leads to phosphorylation of specific EGF receptor tyrosines. *J Biol Chem*. 277:9405-9414.

Moro, L., M. Venturino, C. Bozzo, L. Silengo, F. Altruda, L. Beguinot, G. Tarone, and P. Defilippi. 1998. Integrins induce activation of EGF receptor: role in MAP kinase induction and adhesion-dependent cell survival. *EMBO J*. 17:6622-6632.

Moser, M., K.R. Legate, R. Zent, and R. Fassler. 2009. The tail of integrins, talin, and kindlins. *Science*. 324:895-899.

Mott, H.R., and D. Owen. 2015. Structures of Ras superfamily effector complexes: What have we learnt in two decades? *Crit Rev Biochem Mol Biol*. 50:85-133.

Mouneimne, G., L. Soon, V. DesMarais, M. Sidani, X. Song, S.C. Yip, M. Ghosh, R. Eddy, J.M. Backer, and J. Condeelis. 2004. Phospholipase C and cofilin are required for carcinoma cell directionality in response to EGF stimulation. *J Cell Biol*. 166:697-708.

Mu, D., S. Cambier, L. Fjellbirkeland, J.L. Baron, J.S. Munger, H. Kawakatsu, D. Sheppard, V.C. Broaddus, and S.L. Nishimura. 2002. The integrin alpha(v)beta8 mediates epithelial homeostasis through MT1-MMP-dependent activation of TGF-beta1. *J Cell Biol*. 157:493-507.

Mu, Z., Z. Yang, D. Yu, Z. Zhao, and J.S. Munger. 2008. TGFbeta1 and TGFbeta3 are partially redundant effectors in brain vascular morphogenesis. *Mech Dev*. 125:508-516.

Munger, J.S., X. Huang, H. Kawakatsu, M.J. Griffiths, S.L. Dalton, J. Wu, J.F. Pittet, N. Kaminski, C. Garat, M.A. Matthay, D.B. Rifkin, and D. Sheppard. 1999. The integrin alpha v beta 6 binds and activates latent TGF beta 1: a mechanism for regulating pulmonary inflammation and fibrosis. *Cell*. 96:319-328.

Murphy, J.E., B.E. Padilla, B. Hasdemir, G.S. Cottrell, and N.W. Bunnett. 2009. Endosomes: a legitimate platform for the signaling train. *Proc Natl Acad Sci U S A*. 106:17615-17622.

Naber, H.P., Y. Drabsch, B.E. Snaar-Jagalska, P. ten Dijke, and T. van Laar. 2013. Snail and Slug, key regulators of TGF-beta-induced EMT, are sufficient for the induction of single-cell invasion. *Biochem Biophys Res Commun*. 435:58-63.

Needham, S.R., S.K. Roberts, A. Arkhipov, V.P. Mysore, C.J. Tynan, L.C. Zanetti-Domingues, E.T. Kim, V. Losasso, D. Korovesis, M. Hirsch, D.J. Rolfe, D.T. Clarke, M.D. Winn, A. Lajevardipour, A.H. Clayton, L.J. Pike, M. Perani, P.J. Parker, Y. Shan, D.E. Shaw, and M.L. Martin-Fernandez. 2016. EGFR oligomerization organizes kinase-active dimers into competent signalling platforms. *Nature communications*. 7:13307.

Nevo, J., A. Mai, S. Tuomi, T. Pellinen, O.T. Pentikainen, P. Heikkila, J. Lundin, H. Joensuu, P. Bono, and J. Ivaska. 2010. Mammary-derived growth inhibitor (MDGI) interacts with integrin alpha-subunits and suppresses integrin activity and invasion. *Oncogene*. 29:6452-6463.

Ng, T., D. Shima, A. Squire, P.I. Bastiaens, S. Gschmeissner, M.J. Humphries, and P.J. Parker. 1999. PKCalpha regulates beta1 integrin-dependent cell motility through association and control of integrin traffic. *EMBO J*. 18:3909-3923.

Nielsen, T.O., F.D. Hsu, K. Jensen, M. Cheang, G. Karaca, Z. Hu, T. Hernandez-Boussard, C. Livasy, D. Cowan, L. Dressler, L.A. Akslen, J. Ragaz, A.M. Gown, C.B. Gilks, M. van de Rijn, and C.M. Perou. 2004. Immunohistochemical and clinical characterization of the basal-like subtype of invasive breast carcinoma. *Clinical cancer research : an official journal of the American Association for Cancer Research*. 10:5367-5374.

Ning, Y., T. Buranda, and L.G. Hudson. 2007. Activated epidermal growth factor receptor induces integrin alpha2 internalization via caveolae/raft-dependent endocytic pathway. *J Biol Chem*. 282:6380-6387.

Niu, J., X. Gu, N. Ahmed, S. Andrews, J. Turton, R. Bates, and M. Agrez. 2001. The alphaVbeta6 integrin regulates its own expression with cell crowding: implications for tumour progression. *International journal of cancer. Journal international du cancer*. 92:40-48.

Niu, J., and Z. Li. 2017. The roles of integrin alphavbeta6 in cancer. *Cancer Lett*. 403:128-137.

Normanno, N., A. De Luca, M.R. Maiello, M. Campiglio, M. Napolitano, M. Mancino, A. Carotenuto, G. Viglietto, and S. Menard. 2006. The MEK/MAPK pathway is involved in the resistance of breast cancer cells to the EGFR tyrosine kinase inhibitor gefitinib. *J Cell Physiol*. 207:420-427.

Nystrom, M.L., D. McCulloch, P.H. Weinreb, S.M. Violette, P.M. Speight, J.F. Marshall, I.R. Hart, and G.J. Thomas. 2006. Cyclooxygenase-2 inhibition suppresses alphavbeta6 integrin-dependent oral squamous carcinoma invasion. *Cancer Res*. 66:10833-10842.

O'Toole, T.E., D. Mandelman, J. Forsyth, S.J. Shattil, E.F. Plow, and M.H. Ginsberg. 1991. Modulation of the affinity of integrin alpha IIb beta 3 (GPIIb-IIIa) by the cytoplasmic domain of alpha IIb. *Science*. 254:845-847.

Oda, K., Y. Matsuoka, A. Funahashi, and H. Kitano. 2005. A comprehensive pathway map of epidermal growth factor receptor signaling. *Mol Syst Biol*. 1:2005 0010.

Odintsova, E., J. Voortman, E. Gilbert, and F. Berditchevski. 2003. Tetraspanin CD82 regulates compartmentalisation and ligand-induced dimerization of EGFR. *Journal of cell science*. 116:4557-4566.

Offenhauser, N., A. Borgonovo, A. Disanza, P. Romano, I. Ponzanelli, G. Iannolo, P.P. Di Fiore, and G. Scita. 2004. The eps8 family of proteins links growth factor stimulation to actin reorganization generating functional redundancy in the Ras/Rac pathway. *Mol Biol Cell*. 15:91-98.

Ogiso, H., R. Ishitani, O. Nureki, S. Fukai, M. Yamanaka, J.H. Kim, K. Saito, A. Sakamoto, M. Inoue, M. Shirouzu, and S. Yokoyama. 2002. Crystal structure of the complex of human epidermal growth factor and receptor extracellular domains. *Cell*. 110:775-787.

Onodera, Y., J.M. Nam, A. Hashimoto, J.C. Norman, H. Shirato, S. Hashimoto, and H. Sabe. 2012. Rab5c promotes AMAP1-PRKD2 complex formation to enhance beta1 integrin recycling in EGF-induced cancer invasion. *J Cell Biol*. 197:983-996.

Oria, R., T. Wiegand, J. Escribano, A. Elosegui-Artola, J.J. Uriarte, C. Moreno-Pulido, I. Platzman, P. Delcanale, L. Albertazzi, D. Navajas, X. Trepat, J.M. Garcia-Aznar, E.A. Cavalcanti-Adam, and P. Roca-Cusachs. 2017. Force loading explains spatial sensing of ligands by cells. *Nature*. 552:219-224.

Ory, S., H. Brazier, and A. Blangy. 2007. Identification of a bipartite focal adhesion localization signal in RhoU/Wrch-1, a Rho family GTPase that regulates cell adhesion and migration. *Biol Cell*. 99:701-716.

Otero, M.G., M. Alloatti, L.E. Cromberg, A. Almenar-Queralt, S.E. Encalada, V.M. Pozo Devoto, L. Bruno, L.S. Goldstein, and T.L. Falzone. 2014. Fast axonal transport of the proteasome complex depends on membrane interaction and molecular motor function. *Journal of cell science*. 127:1537-1549.

Page-McCaw, A., A.J. Ewald, and Z. Werb. 2007. Matrix metalloproteinases and the regulation of tissue remodelling. *Nat Rev Mol Cell Biol*. 8:221-233.

Palamidessi, A., E. Frittoli, N. Ducano, N. Offenhauser, S. Sigismund, H. Kajiho, D. Parazzoli, A. Oldani, M. Gobbi, G. Serini, P.P. Di Fiore, G. Scita, and L. Lanzetti. 2013. The GTPase-activating protein RN-tre controls focal adhesion turnover and cell migration. *Curr Biol*. 23:2355-2364.

Pankov, R., E. Cukierman, B.Z. Katz, K. Matsumoto, D.C. Lin, S. Lin, C. Hahn, and K.M. Yamada. 2000. Integrin dynamics and matrix assembly: tensin-dependent translocation of alpha(5)beta(1) integrins promotes early fibronectin fibrillogenesis. *J Cell Biol*. 148:1075-1090.

Park, S., and C.D. James. 2003. Lanthionine synthetase components C-like 2 increases cellular sensitivity to adriamycin by decreasing the expression of P-glycoprotein through a transcription-mediated mechanism. *Cancer Res*. 63:723-727.

Parsons, M., M.D. Keppler, A. Kline, A. Messent, M.J. Humphries, R. Gilchrist, I.R. Hart, C. Quittau-Prevostel, W.E. Hughes, P.J. Parker, and T. Ng. 2002. Site-directed perturbation of protein kinase C- integrin interaction blocks carcinoma cell chemotaxis. *Mol Cell Biol*. 22:5897-5911.

Paszek, M.J., C.C. DuFort, O. Rossier, R. Bainer, J.K. Mouw, K. Godula, J.E. Hudak, J.N. Lakins, A.C. Wijekoon, L. Cassereau, M.G. Rubashkin, M.J. Magbanua, K.S. Thorn, M.W. Davidson, H.S. Rugo, J.W. Park, D.A. Hammer, G. Giannone, C.R. Bertozzi, and V.M. Weaver. 2014. The cancer glycocalyx mechanically primes integrin-mediated growth and survival. *Nature*. 511:319-325.

Paul, N.R., G. Jacquemet, and P.T. Caswell. 2015. Endocytic Trafficking of Integrins in Cell Migration. *Curr Biol*. 25:R1092-1105.

Pedersen, M.W., M. Meltorn, L. Damstrup, and H.S. Poulsen. 2001. The type III epidermal growth factor receptor mutation. Biological significance and potential target for anti-cancer therapy. *Ann Oncol*. 12:745-760.

Pellinen, T., A. Arjonen, K. Vuoriluoto, K. Kallio, J.A. Fransen, and J. Ivaska. 2006. Small GTPase Rab21 regulates cell adhesion and controls endosomal traffic of beta1-integrins. *J Cell Biol*. 173:767-780.

Piccolo, S., S. Dupont, and M. Cordenonsi. 2014. The biology of YAP/TAZ: hippo signaling and beyond. *Physiol Rev*. 94:1287-1312.

Plotnikov, S.V., A.M. Pasapera, B. Sabass, and C.M. Waterman. 2012. Force fluctuations within focal adhesions mediate ECM-rigidity sensing to guide directed cell migration. *Cell*. 151:1513-1527.

Poeter, M., S. Radke, M. Koese, F. Hessner, A. Hegemann, A. Musiol, V. Gerke, T. Grewal, and U. Rescher. 2013. Disruption of the annexin A1/S100A11 complex increases the migration and clonogenic growth by dysregulating epithelial growth factor (EGF) signaling. *Biochimica et biophysica acta*. 1833:1700-1711.

Pollard, T.D. 2016. Actin and Actin-Binding Proteins. *Cold Spring Harb Perspect Biol*. 8.

Pollard, T.D. 2017. What We Know and Do Not Know About Actin. *In* The Actin Cytoskeleton. B.M. Jockusch, editor. Springer International Publishing, Cham. 331-347.

Pollard, T.D., and J.A. Cooper. 2009. Actin, a central player in cell shape and movement. *Science*. 326:1208-1212.

Pouwels, J., J. Nevo, T. Pellinen, J. Ylanne, and J. Ivaska. 2012. Negative regulators of integrin activity. *J Cell Sci*. 125:3271-3280.

Purba, E.R., E.I. Saita, and I.N. Maruyama. 2017. Activation of the EGF Receptor by Ligand Binding and Oncogenic Mutations: The "Rotation Model". *Cells*. 6.

Raab-Westphal, S., J.F. Marshall, and S.L. Goodman. 2017. Integrins as Therapeutic Targets: Successes and Cancers. *Cancers (Basel)*. 9.

Raiborg, C., and H. Stenmark. 2009. The ESCRT machinery in endosomal sorting of ubiquitylated membrane proteins. *Nature*. 458:445-452.

Rainero, E., P.V.E. van den Berghe, and J.C. Norman. 2013. Internalisation, Endosomal Trafficking and Recycling of Integrins During Cell Migration and Cancer Invasion. *In* Vesicle Trafficking in Cancer. Y. Yarden and G. Tarcic, editors. Springer New York, New York, NY. 327-359.

Ramos, D.M., M. But, J. Regezi, B.L. Schmidt, A. Atakilit, D. Dang, D. Ellis, R. Jordan, and X. Li. 2002. Expression of integrin beta 6 enhances invasive behavior in oral squamous cell carcinoma. *Matrix Biol*. 21:297-307.

Ramsay, A.G., M.D. Keppler, M. Jazayeri, G.J. Thomas, M. Parsons, S. Violette, P. Weinreb, I.R. Hart, and J.F. Marshall. 2007. HS1-associated protein X-1 regulates carcinoma cell migration and invasion via clathrin-mediated endocytosis of integrin alphavbeta6. *Cancer Res*. 67:5275-5284.

Rantala, J.K., J. Pouwels, T. Pellinen, S. Veltel, P. Laasola, E. Mattila, C.S. Potter, T. Duffy, J.P. Sundberg, O. Kallioniemi, J.A. Askari, M.J. Humphries, M. Parsons, M. Salmi, and J. Ivaska. 2011. SHARPIN is an endogenous inhibitor of beta1-integrin activation. *Nat Cell Biol*. 13:1315-1324.

Reynolds, A.R., I.R. Hart, A.R. Watson, J.C. Welti, R.G. Silva, S.D. Robinson, G. Da Violante, M. Gourlaouen, M. Salih, M.C. Jones, D.T. Jones, G. Saunders, V. Kostourou, F. Perron-Sierra, J.C. Norman, G.C. Tucker, and K.M. Hodivala-Dilke. 2009. Stimulation of tumor growth and angiogenesis by low concentrations of RGD-mimetic integrin inhibitors. *Nat Med*. 15:392-400.

Reynolds, L.E., L. Wyder, J.C. Lively, D. Taverna, S.D. Robinson, X. Huang, D. Sheppard, R.O. Hynes, and K.M. Hodivala-Dilke. 2002. Enhanced pathological angiogenesis in mice lacking beta3 integrin or beta3 and beta5 integrins. *Nat Med*. 8:27-34.

Ribeiro, P.S., F. Josue, A. Wepf, M.C. Wehr, O. Rinner, G. Kelly, N. Tapon, and M. Gstaiger. 2010. Combined functional genomic and proteomic approaches identify a PP2A complex as a negative regulator of Hippo signaling. *Mol Cell*. 39:521-534.

Riedl, J., A.H. Crevenna, K. Kessenbrock, J.H. Yu, D. Neukirchen, M. Bista, F. Bradke, D. Jenne, T.A. Holak, Z. Werb, M. Sixt, and R. Wedlich-Soldner. 2008. Lifeact: a versatile marker to visualize F-actin. *Nat Methods*. 5:605-607.

Riggs, K.A., N. Hasan, D. Humphrey, C. Raleigh, C. Nevitt, D. Corbin, and C. Hu. 2012. Regulation of integrin endocytic recycling and chemotactic cell migration by syntaxin 6 and VAMP3 interaction. *Journal of cell science*. 125:3827-3839.

Roberts, M., S. Barry, A. Woods, P. van der Sluijs, and J. Norman. 2001. PDGF-regulated rab4-dependent recycling of alphavbeta3 integrin from early endosomes is necessary for cell adhesion and spreading. *Curr Biol*. 11:1392-1402.

Robertson, J., G. Jacquemet, A. Byron, M.C. Jones, S. Warwood, J.N. Selley, D. Knight, J.D. Humphries, and M.J. Humphries. 2015. Defining the phospho-adhesome through the phosphoproteomic analysis of integrin signalling. *Nature communications*. 6:6265.

Rojas, M., S. Yao, and Y.Z. Lin. 1996. Controlling epidermal growth factor (EGF)-stimulated Ras activation in intact cells by a cell-permeable peptide mimicking phosphorylated EGF receptor. *J Biol Chem*. 271:27456-27461.

Roskoski, R., Jr. 2014. The ErbB/HER family of protein-tyrosine kinases and cancer. *Pharmacol Res*. 79:34-74.

Rossier, O., V. Octeau, J.B. Sibarita, C. Leduc, B. Tessier, D. Nair, V. Gatterdam, O. Destaing, C. Albiges-Rizo, R. Tampe, L. Cognet, D. Choquet, B. Lounis, and G. Giannone. 2012. Integrins beta1 and beta3 exhibit distinct dynamic nanoscale organizations inside focal adhesions. *Nature cell biology*. 14:1057-1067.

Roy, M., Z. Li, and D.B. Sacks. 2005. IQGAP1 is a scaffold for mitogen-activated protein kinase signaling. *Mol Cell Biol*. 25:7940-7952.

Rozario, T., and D.W. DeSimone. 2010. The extracellular matrix in development and morphogenesis: a dynamic view. *Dev Biol*. 341:126-140.

Sachse, M., S. Urbe, V. Oorschot, G.J. Strous, and J. Klumperman. 2002. Bilayered clathrin coats on endosomal vacuoles are involved in protein sorting toward lysosomes. *Mol Biol Cell*. 13:1313-1328.

Saegusa, J., S. Yamaji, K. Ieguchi, C.Y. Wu, K.S. Lam, F.T. Liu, Y.K. Takada, and Y. Takada. 2009. The direct binding of insulin-like growth factor-1 (IGF-1) to integrin alphavbeta3 is involved in IGF-1 signaling. *J Biol Chem*. 284:24106-24114.

Sahai, E., M.F. Olson, and C.J. Marshall. 2001. Cross-talk between Ras and Rho signalling pathways in transformation favours proliferation and increased motility. *EMBO J*. 20:755-766.

Samson, T., C. Welch, E. Monaghan-Benson, K.M. Hahn, and K. Burridge. 2010. Endogenous RhoG is rapidly activated after epidermal growth factor stimulation through multiple guanine-nucleotide exchange factors. *Mol Biol Cell*. 21:1629-1642.

Sander, E.E., J.P. ten Klooster, S. van Delft, R.A. van der Kammen, and J.G. Collard. 1999. Rac downregulates Rho activity: reciprocal balance between both GTPases determines cellular morphology and migratory behavior. *J Cell Biol*. 147:1009-1022.

Savio, M.G., N. Wollscheid, E. Cavallaro, V. Algisi, P.P. Di Fiore, S. Sigismund, E. Maspero, and S. Polo. 2016. USP9X Controls EGFR Fate by Deubiquitinating the Endocytic Adaptor Eps15. *Curr Biol*. 26:173-183.

Sawada, Y., M. Tamada, B.J. Dubin-Thaler, O. Cherniavskaya, R. Sakai, S. Tanaka, and M.P. Sheetz. 2006. Force sensing by mechanical extension of the Src family kinase substrate p130Cas. *Cell*. 127:1015-1026.

Saxena, M., S. Liu, B. Yang, C. Hajal, R. Changede, J. Hu, H. Wolfenson, J. Hone, and M.P. Sheetz. 2017. EGFR and HER2 activate rigidity sensing only on rigid matrices. *Nature materials*. 16:775-781.

Schaefer, L., and R.M. Schaefer. 2010. Proteoglycans: from structural compounds to signaling molecules. *Cell Tissue Res*. 339:237-246.

Schiller, H.B., C.C. Friedel, C. Boulegue, and R. Fassler. 2011. Quantitative proteomics of the integrin adhesome show a myosin II-dependent recruitment of LIM domain proteins. *EMBO Rep*. 12:259-266.

Schiller, H.B., M.R. Hermann, J. Polleux, T. Vignaud, S. Zanivan, C.C. Friedel, Z. Sun, A. Raducanu, K.E. Gottschalk, M. Thery, M. Mann, and R. Fassler. 2013. beta1- and alphav-class integrins cooperate to regulate myosin II during rigidity sensing of fibronectin-based microenvironments. *Nature cell biology*. 15:625-636.

Schlaepfer, D.D., S.K. Hanks, T. Hunter, and P. van der Geer. 1994. Integrin-mediated signal transduction linked to Ras pathway by GRB2 binding to focal adhesion kinase. *Nature*. 372:786-791.

Schneider, I.C., C.K. Hays, and C.M. Waterman. 2009. Epidermal growth factor-induced contraction regulates paxillin phosphorylation to temporally separate traction generation from de-adhesion. *Mol Biol Cell*. 20:3155-3167.

Schwartz, M. 2004. Rho signalling at a glance. *Journal of cell science*. 117:5457-5458.

Scita, G., J. Nordstrom, R. Carbone, P. Tenca, G. Giardina, S. Gutkind, M. Bjarnegard, C. Betsholtz, and P.P. Di Fiore. 1999. EPS8 and E3B1 transduce signals from Ras to Rac. *Nature*. 401:290-293.

Scita, G., P. Tenca, L.B. Areces, A. Tocchetti, E. Frittoli, G. Giardina, I. Ponzanelli, P. Sini, M. Innocenti, and P.P. Di Fiore. 2001. An effector region in Eps8 is responsible for the activation of the Rac-specific GEF activity of Sos-1 and for the proper localization of the Rac-based actin-polymerizing machine. *J Cell Biol*. 154:1031-1044.

Scott, K.A., C.H. Arnott, S.C. Robinson, R.J. Moore, R.G. Thompson, J.F. Marshall, and F.R. Balkwill. 2004. TNF-alpha regulates epithelial expression of MMP-9 and integrin alphavbeta6 during tumour promotion. A role for TNF-alpha in keratinocyte migration? *Oncogene*. 23:6954-6966.

Scott, M.G., V. Pierotti, H. Storez, E. Lindberg, A. Thuret, O. Muntaner, C. Labbe-Jullie, J.A. Pitcher, and S. Marullo. 2006. Cooperative regulation of extracellular signal-regulated kinase activation and cell shape change by filamin A and beta-arrestins. *Mol Cell Biol*. 26:3432-3445.

Seguin, L., J.S. Desgrosellier, S.M. Weis, and D.A. Cheresh. 2015. Integrins and cancer: regulators of cancer stemness, metastasis, and drug resistance. *Trends Cell Biol*. 25:234-240.

Shattil, S.J., C. Kim, and M.H. Ginsberg. 2010. The final steps of integrin activation: the end game. *Nat Rev Mol Cell Biol*. 11:288-300.

Sheppard, D. 2005. Integrin-mediated activation of latent transforming growth factor beta. *Cancer Metastasis Rev*. 24:395-402.

Shi, F., and J. Sottile. 2008. Caveolin-1-dependent beta1 integrin endocytosis is a critical regulator of fibronectin turnover. *Journal of cell science*. 121:2360-2371.

Shi, F., S.E. Telesco, Y. Liu, R. Radhakrishnan, and M.A. Lemmon. 2010. ErbB3/HER3 intracellular domain is competent to bind ATP and catalyze autophosphorylation. *Proc Natl Acad Sci U S A*. 107:7692-7697.

Shtiegman, K., B.S. Kochupurakkal, Y. Zwang, G. Pines, A. Starr, A. Vexler, A. Citri, M. Katz, S. Lavi, Y. Ben-Basat, S. Benjamin, S. Corso, J. Gan, R.B. Yosef, S. Giordano, and Y.

Yarden. 2007. Defective ubiquitinylation of EGFR mutants of lung cancer confers prolonged signaling. *Oncogene*. 26:6968-6978.

Sibilia, M., and E.F. Wagner. 1995. Strain-dependent epithelial defects in mice lacking the EGF receptor. *Science*. 269:234-238.

Sigismund, S., D. Avanzato, and L. Lanzetti. 2017. Emerging functions of the EGFR in cancer. *Mol Oncol*.

Sigismund, S., T. Woelk, C. Puri, E. Maspero, C. Tacchetti, P. Transidico, P.P. Di Fiore, and S. Polo. 2005. Clathrin-independent endocytosis of ubiquitinated cargos. *Proc Natl Acad Sci U S A*. 102:2760-2765.

Simanshu, D.K., D.V. Nissley, and F. McCormick. 2017. RAS Proteins and Their Regulators in Human Disease. *Cell*. 170:17-33.

Singh, C., R.K. Shyanti, V. Singh, R.K. Kale, J.P.N. Mishra, and R.P. Singh. 2018. Integrin expression and glycosylation patterns regulate cell-matrix adhesion and alter with breast cancer progression. *Biochem Biophys Res Commun*. 499:374-380.

Sjoblom, B., A. Salmazo, and K. Djinovic-Carugo. 2008. Alpha-actinin structure and regulation. *Cell Mol Life Sci*. 65:2688-2701.

Slack, R.J., M. Hafeji, R. Rogers, S.B. Ludbrook, J.F. Marshall, D.J. Flint, S. Pyne, and J.C. Denyer. 2016. Pharmacological Characterization of the alphavbeta6 Integrin Binding and Internalization Kinetics of the Foot-and-Mouth Disease Virus Derived Peptide A20FMDV2. *Pharmacology*. 97:114-125.

Smith, M.L., D. Gourdon, W.C. Little, K.E. Kubow, R.A. Eguiluz, S. Luna-Morris, and V. Vogel. 2007. Force-induced unfolding of fibronectin in the extracellular matrix of living cells. *PLoS Biol*. 5:e268.

Smythe, E., and K.R. Ayscough. 2006. Actin regulation in endocytosis. *Journal of cell science*. 119:4589-4598.

Sokolowska, E., M. Presler, E. Goyke, R. Milczarek, J. Swierczynski, and T. Sledzinski. 2017. Orlistat Reduces Proliferation and Enhances Apoptosis in Human Pancreatic Cancer Cells (PANC-1). *Anticancer Res*. 37:6321-6327.

Soosairajah, J., S. Maiti, O. Wiggan, P. Sarmiere, N. Moussi, B. Sarcevic, R. Sampath, J.R. Bamburg, and O. Bernard. 2005. Interplay between components of a novel LIM kinase-slingshot phosphatase complex regulates cofilin. *EMBO J*. 24:473-486.

Sorkin, A., and L.K. Goh. 2008. Endocytosis and intracellular trafficking of ErbBs. *Experimental cell research*. 314:3093-3106.

Sorkin, A., and L.K. Goh. 2009. Endocytosis and intracellular trafficking of ErbBs. *Experimental cell research*. 315:683-696.

Sorkin, A., S. Krolenko, N. Kudrjavtceva, J. Lazebnik, L. Teslenko, A.M. Soderquist, and N. Nikolsky. 1991. Recycling of epidermal growth factor-receptor complexes in A431 cells: identification of dual pathways. *J Cell Biol*. 112:55-63.

Sorkin, A., and M. von Zastrow. 2009. Endocytosis and signalling: intertwining molecular networks. *Nat Rev Mol Cell Biol*. 10:609-622.

Sottile, J., and J. Chandler. 2005. Fibronectin matrix turnover occurs through a caveolin-1-dependent process. *Mol Biol Cell*. 16:757-768.

Soule, H.D., J. Vazguez, A. Long, S. Albert, and M. Brennan. 1973. A human cell line from a pleural effusion derived from a breast carcinoma. *J Natl Cancer Inst*. 51:1409-1416.

Sousa, L.P., I. Lax, H. Shen, S.M. Ferguson, P. De Camilli, and J. Schlessinger. 2012. Suppression of EGFR endocytosis by dynamin depletion reveals that EGFR signaling occurs primarily at the plasma membrane. *Proc Natl Acad Sci U S A*. 109:4419-4424.

Sproat, C. 2017. Investigating integrin αvβ6 activation status in breast cancer. Vol. PhD. Queen Mary University of London.

Sripathi, S.R., O. Sylvester, W. He, T. Moser, J.Y. Um, F. Lamoke, W. Ramakrishna, P.S. Bernstein, M. Bartoli, and W.J. Jahng. 2016. Prohibitin as the Molecular Binding Switch in the Retinal Pigment Epithelium. *Protein J*. 35:1-16.

Steinberg, F., K.J. Heesom, M.D. Bass, and P.J. Cullen. 2012. SNX17 protects integrins from degradation by sorting between lysosomal and recycling pathways. *J Cell Biol*. 197:219-230.

Stenmark, H. 2009. Rab GTPases as coordinators of vesicle traffic. *Nat Rev Mol Cell Biol*. 10:513-525.

Stoten, C.L., and J.G. Carlton. 2018. ESCRT-dependent control of membrane remodelling during cell division. *Semin Cell Dev Biol*. 74:50-65.

Streuli, C.H., and N. Akhtar. 2009. Signal co-operation between integrins and other receptor systems. *The Biochemical journal*. 418:491-506.

Stupp, R., M.E. Hegi, T. Gorlia, S.C. Erridge, J. Perry, Y.K. Hong, K.D. Aldape, B. Lhermitte, T. Pietsch, D. Grujicic, J.P. Steinbach, W. Wick, R. Tarnawski, D.H. Nam, P. Hau, A. Weyerbrock, M.J. Taphoorn, C.C. Shen, N. Rao, L. Thurzo, U. Herrlinger, T. Gupta, R.D. Kortmann, K. Adamska, C. McBain, A.A. Brandes, J.C. Tonn, O. Schnell, T. Wiegel, C.Y. Kim, L.B. Nabors, D.A. Reardon, M.J. van den Bent, C. Hicking, A. Markivskyy, M. Picard, M. Weller, R. European Organisation for, C. Treatment of, C. Canadian Brain Tumor, and C.s. team. 2014. Cilengitide combined with standard treatment for patients with newly diagnosed glioblastoma with methylated MGMT promoter (CENTRIC EORTC 26071-22072 study): a multicentre, randomised, open-label, phase 3 trial. *Lancet Oncol*. 15:1100-1108.

Sun, Z., S.S. Guo, and R. Fassler. 2016. Integrin-mediated mechanotransduction. *J Cell Biol*. 215:445-456.

Sweeney, C., D. Fambrough, C. Huard, A.J. Diamonti, E.S. Lander, L.C. Cantley, and K.L. Carraway, 3rd. 2001. Growth factor-specific signaling pathway stimulation and gene expression mediated by ErbB receptors. *J Biol Chem*. 276:22685-22698.

Swindle, C.S., K.T. Tran, T.D. Johnson, P. Banerjee, A.M. Mayes, L. Griffith, and A. Wells. 2001. Epidermal growth factor (EGF)-like repeats of human tenascin-C as ligands for EGF receptor. *J Cell Biol*. 154:459-468.

Takahashi, M., Y. Li, T.J. Dillon, and P.J. Stork. 2017. Phosphorylation of Rap1 by cAMP-dependent Protein Kinase (PKA) Creates a Binding Site for KSR to Sustain ERK Activation by cAMP. *J Biol Chem*. 292:1449-1461.

Tan, M.H., N.J. Nowak, R. Loor, H. Ochi, A.A. Sandberg, C. Lopez, J.W. Pickren, R. Berjian, H.O. Douglass, Jr., and T.M. Chu. 1986. Characterization of a new primary human pancreatic tumor line. *Cancer Invest*. 4:15-23.

Tanaka, T., Y. Zhou, T. Ozawa, R. Okizono, A. Banba, T. Yamamura, E. Oga, A. Muraguchi, and H. Sakurai. 2018. Ligand-activated epidermal growth factor receptor (EGFR) signaling governs endocytic trafficking of unliganded receptor monomers by non-canonical phosphorylation. *J Biol Chem*. 293:2288-2301.

Tao, R.H., and I.N. Maruyama. 2008. All EGF(ErbB) receptors have preformed homo- and heterodimeric structures in living cells. *Journal of cell science*. 121:3207-3217.

Thomas, G.J., M.P. Lewis, I.R. Hart, J.F. Marshall, and P.M. Speight. 2001a. AlphaVbeta6 integrin promotes invasion of squamous carcinoma cells through up-regulation of matrix metalloproteinase-9. *Int J Cancer*. 92:641-650.

Thomas, G.J., M.P. Lewis, S.A. Whawell, A. Russell, D. Sheppard, I.R. Hart, P.M. Speight, and J.F. Marshall. 2001b. Expression of the alphavbeta6 integrin promotes migration and invasion in squamous carcinoma cells. *J Invest Dermatol*. 117:67-73.

Thomas, G.J., M.L. Nystrom, and J.F. Marshall. 2006. Alphavbeta6 integrin in wound healing and cancer of the oral cavity. *Journal of oral pathology & medicine : official publication of the International Association of Oral Pathologists and the American Academy of Oral Pathology*. 35:1-10.

Thomas, G.J., S. Poomsawat, M.P. Lewis, I.R. Hart, P.M. Speight, and J.F. Marshall. 2001c. alpha v beta 6 Integrin upregulates matrix metalloproteinase 9 and promotes migration of normal oral keratinocytes. *J Invest Dermatol*. 116:898-904.

Thomas, M., M. Felcht, K. Kruse, S. Kretschmer, C. Deppermann, A. Biesdorf, K. Rohr, A.V. Benest, U. Fiedler, and H.G. Augustin. 2010. Angiopoietin-2 stimulation of endothelial cells induces alphavbeta3 integrin internalization and degradation. *J Biol Chem*. 285:23842-23849.

Threadgill, D.W., A.A. Dlugosz, L.A. Hansen, T. Tennenbaum, U. Lichti, D. Yee, C. LaMantia, T. Mourton, K. Herrup, R.C. Harris, and et al. 1995. Targeted disruption of mouse EGF receptor: effect of genetic background on mutant phenotype. *Science*. 269:230-234.

Tocchetti, A., S. Confalonieri, G. Scita, P.P. Di Fiore, and C. Betsholtz. 2003. In silico analysis of the EPS8 gene family: genomic organization, expression profile, and protein structure. *Genomics*. 81:234-244.

Tod, J., C.J. Hanley, M.R. Morgan, M. Rucka, T. Mellows, M.A. Lopez, P. Kiely, K.A. Moutasim, S.J. Frampton, D. Sabnis, D.R. Fine, C. Johnson, J.F. Marshall, G. Scita, V. Jenei, and G.J. Thomas. 2017. Pro-migratory and TGF-beta-activating functions of alphavbeta6 integrin in pancreatic cancer are differentially regulated via an Eps8-dependent GTPase switch. *J Pathol*.

Tomas, A., C.E. Futter, and E.R. Eden. 2014. EGF receptor trafficking: consequences for signaling and cancer. *Trends Cell Biol*. 24:26-34.

Travis, M.A., J.D. Humphries, and M.J. Humphries. 2003. An unraveling tale of how integrins are activated from within. *Trends Pharmacol Sci*. 24:192-197.

Vaggi, F., A. Disanza, F. Milanesi, P.P. Di Fiore, E. Menna, M. Matteoli, N.S. Gov, G. Scita, and A. Ciliberto. 2011. The Eps8/IRSp53/VASP network differentially controls actin capping and bundling in filopodia formation. *PLoS Comput Biol*. 7:e1002088.

Valdembri, D., P.T. Caswell, K.I. Anderson, J.P. Schwarz, I. Konig, E. Astanina, F. Caccavari, J.C. Norman, M.J. Humphries, F. Bussolino, and G. Serini. 2009. Neuropilin-1/GIPC1 signaling regulates alpha5beta1 integrin traffic and function in endothelial cells. *PLoS Biol*. 7:e25.

Valiathan, R.R., M. Marco, B. Leitinger, C.G. Kleer, and R. Fridman. 2012. Discoidin domain receptor tyrosine kinases: new players in cancer progression. *Cancer Metastasis Rev*. 31:295-321.

Van Aarsen, L.A., D.R. Leone, S. Ho, B.M. Dolinski, P.E. McCoon, D.J. LePage, R. Kelly, G. Heaney, P. Rayhorn, C. Reid, K.J. Simon, G.S. Horan, N. Tao, H.A. Gardner, M.M. Skelly, A.M. Gown, G.J. Thomas, P.H. Weinreb, S.E. Fawell, and S.M. Violette. 2008. Antibody-mediated blockade of integrin alpha v beta 6 inhibits tumor progression in vivo by a transforming growth factor-beta-regulated mechanism. *Cancer Res*. 68:561-570.

van der Flier, A., and A. Sonnenberg. 2001. Function and interactions of integrins. *Cell Tissue Res*. 305:285-298.

Vanhaesebroeck, B., S.J. Leevers, K. Ahmadi, J. Timms, R. Katso, P.C. Driscoll, R. Woscholski, P.J. Parker, and M.D. Waterfield. 2001. Synthesis and function of 3-phosphorylated inositol lipids. *Annu Rev Biochem*. 70:535-602.

Veevers-Lowe, J., S.G. Ball, A. Shuttleworth, and C.M. Kielty. 2011. Mesenchymal stem cell migration is regulated by fibronectin through alpha5beta1-integrin-mediated activation of PDGFR-beta and potentiation of growth factor signals. *Journal of cell science*. 124:1288-1300.

Vieira, A.V., C. Lamaze, and S.L. Schmid. 1996. Control of EGF receptor signaling by clathrin-mediated endocytosis. *Science*. 274:2086-2089.

Vogel, V. 2006. Mechanotransduction involving multimodular proteins: converting force into biochemical signals. *Annu Rev Biophys Biomol Struct*. 35:459-488.

Wagner, N., J. Lohler, E.J. Kunkel, K. Ley, E. Leung, G. Krissansen, K. Rajewsky, and W. Muller. 1996. Critical role for beta7 integrins in formation of the gut-associated lymphoid tissue. *Nature*. 382:366-370.

Wang, H., H. Jin, and A.C. Rapraeger. 2015. Syndecan-1 and Syndecan-4 Capture Epidermal Growth Factor Receptor Family Members and the alpha3beta1 Integrin Via Binding Sites in Their Ectodomains: NOVEL SYNSTATINS PREVENT KINASE CAPTURE AND INHIBIT alpha6beta4-INTEGRIN-DEPENDENT EPITHELIAL CELL MOTILITY. *J Biol Chem*. 290:26103-26113.

Wang, H.B., M. Dembo, S.K. Hanks, and Y. Wang. 2001. Focal adhesion kinase is involved in mechanosensing during fibroblast migration. *Proc Natl Acad Sci U S A*. 98:11295-11300.

Wang, J., J. Wu, J. Hong, R. Chen, K. Xu, W. Niu, C. Peng, E. Liu, J. Wang, S. Liu, M. Agrez, and J. Niu. 2011a. PKC promotes the migration of colon cancer cells by regulating the internalization and recycling of integrin alphavbeta6. *Cancer Lett*. 311:38-47.

Wang, P., Y. Bai, B. Song, Y. Wang, D. Liu, Y. Lai, X. Bi, and Z. Yuan. 2011b. PP1A-mediated dephosphorylation positively regulates YAP2 activity. *PLoS One*. 6:e24288.

Wang, Q., G. Villeneuve, and Z. Wang. 2005. Control of epidermal growth factor receptor endocytosis by receptor dimerization, rather than receptor kinase activation. *EMBO Rep*. 6:942-948.

Wang, W., R. Eddy, and J. Condeelis. 2007. The cofilin pathway in breast cancer invasion and metastasis. *Nat Rev Cancer*. 7:429-440.

Waterman, H., M. Katz, C. Rubin, K. Shtiegman, S. Lavi, A. Elson, T. Jovin, and Y. Yarden. 2002. A mutant EGF-receptor defective in ubiquitylation and endocytosis unveils a role for Grb2 in negative signaling. *EMBO J*. 21:303-313.

Waterman, H., and Y. Yarden. 2001. Molecular mechanisms underlying endocytosis and sorting of ErbB receptor tyrosine kinases. *FEBS letters*. 490:142-152.

Weinreb, P.H., K.J. Simon, P. Rayhorn, W.J. Yang, D.R. Leone, B.M. Dolinski, B.R. Pearse, Y. Yokota, H. Kawakatsu, A. Atakilit, D. Sheppard, and S.M. Violette. 2004. Function-blocking integrin alphavbeta6 monoclonal antibodies: distinct ligand-mimetic and nonligand-mimetic classes. *J Biol Chem*. 279:17875-17887.

White, D.P., P.T. Caswell, and J.C. Norman. 2007. alpha v beta3 and alpha5beta1 integrin recycling pathways dictate downstream Rho kinase signaling to regulate persistent cell migration. *J Cell Biol*. 177:515-525.

Whittaker, C.A., and R.O. Hynes. 2002. Distribution and evolution of von Willebrand/integrin A domains: widely dispersed domains with roles in cell adhesion and elsewhere. *Mol Biol Cell*. 13:3369-3387.

Wiley, H.S., J.J. Herbst, B.J. Walsh, D.A. Lauffenburger, M.G. Rosenfeld, and G.N. Gill. 1991. The role of tyrosine kinase activity in endocytosis, compartmentation, and down-regulation of the epidermal growth factor receptor. *J Biol Chem*. 266:11083-11094.

Winograd-Katz, S.E., R. Fassler, B. Geiger, and K.R. Legate. 2014. The integrin adhesome: from genes and proteins to human disease. *Nat Rev Mol Cell Biol*. 15:273-288.

Wolanska, K.I., and M.R. Morgan. 2015. Fibronectin remodelling: cell-mediated regulation of the microenvironment. *Biochem Soc Trans*. 43:122-128.

Wolfenson, H., I. Lavelin, and B. Geiger. 2013. Dynamic regulation of the structure and functions of integrin adhesions. *Dev Cell*. 24:447-458.

Worthington, J.J., J.E. Klementowicz, and M.A. Travis. 2011. TGFbeta: a sleeping giant awoken by integrins. *Trends Biochem Sci*. 36:47-54.

Wu, J., T. Vallenius, K. Ovaska, J. Westermarck, T.P. Makela, and S. Hautaniemi. 2009. Integrated network analysis platform for protein-protein interactions. *Nat Methods*. 6:75-77.

Xia, H., R.S. Nho, J. Kahm, J. Kleidon, and C.A. Henke. 2004. Focal adhesion kinase is upstream of phosphatidylinositol 3-kinase/Akt in regulating fibroblast survival in response to contraction of type I collagen matrices via a beta 1 integrin viability signaling pathway. *J Biol Chem*. 279:33024-33034.

Xiong, J.P., T. Stehle, B. Diefenbach, R. Zhang, R. Dunker, D.L. Scott, A. Joachimiak, S.L. Goodman, and M.A. Arnaout. 2001. Crystal structure of the extracellular segment of integrin alpha Vbeta3. *Science*. 294:339-345.

Xiong, J.P., T. Stehle, R. Zhang, A. Joachimiak, M. Frech, S.L. Goodman, and M.A. Arnaout. 2002. Crystal structure of the extracellular segment of integrin alpha Vbeta3 in complex with an Arg-Gly-Asp ligand. *Science*. 296:151-155.

Yada, E., S. Wada, S. Yoshida, and T. Sasada. 2018. Use of patient-derived xenograft mouse models in cancer research and treatment. *Future Sci OA*. 4:FSO271.

Yamada, K.M., and S. Even-Ram. 2002. Integrin regulation of growth factor receptors. *Nature cell biology*. 4:E75-76.

Yang, G.Y., K.S. Xu, Z.Q. Pan, Z.Y. Zhang, Y.T. Mi, J.S. Wang, R. Chen, and J. Niu. 2008. Integrin alpha v beta 6 mediates the potential for colon cancer cells to colonize in and metastasize to the liver. *Cancer Sci*. 99:879-887.

Yang, X., O.V. Kovalenko, W. Tang, C. Claas, C.S. Stipp, and M.E. Hemler. 2004. Palmitoylation supports assembly and function of integrin-tetraspanin complexes. *J Cell Biol*. 167:1231-1240.

Yang, Z., Z. Mu, B. Dabovic, V. Jurukovski, D. Yu, J. Sung, X. Xiong, and J.S. Munger. 2007. Absence of integrin-mediated TGFbeta1 activation in vivo recapitulates the phenotype of TGFbeta1-null mice. *J Cell Biol*. 176:787-793.

Yao, M., B.T. Goult, B. Klapholz, X. Hu, C.P. Toseland, Y. Guo, P. Cong, M.P. Sheetz, and J. Yan. 2016. The mechanical response of talin. *Nature communications*. 7:11966.

Yarden, Y., and G. Pines. 2012. The ERBB network: at last, cancer therapy meets systems biology. *Nat Rev Cancer*. 12:553-563.

Yarden, Y., and B.Z. Shilo. 2007. SnapShot: EGFR signaling pathway. *Cell*. 131:1018.

Ye, F., A.K. Snider, and M.H. Ginsberg. 2014. Talin and kindlin: the one-two punch in integrin activation. *Front Med*. 8:6-16.

Yu, X., S. Miyamoto, and E. Mekada. 2000. Integrin alpha 2 beta 1-dependent EGF receptor activation at cell-cell contact sites. *Journal of cell science*. 113 (Pt 12):2139-2147.

Zaidel-Bar, R., and B. Geiger. 2010. The switchable integrin adhesome. *Journal of cell science*. 123:1385-1388.

Zaidel-Bar, R., S. Itzkovitz, A. Ma'ayan, R. Iyengar, and B. Geiger. 2007. Functional atlas of the integrin adhesome. *Nature cell biology*. 9:858-867.

Zambruno, G., P.C. Marchisio, A. Marconi, C. Vaschieri, A. Melchiori, A. Giannetti, and M. De Luca. 1995. Transforming growth factor-beta 1 modulates beta 1 and beta 5 integrin receptors and induces the de novo expression of the alpha v beta 6 heterodimer in normal human keratinocytes: implications for wound healing. *J Cell Biol*. 129:853-865.

Zhan, T., M. Poppelreuther, R. Ehehalt, and J. Fullekrug. 2012. Overexpressed FATP1, ACSVL4/FATP4 and ACSL1 increase the cellular fatty acid uptake of 3T3-L1 adipocytes but are localized on intracellular membranes. *PLoS One*. 7:e45087.

Zhang, H., P. Ghai, H. Wu, C. Wang, J. Field, and G.L. Zhou. 2013. Mammalian adenylyl cyclase-associated protein 1 (CAP1) regulates cofilin function, the actin cytoskeleton, and cell adhesion. *J Biol Chem*. 288:20966-20977.

Zhang, X., J. Gureasko, K. Shen, P.A. Cole, and J. Kuriyan. 2006. An allosteric mechanism for activation of the kinase domain of epidermal growth factor receptor. *Cell*. 125:1137-1149.

Zhao, B., X. Wei, W. Li, R.S. Udan, Q. Yang, J. Kim, J. Xie, T. Ikenoue, J. Yu, L. Li, P. Zheng, K. Ye, A. Chinnaiyan, G. Halder, Z.C. Lai, and K.L. Guan. 2007. Inactivation of YAP oncoprotein by the Hippo pathway is involved in cell contact inhibition and tissue growth control. *Genes Dev*. 21:2747-2761.

Zheng, X., H. Baker, W.S. Hancock, F. Fawaz, M. McCaman, and E. Pungor, Jr. 2006. Proteomic analysis for the assessment of different lots of fetal bovine serum as a

raw material for cell culture. Part IV. Application of proteomics to the manufacture of biological drugs. *Biotechnol Prog*. 22:1294-1300.

Zwick, E., P.O. Hackel, N. Prenzel, and A. Ullrich. 1999. The EGF receptor as central transducer of heterologous signalling systems. *Trends Pharmacol Sci*. 20:408-412.

Appendix

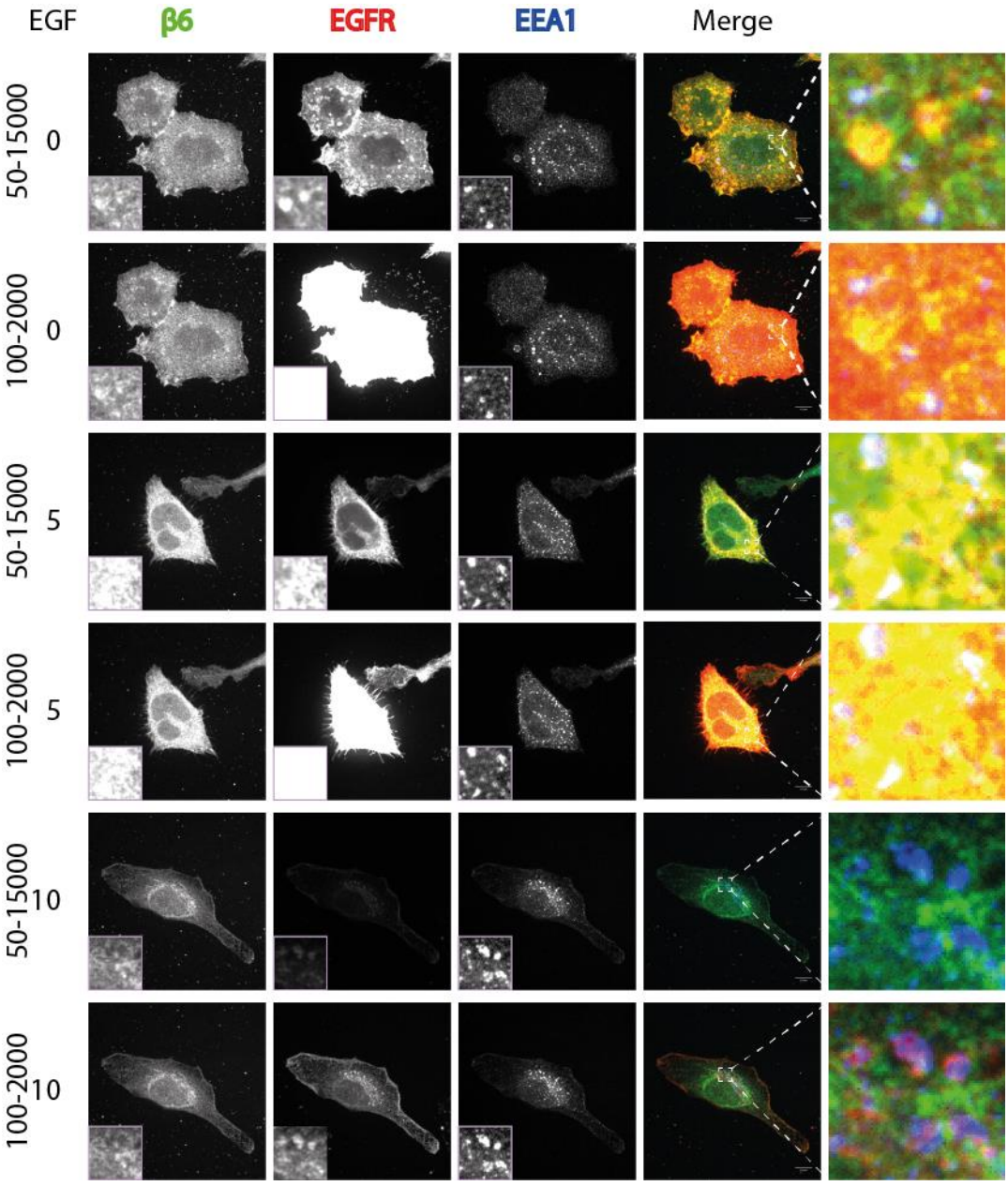

Figure S1 A: EGF stimulation induces colocalisation of β6 and EGFR with EEA1. MDA-MB-468 cells, co-stained for β6, EGFR (D38B1) and EEA1. Single z slice shown for a juxtamembrane section of the cell. EGF stimulation shown in minutes. EGFR is shown at 50 - 15000 and 100 - 2000 intensity arbitrary units for 0, 5 and 10-minute timepoints. Scale bar = 10 µm. N= 2, n= 13 - 20 cells per timepoint.

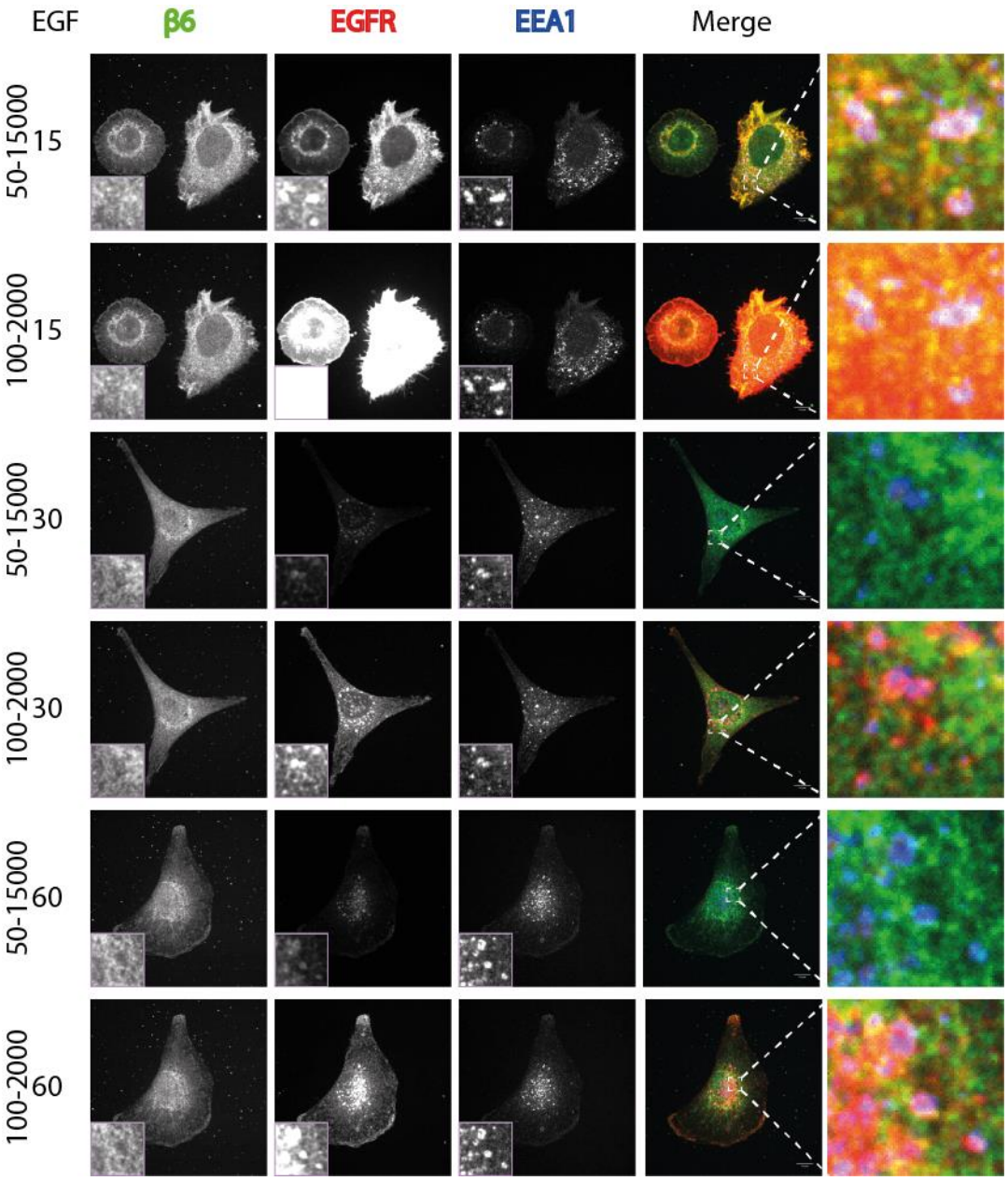

Figure S1 B: EGF stimulation induces colocalisation of β6 and EGFR with EEA1. MDA-MB-468 cells, co-stained for β6, EGFR (D38B1) and EEA1. Single z slice shown for a juxtamembrane section of the cell. EGF stimulation shown in minutes. EGFR is shown at 50- 15000 and 100 - 2000 intensity arbitrary units for 15, 30 and 60-minute timepoints. Scale bar = 10 µm. N= 2, n= 13 - 20 cells per timepoint.

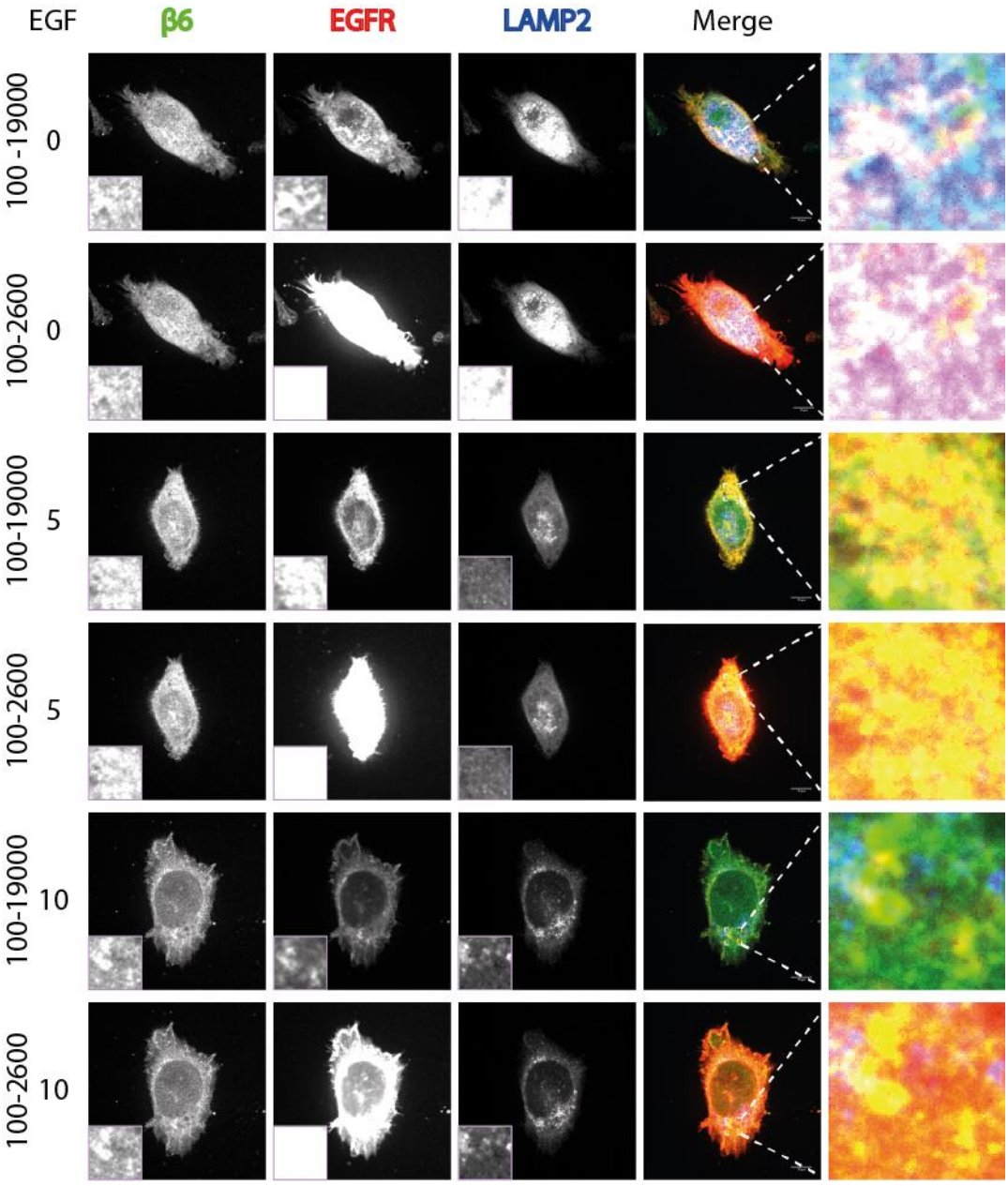

Figure S.2 A: EGF stimulation induces colocalisation of EGFR with LAMP2. MDA-MB-468 cells, co-stained for β6, EGFR (D38B1) and LAMP2. Cells were pre-incubated with the lysosomal and proteasomal inhibitors folimycin and epoxomicin, respectively. Single z-slice shown for a juxtamembrane section of the cell. EGF stimulation shown in minutes. EGFR is shown at 100 - 19000 and 100 - 2600 intensity arbitrary units for 0, 5 and 10-minute timepoints. Scale bar = 10 µm. N=1, n= 15 - 20 cells per timepoint.

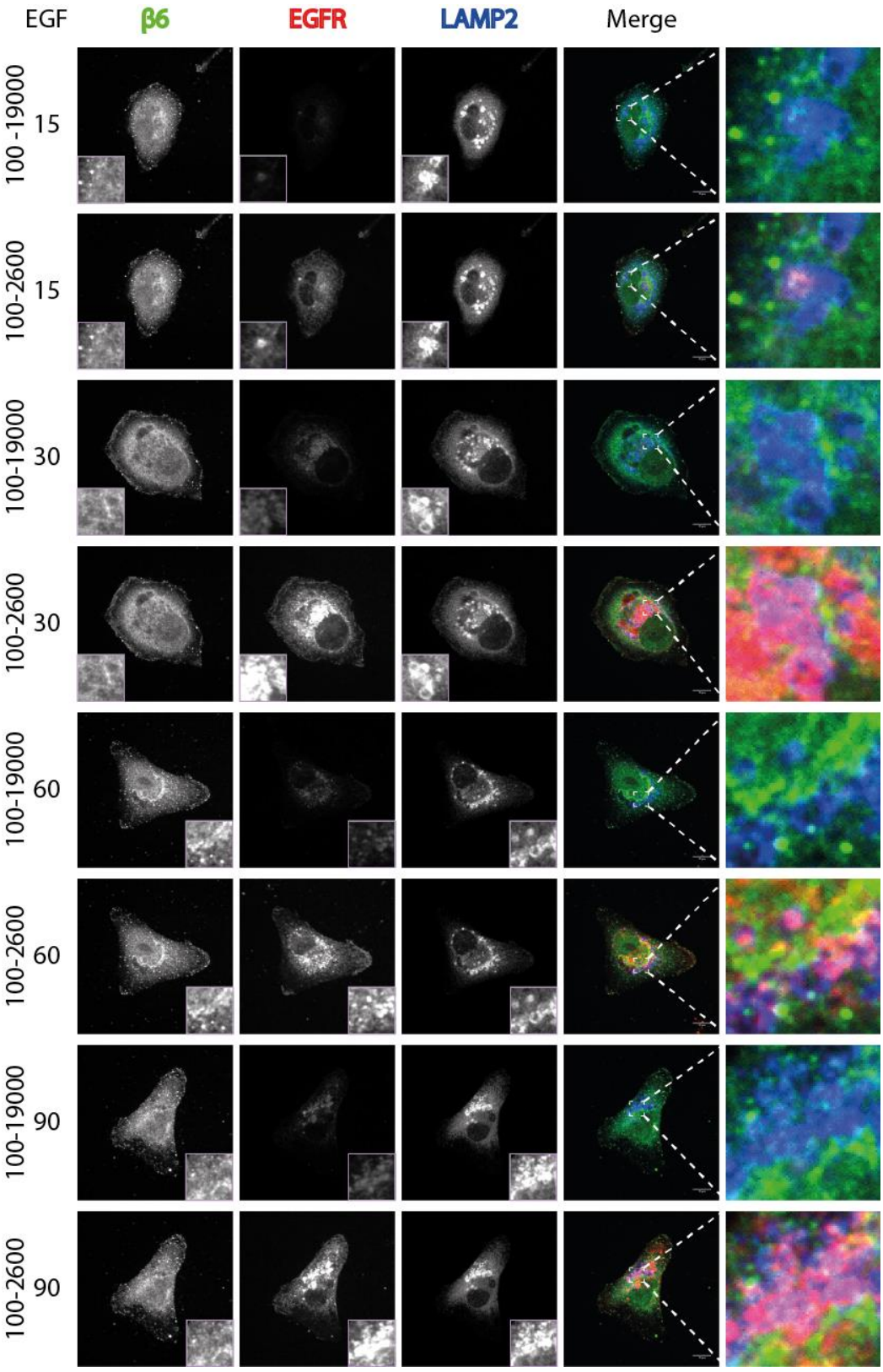

Figure S.2 B: EGF stimulation induces colocalisation of EGFR with LAMP2. MDA-MB-468 cells, co-stained for β6, EGFR (D38B1) and LAMP2. Cells were pre-incubated with the lysosomal and proteasomal inhibitors folimycin and epoxomicin, respectively. Single z-slice shown for a juxtamembrane section of the cell. EGF stimulation shown in minutes. EGFR is shown at 100 - 19000 and 100 - 2600 intensity arbitrary units for 15, 30, 60 and 90 minutes. Scale bar = 10 µm. N=1, n= 15 - 20 cells per timepoint.

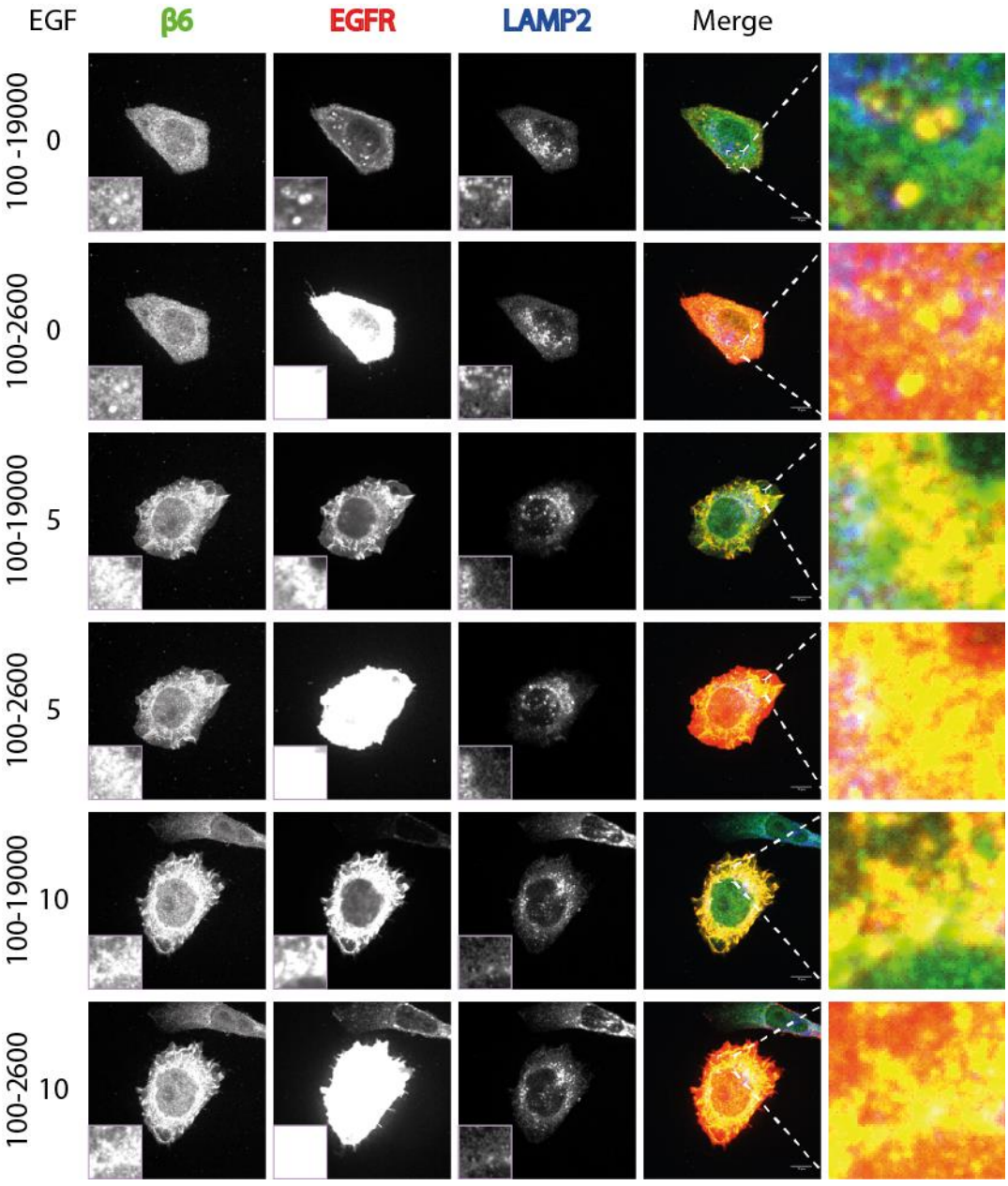

Figure S.3 A: EGF stimulation induces colocalisation of β6 and EGFR with LAMP2. MDA-MB-468 cells, co-stained for β6, EGFR (D38B1) and LAMP2. DMSO vehicle control for Folimycin and epoxomicin lysosomal and proteasomal inhibitors. Single z-slice shown for a juxtamembrane section of the cell. EGF stimulation shown in minutes. EGFR is shown at 100 - 19000 and 100 - 2600 intensity arbitrary units for 0, 5 and 10-minute timepoints. Scale bar = 10 µm. N=1, n= 8 - 24 cells per timepoint.

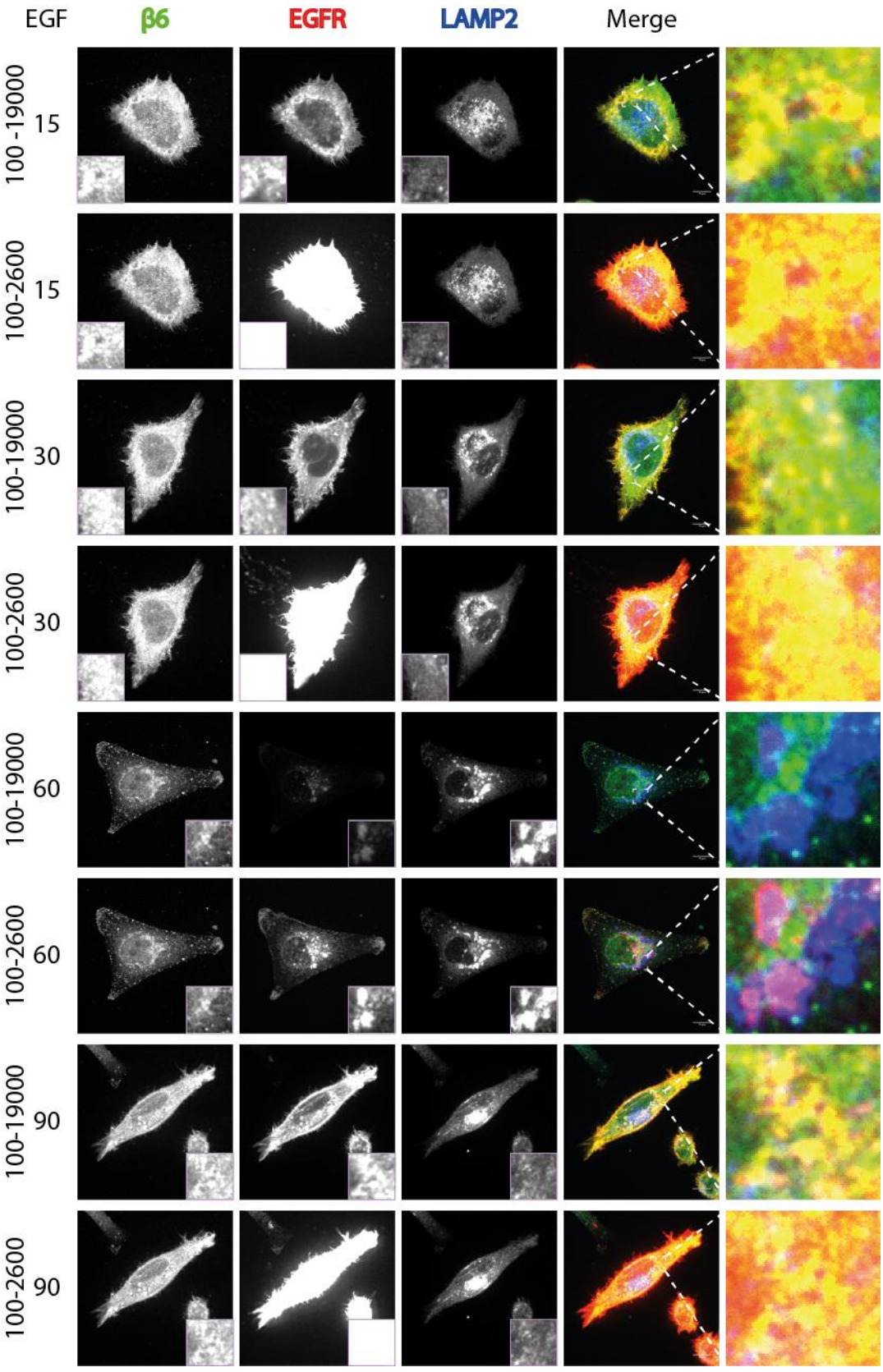

Figure S.3 B: EGF stimulation induces colocalisation of β6 and EGFR with LAMP2. MDA-MB-468 cells, co-stained for β6, EGFR (D38B1) and LAMP2. DMSO vehicle control for Folimycin and epoxomicin lysosomal and proteasomal inhibitors. Single z-slice shown for a juxtamembrane section of the cell. EGF stimulation shown in minutes. EGFR is shown at 100 - 19000 and 100 - 2600 intensity arbitrary units for 15, 30, 60 and 90 minutes. Scale bar = 10 µm. N=1, n= 8 - 24 cells per timepoint.

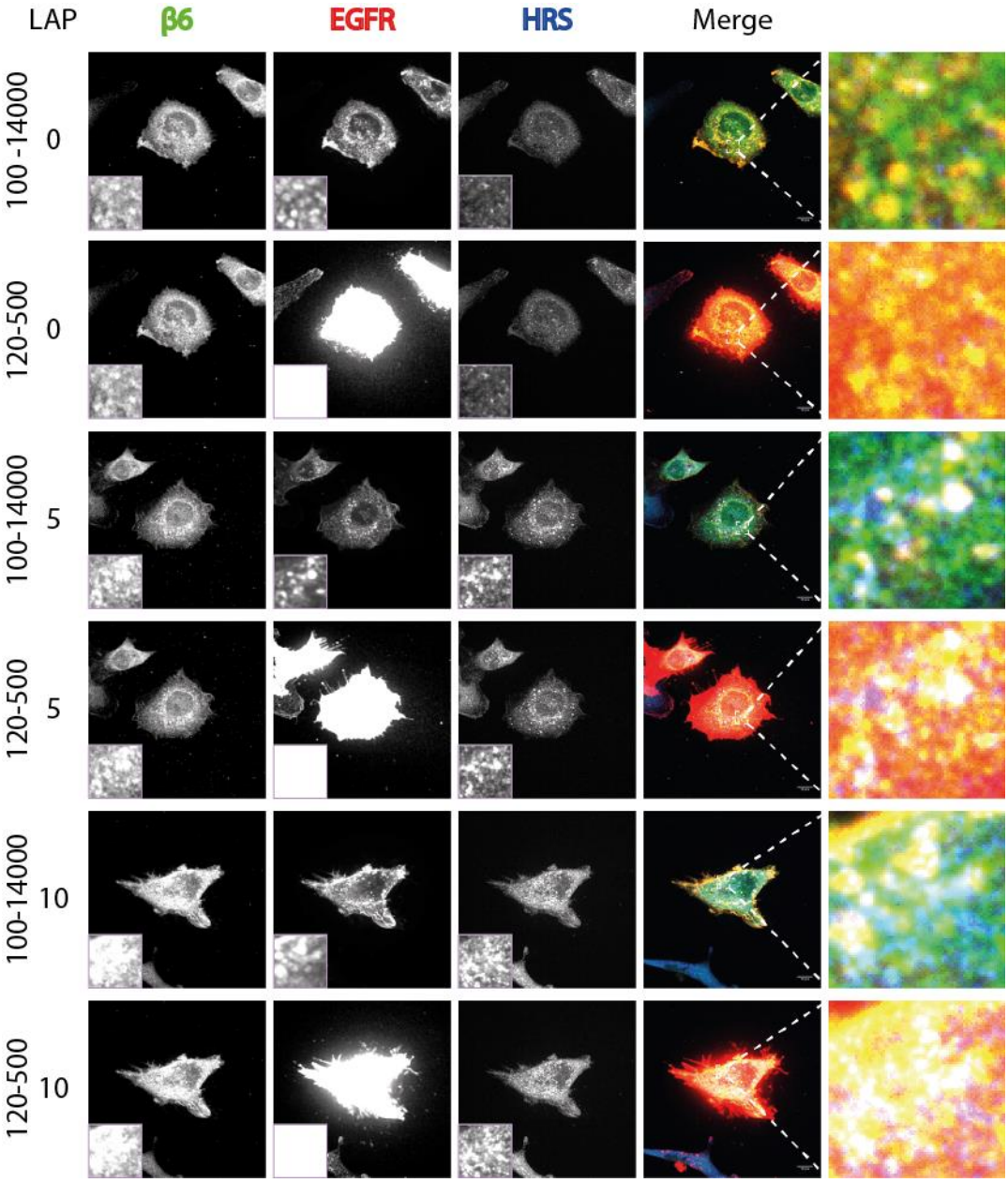

Figure S4 A: LAP stimulation induces colocalisation of β6 and EGFR with HRS. MDA-MB-468 cells, co-stained for β6, EGFR (D38B1) and HRS. Single z-slice shown for a juxtamembrane section of the cell. LAP stimulation shown in minutes. EGFR is shown at 100 - 14000 and 120 - 500 intensity arbitrary units for 0, 5 and 10-minute timepoints. Scale bar = 10 µm. N=2, n= 13 - 19 cells per condition.

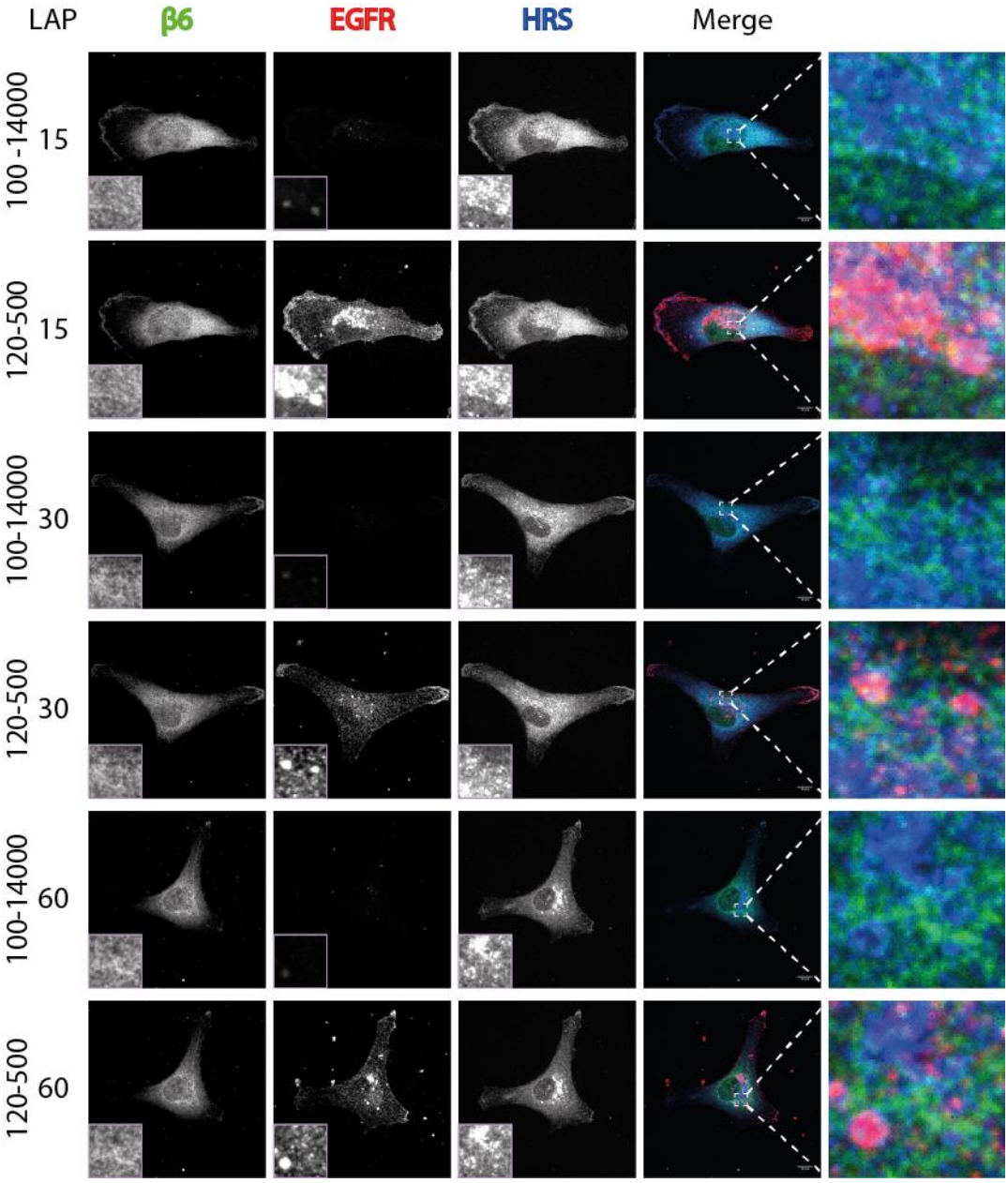

Figure S4 B: LAP stimulation induces colocalisation of β6 and EGFR with HRS. MDA-MB-468 cells, co-stained for β6, EGFR (D38B1) and HRS. Single z-slice shown for a juxtamembrane section of the cell. LAP stimulation shown in minutes. EGFR is shown at 100 - 14000 and 120 - 500 intensity arbitrary units for 15, 30 and 60-minute timepoints. Scale bar = 10 µm. N=2, n= 13 - 19 cells per condition.

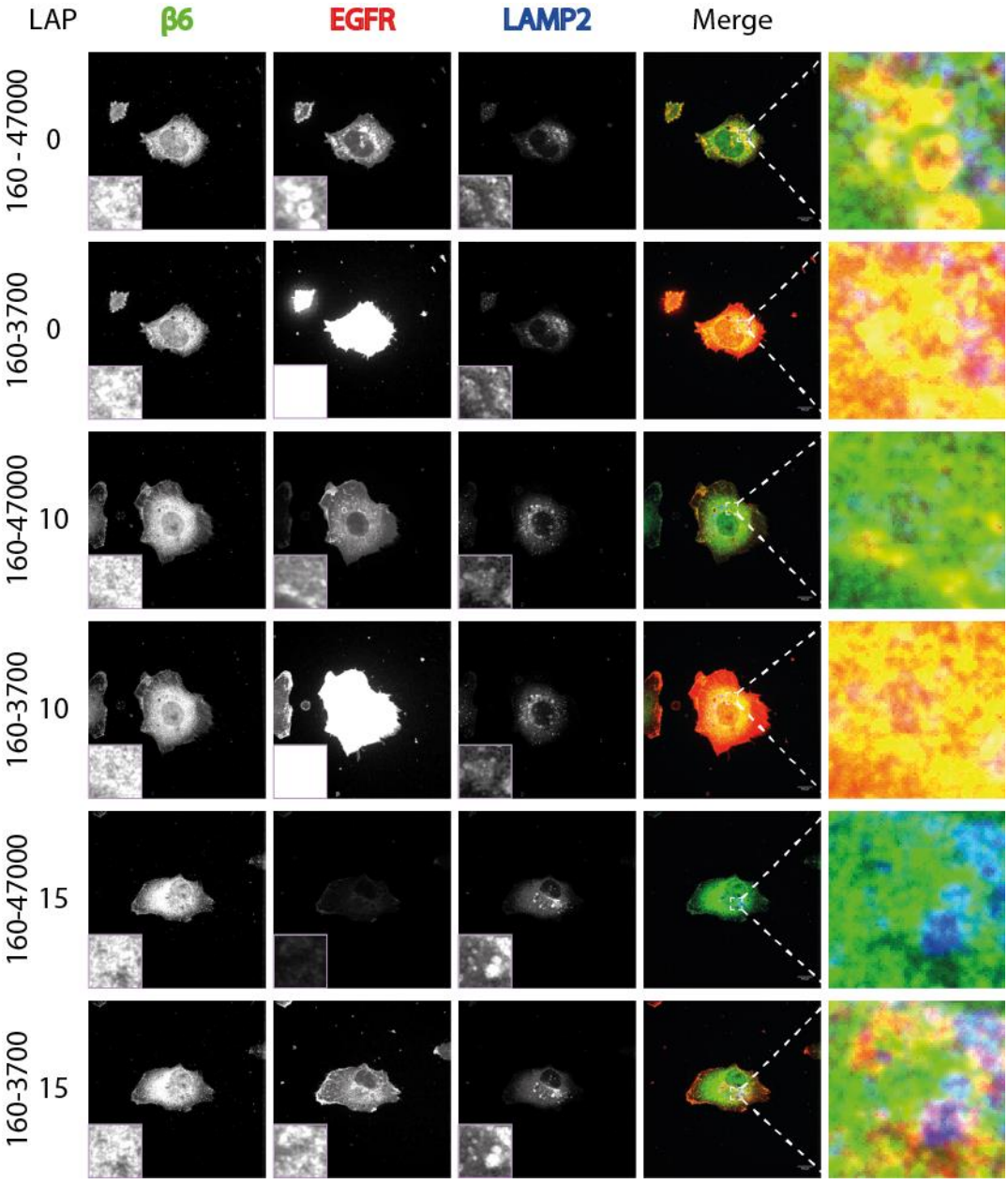

Figure S5 A: LAP stimulation induces colocalisation of EGFR with LAMP2. MDA-MB-468 cells, co-stained for β6, EGFR (D38B1) and LAMP2. DMSO vehicle control. Single z-slice shown for a juxtamembrane section of the cell. LAP stimulation shown in minutes. EGFR is shown at 160 - 47000 and 160 - 3700 intensity arbitrary units for 0, 10 and 15-minute timepoints. Scale bar = 10 µm. N=1, n= 15-17 cells per condition

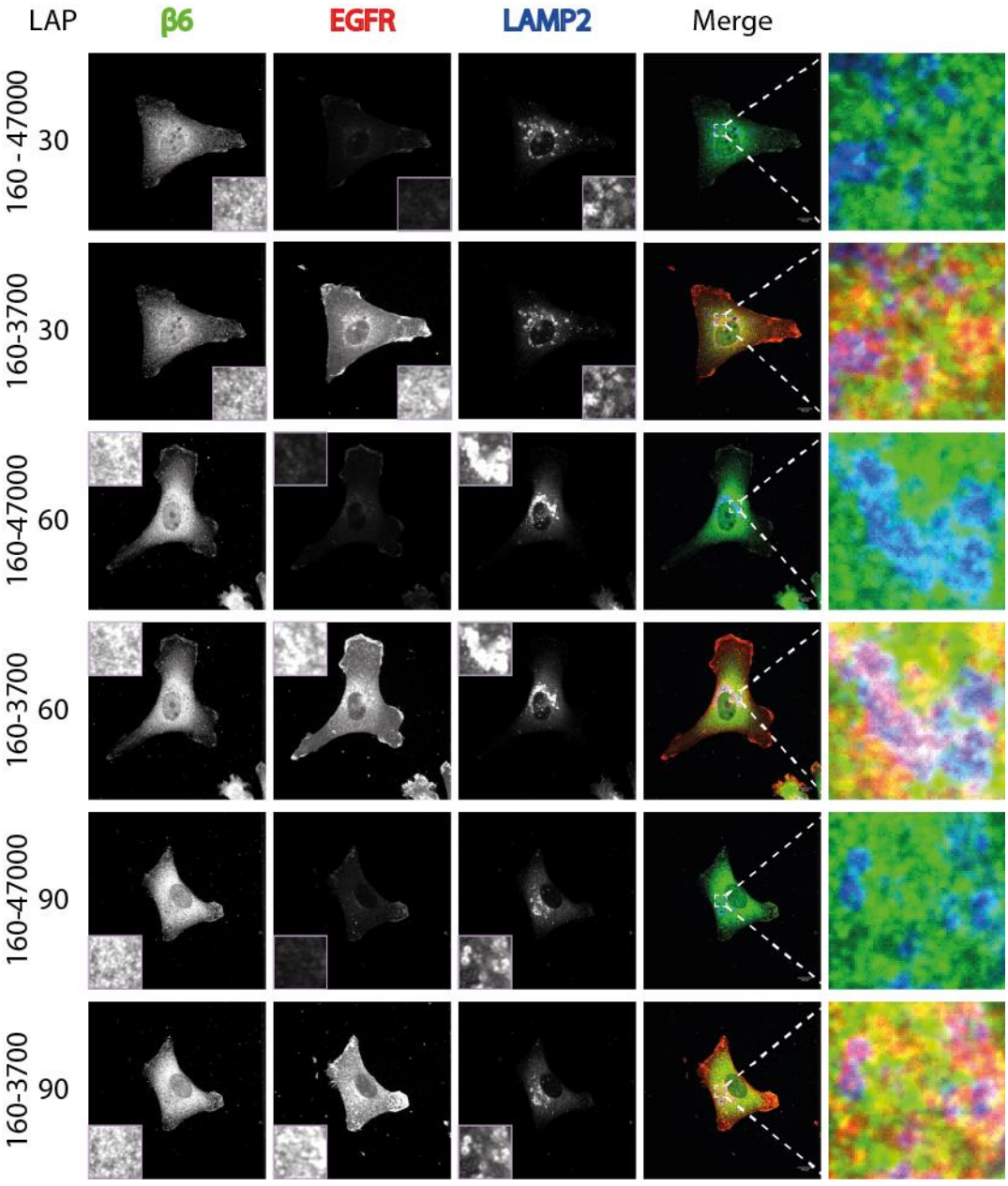

Figure S5 B: LAP stimulation induces colocalisation of EGFR with LAMP2. MDA-MB-468 cells, co-stained for β6, EGFR (D38B1) and LAMP2. DMSO vehicle control. Single z-slice shown for a juxtamembrane section of the cell. LAP stimulation shown in minutes. EGFR is shown at 160 - 47000 and 160 - 3700 intensity arbitrary units for 0, 10 and 15-minute timepoints. Scale bar = 10 µm. N=1, n= 15-17 cells per condition.

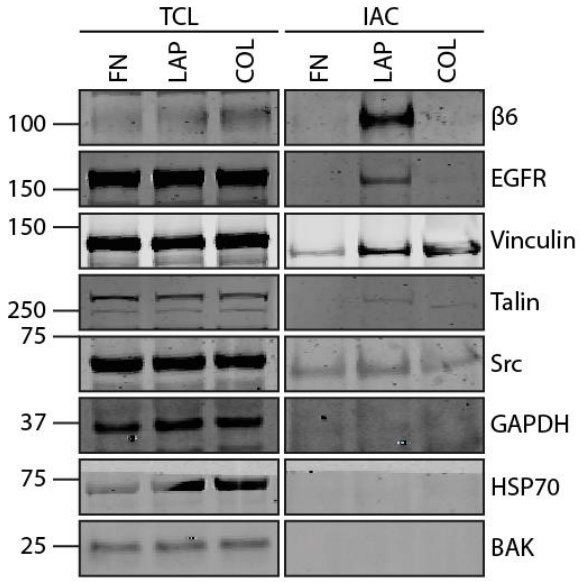

Figure S6: Validation of integrin-associated complex enrichment. Western blotting in total cell lysate (TCL) and isolated integrin-associated complexes (IAC) for the adhesome components integrin β6, vinculin, talin, src (GD11), EGFR (sc-03), and negative control proteins GAPDH, HSP70, and BAK from other subcellular compartments. Blots of N2 that was analysed subsequently by mass spectrometry.

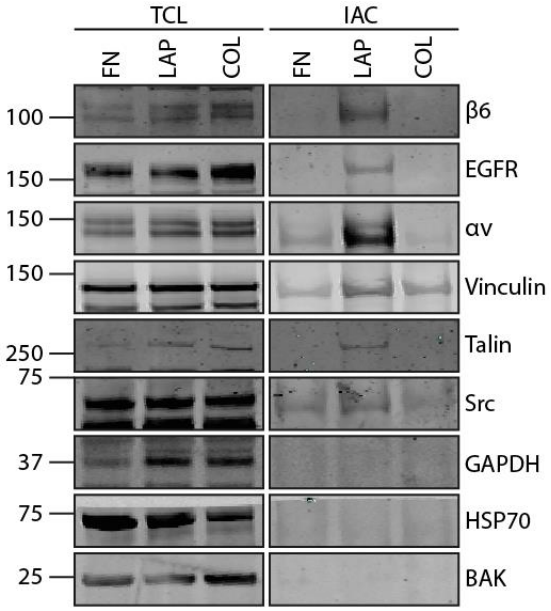

Figure S7: Validation of integrin-associated complex enrichment. Western blotting in total cell lysate (TCL) and isolated integrin-associated complexes (IAC) for the adhesome components integrin β6, αv, vinculin, talin, Src (GD11), EGFR (sc-03), and negative control proteins GAPDH, HSP70, and BAK from other subcellular compartments. Blots of N3 that was analysed subsequently by mass spectrometry.

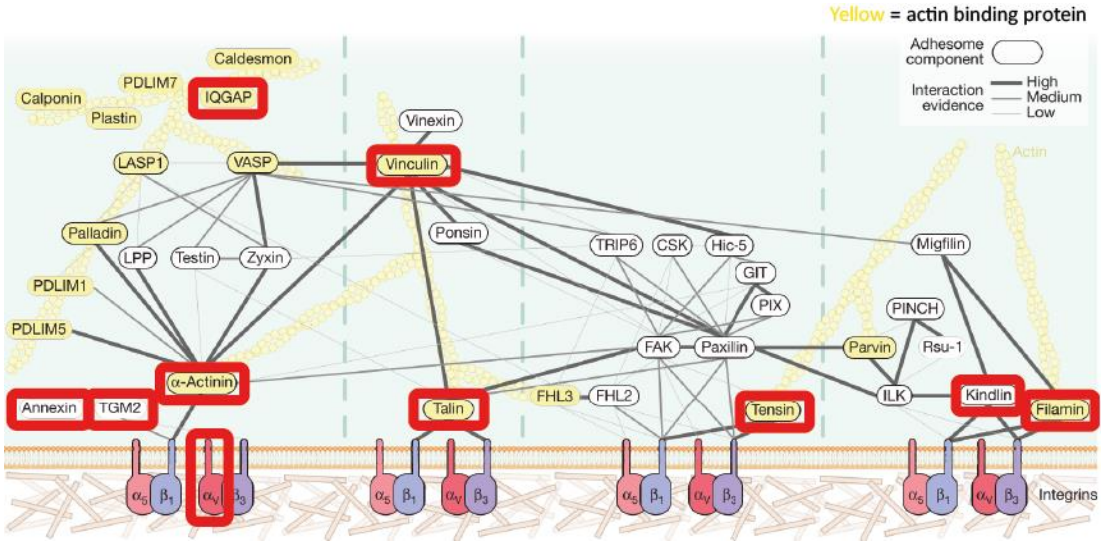

Figure S8: Representation of consensus adhesome proteins represented in the IAC dataset. Figure is adapted from Horton *et al* depicting a schematic of key signalling axes formed by the consensus adhesome proteins (Horton et al., 2015b). Proteins outlined with a red box indicate connected consensus adhesome proteins that were present in our IAC dataset.

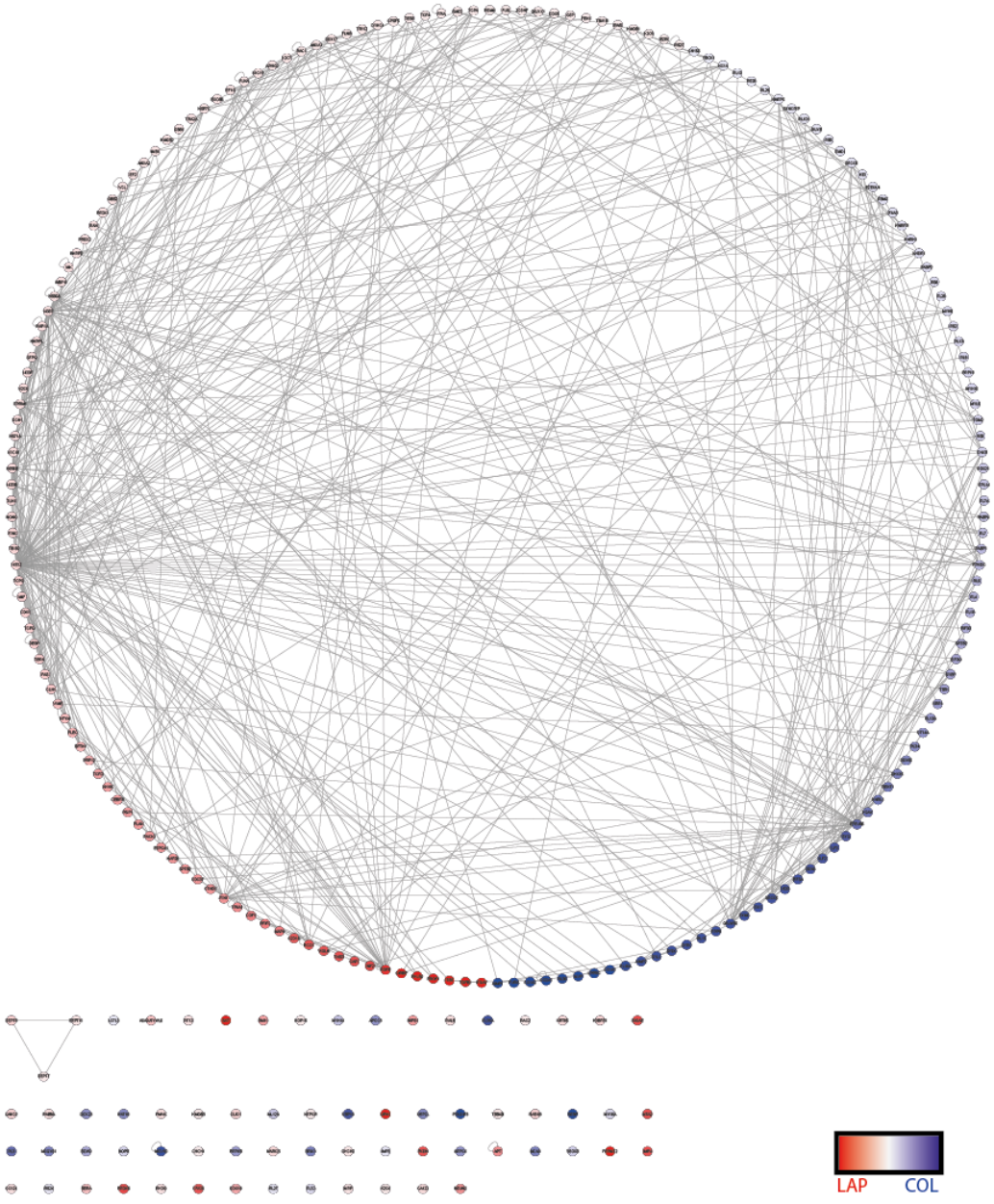

Figure S9: ≥ 1.5-fold different proteins on LAP versus collagen. Total number of proteins = 256. Nodes represent proteins and edges are known interactions. Node colour red to blue gradient = log2 fold enrichment LAP/collagen.

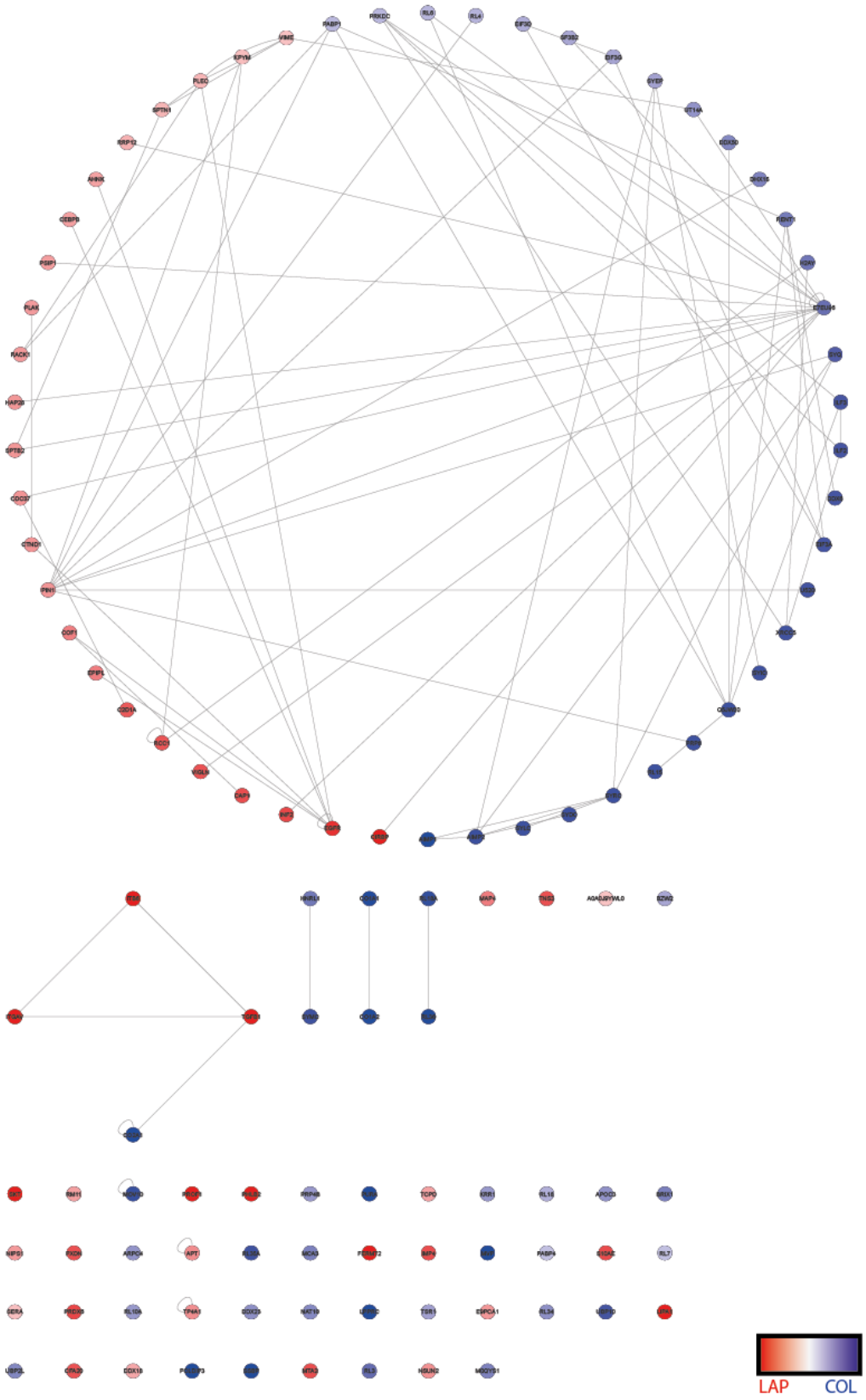

Figure S10: ≥ 5-fold different proteins on LAP versus collagen. Total number of proteins = 113. Nodes represent proteins and edges are known interactions. Node colour red to blue gradient = log2 fold enrichment LAP/collagen.

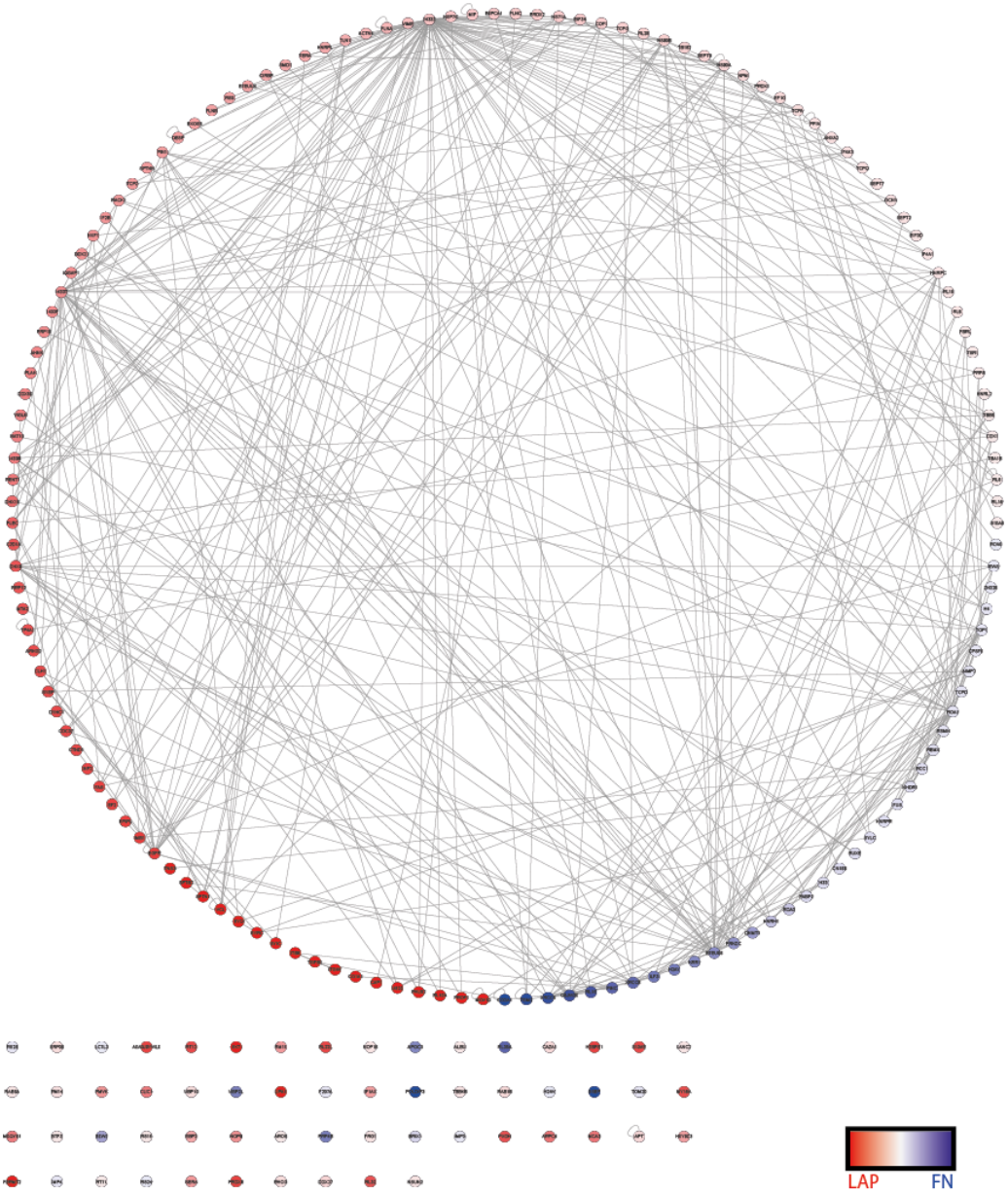

Figure S11: ≥ 1.5-fold different proteins on LAP versus fibronectin. Total number of proteins = 201. Nodes represent proteins and edges are known interactions. Node colour red to blue gradient = log2 fold enrichment LAP/FN.

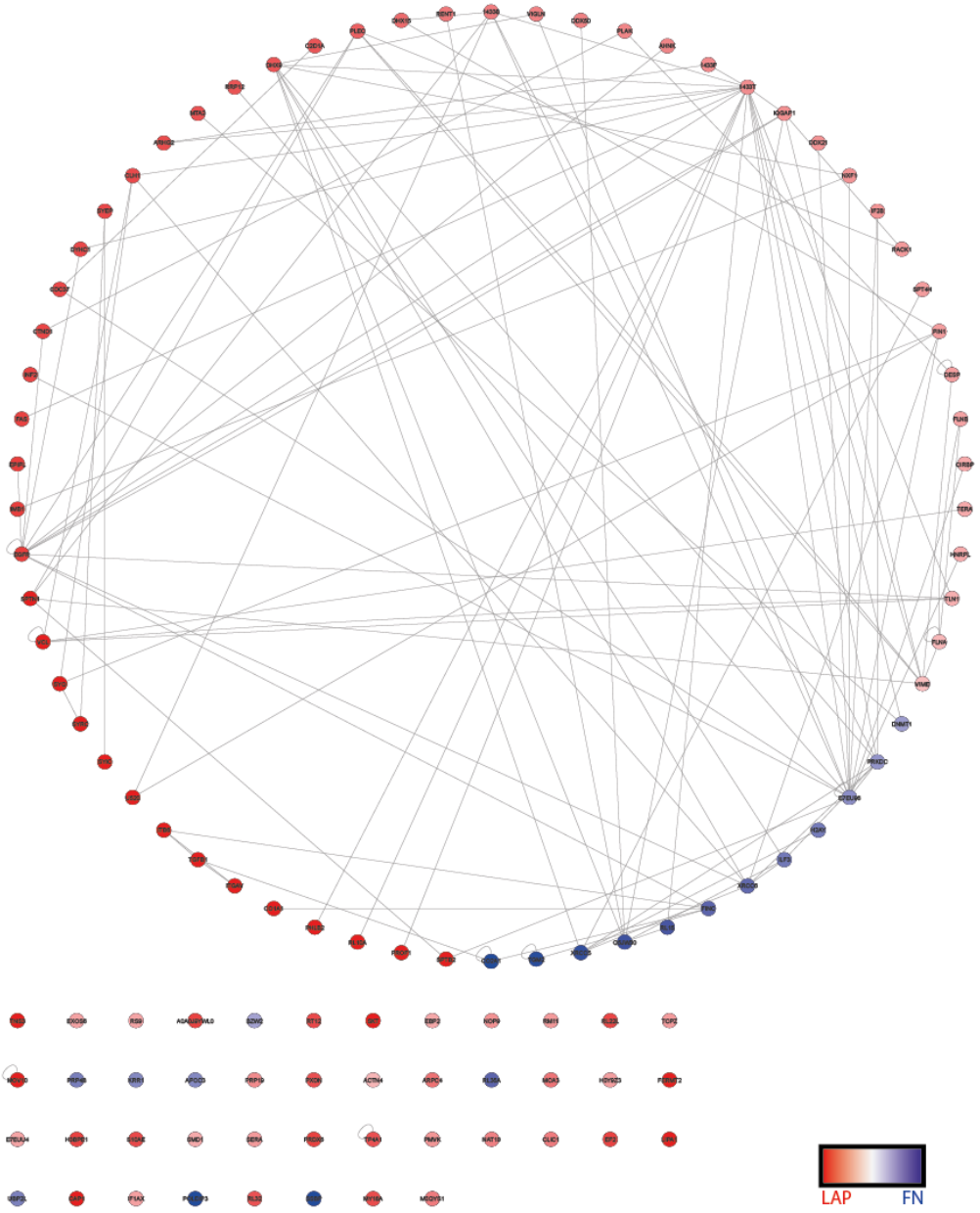

Figure S12: ≥ 5-fold different proteins on LAP versus fibronectin. Total number of proteins = 110. Nodes represent proteins and edges are known interactions. Node colour red to blue gradient = log2 fold enrichment LAP/FN.

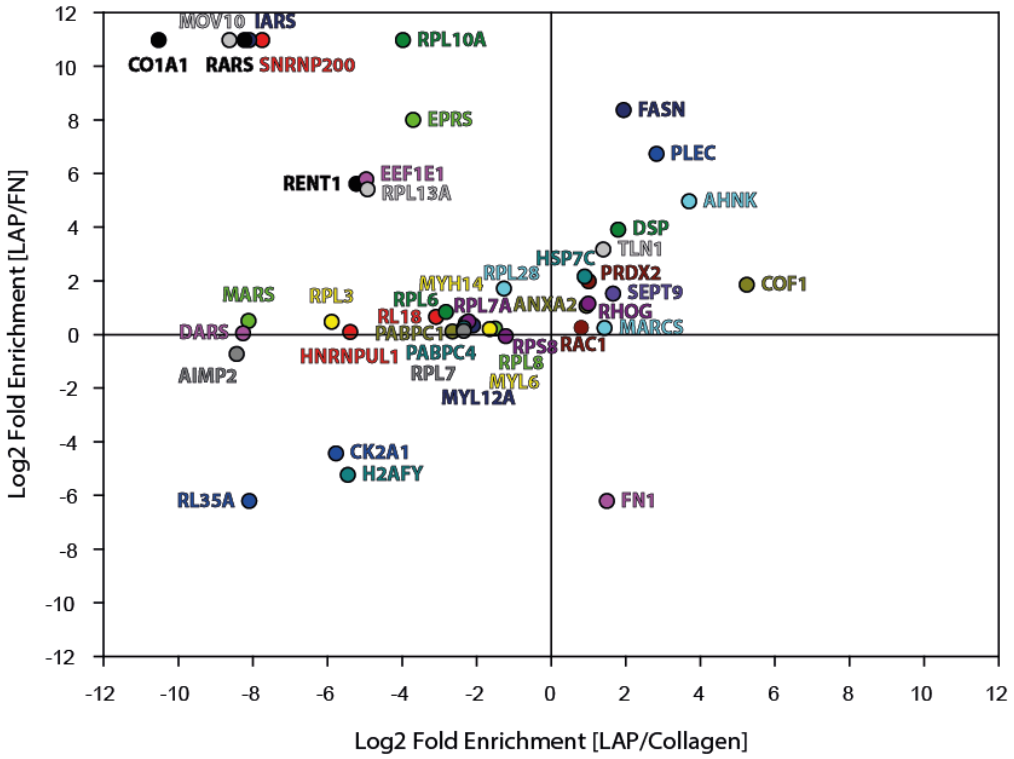

Figure S13: Statistically significantly different proteins between ligands. Analysis of variance (ANOVA) between LAP, FN and collagen ligands normalized spectral abundance factor (NSAF) values. Proteins are mapped by log2 fold enrichment of LAP/ FN and LAP/collagen. Statistical significance p=<0.01. Gene names colour co-ordinated with the corresponding data point symbol.

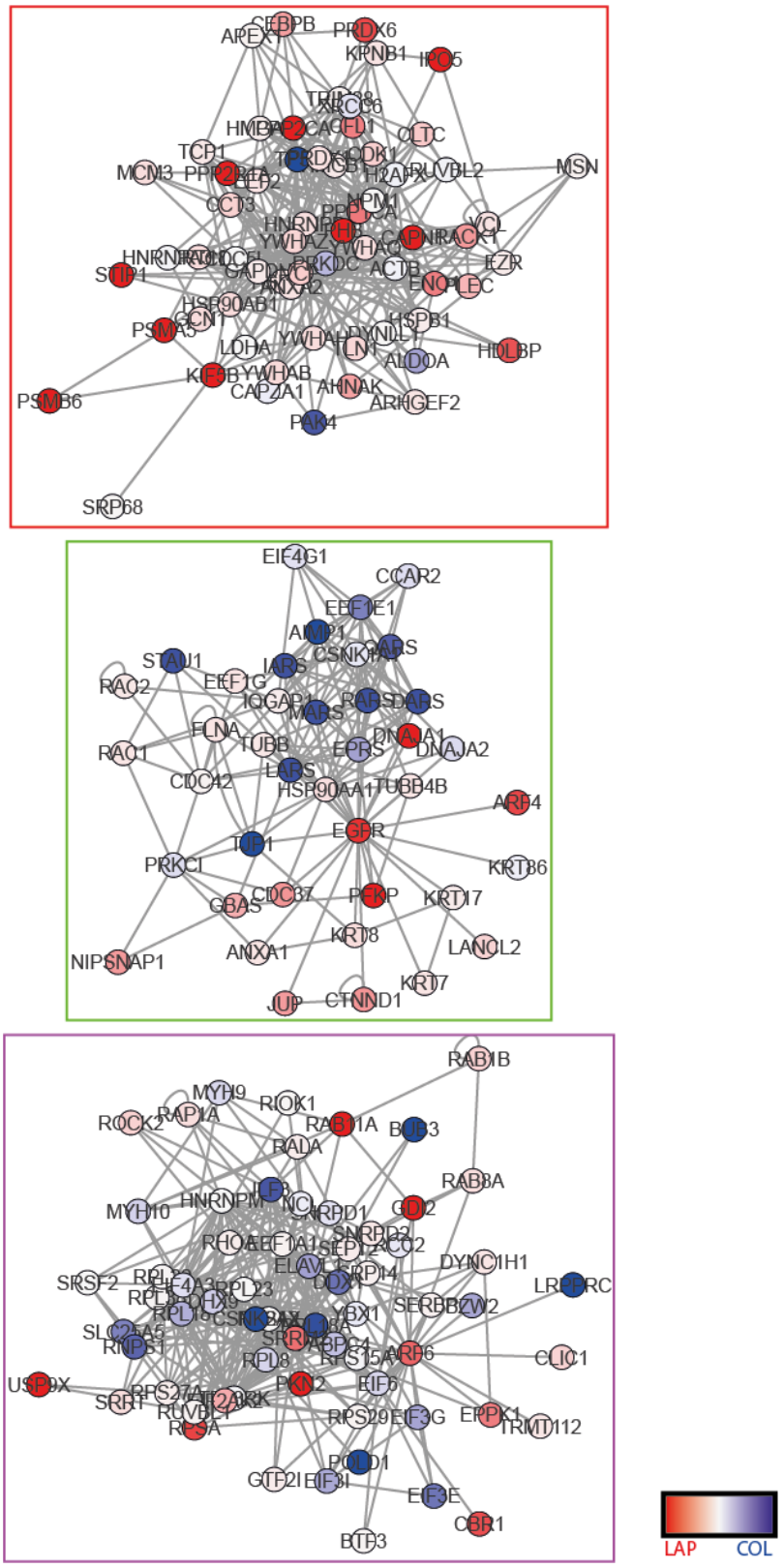

Figure S14: Endocytosis term large subnetwork clusters. Large clusters from which smaller clusters in figure 4.16 were derived. Clusters are colour matched, with a continuous outline for the large cluster, and dashed outline for the smaller derivative. Clusters are from proteins associated with the endocytosis KEGG term group and their one-hop interactors. Inter-cluster interactions are not shown. Nodes represent proteins, and edges are known interactions. Node colour red to blue gradient = log2 fold enrichment LAP/collagen.

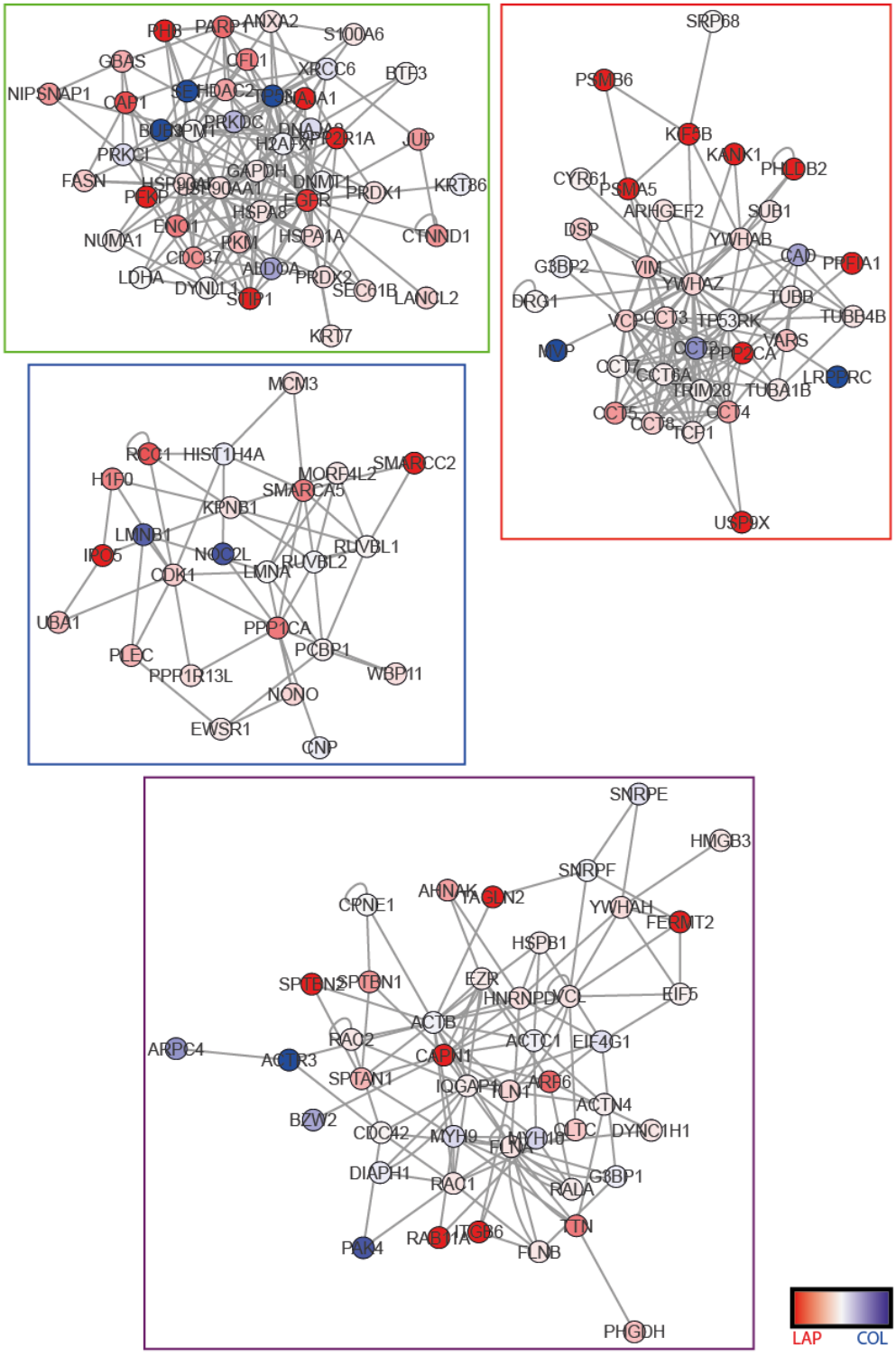

Figure S15: Hippo signalling pathway term large subnetwork clusters. Large clusters from which smaller clusters in figure 4.17 were derived. Clusters are colour matched, with a continuous outline for the large cluster, and dashed outline for the smaller derivative. Clusters are from proteins associated with the hippo signalling pathway KEGG term group and their one-hop interactors. Inter-cluster interactions are not shown. Nodes represent proteins, and edges are known interactions. Node colour red to blue gradient = log2 fold enrichment LAP/collagen.

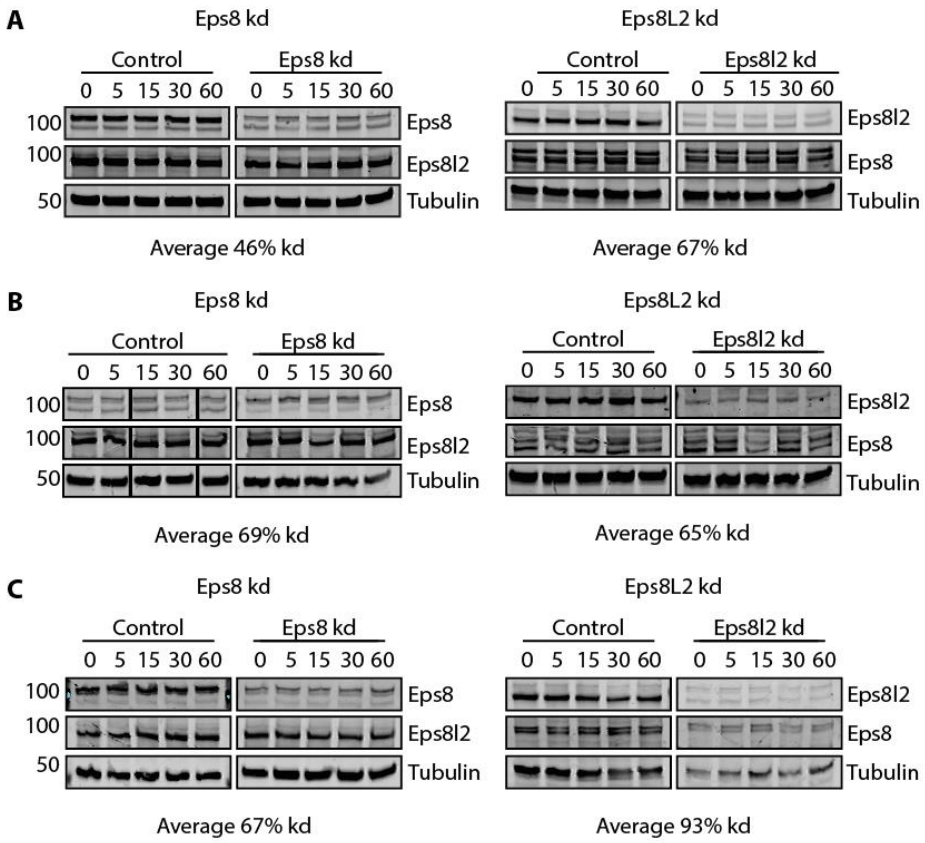

Figure S16: Knockdown levels of Eps8 and Eps8L2. Immunoblotting levels of Eps8, Eps8L2 and tubulin for replicate 1 (A), 2 (B) and 3 (C). Average percentage knockdown quoted for all EGF stimulation timepoints. (C) Replicate 3 half the amount of Eps8L2 sample protein was loaded (5 µg for kd, 10 µg for control samples).